Epoxy Resin Chemistry

Epoxy Resin Chemistry

Ronald S. Bauer, EDITOR

Shell Development Company

Based on a symposium sponsored

by the Division of

Organic Coatings and Plastics

at the 176th Meeting of the

American Chemical Society,

Miami Beach, Florida,

September 11–15, 1978.

ACS SYMPOSIUM SERIES 114

ACS Symposium Series

M. Joan Comstock, *Series Editor*

FOREWORD

The ACS SYMPOSIUM SERIES was founded in 1974 to provide a medium for publishing symposia quickly in book form. The format of the Series parallels that of the continuing ADVANCES IN CHEMISTRY SERIES except that in order to save time the papers are not typeset but are reproduced as they are submitted by the authors in camera-ready form. Papers are reviewed under the supervision of the Editors with the assistance of the Series Advisory Board and are selected to maintain the integrity of the symposia; however, verbatim reproductions of previously published papers are not accepted. Both reviews and reports of research are acceptable since symposia may embrace both types of presentation.

PREFACE

Since their commercial introduction into the United States in the late 1940's, epoxy resins have established themselves as unique building blocks for high performance coatings, adhesives, and reinforced plastics. Over the past five years epoxy resin sales have experienced an annual growth rate of about 8%. In 1978, production in this country exceeded 310 million pounds, and domestic sales were greater than 280 million pounds. This sustained growth of epoxy resins is a result of the wide range of properties that can be achieved with these versatile materials; uses range from coatings for the ubiquitous beverage can to high performance adhesions in spacecraft as well as for encapsulating their sophisticated electronic components.

Work still continues as pressures for more environmentally acceptable and energy efficient systems, and demands for even higher performance, challenge the polymer chemist. This volume covers some of the new resins, curing agents, and application techniques along with new ideas about the chemistry and properties of existing epoxy resin systems. Although comprehensive coverage of this field is not possible in our symposium, it is hoped the papers presented here will help stimulate polymer chemists to answer the challenges facing them.

Shell Development Company   RONALD S. BAUER
Houston, Texas 77001
May 21, 1979

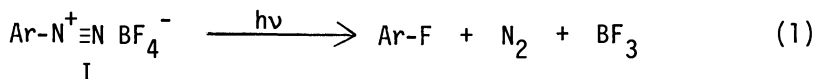# The Photoinitiated Cationic Polymerization of Epoxy Resins

J. V. CRIVELLO and J. H. W. LAM

General Electric Corporate Research and Development Center, Schenectady, NY 12301

The importance of epoxy resins in the fabrication of surface coatings is well recognized in the coatings and plastics industry. In fact, the chief use of epoxy resins, amounting to over 100 million pounds last year, was for coating applications (1). Traditionally, these coatings have been applied from solvents and cured by a baking process. Current efforts to reduce the amount of energy required to carry out coating processes as well as an increasing concern for the environment have provided the impetus to begin the search for new curing chemistry and coating application techniques which circumvent these problems.

Ultraviolet curing has emerged as a rapidly growing method for the fabrication of essentially pollution-free coatings, having only a fraction of the energy requirements of traditional thermally cured materials. At the same time, the generally excellent properties of the coatings which are obtained using uv curing resins together with their high application and cure speeds have made it attractive for many industries to install uv-cure lines.

While the bulk of the work in uv curing to date has involved the radical polymerization of vinyl compounds, during the past five years discovery of several new photoinitiator compounds now makes it possible to effect the uv-cure of epoxy resins by a cationic process. With such systems, solventless liquid epoxy resins can be cured continuously at very high line speeds using approximately one tenth the energy which would be consumed by a comparable thermal process. The first of these new photoinitiators are the aryldiazonium salts (I) (2,3,4,5). When these compounds are irradiated using uv light, a fluoroaromatic compound, nitrogen and the strong Lewis acid, boron trifluoride, are produced (equation 1).

$$Ar-\overset{+}{N}{\equiv}N\ BF_4^- \xrightarrow{h\nu} Ar-F\ +\ N_2\ +\ BF_3 \tag{1}$$
$$I$$

If the photolysis of an aryldiazonium salt is conducted in the

presence of an epoxy resin, boron trifluoride catalyzes the
cationic polymerization of the resin. Due to the production of
nitrogen as a byproduct of the photolysis of aryldiazonium salts,
the major uses of coating systems employing these photoinitiators
lies primarily in thin film applications such as container coat-
ings (6) and photoresists (7).
     Recently, we have reported that diaryliodonium salts (II)
are a second class of highly efficient photoinitiators for the

$$Ar-\overset{+}{I}-Ar'$$
$$X^-$$

$$X^- = BF_4^-, AsF_6^-, PF_6^-, SbCl_6^-, \text{etc.}$$

II
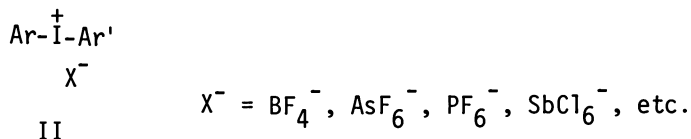
cationic ring opening polymerization of epoxy resins (8,9).
Parallel work in two other laboratories has led to the same con-
clusion (10, 11). Mechanistic studies have shown that on photol-
ysis, diaryliodonium salts liberate strong Brønsted acids of the
type, HX, which subsequently initiate cationic polymerization.
     In this paper, we would like to report some recent work
which has led to the development of triarylsulfonium salts (III)
as a third class of useful photoinitiators for cationic polymeri-
zation and in particular, describe their application to the
polymerization of epoxides.

$$\begin{array}{c} Ar' \\ | \\ Ar-\overset{+}{S} \quad X^- \\ | \\ Ar'' \end{array}$$

III
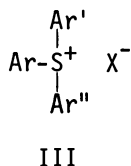
Results and Discussion

     In our laboratory, we have found that triarylsulfonium
salts (III) in which the anions are of the type BF_4^-, AsF_6^-, PF_6^-,
SbF_6^-, etc., are excellent photoinitiators for the polymerization
of epoxy resins as well as a variety of other monomers (12, 13).
Similar results have also been reported by another group of
investigators (14).
     Triarylsulfonium salts may be conveniently prepared via a
number of synthetic routes. In equations 2, 3 and 4 are shown
three of the most direct preparative methods.

$$6ArH + S_2Cl_2 + 3Cl_2 \xrightarrow{AlCl_3} 2(Ar)_3S^+Cl^- + 6HCl \quad (2)$$

$$\begin{array}{c} Ar \\ \diagdown \\ \diagup \\ Ar \end{array} S \to O + Ar'-MgBr \xrightarrow[\text{reflux}]{\text{benzene}} \begin{array}{c} Ar \\ \diagdown \\ \diagup \\ Ar \end{array} S^+-Ar' \ X^- + MgBrOH \quad (3)$$

$$(Ar)_2S \ + \ (Ar')_2I^+ \ X^- \ \xrightarrow{\ Cu^{II} \ (cat)\ } \ Ar_2Ar'S^+ \ X^- \ + \ Ar'I \quad (4)$$
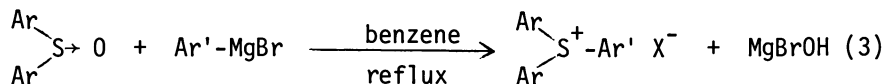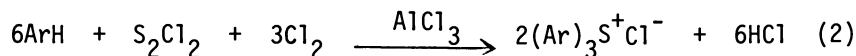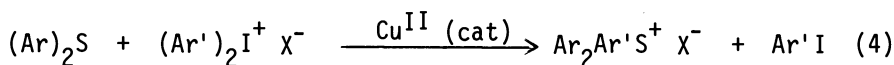
Although the reaction shown in equation 2 is simple and direct, the products which are obtained are generally impure (15). The condensation of diarylsulfoxides with Grignard reagents (equation 3) gives pure triarylsulfonium salts; however, the overall yields are generally of the order of 20-30% (16). In a very recent publication from this laboratory, we described a general synthesis which affords these compounds in high yields (17). This new route involves the copper (II) catalyzed arylation of diaryl-iodonium salts with diarylsulfides (equation 4).

Both of the methods shown in equations 2 and 3 give rise to triarylsulfonium halides which are inactive as photoinitiators for cationic polymerization. These salts must, therefore, be converted to the corresponding salts in which the anion is of the type $X^- = BF_4^-$, AsF_6^-, PF_6^-, etc. This conversion may be accomplished using either of the two methods shown in equation 5.

$$Ar_3S^+ \ Cl^- \ \xrightarrow[\ OH^-\ ]{Ag_2O} \ Ar_3S^+ \ OH^- \ + \ AgCl$$

$$\downarrow HX$$

$$\xrightarrow{NaX} \ Ar_3S^+ \ X^- \qquad (5)$$
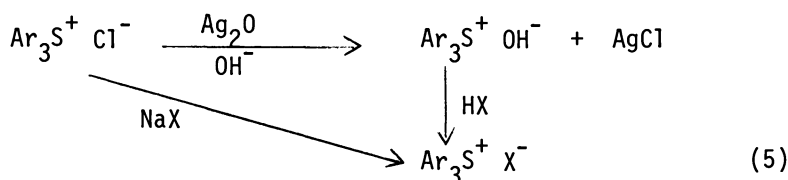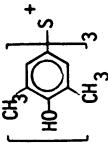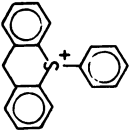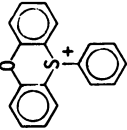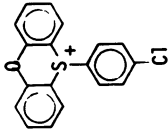
Using the above synthesis, a wide variety of triarylsulfonium salt photoinitiators can be prepared. In Table 1 are shown some representative triarylsulfonium salt photoinitiators which were prepared during the course of this research. All the compounds in this table are well characterized crystalline compounds with well defined melting points, elemental analyses, ultraviolet, proton, and ^{13}C nmr spectra (17). The ability of triarylsulfonium salts bearing non-nucleophilic counterions to serve as photoinitiators is completely general and includes all the symmetrical, unsymmetrical, substituted and unsubstituted as well as polynuclear and heterocyclic salts shown in Table 1.

In contrast to radical photoinitiators which are also generally thermally unstable, triarylsulfonium salts display a surprising level of thermal stability. Figure 1 shows the thermogravimetric analysis curves for triphenylsulfonium hexafluoroarsenate performed in air and nitrogen at a heating rate of 10°C/minute. In both cases, thermal decomposition is not observed below 350°C. This high level of thermal stability is reflected in the extremely long shelf lifes of epoxy resins sensitized with triarylsulfonium salt photoinitiators. Figure 2 shows the plots of the increase in solution viscosity versus time in months for various concentrations of $(C_6H_5)_3S^+$ AsF_6^- in the highly reactive bisepoxide, 4-vinylcyclohexene dioxide. Only a slight increase in the overall solution viscosity was noted

Table 1

Preparation of Triarylsulfonium Salts

Cation	Anion	Mp (°C)	λ_{max} (ϵ)		Elemental Analysis		
					C	H	S
	BF_4^-	191-193	227(21,000) 298(10,000)	calc. fnd.	61.71 62.00	4.28 4.31	9.14 9.33
	AsF_6^-	195-197	227(21,000) 298(10,000)	calc. fnd.	47.63 47.78	3.31 3.41	7.06 7.06
	PF_6^-	133-136	237(20,400) 249(19,700)	calc. fnd.	56.90 57.05	4.96 5.03	6.90 7.09
	AsF_6^-	-	225(21,740) 280(10,100)	calc. fnd.	46.49 46.70	3.88 3.98	5.90 6.00
	BF_4^-	162-165	243(24,700) 278(4,900)	calc. fnd.	64.28 64.32	5.35 5.41	8.16 7.91
	AsF_6^-	111-112	275(42,100) 287(36,800) 307(24,000)	calc. fnd.	50.00 50.10	3.95 4.01	6.67 7.23

Table 1, continued:

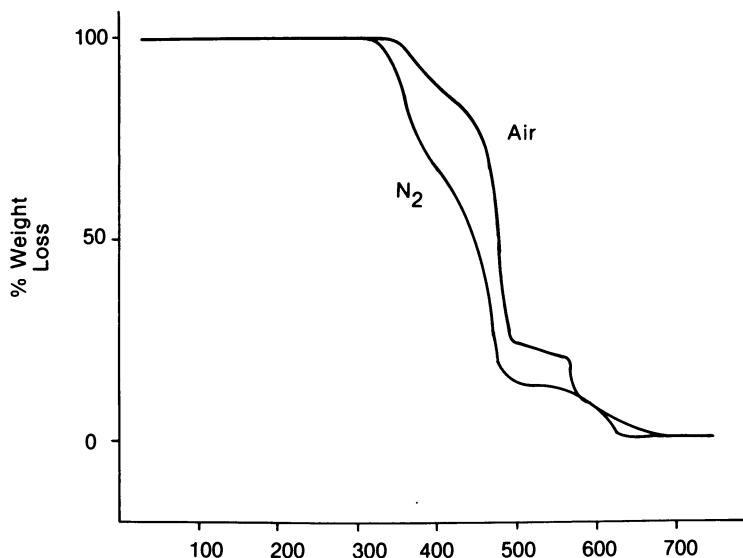| Cation	Anion	Mp(°C)	$\lambda_{max}(\epsilon)$	Elemental Analysis			
					C	H	S
	AsF_6^-	245-251	263(25,200) 280(22,400) 316(7,700)	calc. fnd.	49.39 49.39	4.62 4.59	5.48 5.55
	BF_4^-	168-169	277(25,000) 232(3,100)	calc. fnd.	62.99 62.81	4.14 4.10	8.84 8.96
	AsF_6^-	165-168	238(20,600) 292(5,200)	calc. fnd.	46.35 46.15	2.78 2.76	6.86 6.95
	AsF_6^-	183-187	238(22,600)	calc. fnd.	43.20 43.11	2.40 2.45	6.40 6.31

Figure 1.   Thermogravimetric analysis of $(C_6H_5)_3S^+ AsF_6^-$ in nitrogen and air at a programmed heating rate of $10°C/min$
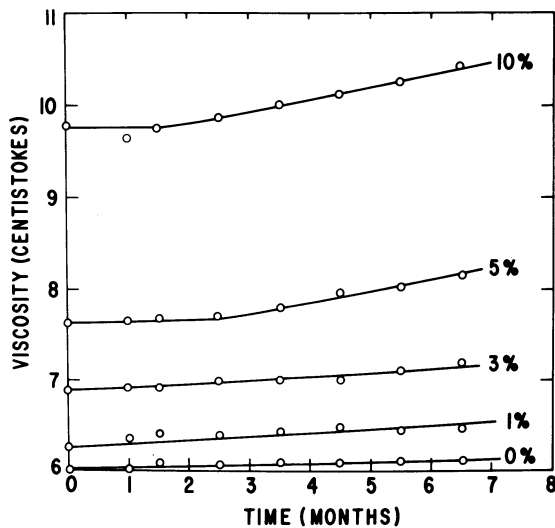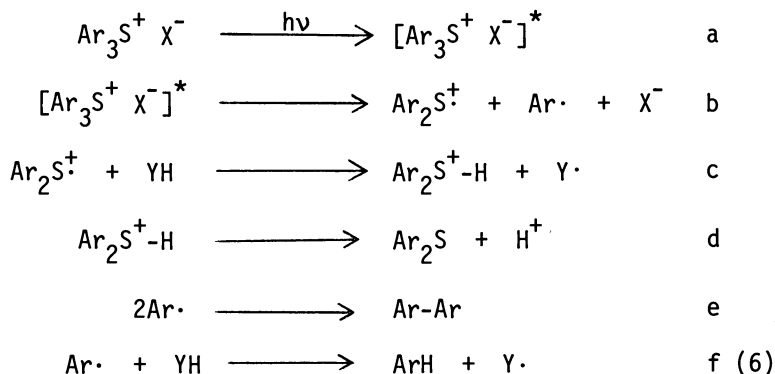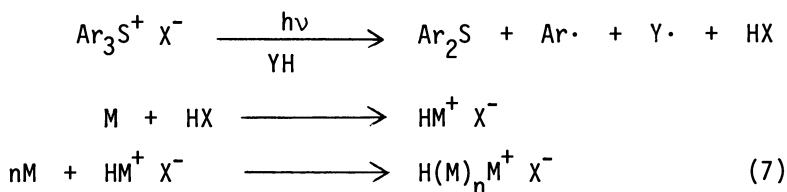

Figure 2.   Solution stability study with various concentrations of $(C_6H_5)_3S^+AsF_6^-$ in 4-vinylcyclohexene dioxide at $55°C$

after one year storage of these solutions in the dark at 55°C.

Although triarylsulfonium salts are highly thermally stable, they undergo rapid photolysis when irradiated at wavelengths from 200-300nm. Under these conditions, efficient ($\Phi_{313,360}$ = 0.17-0.19) homolytic rupture of one of the carbon sulfur bonds results. The following mechanism has been proposed for this photolysis (12).

$$Ar_3S^+ \ X^- \xrightarrow{\quad h\nu \quad} [Ar_3S^+ \ X^-]^* \qquad\qquad a$$

$$[Ar_3S^+ \ X^-]^* \longrightarrow Ar_2S^{+\cdot} + Ar\cdot + X^- \qquad b$$

$$Ar_2S^{+\cdot} + YH \longrightarrow Ar_2S^+\text{-}H + Y\cdot \qquad c$$

$$Ar_2S^+\text{-}H \longrightarrow Ar_2S + H^+ \qquad d$$

$$2Ar\cdot \longrightarrow Ar\text{-}Ar \qquad e$$

$$Ar\cdot + YH \longrightarrow ArH + Y\cdot \qquad f \ (6)$$

Interaction of the radical-cation, $Ar_2S^{+\cdot}$, with the solvent or monomer, YH, in step c results in the release of a proton in step d and the resultant formation of the strong acid, HX. Brønsted acids such as HBF_4, $HAsF_6$, and $HSbF_6$ are well known very reactive initiators for the ring opening polymerization of epoxides (18). Although it is improbable that acids such as those mentioned above exist in the anhydrous state, when they are generated by photolysis in solution, it is likely that immediate protonation of the monomer or the solvent occurs to produce species such as $HM^+ \ X^-$. Subsequent addition of monomer molecules results in propagation and chain growth. The overall process is shown in equation 7.

$$Ar_3S^+ \ X^- \xrightarrow[YH]{\quad h\nu \quad} Ar_2S + Ar\cdot + Y\cdot + HX$$

$$M + HX \longrightarrow HM^+ \ X^-$$

$$nM + HM^+ \ X^- \longrightarrow H(M)_n M^+ \ X^- \qquad (7)$$

Triarylsulfonium salt photoinitiators are capable of polymerizing almost all known types of mono and polyfunctional epoxide containing monomers. The reactivity of these systems depends on a number of factors. The reactivity and number of epoxide groups present play a major role in determining the overall rate and extent of photopolymerization. Monomers most active using diaryliodonium salt photoinitiators are those possessing no functionality other than the epoxide groups, i.e., epoxidized olefins (19). Introduction of functional groups such as ethers,

acetals or esters was found to appreciably attenuate the reactivity of these monomers toward strong protonic acid catalyzed polymerization. Analogous results were observed using triarylsulfonium salt photoinitiators.

While the photochemistry of triarylsulfonium salts is dominated by the structure of the triarylsulfonium cation which is the light absorbing species, the polymerization chemistry is dominated by the nature of the anion. The reason for this derives from the fact that the type of anion present determines what protonic acid is produced on photolysis. As we have already shown, this acid is the species responsible for the polymerization of the epoxide monomer. In Figure 3 is shown plots of the percent conversion to polymer versus time for the uv induced photopolymerization of cyclohexene oxide using 0.02 moles of triphenylsulfonium salts having different anions. Since it has been shown that the quantum efficiencies for photolysis of triphenylsulfonium salts are independent of their anions (12), the differences observed in the curves shown in Figure 3 are due to the relative reactivity of the acids in polymerization. The curve for the SbF_6^- salt was omitted from this figure since polymerization occurred at too fast a rate to be accurately measured. Triarylsulfonium salts may thus be ranked on the basis of their reactivity in the following order with respect to their anions: SbF_6^- > AsF_6^- > PF_6^- > BF_4^-. Similarly, Figure 4 compares the reactivity of these same salts in the photopolymerization of another monomer, styrene oxide. Even on a weight basis, the order of reactivity is the same as noted before although the molecular weight of the triarylsulfonium salt decreases in the order SbF_6^- > AsF_6^- > PF_6^- > BF_4^-.

The above model studies with monofunctional epoxy compounds give considerable insight into the reactivity of various triarylsulfonium salt photoinitiators. However, in terms of coatings, one is primarily interested in the reactivity of these photoinitiators in di- and multifunctional epoxy systems. Determination of the cure rates required to produce tack-free coatings is a generally accepted industry standard for the reactivity of uv cured coatings. In Table 2 are given the cure rates in ft/min which were determined for the cycloaliphatic bisepoxide, 3,4-epoxycyclohexylmethyl-3',4'-epoxycyclohexane carboxylate (ERL 4221) using 1 mole % of triphenylsulfonium BF_4^-, PF_6^-, AsF_6^- and SbF_6^- salts.

A more quantitative measure of the degree of cure as well as the cure rate in uv cure systems can be obtained with the aid of a specially designed differential scanning calorimeter. This device was developed at General Electric (20) and described by the present authors in previous publications (19,21). Figure 5 shows the type of data which can be obtained using this device. When the shutter is opened allowing uv light to strike the sample, immediate exothermic reaction ensues which is recorded as a peak by the strip chart recorder. The time interval from when the shutter is opened to the peak of the exothermic curve is one
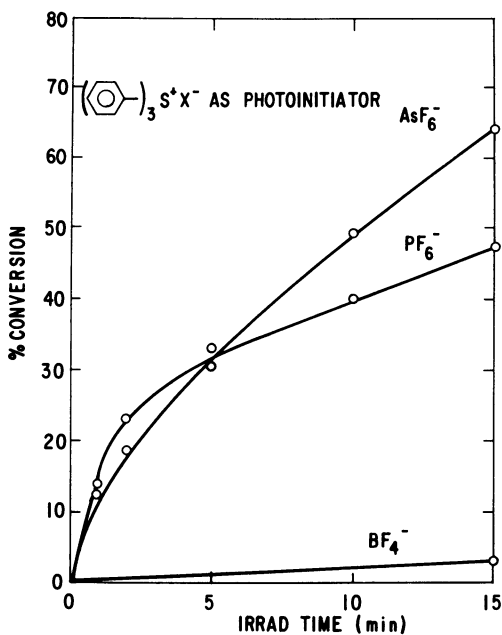
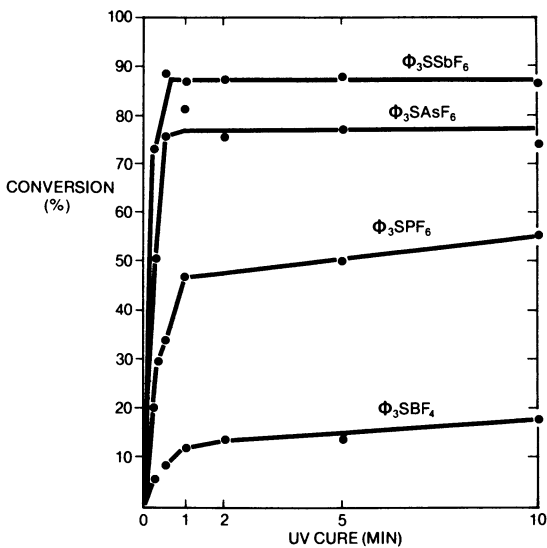Figure 3.   Photopolymerization of cyclohexene oxide using 0.02 mol $(C_6H_5)_3S^+ X^-$ salts

Figure 4.   Photopolymerization of styrene oxide using 10% $(C_6H_5)_3S^+ X^-$ salts

Table 2

UV Cure of ERL 4221 Using Various Triphenylsulfonium Salts

Photoinitiator	Cure Rate (ft/min)*
$(C_6H_5)_3S^+ BF_4^-$	195
$(C_6H_5)_3S^+ PF_6^-$	228
$(C_6H_5)_3S^+ AsF_6^-$	248
$(C_6H_5)_3S^+ SbF_6^-$	280

*1.0 mil films cured using three 200W/in. Hanovia Hg arc
lamps aligned parallel to direction of travel of the
conveyor.

measure of the reactivity of the polymerization system under
study: the shorter the time interval between these two points,
the more reactive the system. In addition, the heat of reaction,
ΔH, can be calculated from the area under the curve. The ΔH val-
ues are a quantitative measure of the extent of polymerization.
Comparing the various curves in Figure 5 leads to the conclusion
that the character of the anion present in the photoinitiator has
a marked effect on both the rate and extent of polymerization.
     Other important rate determining factors in the photoiniti-
ated polymerization of epoxies are the concentration of the
photoinitiator, the wavelength of the irradiating light and its
intensity and the temperature. The influence of these factors
can be conveniently determined using the modified differential
scanning calorimeter (DSC). Figure 6 shows a plot of the effect
of concentration of $(C_6H_5)_3S^+ AsF_6^-$ on the rate of cure of ERL
4221. The optimum cure rates are obtained at concentrations of
2-3% of this photoinitiator. Further increase in the photo-
initiator level does not produce a corresponding increase in the
cure rate,possibly due to light screening effects by the triaryl-
sulfonium salt itself or its photolysis products.
     A DSC study of the effect of light intensity on the cure
rate of ERL 4221 containing 2% by weight $(C_6H_5)_3S^+ AsF_6^-$ is dis-
played in Figure 7. In this figure, I_0 is the incident light
intensity delivered by a GE H3T7 medium pressure mercury arc
lamp ballasted at 200 Watts/inch of arc length and positioned at
20 cm from the samples. As the curve shows, the cure times
approach limiting values at both high and low light levels. At
high light intensities, the system is limited by the absorption
characteristics of photoinitiator, while at very low intensities,
there appears to be some type of threshold or inhibition effect.
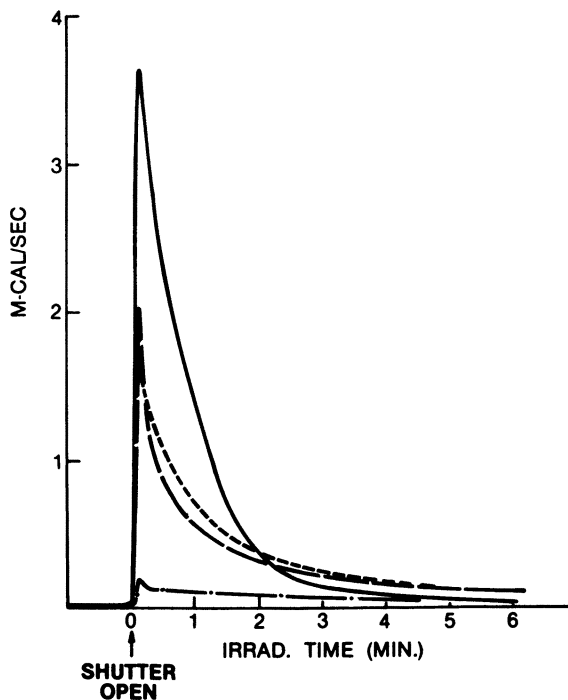
Figure 5.   Photopolymerization of ERL 4221 using 1.5 mol % $(C_6H_5)_3S^+$ X^- salts:
(——) $\phi_3S^+SbF_6^-$; (— —) $\phi_3S^+AsF_6^-$; (———) $\phi_3S^+PF_6^-$; (— · —) $\phi_3S^+BF_4^-$
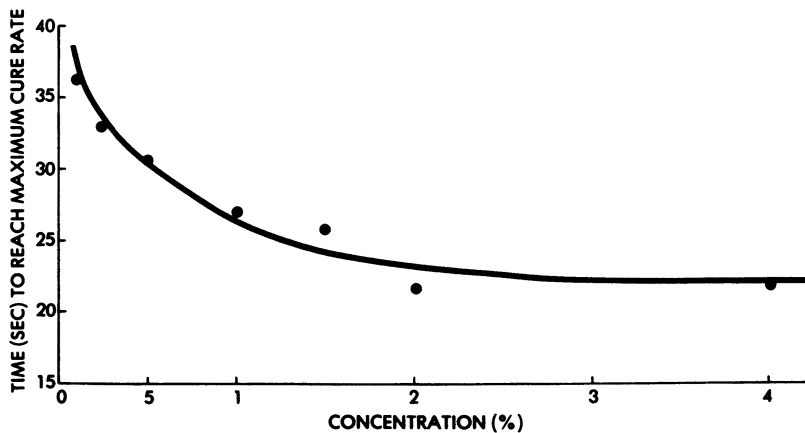
Figure 6.   Concentration dependency of the cure rate of ERL 4221 on %
$(C_6H_5)_3S^+$ AsF_6^-
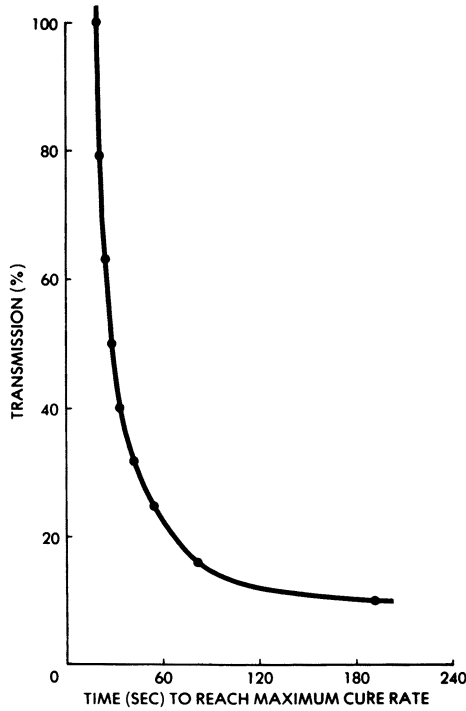
Figure 7.   Effect of light intensity on the cure rate of ERL 4221 with 2%
$(C_6H_5)_3S^+ AsF_6^-$
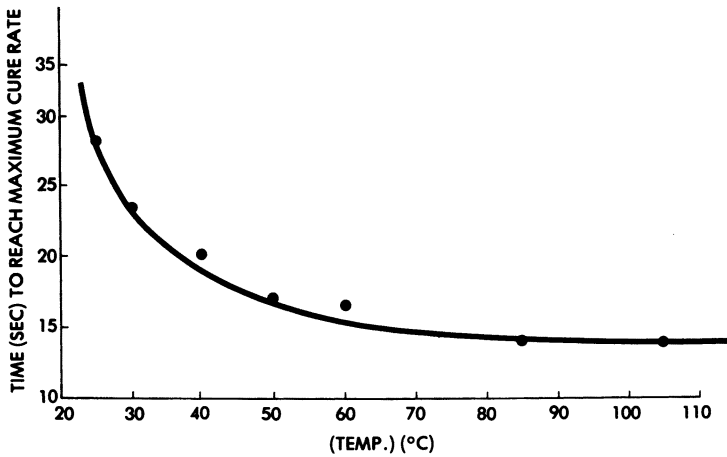
Figure 8.   Effect of temperature on the cure rate of ERL 4221 with 2%
$(C_6H_5)_3S^+ PF_6^-$

Figure 8 shows the effect of temperature in the polymerization of ERL 4221 using 2% $(C_6H_5)_3S^+$ PF_6^- as the photoinitiator. By increasing the temperature from 25°C to 85°C, the time required to reach the maximum cure rate has been decreased by one-half. In all photoinitiated cationic polymerizations employing either diaryliodonium or triarylsulfonium salt photoinitiators, cure at the highest temperature the substrate will allow will give the highest cure rates. Obviously, certain trade offs must be made between the cure temperature and loss of the monomer through volatilization.

Photoinitiated cationic polymerizations of epoxides are unaffected by the presence of atmospheric oxygen. There is, therefore, no need to blanket them with nitrogen. Water and other hydroxyl containing impurities can be tolerated in amounts of 1-2% in most epoxy monomers without seriously affecting their polymerizability. However, the presence of water does change considerably both the rate and extent of polymerization of epoxy monomers. Figure 9 shows the DSC curves for the photopolymerization of both dry ERL 4221 and the same epoxy resin containing 1-2% by weight water using $(C_6H_5)_3S^+$ SbF_6^- as the photoinitiator. The presence of a second peak in the DSC curve of the wet ERL 4221 indicates the presence of another competing chemical process taking place. Basic materials present in uv curable epoxy formulations as either impurities, additives or fillers can inhibit the polymerization and should generally be avoided. UV-opaque fillers can be tolerated to surprising levels. In Figure 10 is shown a plot of the heat of reaction, ΔH, on the level of TiO_2 (anatase) in a formulation containing ERL 4221. The higher the TiO_2 concentration present, the lower the extent of polymerization which takes place due to the screening effect of the pigment. Nevertheless, even at TiO_2 levels of 12%, hard, tack-free coatings can be obtained provided that the coatings are reasonably thin (<1 mil).

In summary, triarylsulfonium salts are a new class of very reactive photoinitiators for the ring opening polymerization of epoxy monomers. By manipulating the various parameters of initiator concentration, initiator type, temperature, and light intensity, one can exercise considerable control over the rate and extent of polymerization of these compounds. Further, the ready commercial availability of epoxy resins of different structural types gives the formulator considerable latitude in the design of uv cured coatings for a wide variety of specialized applications.

Experimental

<u>Materials</u>. Cyclohexene oxide and styrene oxide were dried over calcium hydride, then purified by fractional distillation. 3,4-Epoxycyclohexylmethyl-3',4'-epoxycyclohexane carboxylate (ERL 4221) was obtained from the Union Carbide Company and purified as described above. Triarylsulfonium salts used as photoinitiators
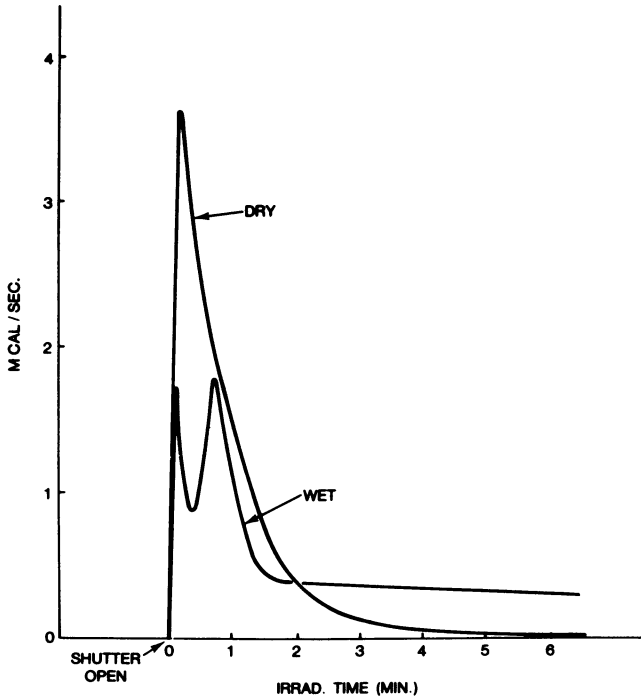
Figure 9.   Effect of water on the photoinitiated polymerization of ERL 4221 containing 1.5 mol % $(C_6H_5)_3S^+ SbF_6^-$
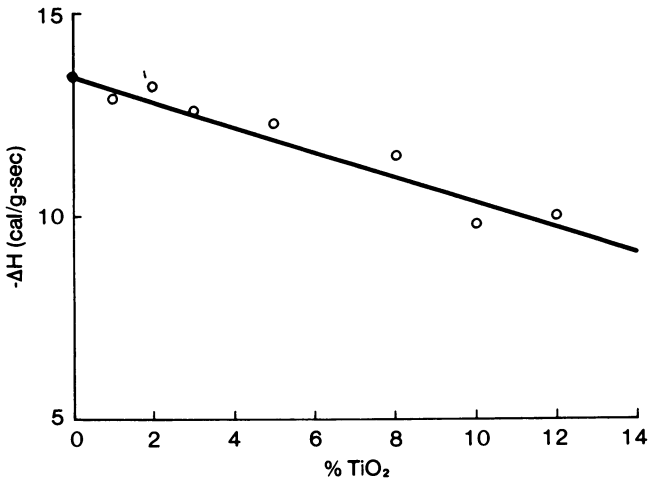
Figure 10.   Effect of TiO_2 on the polymerization of ERL 4221 with 2% $(C_6H_5)_3S^+ SbF_6^-$

in this work were prepared as previously described (12,13).

　　　Photopolymerizations. 5 ml Aliquots of a 0.02 mol/liter solution of the appropriate triphenylsulfonium salt photoinitiator in cyclohexene oxide were placed in sealed pyrex tubes. The tubes were then placed in a "merry-go-round" holder and irradiated using a Hanovia 450W medium pressure mercury arc lamp. The entire apparatus was immersed in a waterbath at 25°C. At appropriate times, the tubes were removed and poured into methanol containing a small amount of NH_4OH. The precipitated polymers were isolated by filtration followed by washing with methanol and drying in vacuo at 60°C overnight.

　　　Differential Scanning Calorimeter Studies. A Perkin Elmer DSC 2 differential scanning calorimeter modified with a GE H3T7 medium pressure mercury arc lamp and a filter system was used in these studies. The apparatus is similar to that described by previous workers from this laboratory (20). Approximately 10 mg samples of the monomer-catalyst solutions were placed in the usual aluminum cups. Except where noted, irradiations were carried out in an isothermal mode at 30°C.

Literature Cited

1. Chemical Economics Handbook, Stanford Research Institute, 1978, 1, 580.0632.

2. Licari, J. J.; Crepeau, W. and Crepeau, P. C., U.S. Patent 3,705,157, Sept. 7, 1965.

3. Schlessinger, S. I., U.S. Patents 3,708,296, Jan. 2, 1973; 3,826,650, July 30, 1974.

4. Watt, W. R., U.S. Patent 3,794,576, Feb. 26, 1974.

5. Feinberg, J. H., U.S. Patents 3,711,390, Jan. 16, 1973; 3,816,281, June 11, 1974; 3,817,845, June 18, 1974; 3,829,369, Aug. 13, 1974.

6. Ludwigsen, R. J., Soc. Mech. Eng., Technical Paper FC 74-533 (1974); J. Rad. Curing, 1975, 2 (1), 10.

7. Schlessinger, S.I., Photogr. Sci. and Eng., 1974, 18(4), 387.

8. Crivello, J. V. and Lam, J. H. W., J. Polym. Sci., Symposium No. 56, 1976, 1-11.

9. Crivello, J. V. and Lam, J. H. W., Macromolecules, 1977, 10(6), 1307.

10. Smith, G. H., Belg. Patent 828,841, Nov. 7, 1975.

11. Belg. Patent 837,782, June 22, 1976, to Imperial Chemical Industries.

12. Crivello, J. V. and Lam, J. H. W., J. Polym. Sci., in press.

13. Crivello, J. V., U.S. Patents 4,058,400 and 4,058,401, Nov. 15, 1977.

14. Belg. Patent 833,472, Mar. 16, 1976, to Imperial Chemical Industries.

15. Pitt, H. M., U.S. Patent 2,807,648, Sept. 24, 1957.

16. Wildi, D.S.; Taylor, S. W. and Potratz, H. A., J. Am. Chem. Soc., 1951, 73, 1965.

17. Crivello, J. V. and Lam, J. H. W., J. Org. Chem., 1978, 43 (15), 3055.

18. May, C. B. and Tanaka, Y., "Epoxy Resin Chemistry and Technology", Marcel Dekker, Inc., New York, 1975, 199-205; Billmeyer, F. W., Jr., "Textbook of Polymer Science", Interscience Pub., New York, 1964, 294.

19. Crivello, J. V.; Lam, J. H. W. and Volante, C. N., J. Rad. Curing, 1977, 4 (3), 2.

20. Moore, J. E.; Schroeter, S. H.; Shultz, A. R. and Stang, L. D., ACS Symposium Series No. 25, 1976, 9.

21. Crivello, J. V.; Lam, J. H. W. and Volante, C. N., Ctgs. and Plast. Preprints, 1977, 37 (2), 4.

Photosensitized Epoxides as a Basis for Light-Curable Coatings

WILLIAM R. WATT

Princeton Research Center, American Can Company, Princeton, NJ 08540

Coatings which harden or "cure" by photoinduced polymeriza-
tion offer a way to reduce air pollution and to conserve energy.
With such coatings, the change from liquid to solid is accom-
plished by an increase in molecular weight rather than by removal
of solvent.

Although there has been increasing interest in light-curable
coatings over the past decade, most published investigations deal
with coatings based on free-radical polymerization. Much less has
been written about light-curable coatings based on ionic polymeri-
zation; and what has been written is of relatively recent origin.
One of the earliest descriptions of this subject was a paper pre-
sented by the author in 1974 describing photosensitized epoxide
coatings which cure by cationic polymerization on exposure to
ultraviolet radiation (1). Since that time, several technical
papers concerned with coatings based on photoinduced cationic
polymerization have appeared (2-11).

Photoinitiators for Cationic Polymerization of Epoxides

The development of light-curable epoxide coatings depends on
the availablility of a suitable photoinitiator. Several compounds
are known (see Table I) which will initiate cationic polymeriza-
tion on exposure to light, but not all of these are suitable for
use in commercial coating operations. Some are costly, and their
use in coatings applications would be uneconomical. With others,
the rates of polymerization are too slow to be of interest in
high-speed coating operations. These photoinitiators have gener-
ally not been available as off-the-shelf items from chemical
suppliers. The necessity to synthesize them, together with the
fact that their use as photoinitiators is protected by patents,
has been a hindrance to their widespread use. From such informa-
tion as is available, it appears that among the compounds listed
in Table I, the onium salts show the greatest promise of meeting

Table I. Photoinitiators for Cross-Linking of Epoxides

Type	Reference
1) Unsaturated nitrosamines (activated by light and heat)	(54)
2) Diazonium Fluoroborates	(14)
3) Diazonium Perchlorates; Perfluorocarboxylates	(15)
4) Fluorinated alkane sulfonic acid salts of silver and thallium; or a metal salt of a polyboron acid and a silver halide or aromatic halide.	(55)
5) Cyclopentadienylmanganese tricarbonyl compounds	(56)
6) Bis(perfluoroalkylsulfonyl) methane silver salt	(57)
7) Diazonium salts other than tetrafluoroborates	(18)
8) Aryliodonium salts	(35) (36) (37)
9) Aryliodonium salts plus a cationic dye	(40)
10) Diazonium difluorophosphate, phosphotungstate, phosphomolybdate, tungstogermanate, silicotungstate and molybdosilicate	(58)
11) Group VIa Aromatic onium salts	(47)
12) Group Va Aromatic onium salts	(44)
13) Thiopyryllium salts	(9)

the requirements of commercial coatings. On photolysis, they will
initiate polymerization of some epoxides, and they have the capa-
city to promote the rapid cure required in high-speed coating
operations.

Three types of onium salts most often mentioned in the liter-
ature as photoinitiators for epoxide polymerization are diazonium
salts, aryliodonium salts and onium salts of the elements of
Groups Va and VIa. Representative examples of each type are shown
in Table II.

Diazonium Salts. The first use of a diazonium salt as an
initiator for cationic polymerization of cyclic ethers was re-
ported in 1965 by Dreyfuss and Dreyfuss (12), who announced the
polymerization of tetrahydrofuran initiated by thermal decompo-
sition of a "new catalyst" which they identified as benzene-
diazonium hexafluorophosphate. (In a later publication (13) this
material was correctly identified as ρ-chlorobenzenediazonium
hexafluorophosphate).

In the same year, a patent was issued to Licari and Crepeau
(14) for the photoinduced polymerization of epoxide resins by
diazonium tetrafluoroborates for use in the encapsulation of
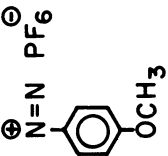electronic components and the preparation of circuit boards.
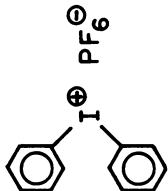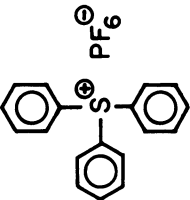
In 1966, E. Fischer was granted a U.S. patent (15) claiming
a method for polymerizing cyclic ethers by means of diazonium
salts of perchloric acid and perfluorocarboxylic acids decomposed
by heat and/or ultraviolet radiation. The storage stability of
mixtures of these salts with cyclic ethers was poor, and the
handling of diazonium perchlorates would require special consider-
ation before introduction into large-scale coating operations.

Dreyfuss and Dreyfuss (13) reported that ρ-chlorobenzene-
diazonium hexafluorophosphate was not a very effective initiator
for polymerization of epoxides, based on an observation that
thermal decomposition of the diazonium salt in the presence of
propylene oxide did not yield a high molecular weight polymer.

However, S. I. Schlesinger found that epoxides could be poly-
merized by a wide variety of diazonium salts, including ρ-chloro-
benzenediazonium hexafluorophosphate, on exposure to ultraviolet
radiation (16, 17). He delineated differences in behavior between
various salts and identified those which are most effective in
promoting rapid polymerization to high molecular weight. In par-
ticular, he showed that the hexafluorophosphates are much more
effective as photoinitiators than the tetrafluoroborates (18).

More than one mechanism has been proposed to explain the
catalytic activity of diazonium salts in initiating polymerization
of cyclic ethers. Dreyfuss and Dreyfuss (13) postulated that
initiation involves hydrogen abstraction from the cyclic ether by
a carbenium ion formed via decomposition of the diazonium salt,
followed by polymerization via tertiary oxonium ions associated
with PF_6^- counterions. The polymerization reactions studied by
Dreyfuss and Dreyfuss were initiated by thermal decomposition of

Table II. Representative Onium Salt Photoinitiators

STRUCTURE		
p-METHOXYBENZENEDIAZONIUM HEXAFLUOROPHOSPHATE PM	DIPHENYLIODONIUM HEXAFLUOROPHOSPHATE DPI	TRIPHENYLSULFONIUM HEXAFLUOROPHOSPHATE TPS
REFERENCES		
A) SCHLESINGER, S.I., US PATENT 3,708,206	A) CRIVELLO,J.V. & J.H.W. LAM, J.POLY.SCI., SYMPOSIUM #56, 383-395 (1976)	A) KNAPCZYK,J.W.,W.E.MC EWEN, JACS, 91, 145 (1969)
B) FEINBERG, J.H. US PATENT 3,829,369	B) CRIVELLO,J.V. & J.H.W.LAM, MACROMOLECULES, 10, #6, 1307-1315 (1977)	B) CRIVELLO, J.V. ET AL, J. RADIATION CURING 5 (1) JAN. 1978
C) WATT, W.R. US PATENT 3,794,576		

the salt rather than photolysis. Their mechanism would account
for a "dark reaction", explaining the limited storage stability of
some photosensitized epoxides in the absence of light.
    The Schieman reaction (19) was cited by Schlesinger (16) and
by Licari and Crepeau (14) as the probable mechanism by which
initiators for cationic polymerization are released by diazonium
salts. Rutherford et al (20) showed side reactions to be mini-
mized when the diazonium salt is a hexafluorophosphate.
    Although heat is generally used to promote decomposition of
diazonium salts by the Schieman reaction, the reaction has been
shown to occur also under the influence of ultraviolet radiation
(21, 22):

$$R\text{—}\bigcirc\text{—}\overset{\oplus}{N}=N \quad \overset{\ominus}{PF_6} \quad \xrightarrow{U.V.} \quad R\text{—}\bigcirc\text{—}F + N_2 + PF_5$$
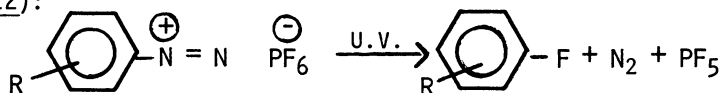
Phosphorous pentafluoride was shown by Muetterties (23, 24)
to initiate polymerization of cyclic ethers to high-molecular-
weight polymers.
    The release of a Lewis acid such as BF_3 or PF_5 in the pre-
sence of a material capable of undergoing cationic polymerization
would be expected to yield polymeric products, and the photo-
induced polymerization of epoxides can be explained according to
the mechanism for cationic polymerization proposed by Rose (25)
and others (26, 27, 28).
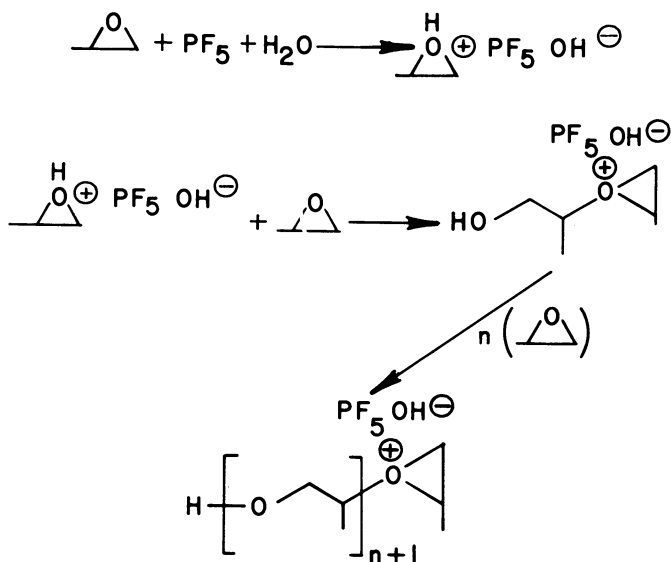
The length of time required for a coating to go from the liquid state in which it is laid down on the substrate to a solid nontacky state is dependent upon the concentration of photo-initiator. Coatings containing various amounts of ρ-methoxy-benzenediazonium hexafluorophosphate (PM) were applied at a thickness of 0.2-0.3 mil to aluminum, and the time to become tack-free following two seconds' exposure to a General Electric UA-3 mercury arc (60 watts per inch) was determined. Coatings containing 1.0 to 1.2 parts of PM per 100 parts of epoxide cured rapidly. Tack-free times of less than one second could not be measured accurately, and there appeared little advantage in using larger amounts of photoinitiator.. At lower concentrations of photoinitiator there was a drastic increase in the time required for the coating to become nontacky, particularly at concentrations below 0.6 parts of photoinitiator per 100 parts of epoxide.

Table III.   Effect of Photoinitiator Concentration on Rate of Cure

Amount of Photoinitiator[1] per 100 grams of ECC*		Tack-Free Time[2] (seconds)
Grams	Moles	
0.2	0.0007	60+
0.4	0.0014	60+
0.6	0.0021	4
1.0	0.0035	3
1.2	0.0043	1
1.4	0.0050	1

(1) ρ-Methoxybenzenediazonium hexafluorophosphate (PM)

(2) Time following two seconds' exposure to G.E. UA-3 mercury arc at a distance of 4.5 inches for 0.2-0.3 mil coating on aluminum to become tack free.

*   ECC = 3,4-Epoxy cyclohexylmethyl-3,4-epoxy cyclo-hexane carboxylate.

The amount of radiation required to decompose the PM photo-initiator in a coating 0.2-0.3 mil thick on aluminum was determined spectrophotometrically by changes in the ultraviolet absorbance following exposure to a mercury arc (29). By this method it was determined that more than 90% of the PM was photo-lyzed during two seconds' exposure to the UA-3 arc at a distance of 4.5 inches (see Figure 1). The radiation dose received by the sample under these conditions was 0.70 joule/cm^2.

In mixtures of epoxides and diazonium salts, there is generally a "dark reaction" which takes place even in the absence of ultraviolet radiation. Mixtures stored in the dark at average room temperatures will gradually become more viscous and eventually solidify. The rate at which this occurs is influenced by
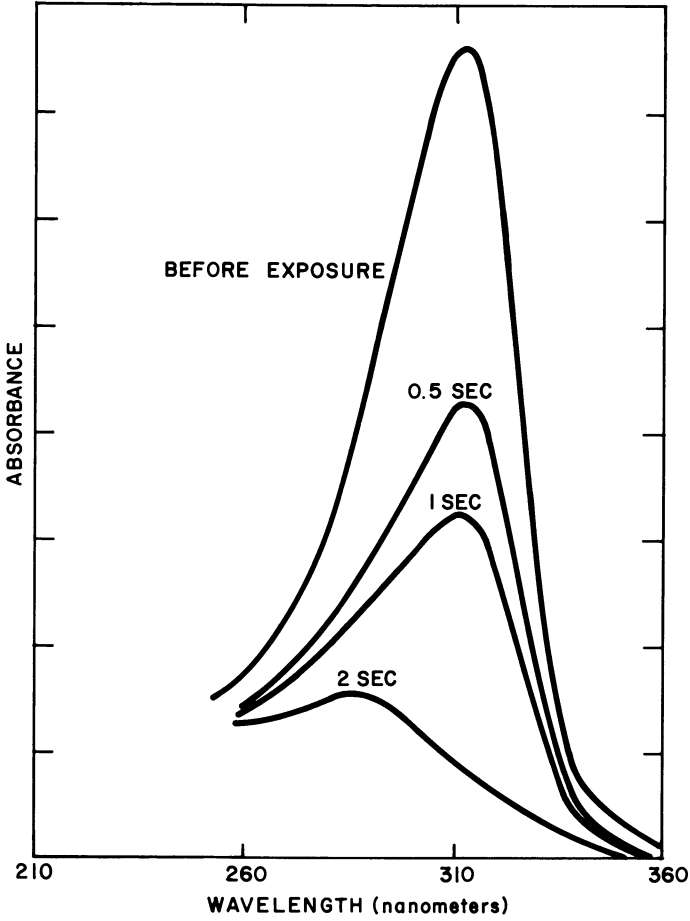
Figure 1.   Change in UV absorbance of a photosensitized coating on exposure to the mercury arc (Photosensitizer = PM)

several factors, including storage temperature and sample size. It is strongly dependent upon the epoxides which are present.

Some epoxides react very shortly after mixing with a diazonium salt. Epoxides such as allyl glycidyl ether, vinyl cyclohexene dioxide and butanediol diglycidyl ether react vigorously when mixed with ρ-chlorobenzenediazonium hexafluorophosphate, evolving heat and forming solid products. Diglycidyl ethers of bisphenol "A" (DGEBA) gel slowly over a period of several hours. Other epoxy resins show a very gradual increase in viscosity over a period of days or weeks (see Table IV).

Another factor influencing storage stability of photosensitized epoxides is the structure of the aromatic diazonium salt. The nature and position of substituents on the benzene ring of the diazonium salt significantly influences reactivity toward epoxides (see Table V).

Storage stability can be further improved by addition of "stabilizers" which inhibit the dark reaction without retarding rate of cure. Materials fitting the description of Lewis Bases or electron-donor compounds are generally effective in inhibiting the dark reaction. Many compounds of this type, however, tend to quench the cationic reaction completely, so that curing does not occur even on exposure to ultraviolet radiation.

There are some donor compounds which, while not completely preventing the dark reaction, will inhibit it and, at the same time, not interfere with the curing reaction. Cyclic amides (30), nitriles (31), substituted ureas (32) and sulfoxides (33) have been shown to promote storage stability of photosensitized epoxides without preventing rapid cure when exposed to ultraviolet radiation.

Figure 2 illustrates the effect of an added stabilizer (N-methylpyrrolidone) on storage stability of a mixture of epoxy resins.

Stabilization of photosensitive epoxides by electron donor compounds is probably due to formation of a complex with the Lewis acid which is slowly liberated by decomposition of the diazonium salt on storage (23, 34).

Diaryliodonium Salts. The use of diaryliodonium salts as photoinitiators for epoxide polymerization was first described in Belgian Patents issued in 1975 and 1976 (35, 36, 37). Diaryliodonium salts had been used earlier in photoinduced polymerization (38), but they were used for free-radical polymerizations.
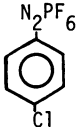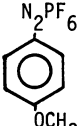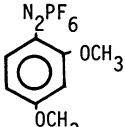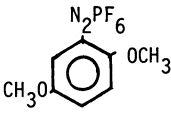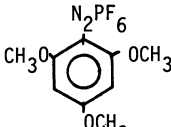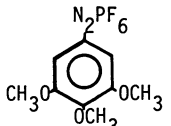
Diaryliodonium salts are not strong absorbers of light at wavelengths above 300 nanometers (4, 39). They do not make efficient use of the output of the high-pressure mercury arc and, as a result, cure initiated by diaryliodonium salts is apt to be slow and to require longer exposure than is the case with diazonium salts. Rates of cure can be increased by adding to the diaryliodonium salt a photosensitizer which absorbs longer wavelength radiation and permits curing under sources of visible

Table IV. Reactivity of Epoxides Toward Diazonium Salt

EPOXIDE	Epoxy Value	Result when mixed with p-chlorobenzenediazonium·PF_6
Vinyl cyclohexene dioxide	1.39	Vigorous exothermal reaction
Allyl glycidyl ether	0.87	"
Butanediol diglycidyl ether	0.75	"
3,4-Epoxy cyclohexylmethyl-3,4-epoxy cyclohexane carboxylate	0.74	Viscosity goes from 470 to 2600 cps in 5 days
DGEBA (Vis. @25°C 4000-6000 cps)	0.57	Gels in 20 hours
Epoxy phenol novolak (Vis. @52°C 1400-2000 cps)	0.56	---
Bis(3,4-Epoxy-6-methyl cyclohexyl methyl) adipate	0.47	928 to 1885 cps in 5 days
C_{12-14} alkyl glycidyl ether	0.35	8 to 30 cps in 5 days

Table V. Benzenediazonium Hexafluorophosphates Influence of Substituents

Photoinitiator	Melting Point ($^\circ C$)	Ultraviolet Absorption Maxima (nm)	Cure Time[1] (seconds)	Potlife[2] (hours)
N_2PF_6 — Cl (para)	162-164	273	1	Gelled within 24 hours
N_2PF_6 — OCH_3 (para)	149-151	313	1	28
N_2PF_6 — OCH_3, OCH_3	132	230 300 335	1	96
N_2PF_6 — OCH_3, CH_3O	116	232 305 400	1	Gelled within 24 hours
N_2PF_6 — CH_3O, OCH_3, OCH_3	188	302 343	1	300
N_2PF_6 — CH_3O, OCH_3, OCH_3	122 Exothermal	355	3	Gelled within 24 hours

[1] *Time for ECC containing one pph photoinitiator to become tack-free following two seconds' exposure to GE UA-3 mercury arc at 4.5 inches. Sample temperature = 30°C.*

[2] *Length of time in storage at 40°C for doubling of viscosity of formulation consisting of 55 parts DGEBA, 30 parts ECC, 15 parts C_{12-14} alkyl glycidyl ether and 1 part photoinitiator.*

Figure 2.   Effect of electron donor compound on storage stability of photosensi-tized epoxide mixture stored at 40°C (Photosensitizer = PM): (A) without N-methylpyrrolidone; (B) 0.005% N-methylpyrrolidone added; (C) 0.02% N-methyl-pyrrolidone added; (D) 0.06% N-methylpyrrolidone added

light (40).

The mechanism by which diaryliodonium salts initiate poly-
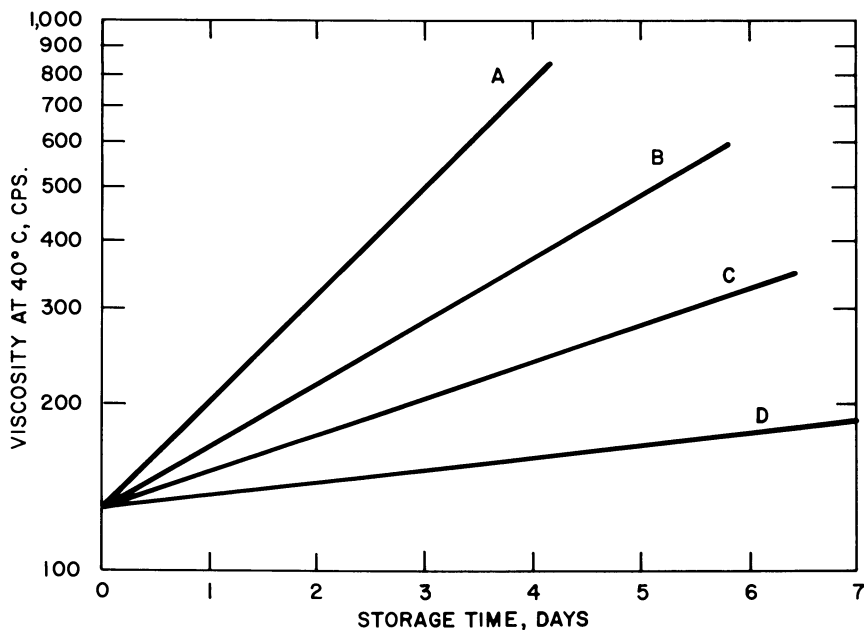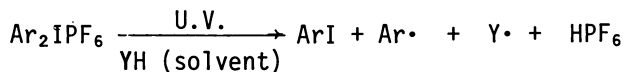merization of epoxides has been explained as involving acids
produced from photolysis of the diaryliodonium salt ($\underline{2}$, $\underline{3}$, $\underline{4}$):

$$Ar_2IPF_6 \xrightarrow[\text{YH (solvent)}]{\text{U.V.}} ArI + Ar\cdot + Y\cdot + HPF_6$$

This is followed by cationic polymerization of the epoxide initi-
ated by the proton from HPF_6.

The diaryliodonium metal halide complex salts are not
commercially available at this writing. Methods for their pre-
paration are reviewed in a paper by Crivello and Lam ($\underline{4}$).

Sulfonium Salts. Other onium salts beside the diazonium and
halonium salts will, on exposure to light, initiate polymerization
of epoxides and other monomers capable of undergoing cationic
polymerization. The use of onium salts of the elements of Groups
Va and VIa was first described in 1975 ($\underline{41}$, $\underline{42}$) and 1976 ($\underline{43}$).
More recently, U.S. patents have been granted covering the use of
onium salts of the elements of Groups Va ($\underline{44}$, $\underline{45}$) and VIa ($\underline{46}$,
$\underline{47}$) with epoxides and with other monomers which are known to
polymerize cationically.

There seems to be some confusion concerning the necessity to
add photosensitizers to increase spectral absorbance in order to
obtain rapid cure of epoxides containing triarylsulfonium salts.
The aromatic sulfonium complex salts are claimed to be photosen-
sitive only to the shorter wavelength radiation ($\underline{5}$, $\underline{39}$), and they
have been reported to be slightly less photoreactive than diaryl-
iodonium salts ($\underline{6}$). The limited spectral response has been cited
as a serious inherent limitation with respect to their use as
photoinitiators in photosensitive compositions ($\underline{48}$). It was
shown that a coating made up of 4 parts triphenylsulfonium hexa-
fluorophosphate (TPS) in 100 parts of an epoxy resin (DER 331)
failed to cure in 5 minutes' exposure to a G.E. H3T7 mercury arc;
but following addition of .02 parts of 2-ethyl-9,10-dimethoxy-
anthracene, curing occurred in fifteen seconds.

On the other hand, it has been reported that triarylsulfonium
salts are very reactive photoinitiators for the ring opening of
epoxy monomers ($\underline{7}$). It was also reported ($\underline{49}$) that a coating com-
posed of 4% by weight of triphenylsulfonium hexafluorophosphate in
3,4-epoxy cyclohexylmethyl-3,4-epoxy cyclohexane carboxylate cured
in 20 seconds' exposure.

It has been postulated ($\underline{6}$) that photolysis of Group Va and
VIa onium salts proceeds as shown below, and that the acid HPF_6
then initiates ring opening and polymerization of the epoxide.
This is similar to the mechanism proposed by Dreyfuss and Dreyfuss
($\underline{13}$). The nonnucleophilic counterion PF_6^- does not react with the
growing cationic species

$$AR_3SPF_6 \xrightarrow[YH]{U.V.} Ar_2S + ArH + Y\cdot + HPF_6$$
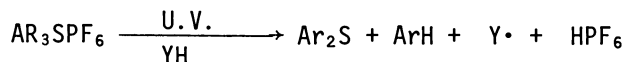
The arylsulfonium metal halide complex salts are not readily available. Triphenylsulfonium hexafluorophosphate can be pre-pared from diphenyliodonium hexafluorophosphate by heating with phenyl sulfide, as described by Knapczyk and McEwen (59), or by reaction of phenyl magnesium bromide with diphenylsulfoxide followed by reaction with hexafluorophosphoric acid according to the procedure of Wildi, Taylor and Potratz (60).

Comparison of Photoinitiators

Two properties of fundamental importance to the successful functioning of a photoinitiator for light-curable coatings are cure rate and storage stability of the photosensitized formu-lations. In high-speed coating operations, the interval between application of the coating and rolling up or stacking of the coated substrate is often no more than a few seconds. In this brief interval the coating must be converted from a free-flowing liquid to a nontacky solid.

While capable of rapid cure, the coating must be sufficiently stable that it does not undergo appreciable change in the period between addition of the photoinitiator and application to the object being coated. This interval may be a few hours (on-site mixing) or several months, as would be the case with coatings prepared at a central location and stored for extended periods prior to distribution and use.

Comparison of Rates of Cure. The rate at which coatings cure is generally based on personal judgment of the time required to become nontacky to the touch. The test is simple and widely used, but it is highly subjective.
We have developed an instrument which eliminates much of the subjectivity of the touch test. This instrument, which is illus-trated in Figure 3, consists of an oscillating stage which carries a coated metal coupon into an enclosure containing a shuttered mercury arc (G.E. UA-3, 60 watts per inch) in a parabolic reflec-tor. When the oscillating stage enters the enclosure, a shutter opens, exposing the coated coupon to the ultraviolet radiation from the mercury arc. At the end of a measured interval, the shutter closes, and the oscillating stage retracts.

The shutter operates on a timer, permitting variations in exposure time from one second to fifteen minutes.
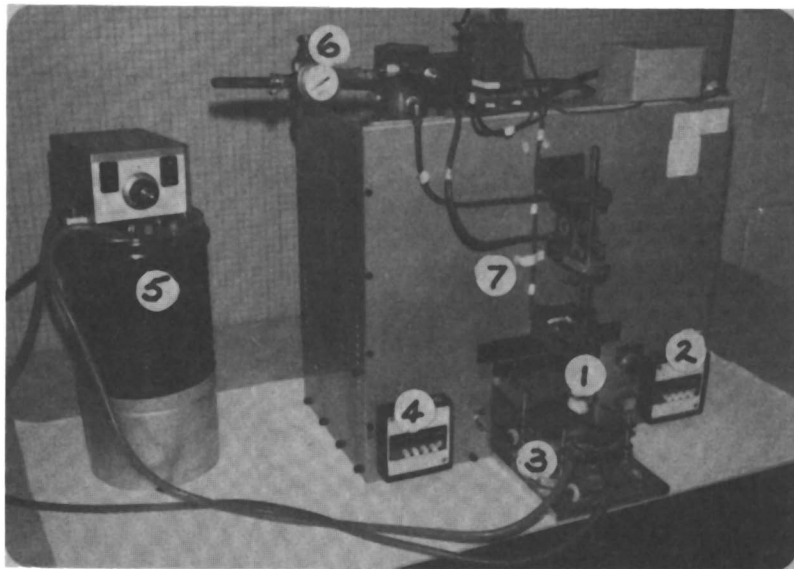
*Figure 3.   Device for measuring tack-free time: (1) probe (absorbent cotton);
(2) timer controlling interval between exposure and activation of probe; (3) oscil-
lating stage; (4) exposure timer; (5) constant temperature bath and circulator;
(6) air pressure regulator controlling pressure on probe; (7) General Electric UA-3
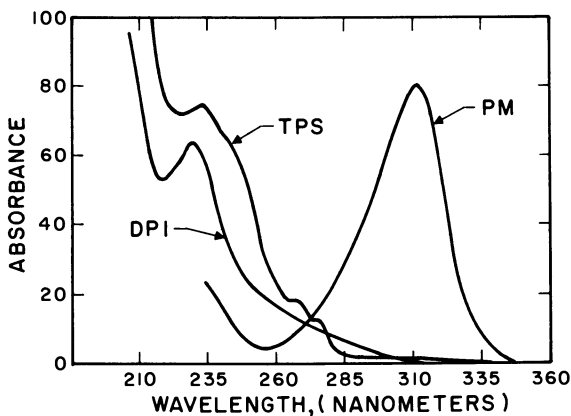mercury arc, reflector, and shutter (inside enclosure)*

Figure 4.   UV absorbance spectra of onium salt photoinitiators

When the shutter closes and the stage retracts, a second timer is activated which controls the interval between exposure and administration of the tack test. This interval can also be varied from one second to 15 minutes in increments of one second.

The tack test is administered by a small air-driven piston, to one end of which is attached a probe consisting of a ball of absorbent cotton. Pressure on the probe is controlled by air pressure driving the piston. A tacky coating is readily recognized by the tendency of cotton linters to adhere to it. The number of seconds following exposure for a coating to become hard enough that it does not pull cotton linters from the probe is defined as the "tack-free time".

An advantage of measuring independently both the exposure time and the interval between exposure and the disappearance of tack is that it allows a separation of the effects of ultraviolet radiation and the effects of heat.

The photoinduced curing of epoxides involves two steps:

1. Photodecomposition of the initiator
2. Polymerization of the epoxide

Ultraviolet radiation is required only for the first step. The second step, while independent of UV radiation, is influenced by heat. Continuous exposure to a mercury arc to determine tack-free time can influence the course of the polymerization because of an increase in temperature of coating and substrate caused by the intense heat of the mercury arc. To avoid this complication and to maintain control of the temperature of the coating during cure, exposure to the mercury arc was generally limited to two seconds. This proved adequate to give a tack-free condition within one second following exposure for the most reactive epoxides.

The PM and TPS photoinitiators generally gave shorter tack-free times than DPI; and at the lower concentration level, PM was somewhat more effective than TPS. This can be attributed to the more efficient use of the mercury arc radiation by the PM photoinitiator, which has an absorption peak at 313 nanometers (Figure 4), corresponding to a peak in the emission spectrum of the mercury arc. Absorption maxima for DPI and TPS are at the lower end of the spectrum, far removed from the peak output of the high pressure mercury arc.

An explanation of the differences in cure rate between DPI and TPS is less obvious, as the absorption spectra of these two compounds are similar. Depending on the method of preparation, however, the TPS photoinitiator frequently shows some absorbance in the spectral region between 290 and 340 nm, overlapping the band at 310 in the mercury lamp emission spectrum. This may be the result of a fortuitous contaminant not completely removed in synthesis and purification of the TPS photoinitiator.

Differences in catalytic activity of the three photoinitiators are most obvious when the coatings are exposed to a source of predominantly visible light, such as sunlight, or to a source of shortwave radiation, such as a germicidal lamp. Table VI shows the time required for 3,4-epoxycyclohexylmethyl-3,4-epoxy-cyclohexane carboxylate (ECC) photosensitized with the three photoinitiators to become tack-free when exposed to various sources of light.

Table VI.   Comparison of Photoinitiators

Effect of Radiation Source on Rate of Cure of
3,4-epoxycyclohexylmethyl-3,4-epoxycyclohexane carboxylate
Photosensitized with PM, DPI or TPS

Radiation Source, Exposure Time	TACK-FREE TIME, seconds		
	PM	DPI	TPS
UA-3 (60W/in), 2 seconds	2	60	5
" " 4 "	1	5	1
Sunlight (continuous exposure)	25-30	NC*	NC*
Germicidal lamp (continuous exposure)	75	35	15

Did not cure in 30 minutes continuous exposure

It can be seen that under the influence of sunlight, PM will initiate polymerization readily, while neither DPI nor TPS produces a cure. Under the germicidal lamp, which emits 254 nm radiation almost exclusively, the situation is reversed, with DPI and TPS which are strong absorbers of the shorter wavelength radiation, being somewhat more effective than PM.

Storage Stability of Photosensitized Epoxides. Storage stability of photosensitized formulations is dependent upon many factors, such as temperature, sample size, structure and concentration of the photoinitiator, exclusion of light and the presence of impurities. Tests were run under parallel conditions using a mixture of epoxides known to give a short potlife with the PM photoinitiator to compare storage stability of the same formulation photosensitized with DPI or TPS.
Storage stability was determined by periodic measurement of viscosity. Results are summarized in Table VII.

Table VII. Comparison of PM, DPI, and TPS: Potlife of
an Unstabilized Formulation @ 40°C

Photoinitiator	Time for Viscosity to Double
PM	< 12 hours
DPI	13 days
TPS	No change after 6 months

Characteristics of the Curing Process

Dreyfuss and Dreyfuss (13) showed that the cationic polymerization of cyclic ethers has the characteristics of a "living" polymerization, in that there appears to be a lack of termination except through reaction of the cationic growing chain end with impurities; and that eventually a steady state is attained where the living polymer is in equilibrium with its monomer.

In the photoinitiated cationic polymerization of epoxides, UV energy is required only to cause decomposition of the photosensitive salt releasing the materials which initiate polymerization. Once this has been done, the propagation of polymerization continues without further input of UV energy. Crosslinking continues long after exposure to ultraviolet radiation has been stopped. The practical consequence of this is that the coated substrate can be rolled up or stacked as soon as the surface becomes nontacky. Curing will continue in storage.

Evidence of this continuing reaction can be obtained spectrophotometrically. The infrared spectrum of a photosensitized coating on an aluminum substrate showed an absorption band at 910 cm^{-1}, as shown in Figure 5. Immediately after curing to a tack-free surface, the infrared absorbance at 910 cm^{-1} had diminished. After standing 20 hours longer in the absence of light, it had all but disappeared, indicating disappearance of nearly all unreacted epoxide groups.

Evidence of a continuing reaction was also obtained by S. I. Schlesinger (17) who noted an increase in the number of steps on a photographic step tablet proportional to the delay between exposure and development.

Changes in the solvent and abrasion resistance of cured coatings with age following exposure also gave evidence of a "living" polymerization. Resistance of coatings to methyl ethyl ketone immediately after exposure is generally poor, even though the coatings are nontacky. These same coatings an hour or more later exhibit excellent resistance to MEK.
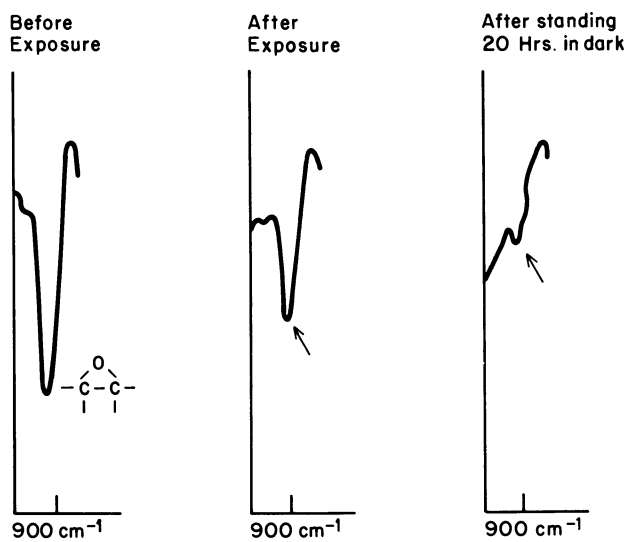
*Figure 5.   IR spectrum showing disappearance of epoxide band at 910 cm⁻¹ fol-
lowing exposure of photosensitized coating to mercury arc*

Effect of Epoxide Structure on Rate of Cure. The rate at
which photosensitized epoxides are converted from the liquid to
the solid state is influenced by the epoxide structure. Some
photosensitized epoxides remain liquid even after prolonged expo-
sure to the output of a mercury arc, while others solidify in
less than one second. Rates at which various epoxides become
tack-free are shown in Table VIII.

Epoxidized olefins show the highest rates of cure. In the
formulation of coatings, it is generally necessary to use a mix-
ture of epoxy resins in order to obtain the rheology needed for
application or to obtain the particular properties required by
the end use of the object being coated. Coatings to be cured at
ambient conditions generally require some aliphatic epoxide for
rapid cure (50). The data in Table IX illustrates the effect of
including a cycloaliphatic epoxide in coating formulations which
are to be cured under ambient conditions.

Epoxides which cure relatively slowly or not at all at
ordinary temperatures can be used as components of mixtures con-
taining 3,4-epoxycyclohexylmethyl-3,4-epoxycyclohexane carboxylate
(ECC), in which case the rate of cure is dependent upon the amount
of ECC in the mixture.

Mixtures of epoxides which are slow to cure at ordinary tem-
peratures will cure more rapidly at elevated temperatures (3).
The effects of temperature on rate of cure of mixtures of a cyclo-
aliphatic epoxide and a DGEBA resin are shown in Table X.
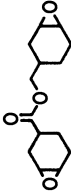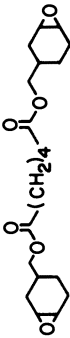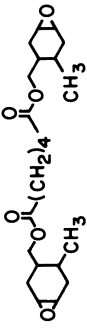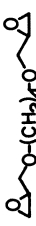
Effect of Humidity on Rate of Cure

Cationic polymerization is terminated by the presence of
contaminants, including water. In experiments to note the com-
bined effects of temperature and humidity on tack-free time,
temperature of the substrate was controlled by means of the
oscillating stage, as described above, and humidity was controlled
by conducting the experiments in an environmental chamber. Re-
sults are shown in Table XI.

At relative humidities of 65% or less the effect on tack-
free time ranged from negligible to slight with epoxides contain-
ing the PM or TPS photoinitiators. With DPI, results were
strongly dependent upon the epoxide. The 3:1 mixture of cyclo-
aliphatic diepoxide and DGEBA resin showed no change in tack-free
time when humidity was raised from 45% to 65%; but the tack-free
time of the 3:1 mixture of cycloaliphatic diepoxide and butane-
diol diglycidyl ether increased significantly.

High humidity (85%) caused a drastic increase in tack-free
time when the substrate was maintained at 35°C or less. When the
substrate temperature was raised to 45°C, the effect of high
humidity on tack-free time was overcome and rapid cure was ob-
served. Under commercial UV curing conditions (i.e., multiple
200 watt per inch lamps and no control of substrate temperature),
coatings would ordinarily reach or exceed 45°C on exposure to the
mercury arcs and this would tend to obscure the effects of high
humidity.

Table VIII. Tack-Free Time of Various Epoxides Photosensitized
with PM, DPI, or TPS

EPOXIDES	TACK-FREE TIME, SECONDS **					
	PM		DPI		TPS	
	0.005*	0.01*	0.005*	0.01*	0.005*	0.01*
(epoxide, —(CH₂)₄— diepoxide)	—	—	3	—	—	—
(cyclohexane diester epoxide)	—	—	15	2	—	—
(epoxide O–(CH₂)₄ ester)	6	4	60+	17	7	4
(epoxide O–(CH₂)₄ ester, CH₃ substituted)	60+	10	60+	60	60+	10
(diglycidyl O–(CH₂)₄–O)	60+	40	60+	60+	60+	60+
(bisphenol diglycidyl, EEW 175)	60+	30	60+	40	60+	60+
(bisphenol diglycidyl, EEW 189)	60+	30	60	35	60+	60+

* CONCENTRATION IN MOLES OF PHOTOINITIATOR PER GRAM EQUIVALENT WEIGHT OF EPOXIDE

** TIME TO BECOME TACK-FREE FOLLOWING TWO SECONDS EXPOSURE TO GENERAL ELECTRIC UA-3 (60 WATTS/INCH) MERCURY ARC AT 4.5 INCHES. TEMPERATURE OF SUBSTRATE 30°C.

Table IX.   Correlation of Viscosity, Epoxy Value, and Cure Time of Epoxide
Coating Showing Dependence of Rapid Cure on Cycloaliphatic Epoxide

EPOXIDE COATING COMPOSITION
Parts by Weight[1]

Resin 1	Resin 2	Resin 3	Resin 4	Vis @ 25°C (cps)	Epoxy Value	Cure Time[2] (seconds)
20	50	--	--	10	0.54	NC[3]
20	80	--	--	13	0.67	NC
20	--	80	--	100	0.64	4
--	80	--	20	31	0.69	NC
--	--	80	20	841	0.67	2
--	50	--	50	110	0.64	NC
--	--	50	50	2253	0.62	5
10	10	--	80	622	0.53	NC
10	--	10	80	1504	0.53	9
10	40	--	50	94	0.60	NC
10	--	40	50	618	0.59	5
10	70	--	20	28	0.66	NC
10	--	70	20	314	0.63	3
5	80	--	15	24	0.67	NC

[1]*Each composition contained 1 pph PM*

[2]*No. seconds continuous exposure to UA-3 Hg Arc @ 4.5 inches for coating to become tack-free*

[3]*NC = No cure after 60 seconds exposure*

*0.2–0.3 mil coating on aluminum

Resin 1 = C_{12-14} alkyl glycidyl ether

Resin 2 = Butanediol diglycidyl ether

Resin 3 = 3,4-epoxycyclohexylmethyl-3,4-epoxycyclohexane carboxylate

Resin 4 = DGEBA (vis.@25°C = 4000–6000 cps; EEW = 172–178)

Table X. Rate of Cure of DGEBA Resin
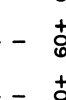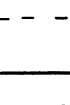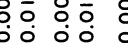
Relationship between amount of cycloaliphatic epoxide
    added and cure rate at various temperatures

ECC ADDED	Tack-free Time (seconds)				
(pph)	@23°	@30°	@40°	@50°	@60°
None	60+	60+	20	5	1
2	60+	60+	17	4	1
5	60+	60+	17	2	1
10	60+	55	13	1	1
15	60+	45	4	1	1
25	25	3	1	1	1
35	4	2	1	1	1

*0.2-0.3 mil coatings on aluminum exposed to G.E. UA-3 for
    4 secs. at 4.5 inches.*

Photoinitiator: PM (1.3 parts per 100 parts epoxide)

Table XI.   Comparison of Photoinitiators (PM, DPI, TPS)—Influence
of Temperature and Humidity on Tack-Free Time

EPOXIDE	PHOTOINITIATOR		TACK-FREE TIME, SECONDS[2]								
	TYPE	CONC.[1]	45%RH			65%RH			85%RH		
			25°	35°	45°	25°	35°	45°	25°	35°	45°
EPOXY EQ.WT.= 140 VIS. AT 25°C=550 CPS	PM	0.005	—	—	—	—	—	—	60+	2	—
		0.01	—	—	—	—	—	—	60+	—	—
	DPI	0.005	30	10	4	60+	60+	60+	60+	60+	60+
		0.01	2	—	—	35	2	—	60+	60+	—
	TPS	0.005	—	—	—	—	—	—	60+	2	—
		0.01	—	—	—	—	—	—	60+	—	—
3 PARTS (structure) +1 PART O(CH₂)₄O (structure) EPOXY EQ.WT.=138 VIS. AT 25°C=80 CPS	PM	0.005	2	—	—	5	—	—	60+	13	—
		0.01	—	—	—	4	—	—	60+	7	—
	DPI	0.005	20	14	9	60+	35	15	60+	60+	25
		0.01	18	6	2	60+	15	3	60+	60+	5
	TPS	0.005	4	2	—	13	3	—	60+	45	2
		0.01	—	—	—	5	—	—	60+	10	—
3 PARTS (structure) +1 PART (structure) EPOXY EQ.WT.= 149 VIS. AT 25°C=865 CPS	PM	0.005	—	—	—	—	—	—	60+	—	—
		0.01	—	—	—	—	—	—	60+	—	—
	DPI	0.005	—	—	—	—	—	—	60+	—	—
		0.01	—	—	—	—	—	—	60+	—	—
	TPS	0.005	—	—	—	—	—	—	60+	2	—
		0.01	—	—	—	—	—	—	60+	—	—

[1] MOLES PHOTOINITIATOR PER GRAM EQ. WT. OF EPOXIDE.
[2] TIME FOLLOWING EXPOSURE TO UV FOR COATING TO BECOME TACK-FREE (COTTONBALL TEST).

Maintaining the substrate at lower temperatures in a humid
atmosphere undoubtedly causes condensation of moisture on the
substrate and coating. Excess water will complex with the acidic
initiator promoting preferentially the hydrolysis of epoxy groups.
The net effect is to consume epoxy groups which do not contribute
to crosslinking (53).

Volatility of Photosensitized Epoxy Coatings

A principal motivating factor in the development of light-
curable coatings is the reduction in vaporization of materials
which would contribute to air pollution. It is therefore desir-
able to minimize the amount of low-molecular-weight material in
a coating formulation. However, viscosity limitations imposed by
the method of applying the coating to the substrate require the
inclusion of some low-molecular-weight material.

Low-viscosity epoxide monomers are available which have high
boiling points and low vapor pressures. However, the nature of
the curing process involves conditions conducive to evaporation.
The coating is applied in the form of a thin film with a very
large surface. It is subjected to radiation from a high-intensity
mercury arc which includes significant infrared radiation.
Further, the coated surface is generally moving at a high veloc-
ity, creating a strong flow of air over the surface.
The volatility of light-curable epoxy formulations was
determined by observing changes in weight at three stages:

- After coating but before exposure
- After exposure
- After baking at 110°C for 2 hours at 1 mm pressure

Coatings were applied at a thickness of approximately 0.3 mil
to weighed aluminum sheets. The total weight of coating was
between 50 and 60 milligrams. Sheets coated with uncured formu-
lations were allowed to stand on the platform of an analytical
balance for ten minutes at ambient conditions. This is consider-
ably longer than the normal interval between coating and exposure
in a standard coating operation, but it was desired to provide
exaggerated test conditions.
Coated plates were then exposed to the mercury arc until the
coating was tack-free. After being returned to equilibrium with
room temperature, the coated plates were weighed again. The
aluminum plates with cured coatings were then placed in a vacuum
oven and baked as described above.
The method is sensitive to changes of 0.1 milligram or 0.2%
of the original coating weight.
It was found that the wet coatings could stand for more than
ten minutes with no measurable change in weight, indicating no
significant evaporation would be likely to occur in the brief
interval between application of the coating and irradiation.

Surprisingly, following exposure to the mercury arc, the coatings do not lose weight, but actually increase in weight. This gain in weight on exposure to the mercury arc has been observed consistently over several hundred samples. It is a very real effect and can be rationalized on the basis of termination of the polymerization by water, probably absorbed from the humidity in the atmosphere.

Finally, the cured coatings were baked two hours at 110°C under vacuum (less than 1 mm Hg), to remove any residual volatiles in the cured coating. The results shown in Table XII indicate weight losses ranging from 0.28 to nearly 7%, depending on composition of the coating.

Preparation of ρ-Methoxybenzenediazonium Hexafluorophosphate

Sixty milliliters (0.30 mole) of 5M hydrochloric acid was added to 12.3 grams (0.10 mole) of ρ-anisidine, and the mixture was stirred with heating until all solids dissolved. The solution was diluted with 100 ml. of distilled water and cooled on an ice-salt bath. At about 0°C, crystals began to form.

Separately, a solution of 6.9 grams (0.10 mole) of sodium nitrite in 50 ml. of distilled water was prepared and cooled to 5°C.

The nitrite solution was added slowly to the stirred acid solution, dropping the nitrite directly into the acid, not along the walls of the container. Rate of addition was regulated so that the temperature of the reaction mixture did not exceed 8°C.

Stirring at 0°C was continued for 10-15 minutes, then 15 ml. of 65% aqueous hexafluorophosphoric acid was slowly added, keeping the temperature of the reaction mixture below 8°C. (Caution: HPF_6 attacks glass. All plastic containers and labware should be used for handling and transferring this acid.)

Stirring and cooling were continued for 10-15 minutes after all the HPF_6 had been added.

The precipitated product was recovered by filtration, washed with cold water until free of chlorine ($AgNO_3$ test) and air dried on the filter.

The crude product was recrystallized from methanol. Nineteen grams (68% yield) of a white crystalline product (m.p. 150-151°C) was obtained.

Table XII.   Changes in Weight of Light Curable Epoxide Coatings[1]
During Various Stages of Processing

PERCENT CHANGE IN WEIGHT

Coating Formula	On standing 10 mins @ 23°C	On exposure to mercury arc[2]	During bake[3]
A	Nil	+2.24	-0.28
B	Nil	+2.33	-6.88
C	Nil	+2.72	-2.40
D	Nil	+1.37	-1.21

[1]*Coating 0.2–0.3 mil thick on aluminum*
[2]*200 watts per inch*
[3]*2 hours at 110°C under vacuum (less than 1 mm Hg)*

Conclusions

The crosslinking of epoxides initiated by acidic products of photolysis is a promising concept for the development of non-polluting, energy-conserving coatings. It is possible to formulate compositions from readily available epoxy resins and monomers which can be applied by conventional coating machinery and which cure rapidly enough for high speed coating operations.

Onium salts have many of the characteristics required of photosensitive initiators for light-curable coatings. Aryldiazonium, aryliodonium and arylsulfonium salts all initiate rapid cure. Storage life of photosensitized formulations ranges from a few hours to more than six months, depending upon structure of the photoinitiator, composition of the coating and storage conditions.

The cationic process is not inhibited by oxygen. Curing can be initiated in air under natural sunlight or low-intensity mercury arcs whose useful lifetime is several times that of the high-intensity arcs used in free-radical curing processes.

Typical of cationic polymerization, the rate of cure is influenced by temperature and the presence of moisture. By a judicious choice of epoxides, it is possible to formulate coatings which cure rapidly under ambient conditions.

The combination of arylonium salts with selected epoxy resins provides the essentials for a viable system of light-curable coatings and should invite further investigation.

Literature Cited

1. Watt, W. R., "Light Curable Coatings from Photosensitized
    Epoxides", 14th Annual Coatings Symposium, North Dakota State
    University. (1974)

2. Crivello, J. V.;   Lam, J. H. W., J. Polymer Sci., 1976,
    Symposium No. 56, 383-395

3. Crivello, J. V.; Lam, J. H. W.; Volante, C. N. J. Radiation
    Curing, July 1977, 2-16

4. Crivello, J. V.; Lam, J. H. W. Macromolecules, 1977, 10, 6,
    1307-1315

5. Crivello, J. V. "UV Curing: Science and Technology", (S. P.
    Pappas, Ed.), Technology Marketing Corp., Stamford, Conn., 1978

6. Crivello, J. V.; Lam, J. H. W.; Moore, J. E.; Schroeter, S.H.
    J. Radiation Curing, 1978, 5, (1), 2-16

7. Crivello, J. V.; Lam, J. H. W.; Organic Coatings and Plastics
    Preprints, 1978, Am. Chem. Soc., 39, 31-35

8. Watt, W. R., Organic Coatings and Plastics Preprints, 1978
    Am. Chem. Soc., 39, 36-41

9. Ketley, A. D.; Tsao, J. H. Polymer Preprints, 1978, Am. Chem.
    Soc. 19 (2), 656-661

10. Ludwigsen, R. J., Radiation Curing, February 1975, 10-14

11. Tarwid, W. A.; Kester, D. E. Organic Coatings and Plastics
    Preprints, 1977, Am. Chem. Soc. 37, (2), 67-72

12. Dreyfuss, M.P.; Dreyfuss, P. Polymer, 1965, 6, 93

13. Dreyfuss, M.P.; Dreyfuss, P. J. Polymer Sci., 1966, A-1, 4
    2179-2200

14. Licari, J. J.; Crepeau, P. C. US 3,205,157 (North American
    Aviation, Inc.), September 7, 1965

15. Fischer, E. US 3,236,784 (Farbwerke Hoechst AG), February 22,
    1966

16. Schlesinger, S. I., Polymer Sci. and Eng. 1974, 14 (7),513-515

17. Schlesinger, S. I., Photographic Sci. and Eng. 1974, 18 (4),
    387-393

18. Schlesinger, S. I., US 3,708,296 (American Can Co.),
    January 2, 1973

19. Roe, A. Organic Reactions 1949, 5, 193

20. Rutherford, K. G.; Redmond, W.; Rigamonti, J. J. Organic
    Chem. 1961, 26, 5149-52

21. Lee, W. E.; Calvert, J. G.; Malmberg, E. W. JACS 1961, 83,
    1928-34

22. Lewis, E. S.; Halliday, R. E.; Hartung, L. D. JACS 1969, 91
    430

23. Muetterties, E. L. US 2,856,370 (E. I. DuPont de Nemours,Inc)
    Oct. 14, 1958

24. Muetterties, E. L.; Bither, T. A.; Farlow, M. W.; Coffman,
    D. D. J. Inorg. and Nucl. Chem. 1960, 16, 52-59

25. Rose, J. B. "Chemistry of Cationic Polymerization" (P. H.
    Plesch, Ed.), The MacMillan Co., 1963.

26. Flory, P. J. "Principles of Polymer Chemistry", Cornell
    Univ. Press, 1953, p. 219.

27. Billmeyer, F. W., Jr. "Textbook of Polymer Science", J.
    Wiley, 1962, p. 293.

28. Eastham, A. M. Encyclopedia of Polymer Sci. and Tech., 1965,
    3, 35

29. Pobiner, H. Analytica Chim. Acta, 1978, 96, 153-163

30. Watt, W. R. US 3,721,617 (American Can Co.) March 20, 1973

31. Watt, W. R. US 3,721,616 (American Can Co.) March 20, 1973

32. Feinberg, J. H. US 3,771,390 (American Can Co.) Jan. 16, 1973

33. Feinberg, J. H. US 3,771,391 (American Can Co.) Jan. 16, 1973

34. Laubengayer, A. W.; Sears, D. S. JACS 1945, 67, 164-166

35. Belgian Patent 828,669 (General Electric Co.) Sept. 1, 1975

36. Belgian Patent 828,841 (3 M Company) November 7, 1975

37. Belgian Patent 837,782 (Imperial Chemical Industries, Ltd)
    July 22, 1976

38. Smith, G. H. US 3,741,769 (3 M Company) June 26, 1973

39. Barton, R. W. US 4,090,936 (3 M Company) May 23, 1978

40. Crivello, J. V.; Schroeter, S. H. US 4,026,705 (General Electric Co.) May 31, 1977

41. Belgian Patent 828,668 (General Electric Co.) Sept. 1, 1975

42. Belgian Patent 828,670 (General Electric Co.) Sept. 1, 1975

43. Belgian Patent 833,472 (Imperial Chemical Industries, Ltd) March 16, 1976

44. Crivello, J. V. US 4,069,055 (General Electric Co.) January 17, 1978

45. Crivello, J. V. US 4,069,056 (General Electric Co.) January 17, 1978

46 Crivello, J. V. US 4,058,400 (General Electric Co.) November 15, 1978

47. Crivello, J. V. US 4,058,401 (General Electric Co.) November 15, 1978

48. Smith, G. H. US 4,069, 054 (3 M Company) January 17, 1978

49. Belgian Patent 833,472 (Imperial Chemical Industries, Ltd) March 16, 1976

50. Watt, W. R. US 3,936,557 (American Can Co.) February 3, 1976

51. Sims, I. D. J. Chem. Soc. 1964, 864-865

52. Dreyfuss, M. P.; Dreyfuss, P. Macromolecules 1968, 1, (5), 437-441

53. Lee, H.; Neville, K. "Handbook of Epoxy Resins", McGraw-Hill 1967, 11-2.

54. British Patent 912,022 (3 M Company), December 5, 1962

55. Cripps, H. N. US 3,347,676 (E. I. DuPont de Nemours, Inc.) October 17, 1967

56. Anderson, W. S. US 3,709,861 (Shell Oil Co.) Dec. 14, 1970

57. Kropp, J. E. US 3,586,616 (3 M Company) June 22, 1971

58. deMoira, P. P.; Murphy, J. P. US 3,930,858 (Ozalid Co.,Inc.),
     January 6, 1976

59. Knapczyk, J. W.; McEwen, W. E. JACS 1969, 91, 145-150

60. Wildi, D. S.; Taylor, S. W.; Potratz, H. A., JACS 1951, 73,
     1965-1967

Quaternary Phosphonium Compound Latent Accelerators for Anhydride-Cured Epoxy Resins

JAMES D. B. SMITH

Westinghouse Research and Development Center, Pittsburgh, PA 15235

Epoxy resins are used extensively in the electrical industry as insulation materials. In particular, they are used in conjunction with mica to insulate sophisticated rotating electrical equipment, such as turbine generators, A.C. motors, and traction motors. They also find widespread use in transformer and power circuit breaker insulation applications. It can be stated that, at the present time, epoxy resins would appear to be the material of choice for the abovementioned applications because of their overall superior properties compared to other thermoset polymeric resins such as polyesters, polyurethanes and acrylics. Among these superior properties exhibited by epoxy resins are higher bond strengths, higher mechanical properties, lower shrinkage, higher resistance to hydrolytic and chemical degradation, good electrical properties and ease of processing and fabrication.(1,2)

Many of the above cited applications utilize solventless epoxy resins containing "latent" catalysts which are designed to be unreactive at room temperature but will give rapid cure of resin with the application of heat.

A considerable amount of effort has been devoted in recent years, mainly in industrial laboratories, to develop improved "latent" catalysts for curing epoxy resins. This has been particularly the case in the manufacture of electrical equipment, such as motors, transformers and generators where epoxy resins are utilized in such diverse processes as casting, potting, encapsulation, and vacuum pressure impregnation (vpi). For reasons of economy and convenience, it is normal practice to store "one-package" epoxy resins (i.e., catalyzed resins) in large storage tanks (typically 2,000 to 10,000 gallons) in close proximity to the processing area. Thus, adequate catalyzed storage stability at ambient combined with efficient reactivity and cure at elevated temperatures are necessary prerequisites.

Properties Required of Latent Catalysts. The specific properties required by an ideal "latent" catalyst would be the following:

(a) It should give rapid cure of epoxy resins at moderately
elevated temperatures (i.e., 120°-180°C).

(b) It should be completely miscible with the resins at all
temperatures. This is particularly true of impregnating resins.

(c) The storage life of the catalyzed resin should be
indefinite. In practice, the viscosity of the resin should not
change appreciably at room temperature over periods ranging from
several months to years.

(d) It should not adversely affect the properties of the
cured resin (e.g., tensile and electrical properties).

The need for fast gel times in this application is because of
the tendency for the impregnating resin to drain out during cure,
thereby leaving voids in the insulation. In practice, it has been
found that, to avoid excessive void formation, the gel times of
the impregnating resins should be less than 30 min at the cure
temperature.

Experience in the electrical industry has also shown that
thorough impregnation of the "groundwall" insulation materials
(e.g., mica flake paper) becomes difficult if the viscosity of the
resin increases above 1,000 cps (as measured at 25°C). The
impregnation process, however, with more viscous resins, can be
made more effective by using higher pressures and elevated temper-
atures, but this is not always desirable or possible in production.

Previous Work on Latent Catalysts for Epoxy Resins. Numerous
patents (3,4,5) have been issued in recent years on the develop-
ment of latent catalysts for DGEBA (i.e., diglycidylether of bis-
phenol 'A') resins, but most fulfill only a few of the conditions
outlined above. One of the most successful of these has been the
boron trifluoride–monoethylamine complex (6). However, one of the
serious disadvantages of this particular latent catalyst is the
poor electrical properties at elevated temperatures of the epoxy
resin in the cured state (7).

To improve high temperature stability over amine cured systems
and to give better physical and electrical properties above their
heat distortion temperatures, it has been general practice in
epoxy resin systems to use anhydride curing agents with DGEBA
epoxy resins (8). Most anhydride formulations require elevated-
temperature cures with the ultimate properties dependent on post-
cures at temperatures of 150°C or higher.

For most commercial applications, it is necessary to add some
form of accelerator to the formulation to speed the rate of cure.
Both acidic and basic accelerators can be used. Consequently,
several latent accelerators have appeared on the commercial scene
in recent years. Included among these are quaternary ammonium
halides such as benzyltrimethylammonium chloride (9), stannous
octoate (5), zinc stearate (10), 'extra-coordinate' siliconate
salts (11), triethanolamine borate (12), triethanolamine titanate
(13), and various other metal chelates (14). However, all of
these materials have been rejected for one reason or another and

the quest for improved latent accelerators for anhydride cured
epoxy resins has continued.

Quaternary Phosphonium Compounds. Recent work (15,16) at our
laboratories has revealed a new family of latent accelerators.
This new family of compounds is derived from the salts of tertiary
organo-phosphines and aryl or alkyl halides which have the general
structural formula:

$$R_2 \; — \; \overset{\displaystyle R_1}{\underset{\displaystyle R_3}{\overset{|}{\underset{|}{P^+}}}} \; — \; R_4 \qquad X^-$$
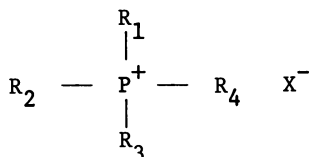
where R_1, R_2, R_3 and R_4 are alkyl or aryl groups and X^- is
halogen, acetate, or dimethylphosphate anion.
    Most of the data reported here will be concerned with bis-
phenol 'A' epoxy resin systems cured with the liquid anhydride,
1-methyltetrahydrophthalic anhydride (the Union Carbide commercial
designation for this material is ZZLA-0334). However, these
quaternary phosphonium compounds have also been shown to be
effective with other anhydrides such as hexahydrophthalic anhy-
dride (HHPA).

Experimental

    Different Quaternary Phosphonium Compounds Evaluated. Seven
different quaternary phosphonium salts were evaluated in this
work:
     i) Methyltrioctylphosphonium dimethylphosphate (MTOP-DMP),
    ii) Tetrabutylphosphonium acetate (TBPA),
   iii) Methyltributylphosphonium dimethylphosphate (MTBP-DMP),
    iv) Benzyltriphenylphosphonium chloride (BTPPC),
     v) Tetrabutylphosphonium chloride (TBPC),
    vi) Methyltriphenylphosphonium dimethylphosphate (MTPP-DMP),
   vii) Triphenylethylphosphonium iodide (TPEPI).
    With the exception of TPEPI, supplied by Arapahoe Chemical
Company, Boulder, CO, all of the phosphonium compounds were
supplied by Cincinnati Milacron, Reading, OH. The chemical
structures of the various quaternary phosphonium compounds are
shown in Table I.
    Most of the evaluation studies were made using a 1:1
stoichiometric bisphenol 'A' epoxy-anhydride formulation. The
various quaternary phosphonium compounds were added at a 0.01 to
0.25% level (based on the combined anhydride and epoxy resin
weights). With the exception of MTPP-DMP, which showed partial
insolubility in the resin formulation, excellent solubilities at
ambient temperature were found.

Table I.   The Structures of the Various
Quaternary Phosphonium Compounds

Phosphonium Compound	R_1	R_2	R_3	R_4	X
MTOP-DMP	CH_3	C_8H_{17}	C_8H_{17}	C_8H_{17}	$^-O\overset{O}{\overset{\|}{P}}(OCH_3)_2$
TBPA	C_4H_9	C_4H_9	C_4H_9	C_4H_9	$^-O\overset{O}{\overset{\|}{C}}CH_3 : CH_3\ COOH$
MTBP-DMP	CH_3	C_4H_9	C_4H_9	C_4H_9	$^-O\overset{O}{\overset{\|}{P}}(OCH_3)_2$
BTPPC	$C_6H_5CH_2$	C_6H_5	C_6H_5	C_6H_5	^-Cl
TBPC	C_4H_9	C_4H_9	C_4H_9	C_4H_9	^-Cl
MTPP-DMP	CH_3	C_6H_5	C_6H_5	C_6H_5	$^-O\overset{O}{\overset{\|}{P}}(OCH_3)_2$
TPEPI	C_2H_5	C_6H_5	C_6H_5	C_6H_5	^-I

Gel Time Data.   Initially, gel times were recorded on 10 g
samples of resin in 2 in. diameter aluminum dishes over the
temperature range 135°C to 170°C.   Later, to give improved
accuracy, the gel time measurements were made in 19 x 150 mm test
tubes in a constant temperature silicone oil bath using a Sunshine
Gel Meter.

Storage Stability Data.   Storage stability characteristics of
the formulations were followed at room temperature (i.e., 25°C)
using a Gardner-Holdt bubble viscometer (ASTM #D154-56).   Termi-
nation of a sample's catalyzed lifetime (i.e., storage life) was
taken to be when the viscosity reached a value of 1,000 cps at
25°C.

Electrical Data.   The electrical properties of cured speci-
mens of the epoxy resin, containing various quaternary phosphonium
compounds, were obtained on 2 in. diameter discs (0.125 in. to
0.25 in. thick) using standard procedures (ASTM #D150-65T).   In
these tests, the power factor (100 x tan δ) and dielectric con-
stant (ε') data were usually measured at 150°C (and a frequency of
60 Hz) on resin samples which had been cured for 16 h at 135°C
+ 5 h at 150°C.

Results

The data shown in Tables II and III indicate the effective-
ness of two of the phosphonium compounds as accelerators for
epoxy-anhydride resins.   From the data in Table II, it is noted

Table II. Gel Time Data for Quaternary
Phosphonium Latent Accelerators
in Epoxy-Anhydride Resins

Latent Accelerator	Concentration (% w/w) in Epoxy-Anhydride Resin	Gel Time Data (min)		
		135°C	150°C	170°C
Methyltrioctylphosphonium dimethylphosphate (MTOP-DMP)	0.02	--	90	35
	0.04	115	55	25
	0.06	75	45	15
	0.10	50	15	10
Tetrabutylphosphonium acetate (TBPA)	0.02	120	65	30
	0.04	75	40	15
	0.06	60	30	10
	0.08	50	25	--
Methyltributylphosphonium dimethylphosphate (MTBP-DMP)	0.02	--	85	35
	0.04	110	50	25
	0.06	75	40	13
Benzyltriphenylphosphonium chloride (BTPPC)	0.02	--	60	--
	0.10	--	15	--
Tetrabutylphosphonium chloride (TBPC)	0.02	--	60	--
	0.10	--	15	--
Methyltriphenylphosphonium dimethylphosphate (MTPP-DMP)	0.02	--	--	90
Triphenylethylphosphonium iodide (TPEPI)	0.02	125	65	30
None	--	>1000	>600	>450

Table III. Viscosity (Storage) Data for Quaternary
            Phosphonium Latent Accelerators in
            Epoxy-Anhydride Resins

Latent Accelerator	Concentration (% w/w) in Epoxy-Anhydride Resin	Storage Stability Time (Days at 25°C) for Resin Viscosity to Reach	
		500 cps	1000 cps
Methyltrioctylphosphonium dimethylphosphate (MTOP-DMP)	0.02	90	130
	0.04	60	85
	0.06	33	56
	0.10	25	45
Tetrabutylphosphonium acetate (TBPA)	0.02	70	112
	0.04	45	80
	0.06	30	42
	0.10	15	21
Methyltributylphosphonium dimethylphosphate (MTBP-DMP)	0.01	120	160
	0.02	70	115
	0.04	50	85
Benzyltriphenylphosphonium chloride (BTPPC)	0.02	60	90
	0.10	20	28
Tetrabutylphosphonium chloride (TBPC)	0.02	65	90
	0.10	18	30
Methyltriphenylphosphonium dimethylphosphate (MTPP-DMP)	0.02	115	150
Triphenylethylphosphonium iodide (TPEPI)	0.02	60	85
None	--	150	300

that fast gel times (i.e., < 60 minutes) can be obtained with
small amounts of accelerator (e.g., 0.06%), particularly at
temperatures above 150°C. In the absence of accelerator, the
epoxy-anhydride resin showed very sluggish curing properties, the
gel time at 150°C being in excess of 10 hours.

Appreciable latency is shown by these phosphonium compounds
as demonstrated by the storage data shown in Table III. Using
1,000 cps (at 25°C) as being the limiting viscosity, "storage
lifetime" values can be assigned to each of the phosphonium com-
pounds as indicated in Table III. It would appear that the non-
halide phosphonium compounds (e.g., MTOP-DMP and MTBP-DMP) exhibit
higher latency than those containing halides. These differences
may be linked to the presence of impurities or hydrolyzed by-
products in the halide compounds. In this respect, it was noted
that two of the materials investigated (i.e., BTPPC and TBPC) had
pungent odors, suggesting the presence of free organo-phosphine;
presumably resulting from sample degradation or hydrolysis. The
three phosphonium compounds showing the best compromise between
storage lifetime and catalytic effectiveness were MTOP-DMP, MTBP-
DMP and TBPA.

The electrical properties of the cured resins, containing
various quaternary phosphonium additives are shown in Table IV.
The data indicate that the lowest power factor (100 x tan δ) and
dielectric constant (ε') values, as measured at 150°C, are shown
by the samples containing MTOP-DMP and MTBP-DMP. There would
appear to be a trend in these electrical data in that the samples
containing halide anionic species (e.g., chloride and iodide)
apparently exhibit higher power factor and dielectric constant
values than the non-halide phosphonium additives. This is not too
surprising because of the more polar nature of the halide ions
compared to anions such as dimethylphosphate.

In the highest voltage electrical applications (i.e., >15 kV)
in which these epoxy resins would be used, the insulation require-
ments are such that a power factor value of <15% and a dielectric
constant of <6.0 (as measured at 150°C) are desirable. This
would then imply that epoxy resins containing MTOP-DMP and MTBP-
DMP would be acceptable for this application, whereas TBPA would
be marginal and TBPC and TPEPI would be unsuitable.

Discussion

Comparison with Other Latent Accelerators. To illustrate the
effectiveness of these quaternary phosphonium salts as acceler-
ators for anhydride cured epoxy resins, a comparison of MTOP-DMP
and TBPA with other well-known accelerators is given in Table V.
The data were obtained from work done in this laboratory using the
same resin systems. To make the comparison valid, the concentra-
tion given for each of these materials has been converted from
"phr" to "moles/200 g resin". Thus, the comparison is made on a
molecular concentration basis instead of weight. Gel times were

Table IV. Electrical Properties of Cured Epoxy-Anhydride
           Resins Containing Various Quaternary
           Phosphonium Compounds*

Quaternary Phosphonium Compound*	Electrical Properties** at 150°C, 60 Hz	
	% Power Factor (100 x tan δ)	Dielectric Constant (ε')
Methyltrioctylphosphonium dimethylphosphate	8.8	4.1
Methyltributylphosphonium dimethylphosphate	8.3	5.9
Tetrabutylphosphonium acetate	17.0	4.7
Tetrabutylphosphonium chloride	29.6	6.2
Triphenylethylphosphonium iodide	39.4	6.4

*Phosphonium compound added at ∿ 0.05% (w/w) on resin.
**Resin samples cured 16 h at 135°C + 5 h at 150°C.

Table V. Relative Reactivities of Different
          Accelerators in Epoxy-Anhydride Resins

Accelerator	Relative Reactivity (R) (R x 10^{-4} min moles)
MTOP-DMP	187.3
TBPA	190.1
Benzyltriethylammonium iodide	216.0
1-Methylimidazole	350.0
2-Methylimidazole	259.0
Zinc stearate	3165.0
Zinc oleate	1592.0
N,N-diethylethanolamine	213.5

(R) = Gel time$_{135°C}$ x accelerator concentration (moles/200 g).

recorded at 135°C as shown in Table II, and the measure of
relative reactivity (R) of each of the accelerators is given by
the expression

(R) = [Time to reach gel point, minutes] x [Molar concentration
        of accelerator, (moles/200 g resin)]

Examination of the above equation shows that the more reactive
the accelerator, the lower the product (R) will be. Data have
thus been calculated at 135°C for these accelerators as shown in
Table V.
    Comparison of these data (Table V) show, quite clearly, how
much more reactive the phosphonium salts are in the resin system
than compounds such as substituted imidazoles and organo-zinc
salts (e.g., zinc stearate and octoate). The only accelerator
that shows substantially more potency than the quaternary phos-
phonium salts is uranyl nitrate. However, this compound is not a
latent accelerator in the sense that storage lifetimes are only
of the order of a few days.

    The Initiation Mechanism with Phosphonium Compounds. Although
further experimental data are needed to give a fuller under-
standing of the reaction mechanisms involved in the latent accel-
eration effect of these quaternary phosphonium compounds in epoxy-
anhydride resins, there is definite indication, at this stage,
that the mechanism does not involve the decomposition of the
phosphonium compound to the free phosphine species (16). The
initiation mechanism probably involves the formation of hydrogen-
bonded phosphonium-epoxy or phosphonium-anhydride complexes which
rearrange on the application of heat to form activated species
resulting in polymerization of the epoxy-anhydride components
(17).

    Quaternary Arsonium and Stibonium Compounds. More recently,
experimental work in this laboratory has revealed that quaternary
arsonium compounds (18) are extremely effective as latent accel-
erators for epoxy-anhydride resins. Surprisingly, it has also
been found that quaternary stibonium compounds are very much less
effective as accelerators than quaternary arsonium, phosphonium
or ammonium compounds. In fact, the order of gelation reactivity
of these compounds with epoxy-anhydride resins would appear to be
as follows:

        Arsonium > Phosphonium > Ammonium > Stibonium
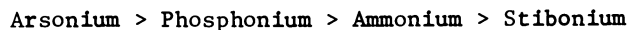
    Since all these elements are in the same group of the
Periodic Table (i.e., Group VA), one might expect the reactivity
trend to continue going from arsonium compounds to stibonium ones.
The fact that stibonium compounds are the least effective in this
group suggests that steric hindrance effects, caused by the larger

stibonium (antimony) cation, may be playing a role.

Summary

Quaternary phosphonium compounds have been found to be extremely effective latent accelerators for anhydride-cured epoxy resins employed in electrical insulation applications. Used at very low concentrations (0.01 to 0.25% level) in these resins, they have been found to give very fast gel times at elevated temperatures combined with very good storage stability properties at room temperature. Results show that the quaternary phosphonium compounds having non-halide anions give the best compromise of gel reactivity, storage stability and electrical properties. Comparison with other types of latent accelerators reveal that the quaternary phosphonium compounds are among the most effective additives yet discovered for epoxy-anhydride resin systems.

Literature Cited

1. Kohn, L. S., in "Epoxy Resin Technology," Edited by
    Paul F. Bruins, Interscience Publishers, New York, 1968,
    Chapter 11, 219-228.
2. Sillars, R. W., in "Electrical Insulating Materials and Their
    Application," Institution of Electrical Engineers Monograph
    Series 14, Peter Peregrinus Ltd., Stevenage, England, 1973,
    192-198.
3. German Patent 1,162,439 to Westinghouse (Nov. 1958).
4. British Patent 869,969 to Shell (June 1961).
5. British Patent 966,917 to Union Carbide (Feb. 1965).
6. Launder, A. J., A.C.S. Div. Org. Coatings Plast. Chem.,
    Preprints, 24, No. 2 (Sept. 1964).
7. Feuchtbaum, R. B., Insulation, 47 (Sept. 1962).
8. Lee, H. and Neville, K., "Handbook of Epoxy Resins," McGraw-
    Hill Book Company, 1967, Chapter 5, p. 20.
9. U.S. Patent 2,928,807 to Devoe & Raynolds Co. (March 1960).
10. Rogers, D. A. and Kauffman, R. N., Westinghouse R&D
    Unpublished Work.
11. Vincent, H. L., Frye, C. L. and Oppliger, P. E., in"Epoxy
    Resins,"Advan. Chem. Ser., 92, R. F. Gould, Ed.,
    American Chemical Society, Washington, D.C., 1970,
    Chapter 14.
12. Langer, S. H. and Elbling, I. N., Ind. Eng. Chem., 49, 1113
    (1957).
13. Langer, S. H., Elbling, I. N., Finestone, A. B. and
    Thomas, W. R., J. Appl. Polym. Sci., V, No. 15, 370 (1961).
14. Belgian Patent 633,330 to CIBA (1963).
15. U.S. Patent 3,759,866 to Westinghouse (Sept. 1973).
16. U.S. Patent 3,784,583 to Westinghouse (Jan. 1974).
17. Smith, J. D. B., J. Appl. Poly. Sci., in Press.
18. U.S. Patent 3,979,355 to Westinghouse (Sept. 1976).

Development of Epoxy Resin-Based Binders for Electrodeposition Coatings with High Corrosion Resistance

W. RAUDENBUSCH

Koninklijke/Shell-Laboratorium, Amsterdam (Shell Research B.V.),
Badhuisweg 3, 1031 CM Amsterdam-Noord, The Netherlands

Electrodeposition (ED) has proved to be a most attractive process for industrial coating, in particular for the priming of automobile bodies. Epoxy resins play a leading role in this field, nearly 6 % of all epoxy resins sold for coatings being used in ED systems.

Until the early 1970s, all ED binders used industrially were based on maleinised natural oils, acidic alkyd resins or epoxy resin esters. Later, binders based on maleinised polybutadiene oils (LMPBs = low-molecular-weight polybutadienes) also came into industrial use, particularly in Western Europe. All these systems were of the anionic type, i.e. their water solubility and their deposition at the anode were due to the presence of carboxylate groups in the binder molecules. More recently, cathodic ED, with binders carrying cationic groups (e.g. $-N^{\oplus}R_2H$), has proved to be an interesting alternative. This paper describes development work directed towards improving the corrosion resistance of anionic, and more briefly, cationic ED binders.

The properties, described in broad terms, of the different classes of anionic binders are shown in Table I. The systems initially used (epoxy esters, maleinised oils and acidic alkyds) generally performed quite well and the rapid rise of the LMPBs, notwithstanding their bath stability problems, was therefore rather surprising.

In fact, the advance of LMPB-based binders was due to one key advantage: their superior corrosion resistance when applied to non-phosphated steel substrates. This property is important in modern automotive applications since most cars now used in Western Europe are of the integral body type on which spray-phosphating always leaves some poorly phosphated or even bare areas. Primers offering good corrosion protection on poorly phosphated steel are thus quite essential for ensuring a long lifetime of modern cars. The superior performance of LMPBs in this respect was ascribed to the low water permeability of polybutadiene films (1). Our more recent work, however, has thrown a different light on this theory.

TABLE I

PERFORMANCE OF ANIONIC ED BINDERS

	Maleinised oils, acidic alkyds	Epoxy resin esters	Maleinised LMPBs
Bath stability	adequate to very good	very good	occasional difficulties
ED properties	good to very good	very good	good to very good
Mechanical coating properties	good to very good	very good	adequate to very good
Corrosion resistance – on phosphated steel – on bare steel	good poor	very good poor	very good very good

Fundamental Studies on the Factors Governing Corrosion Resistance

When comparing two typical ED binders, a commercial LMPB
system and a long-oil epoxy ester, in the standard ASTM salt-spray
test (25 µm clear coatings on bare steel, stoved at 180 °C for
30 min), we first observed that the ratings (good with LMPB, poor
with the epoxy ester) did not depend on the method of application
used (ED or spraying from solvent solution). Therefore, we subse-
quently applied all binders simply from organic solvent solutions,
which greatly speeded up our further work.

Our second observation was that the epoxy ester coatings
failed by loss of adhesion rather than by film degradation. We
assumed that of the different polar groups present (carboxyl, ester,
ether) the carboxyls play the major role in adhesion promotion, and
lose this function upon salt formation with the aqueous alkali
formed during salt-spray testing. Consequently, we inquired which
other, more alkali-resistant, adhesion-promoting groups might be
present in LMPB binders. By infrared spectroscopy we discovered
that during curing of LMPB films at 180 °C for 30 min about 40 % of
the carbon double bonds initially present disappear and substantial
amounts of hydroxyl and (ketonic) carbonyl groups are formed. The
assumption that these groups are primarily responsible for the high
corrosion resistance on bare steel was supported by the fact that
LMPB coatings cured only by air-drying (20 °C/7 d) contained much
less OH and less C=O and showed poor salt-spray ratings.

Elaborating on the hypothesis that hydroxyl groups may be
important alkali-resistant adhesion promotors, we investigated the
salt-spray performance of certain epoxy-resin-based coatings which
after curing contain reasonably well-defined levels of unreacted
hydroxyl groups. One such system consisted of the solid epoxy resin
EPIKOTE 1007 (E-1007) cured with various amounts of hexamethoxy-
methylmelamine (HMMM). When the hydroxyl content of the resin is
known, and the equivalent weight of HMMM is taken as 130 (assuming
for steric reasons that only three of the six available methoxy-
methyl groups are reactive), it is possible to calculate the amount
of residual OH groups in cured coatings quite accurately. These
experiments (see Table II) showed that good salt-spray resistance
on bare steel may be expected if the coating contains between 200
and 400 meq hydroxyl groups per 100 g. It is interesting to note
that good salt-spray resistance appeared to be unrelated to the
degree of crosslinking achieved in this system.

The strong beneficial influence of high hydroxyl levels on
corrosion resistance was also seen in other model experiments, at
least where epoxy resins formed the major coating ingredients.
Some systems, however, most of which were based on alkyds rather
than on epoxies, failed to give similarly good salt-spray ratings
even though their residual OH level was high (300 to 400 meq/100 g).
Thus other factors certainly also play a role. From our subsequent
work, some of these factors appear to be:

TABLE II

PROPERTIES OF "EPIKOTE" 1007/HMMM COATINGS ON BARE STEEL[a]

Exp. no.	E-1007/ HMMM weight ratio	Mechanical properties		Methyl ethyl ketone resistance	ASTM B117-64 salt-spray resistance[b]		Residual OH content of cured films, meq/100 g
		Buchholz hardness	BS impact, direct, in.lb		1 day	8 days	
1	99/1	95	< 5	poor	10	9	350
2	95/5	111	>100	good	10	9	305
3	90/10	115	>100	good	$9\frac{1}{2}$	7	250
4	85/15	133	< 5	very good	2	0	190
5	67/33	154	< 5	very good	0	0	≈0

a. Clear 25 μm coatings applied by spraying from organic solvent solution and stoved at 180 °C for 30 min. Systems contained 0.5 %w of p-toluolsul-fonic acid as catalyst.

b. Ratings: 10 = unaffected, 9 = 5 mm loss of adhesion from scratch, 8 = 10 mm loss of adhesion, 7 = 15 mm loss of adhesion, etc., 0 = total loss of adhesion.

- Susceptibility of cured coatings to alkaline hydrolysis.
- Hydrophilicity of cured films. Poor salt-spray ratings were found to result from the presence of too many polar groups in the coatings.
- Steric (?) factors. Generally we observed that the use of even modest amounts of fatty acids or their esters in OH-rich binders substantially decreases the corrosion resistance. A possible explanation would be sterical shielding of the adhesion-promoting groups by the long fatty acid tails.

Development of Anionic ED Binders with High Corrosion Resistance

The "high-hydroxyl" principle was discovered in experiments in which the coatings were conventionally applied from organic solvent solutions. We then set out to develop ED binders conforming to this principle. Apart from offering good corrosion resistance, such binders must of course meet a number of further requirements, such as

- solubility or dispersibility in water,
- good bath stability,
- good ED behaviour,
- crosslinkability on stoving,
- good mechanical and chemical film properties,
- acceptable preparation methods and costs.

Note: The formulations described in this section are covered by the German Patent Application OLS 2700537, and other applications in a number of countries.

Much of our work was based on the following approach: Into a solid epoxy resin (EPIKOTE type 1001 or 1004) terminal hydroxyl groups were introduced by reacting the epoxy groups with stoichiometric quantities of hydroxy acids such as lactic or, preferably, dimethylolpropionic acid (DMPA). The resulting hydroxyl-rich "backbones" (8-12 OH groups/molecule) were then reacted with a cyclic anhydride such as succinic anhydride (SA) to introduce the carboxyl groups necessary for solubilisation in water:

EPIKOTE
1004

(DMPA)

OH-RICH
BACKBONE

(SA)

WATER-SOLUBLE
RESIN
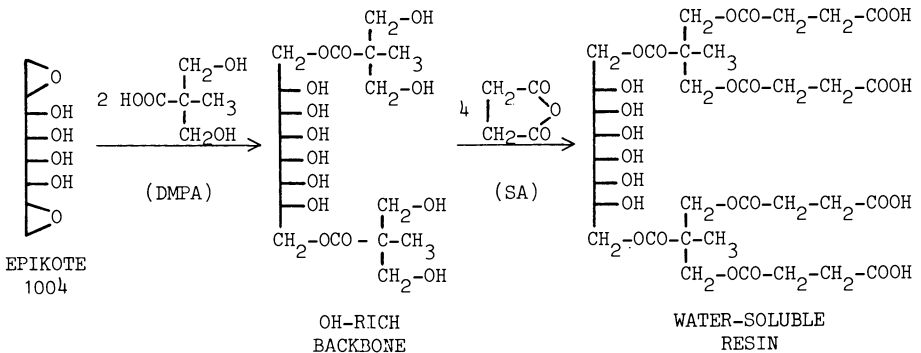
   It soon became clear that these oil-free binders were too
"hard", i.e. when applied by ED they flowed poorly during the
actual deposition step and consequently formed rough coatings (nos.
1 and 2 in Table III). Better-flowing binders were obtained when
the succinic anhydride was replaced by a substituted material, viz.
a premaleinised fatty acid (no. 3, Table III). Unfortunately, how-
ever, this approach always led to a deterioration in salt-spray
resistance, an effect typical for modifications with natural fatty
acids (see above).

   We then discovered that we could improve the softness and the
flow of the binders by incorporating a derivative of a synthetic
fatty acid. This derivative is the glycidyl ester of an α-branched
monocarboxylic acid with 10 carbon atoms and is commercially avail-
able under the trade-name CARDURA E10 (CE 10). Being a monoepoxy
compound, CE 10 could be easily incorporated by reaction with part
of the carboxyl groups present in the binders:

$$CH_2\text{-}OCO\text{-}CH_2\text{-}CH_2\text{-}COOH$$

$$CH_2\text{-}O\text{-}CO\text{-}C\text{-}CH_3$$

$$CH_2\text{-}OCO\text{-}CH_2\text{-}CH_2\text{-}COOH$$

—OH
—OH
—OH
—OH
—OH

$$2\ \ CH_2\text{-}CH\text{-}CH_2\text{-}OCO\text{-}C_9H_{19} \longrightarrow$$

(CE 10)

$$CH_2\text{-}OCO\text{-}CH_2\text{-}CH_2\text{-}COOH$$
$$CH_2\text{-}O\text{-}CO\text{-}C\text{-}CH_3$$
$$CH_2\text{-}OCO\text{-}CH_2\text{-}CH_2\text{-}COOH$$

WATER-SOLUBLE
   RESIN

$$CH_2\text{-}OCO\text{-}CH_2\text{-}CH_2\text{-}COO\text{-}CH_2\text{-}\overset{OH}{CH}\text{-}CH_2\text{-}COO\text{-}C_9H_{19}$$

$$CH_2\text{-}O\text{-}CO\text{-}C\text{-}CH_3$$
$$CH_2\text{-}OCO\text{-}CH_2\text{-}CH_2\text{-}COOH$$

— OH
— OH
— OH
— OH
— OH
— OH

$$CH_2\text{-}OCO\text{-}CH_2\text{-}CH_2\text{-}COO\text{-}CH_2\text{-}\overset{OH}{CH}\text{-}CH_2\text{-}OCO\text{-}C_9H_{19}$$
$$CH_2\text{-}O\text{-}CO\text{-}C\text{-}CH_3$$
$$CH_2\text{-}OCO\text{-}CH_2\text{-}CH_2\text{-}COOH$$

OH-RICH ED BINDER
(No. 4 in Table III)
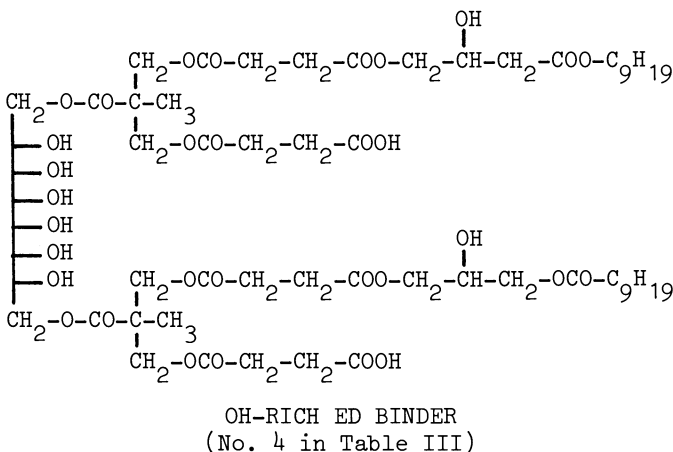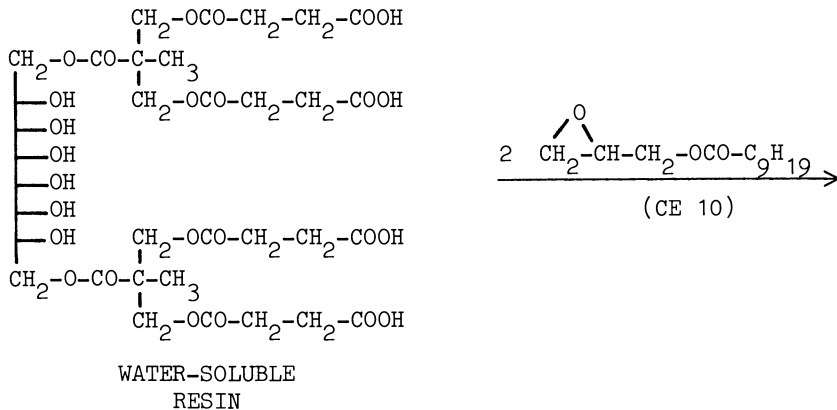
TABLE III

HYDROXYL–RICH ANIONIC ED BINDERS[a]

No.	Binder composition[b] Molar ratios	Hydroxyl content[c], meq/100 g	ED behaviour[d]	Bath stability[d] (7 d/40 °C)	Mechanical coating properties	Salt-spray rating (10 d)
1	E-1004/LA/SA 1/ 2 /1.5	404	poor	fair	good	9[e]
2	E-1004/DMPA/SA 1/ 2 /1.5	479	poor	fair	good	$9\frac{1}{2}$[e]
3	E-1001/DMPA/MAFA 1/ 2 /2	358	good	very good	good	5 - 6[e]
4	E-1004/DMPA/SA/CE 10 1/ 2 / 4 /2	341	good	fair	good	9[f]
5	E-1001/AA/DMPA/TMA/CE 10 2/1/ 2 /2.3/2.4	405	good	very good	good	9[f]
6	Commercial LMPB binder (comparison)	–	good	good	fair	9[f]

a. All binders (except no. 6) combined with HMMM (weight ratio 95/5); 25 μm thick clear coatings applied to bare steel by spraying or by ED, followed by stoving at 180 °C for 30 min.
b. E-1001, E-1004: solid EPIKOTE epoxy resins; LA: lactic acid; DMPA: dimethylol-propionic acid; SA: succinic anhydride; TMA: trimellitic anhydride; MAFA: pre-maleinised fatty acid; CE 10: CARDURA E10; AA: adipic acid.
c. Calculated.
d. 10 % aqueous solutions containing ethylene glycol mono-n-butyl ether (30 % on binders), and triethylamine for neutralisation.
e. Spray-applied coatings;
f. Both ED- and spray-applied coatings;} for salt-spray ratings see Table II.

A binder of this type (no. 4 in Table III), in combination
with small amounts of melamine or phenolic resins as crosslinkers,
showed good ED behaviour and good mechanical film properties. Its
salt-spray resistance was only slightly lower than that of a
CARDURA-free analogue (no. 2 in Table III). CE 10 seems to have a
lesser detrimental effect on the salt-spray resistance than natural
fatty acids, possibly because its hydrocarbon chain is much shorter.

The hydrolytical stability of binder no. 4 was not very good
and our next task was to improve this aspect.

Binders rendered water-soluble by the acidic halfester prin-
ciple contain a hydrolytically weak site, viz. the halfester linkage.

CYCLIC
ANHYDRIDE   ACIDIC HALFESTER
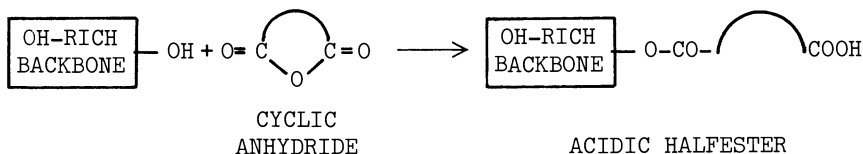
The reason is probably that the saponification of the halfester is
assisted by the neighbouring carboxyl function. We screened the
hydrolytic stability of binders containing different types of half-
esters by storing aqueous solutions (10 % solids content) at 40 $^{\circ}$C
and periodically checking the pH, the conductivity and the ED
behaviour. In this way we found that binders containing halfesters
of maleic or phthalic acid are quite unstable. The stability of
binders with succinic halfesters is better but probably still
insufficient for most industrial applications. Halfesters of tri-
mellitic anhydride (TMA) are considerably more stable than those
of succinic acid. To our surprise we found that modification of the
trimellitic halfesters with the above-mentioned monoepoxide CE 10
enhanced the stability even further. If about equimolar amounts of
TMA and CE 10 are used there are sufficient carboxylic functions
left to guarantee a good solubility of the binders in water:

CARDURA E10-TMA MODIFIED ED BINDER
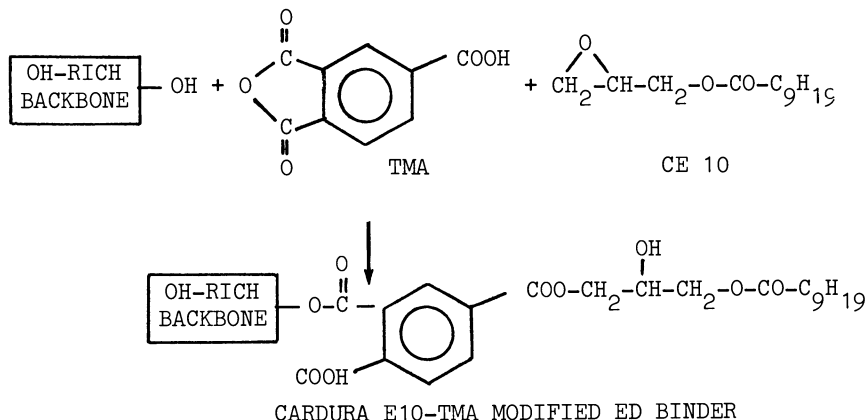
From our laboratory experience we believe that such systems are about as stable as the industrially well-known binders which are rendered water-soluble with premaleinised fatty acids.

A typical hydroxyl-rich binder which is modified with TMA and and CE 10 is no. 5 in Table III. In this binder the backbone is slightly different from that of the preceding binders, i.e., EPIKOTE 1004 is replaced by a combination of EPIKOTE 1001 (two moles) and adipic acid (one mole). This was done to further improve the mechanical properties of the coatings.

With melamine or phenolic resins as crosslinkers binder no. 5 shows an attractive combination of good ED behaviour, good mechanical film properties and high bath stability. Its salt-spray resistance is comparable to that of a commercial LMPB system (no. 6 in Table III). Binder no. 5 also shows self-crosslinking behaviour, i.e. it gives coatings with an interesting level of performance when stoved in the absence of external crosslinkers.

In view of these encouraging results, we decided to submit binder no. 5 to customers under the code LR-2052. Customer reactions so far have been quite positive and our views regarding the high salt-spray resistance of this binder on non-phosphated steel were fully confirmed.

With a view to lowering raw material costs (the DMPA used in binder LR-2052 is rather expensive), we later developed another OH-rich binder, designated LR-2053. This system is based on a linear backbone containing a liquid epoxy resin, EPIKOTE 828, diphenylolpropane, adipic acid and CE 10 (molar ratio 3/2/2/2) and again is rendered water-soluble with a TMA/CE 10 combination (2.5 moles TMA and 2.6 moles CE 10 per mole of backbone). This binder performs as well as LR-2052, with an only marginally lower salt-spray resistance.

With both binders, LR-2052 and LR-2053, we have prepared pigmented ED paints. We used a simple TiO_2 based pigmentation without active ingredients. Typical data for these paints are shown in Table IV. The general performance of both pigmented systems was very satisfactory and the salt-spray ratings were comparable to those of unpigmented coatings.

In conclusion, we can say that it is possible to design anionic ED binders based on epoxy resins which give coatings with a much better salt-spray resistance on bare steel than that of coatings based on conventional anionic binders. The main design features of the epoxy resin based binders are (1) the presence of a sufficiently high level of hydroxyl groups in the crosslinked coatings, and (2) the omission of natural fatty acids. In later work we applied the same principles to cationic ED binders.

Cationic ED Binders

A chief advantage claimed for coatings applied by the cathodic ED is their superior corrosion resistance, and this has been the main incentive for our work in this area. Initially, we tried to establish whether the cathodic deposition process as such would lead to improved corrosion resistance of the coatings. To this end

TABLE IV

PIGMENTED ED PAINTS

		LR-2052	LR-2053
Binder		Setaliet 100[a]	Setaliet 100[a]
Paint composition			
Crosslinking resin			
Binder/crosslinker weight ratio		85/15	85/15
Pigment[b]/binder weight ratio		0.28	0.28
Binder/solvents[c] weight ratio		100/40.5	100/40.5
Degree of neutralisation (triethylamine)		0.83	0.80
Paint solids content,	%w	14.8	14.8
Paint properties			
pH (25 °C)		7.1	7.5
Specific resistance (25 °C),	Ω.cm	1260	1280
Deposition temperature,	°C	30	30
Deposition time,	min	2	2
Deposition voltage,	V	150-175	150-200
Rupture voltage,	V	220	250
Throwing power (Ford test),	cm/V	15/175	16/200
Stability of paint[d] at 28 °C,	weeks	≥4	≥4
Cured film properties[e] (Stoving: 180 °C/30 minutes)			
Film thickness,	μm	22-28	22-28
Film appearance		very good	good
Pendulum hardness (König),	s	195	170
Adhesion (crosshatch, DIN 53151)		Gt 0	Gt 0
Erichsen impact, reverse,	mm	>3	>3
Conical mandrel bend (ASTM D522-60)		passed	passed
Salt-spray resistance (ASTM B117-64; 10 d)[f]		9-9½	8½

a. Thermoreactive phenolic resin (Synthese B.V., Holland).
b. Titanium dioxide/carbon black/clay (weight ratio 36/2/2).
c. Diethylene glycol monobutyl ether/isophorone (weight ratio 2/1).
d. Circulation in open containers, no ultrafiltration.
e. All coatings applied to bare steel.
f. For ratings see Table II.

we modified a given anionic ED binder, LR-38 (a maleinised long-oil
epoxy resin ester modified with a styrene/methacrylic acid copo-
lymer), so that it could be electrodeposited anodically or catho-
dically depending on the pH. Such "amphoteric" behaviour was
achieved by converting the (substituted succinic) anhydride rings
present in LR-38 with 2-dimethylaminoethanol into amino acid
functions, e.g. $\boxed{\text{LR-38}}$— CH-COOH

$$CH_2-COO-CH_2-CH_2-N(CH_3)_2$$
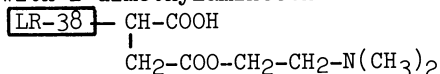
Salt-spray data (for nos. 1 and 2 in Table V) indicated that,
on zinc-phosphated steel, cathodic ED indeed led to considerably
better corrosion resistance. On bare steel, however, both cathodic
and anodic coatings failed completely. Further, we prepared a
number of different, amine-modified epoxy resin esters containing
between 30 and 50 %w of drying fatty acids (e.g. no. 3 in Table V).
These could all be deposited cathodically and again attained excel-
lent salt-spray ratings on phosphated steel but performed poorly
on bare steel. We concluded that cathodic ED prevents phosphate
layer degradation (a well-known phenomenon with anodic ED) and thus
leads to superior corrosion resistance on pretreated steel. On bare
steel the binders performed too poorly to allow comparison between
cathodic and anodic ED.

In the light of our more recent discovery of the "high-
hydroxyl" principle, the poor performance of our early cationic
systems on bare steel can now be explained by their lack of suffi-
cient hydroxyl groups (<100 meq/100 g) and their high fatty acid
levels (30-50 %w). To optimise the corrosion resistance the trend
should be towards essentially oil-free cationic binders preferably
based on epoxy resins and containing high levels of residual OH
groups. It is interesting to note that all these features are
realised in a number of cationic systems proposed in the patent
literature.

In our own work towards cathodic systems with high bare steel
corrosion resistance we first prepared a number of epoxy resin/
amine adducts of the formal composition:

| Secondary amine | | Epoxy resin | | Primary amine | | Epoxy resin | | Secondary amine |
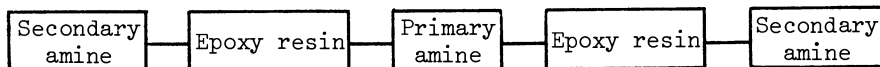
Upon neutralisation (with lactic or acetic acid) these adducts
became water-soluble but showed quite poor ED behaviour, probably
again owing to the absence of flow-promoting entities (no. 4,
Table V). The ED behaviour was much improved by chemical incorpo-
ration of the monoepoxide, CARDURA E10 (no. 5, Table V). Unfortu-
nately, in spite of the many hydroxyl groups present the cure of
these binders with external crosslinkers (melamine or phenolic
resins) was marginal. This undoubtedly is due to the lack of cata-
lysing acidic functions and to the retarding influence of the amino
groups.

We then attempted to incorporate catalysing acidic moieties
into such binders and found that sulfanilic acid (p-NH_2-C_6H_4-SO_3H)
co-reacts with epoxy resins in the presence of other amines,

TABLE V

CATIONIC ED BINDERS[a]

No.	Binder type or molar composition[b]	Hydroxyl content[c], meq/100 g	ED behaviour[d]	Bath stability[d] (14 d/23 °C)	Crosslink-ability[e]	Salt-spray rating[f] (10 days)	
						Phosph. steel (Bonder 97)	Bare steel
1	Amphoteric LR-38 (anodic ED)	0	good	fair	good	8	0
2	Amphoteric LR-38 (cathodic ED)	0	fair	fair	good	$9\frac{1}{2}$	0
3	Amine-modified epoxy resin ester	90	good	fair	good	$9\frac{1}{2}$	0
4	E-1001/Deola/Eola 2/ 2 /1	690	poor	good	marginal	-	-
5[g]	E-1001/Deola/Eola/Sulfa/HD/CE 10 3/ 2 / 1 / 1 /2	590	good	good	marginal	-	-
6[g]	E-1001/Deola/Eola/Sulfa/HD/CE 10 3/ 2 /0.75/0.25 /1 /2.75	550	good	good	good	$9\frac{1}{2}$	$9\frac{1}{2}$

a. 25 μm thick clear coatings applied by ED, followed by stoving at 180 °C for 30 min; binders nos. 4-6 cured with HMMM (weight ratio 80/20).

b. E-1001: solid EPIKOTE epoxy resin; Deola: diethanolamine; Eola: ethanolamine; HD: hexanediamine-1,6; CE 10: CARDURA E10; Sulfa: sulfanilic acid. For binders nos. 1-3 see text.

c. Calculated.

d. 10 % aqueous solutions containing ethylene glycol mono-n-butyl ether (30 %w on binders) and lactic acid for neutralisation (triethylamine with system no. 1).

e. Stoving at 180 °C for 30 min in the presence of 20 % HMMM. Degree of crosslinking assessed from solvent resistance and mechanical coating properties.

f. For ratings see Table II.

g. Formulations nos. 5 and 6 in Table V are covered by recent patent applications.

leaving the -SO₃H group intact. An optimised binder of this type
(no. 6, Table V) crosslinks well and leads to coatings with excel-
lent salt-spray resistance on both phosphated and bare steel. A
drawback of this binder is the rather low pH of the aqueous solu-
tions (4.5-5.0), and work on cathodic systems with higher pH is
therefore being carried out.

From this work we can conclude that the salt-spray resistance
of cationic ED coatings also appears to benefit from a high level
of hydroxyl groups in the cured films.

Abstract

Primer coatings for automobile bodies are generally applied
by electrodeposition (ED) and binders based on epoxy resins play a
leading role in this field. During recent years car manufacturers
have become more stringent regarding the corrosion protection
demanded of ED primers, not only on phosphated but also on non-
pretreated steel. Traditional epoxy resin binders, modified with
drying fatty acids, cannot meet these requirements. In a search for
factors which influence the salt-spray resistance of thin (25 µm)
model coatings on bare steel it was found that a high level of
residual hydroxyl groups in the cured coatings (200-400 milliequi-
valents/100 grams) has a strongly beneficial effect. This discovery
led to the development of epoxy-resin-based anionic ED binders
having very good salt-spray resistance on non-pretreated steel.
Essentially, these binders are oil-free, hydroxyl-rich epoxy resin
esters which are modified with trimellitic anhydride and a flow-
promoting monoepoxy ester (CARDURA E10). The "high-hydroxyl" prin-
ciple also appears to hold for cathodic ED, the applicational
variant increasingly preferred by the industry. The development of
epoxy-resin-based cationic ED binders with high corrosion resis-
tance is discussed.

Acknowledgement

Literature Cited

1. Heidel, K. Chemische Werke Hüls, A.G., 1967, lecture: "Air-
   drying resins on the basis of liquid cis-polybutadiene".

Water-Borne Coatings Prepared from High Molecular Weight Epoxy Resins

EDWARD G. BOZZI and CAMILLA Y. ZENDIG

Epoxy Resins Laboratory, CIBA-GEIGY Corporation, Ardsley, NY 10502

As air pollution controls tighten, as fuel reserves dwindle and as industrial hazards are explored, solvents become increasingly unattractive as diluents for coatings.

Industry has formulated several alternative coating technologies, probably the most advanced and easily substituted being water-borne.

Our water-borne investigations led us recently to the discovery of techniques for preparing oil-in-water emulsions of our highest molecular weight epoxy resins. Known commercially as ARALDITE ® 488, these resins have weight average molecular weights of 15,000–20,000 and are ideal for applications requiring excellent adhesion and formability.

Emulsions of these resins with relatively high solids content can be prepared while the corresponding solvent cuts have viscosities too high for use in coatings. For example, at 40% solids in Cellosolve acetate, ARALDITE 488 has a viscosity of 6000 cP. while the water-borne emulsion at the same solids level is only 1000 cP. For most methods of application the solids content of the solvent cut would have to be dropped below 40% to give a workable viscosity and this would exclude the resin from some important end uses such as can end and 3-piece can body coatings. The resin in its emulsified form, however, has the proper solids/viscosity relationship for this particular end use.

In the emulsified state, the high molecular weight epoxy resin exists as small spherical droplets surrounded by a surfactant which forms a "skin" over the droplets and thus prevents coalescence. While the viscosity within these particles may be great due to the high viscosity of the solvent cut of resin, the overall emulsion viscosity will only be dependent on the total solids content and any water-soluble additives. Therefore, coatings with a high non-volatiles content can be made from a very high molecular weight epoxy resin in its emulsified form but cannot be made from the same resin at an equivalent solids level in a solvent cut.

APPLICATIONS

   Can End Coatings. In most cases, a two-step process is used
when roller coating the interior ends of beer and beverage cans.
After the first resinous coating is applied, the pull-tab is form-
ed and a second coating follows to cover any cracks in the origi-
nal coating due to rivet and scribing operations. If the first
coating were, however, flexible enough to withstand the rivet and
scribing operations, the second repair coating could be elimina-
ted. We have evaluated our high molecular weight epoxy resin
emulsion for this end use and have found that the flexibility in-
herent in the solvent-borne resin has not been lost during emulsi-
fication. At high resin/hardener ratios we found excellent flex-
ibility and pasteurization resistance and good formulation stabil-
ity. Table I compares the properties of the high molecular weight
epoxy emulsion to a "7" type epoxy resin emulsion formulated with
melamine and urea-formaldehyde hardeners.

TABLE I

FORMULATIONS AND PHYSICAL PROPERTIES

FORMULATION NO.	I	II	III
ARALDITE 488 Emulsion, 40% Solids	245	237.5	-
"7" Type Epoxy Emulsion, 50% Solids	-	-	196
Melamine Hardener (Cymel 303)	2	-	2
Urea Formaldehyde Hardener (Beetle 65, 50% in H_2O)	-	10	-
Resin Crosslinker	98/2	95/5	98/2
Wedge Bend (mm)	10	0-1	15-20
Beer Pasteurization (160^oF/45 m)	No Change/Excellent Adhesion	Slight Blush/Excellent Adhesion	Slight Blush/Excellent Adhesion
Stability	14	58+ Weeks	(Separation at 15 Weeks)

   Poor flow and leveling, particularly during roller coating,
and the need for an external catalyst, are, however, problems with

the high molecular weight epoxy emulsion. To solve these two
problems, we formulated the epoxy emulsion with 15-20% of various
water-base alkyds, polyesters and acrylics. After much experimen-
tation we found only a few systems with good film properties and
stability and found in particular one alkyd, Kelsol 3900 from
Spencer-Kellogg, to perform very well with our epoxy resin emul-
sion. Table II shows the formulation evaluated and the properties
of the coating.

<div align="center">

TABLE II

FORMULATION FOR CAN END COATING

</div>

Epoxy Resin Emulsion (40% Solids)	-	73.4
Alkyd (Kelsol 3900) (48.6% Solids)	-	15.1
Melamine Hardener (Cymel 303)	-	4.1
Water	-	7.4
		100.0
Resins/Crosslinking Agent	-	90/10
Epoxy/Alkyd	-	4/1
Solids, %	-	40.8
Viscosity, (#4 Ford Cup), sec.	-	45

<div align="center">

PERFORMANCE PROPERTIES

</div>

Substrate	Treated Aluminum
Application Method	Roller Coated
Cure Schedule (min./°F)	3/400
Appearance	Good Flow and Leveling
209 Can End Immersed in $CaSO_4$, min.	Pass, 6

Beer Pasteurization, 45 m/160°F
(Closed Container)

	Appearance:	No Change
	Adhesion:	Excellent

Water Pasteurization, 45 m/160°F
(Closed Container)

	Appearance:	No Change
	Adhesion:	Excellent
Wedge Bend, mm		22

   Automotive Primer Coatings. To those working in the field
it is generally known that water-borne versions of "7" and "9"
type epoxy resins do not meet the high corrosion resistance re-
quirements for an automotive primer. However, the high crosslink-
ing density and excellent adhesion properties afforded by the high
molecular weight of our epoxy resin should make it ideal for such
end uses.
   Table III shows the formulation and performance properties

of our epoxy resin emulsion and appropriate primer coating fillers
cured with a proprietary water-borne phenolic hardener. The best
property of this coating is its outstanding salt spray resistance.
We obtained over 1500 hours salt spray resistance on Bonderite
P-60 steel, with less than 1 mm creep. Even on cold rolled steel,
the coatings displayed 300 hours resistance ($<$ 3 mm creepage)
while those of a commercial water-borne coating failed after only
24 hours exposure.

TABLE III

FORMULATION FOR AUTOMOTIVE PRIMER COATINGS

Epoxy Resin Emulsion (40% Solids)	–	38.3
Alkyd (Kelsol 3900) (48.6% Solids)	–	13.0
Water-Borne Phenolic Hardener (32% Solids)	–	18.0
Water	–	8.6
Clay	–	6.5
$BaSO_4$	–	13.0
Lampblack	–	1.0
TiO_2	–	1.6
		100.0

Resins/Crosslinking Agent	–	88/12
Epoxy/Alkyd	–	70/30
Solids %	–	48.5
Viscosity, (#4 Ford Cup), sec.	–	50

PERFORMANCE PROPERTIES

Substrate	–	Bonderite P60 Steel
Application Method	–	0.003 mil Doctor Blade
Cure Schedule (min./$^\circ$F)	–	30/325
Appearance	–	Good Flow and Leveling
Salt Spray Resistance	–	1500 Hours, $<$ 1 mm Creep

Other Applications. We have evaluated our epoxy resin emul-
sion with various thermoplastics. Results are shown graphically
in Table IV.

TABLE IV

THERMOPLASTIC MODIFIED EPOXY RESIN EMULSION

THERMOPLASTIC

Polyvinyl Acetate (Gelva S55H, Monsanto)	–	Improved Impact and Acid Resistance
Vinyl Acetate/Acrylic Co-Polymer (Polyco 2151, (Borden)	–	Improved Adhesion and Acid Resistance
Alkyd (Kelsol 3906, Spencer-Kellogg)	–	Improved Flexibility and Dry Time
Acrylic (WS32, Rohm and Haas)	–	Improved Hardness and Dry Time

Adhesion is usually improved while flexibility is maintained when using the high molecular weight epoxy emulsion as an upgrader in water-borne thermoplastic systems.

CONCLUSION

Our investigations of very high molecular weight epoxy resin emulsions as evaluated in can end, automotive primer and thermoplastic-type maintenance coating systems have yielded some very exciting and useful data. The largest technological challenge that remains is in obtaining proper rheology. This problem is helped by the addition of very specific water-soluble resins. Commercial success of the high molecular weight epoxy resin emulsion will depend, therefore, on how well we can solve these rheological problems.

RECEIVED July 16, 1979.

Aqueous Epoxy Resins for Electrical Reinforced Plastics Industry

TERRY L. ANDERSON, JAMES H. MELLOAN, KATHLEEN L. POWELL,
ROLAND R. McCLAIN, J. BRANDON SIMONS, ROBIN L. CONWAY,
and DAVID A. SHIMP

Celanese Polymer Specialties Co., 9800 E. Bluegrass Parkway, Jeffersontown, KY 40299

    The electrical reinforced plastics industry is undergoing
changes as the requirements of printed circuit boards become more
complex. This complexity is compounded by the requirements that
the processes be more environmentally acceptable. EPA acceptable
resins will ultimately be required of the resin producers.
    The purpose of this paper is to present a new water based
epoxy resin system which will meet the current requirements of the
industry. In addition, an experimental system will be presented
which will approach the emerging requirements of the industry.

GENERAL TECHNOLOGY AND RESIN REQUIREMENTS

    Prior to discussing the new water based system, let us review
the basic processes used in making the laminate.
    Figure I gives a flow diagram of the typical laminate process.
    Figure II gives a typical resin and curing agent varnish for-
mula which would be used to make the finished laminate.

Figure I
TYPICAL LAMINATE PROCESS

| Impregnate resin into glass | → | Partially cure resin to a tack free state |
| Stack pre-preg into layers | → | Fully cure resin to bond layers of pre-preg into a laminate |
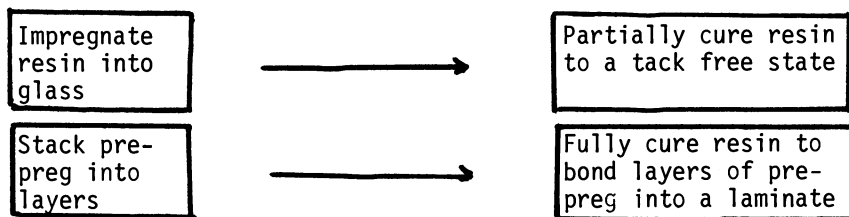
Figure II
TYPICAL ORGANIC SOLVENT VARNISH FORMULA

Epoxy resin @ 80% NVM   125 parts
in organic solvent

Dicyandiamide   4 parts

Organic Solvent   45 parts

Cure Accelerator   0.2 parts

As can be seen in Figures I and II, the processing involves
impregnating the fiberglass with the uncured epoxy resin solution,
and finally fully curing layers of the prepreg with copper foil
into a finished laminate. From this point the laminate is fabri-
cated into a finished printed circuit board.
The epoxy resin solution is typically a halogenated epoxy
resin dissolved in a volatile solvent such as acetone. Various
proprietary resin parameters control such properties as cure speed,
wetting of the glass, and cured state Tg.

NEW WATER BASED SYSTEM (ED-24574)

The above brief discussion is not intended to be a comprehen-
sive review of the processes used but is intended as an overview.
Figure III shows the varnish formula for the new water based
system. The key feature of this varnish system is that no organic
solvent exists in the entire formula.

Figure III
WATER BASED VARNISH FORMULA

Water Based Epoxy @   167 parts
60% NVM

Dicyandiamide   3.2 parts

Water   22 parts

Accelerator   0.3 parts

Several basic problems can exist with a water based resin
when manufacturing prepreg material.
The first problem is a reactivity problem. Early attempts at
preparing water based systems encountered very slow reactivity of
the dicyandiamide with the epoxy resin. This caused very slow
line speeds for the laminator. This problem has been resolved
with ED24574 and the cure response of the system is equal to
organic solvent based standards.
The second problem which can plague a water based system is
one of foaming of the resin. The foaming tendency is considered
common to all water based dispersions and is attributed to the

decrease in surface tension caused by the dispersant. Foaming manifests itself when the glass cloth is pulled continuously through the resin dispersion. Since large volumes of air are introduced into the glass/resin interface a substantial amount of foaming can occur. Wetting problems are then introduced into the prepreg and ultimately into the finished laminate. Unique attention to resin composition has solved the foaming problem for ED-24574. It does not generate foam and the subsequent wetting problems in the finished laminate.

The third problem associated with water based varnishes is poor electrical insulation properties of the laminate after moisture conditioning. This problem is probably the most critical problem because insulation failures of the laminate can lead to electrical failure of the finished printed circuit board. This property is measured by conditioning the finished laminate in a high moisture environment and then testing the dielectric breakdown strength. ED24574 has excellent insulation resistance. This was achieved by a proprietary resin composition.

Solution of the above problems has allowed the ED24574 system to run on commercial treater lines to produce laminates which will pass NEMA FR4 requirements.

PROPERTIES OF ED24574

Figure IV gives the general properties of the new water based resin ED24574. The key properties to note are the electric properties. Specifically, the dielectric breakdown voltage is a safe margin above the minimum requirements. The remainder of the electrical properties are also well above the requirements.

Recently in the industry, requirements on cured state Tg and related phenomena have begun to be requested of the resin suppliers. One of two types of tests has been added over the NEMA FR4 requirements listed in Figure IV. This test is either a measurement of the cured state Tg or a pressure cooker test.

The Tg requirement has increased from about 115-120°C. to a level of 120-130°C. for the cured laminate. The pressure cooker test is run by subjecting the test laminate to 15 psi steam in a conventional pressure cooker for 20-40 minutes. The test laminate is removed from the pressure cooker, conditioned one hour at room temperature and immediately placed in a hot solder bath (about 500°F.). The laminate is then tested for water blistering between the laminate plies. Any visible blistering is considered a failure.

Figure V presents data which compares the ED24574 system with a standard organic solvent based resin system. As can be seen in Figure V the ED24574 formulation does not pass the emerging Tg or pressure cooker requirements of the industry.

Figure IV
PROPERTIES OF LAMINATES PREPARED FROM ED24574

Laminate Properties
Laminates constructed from 12 plies of Style 7628, I-399 finish glass cloth prepreg press cured one hour at 350°F. and 150 psi were tested versus NEMA FR-4 specification limits. Results are listed below:

Laminate Property	Conditioning	NEMA FR-4 Requirements	Test Results
Resin Content (wt. %)	-	-	34
Flexural Strength (psi)			
Lengthwise	23°C., 50% RH	60,000 min.	84,000
Crosswise	23°C., 50% RH	50,000 min.	64,000
Lengthwise	150°C.	-	8500
Izod Impact (ft.-lbs./in. notch)			
Lengthwise	48 hrs. @ 50°C.	7.0 min.	17.6
Crosswise	48 hrs. @ 50°C.	5.5 min.	10.3
Peel Strength (lb. inch width)			
1 oz. copper	20 sec. solder dip	8 min.	11.4
Water Absorption (%)	24 hrs. @ 23°C.	0.20 max.	0.06
	1 hr. @ Boil	-	0.21
Volume Resistivity (megohm-cm)	96 hrs. @ 35°C. & 90% RH	10^6 min.	10^9
Surface Resistivity (megohms)	96 hrs. @ 35°C. & 90% RH	10^4 min.	10^7
Dielectric Constant @ 1 megacycle	23°C., 50% RH	5.2 max.	5.0
	24 hrs. @ 23°C. in water	5.4 max.	5.1
Dissipation Factor @ 1 megacycle	23°C., 50% RH	0.025 max.	0.016
	24 hrs. @ 23°C. in water	0.035	0.017
Dielectric Breakdown (KV) parallel to lamination	23°C., 50% RH	45 min.	> 60
	48 hrs. @ 50°C. in water	40 min.	52
Flammability, per UL94V Burning Time (seconds)	-	-	7

Figure V
COMPARISON OF LAMINATE Tg AND PRESSURE COOKER TEST RESULTS

	Standard Acetone Solution Based Resin	ED24574
Tg (cured laminate)	125°C.	100°C.
20 minutes pressure cooker blistering	Pass	Fail
30 minutes pressure cooker blistering	Pass	Fail

EXPERIMENTAL SYSTEMS

At present it is not clear whether Tg or pressure cooker re-
sults will be required of the epoxy resins in the electrical lami-
nate industry. We have developed an experimental resin in the
laboratory which will pass the new Tg or pressure cooker require-
ments. The results of this experimental system are depicted in
Figure VI and in Figure VII.

Figure VI
LAMINATE TEST RESULTS FOR EXPERIMENTAL RESIN

	Experimental Resin
Tg	119°C.
20 minutes pressure cooker blistering	Pass
30 minutes pressure cooker blistering	Pass

As can be seen from this data in Figure VI substantial improve-
ment over the current ED24574 system has occurred. Both Tg and
electrical data are acceptable for this industry.

CONCLUSION

A new water based epoxy resin system has been developed for
the electrical reinforced plastics industry.

Key features of the ED24574 system are its ability to run on
commercial treater lines without cure speed problems, no foaming
or wetting problems, and finally no insulation resistance pro-
blems after moisture conditioning.

The ED24574 system does not pass the emerging Tg or pressure
cooker requirements. However, an experimental resin does pass
these requirements. It is anticipated that this higher Tg resin
will allow laminates to be made which will pass the emerging re-
quirements of the printed circuit board industry.

Figure VII

PROPERTIES OF LAMINATES PREPARED FROM EXPERIMENTAL RESIN

Laminate Properties

Laminates constructed from 8 plies of Style 7628, I-399 finish glass cloth pre-preg press cured one hour at 350°F. and 150 psi were tested versus NEMA FR-4 specification limits. Results are listed below:

Laminate Property	Conditioning	NEMA FR-4 Requirements	Test Results
Volume Resistivity (megohm-cm)	96 hrs. @ 35°C. & 90% RH	10^6 min.	10^{15}
Surface Resistivity (megohms)	96 hrs. @ 35°C. & 90% RH	10^4 min.	10^{13}
Dielectric Constant @ 1 megacycle	23°C., 50% RH 24 hrs. @ 23°C. in water	5.2 max. 5.4 max.	5.2 5.3
Dissipation Factor @ 1 megacycle	23°C., 50% RH 24 hrs. @ 23°C.	0.025 max. 0.035 max.	.006 .007
Dielectric Breakdown (KV) parallel to laminations	23°C., 50% RH 48 hrs. @ 50°C. in water	45 min. 40 min.	60 56
Flammability, per UL94V Burning Time (seconds)		-	7
Resin Content (%)			38

Epoxide Equivalent Weight Determination by Carbon-13 Nuclear Magnetic Resonance

W. B. MONIZ and C. F. PORANSKI, JR.

Chemistry Division, Naval Research Laboratory, Washington, DC 20375

We have been involved for some time in the development and application of nuclear magnetic resonance (nmr) techniques for the characterization of thermosetting polymers. The effort has been directed toward analysis of both prepolymers and cured resin systems. We have previously described how carbon-13 nmr can aid the analyst distinguish various types of epoxy resins and identify reactive diluents which may be present (1), and have published a comprehensive catalog of proton and carbon-13 nmr spectra of epoxy resins and curing agents (2). We have applied the relatively new technique of proton-enhanced carbon-13 nmr to the analysis of solid, cured epoxy systems (3). It appears that this technique will be useful not only in chemically characterizing cured systems, but also in probing their molecular dynamics.

In this paper we discuss the use of carbon-13 nmr to measure epoxide equivalent weights of epoxy resins based on the diglycidyl ether of bisphenol A (DGEBA). The results obtained to date indicate that the carbon-13 technique could be an attractive alternative to current methods.

Epoxy resins based on DGEBA are represented by the general formula shown below. Commercial resins are mixtures of such structures (oligomers) with various values of n. The epoxide equivalent weight (EEW) measures the number of epoxide groups available for reaction during cure. In a resin composed of oligomers, the EEW is an average for the mixture.

The resin system processing parameters which are of practical importance include EEW, viscosity, and in some cases, the relative
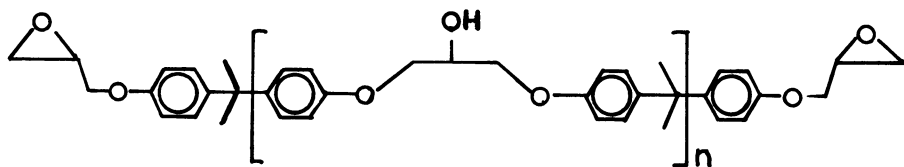
proportions of the various n-oligomers. Zucconi (4), for example, has reported that problems in manufacture and performance of epoxy printed-circuit boards were traced to differences in the oligomer distribution of epoxy resin batches which had met viscosity and EEW specifications. He has developed a quality control procedure based on liquid chromatography for monitoring oligomer distribution. The carbon-13 nmr technique described here measures EEW, but not oligomer distribution.

Dorsey, et al., have described a proton nmr method for EEW determination which uses a measured amount of sym-tetrachloroethane as an internal standard (5). They report results on five resins with EEW's below 300. Hammerich and Willeboordse have analyzed the precision of proton nmr EEW determinations (6). Some of the problems in accurate area measurement they point out, such as carbon-13 satellites and insufficient separation of main peaks, are not of concern in the carbon-13 nmr EEW determination.

While proton nmr is satisfactory for determinations on low and medium EEW epoxy resins, the method loses accuracy as the EEW increases. As shown in Figure 1, the proton nmr spectrum of DER 332LC (EEW$\cong$175) has sharp multiplets and integration of the relative areas is straightforward. But, as the spectrum of EPON 1004 (EEW$\cong$950) shows, when the EEW increases, the multiplets broaden due to overlap with the lines of the aliphatic protons in the bridging groups of the oligomers.

For carbon-13 nmr, the large chemical shift dispersion and the use of proton decoupling obviate such problems. Figure 2 shows carbon-13 nmr spectra of the region of interest for two epoxy resin systems.

The three lines at 44, 50, and 70 ppm form the basis for the carbon-13 nmr method of EEW determination. As n in the general oligomer structure increases, the number of bridging carbons increases, but the number of terminal epoxide groups remains the same, two per oligomer molecule. For the idealized n-oligomer, the ratio of terminal glycidyl ether carbons of types c,d, or e, to bridging carbons (type b) is 2/3n. Now, the intensity of the carbon-13 line at 70 ppm is the sum of the intensities of the line due to the terminal ether methylene carbon, I_e, and those due to the bridging carbons, I_b. Although I_e cannot be measured directly,
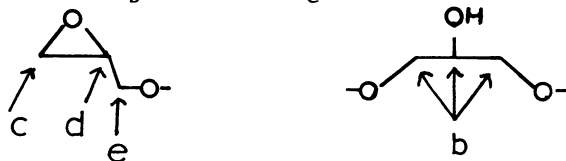
its value can be obtained by measuring the intensity of either the line at 44 ppm (I_c) or 50 ppm (I_d), or their average value, I'. Thus the ratio, 2/3n, can be expressed by $I'/(I_b - I')$ and $n = 2(I_b - I')/3I'$.
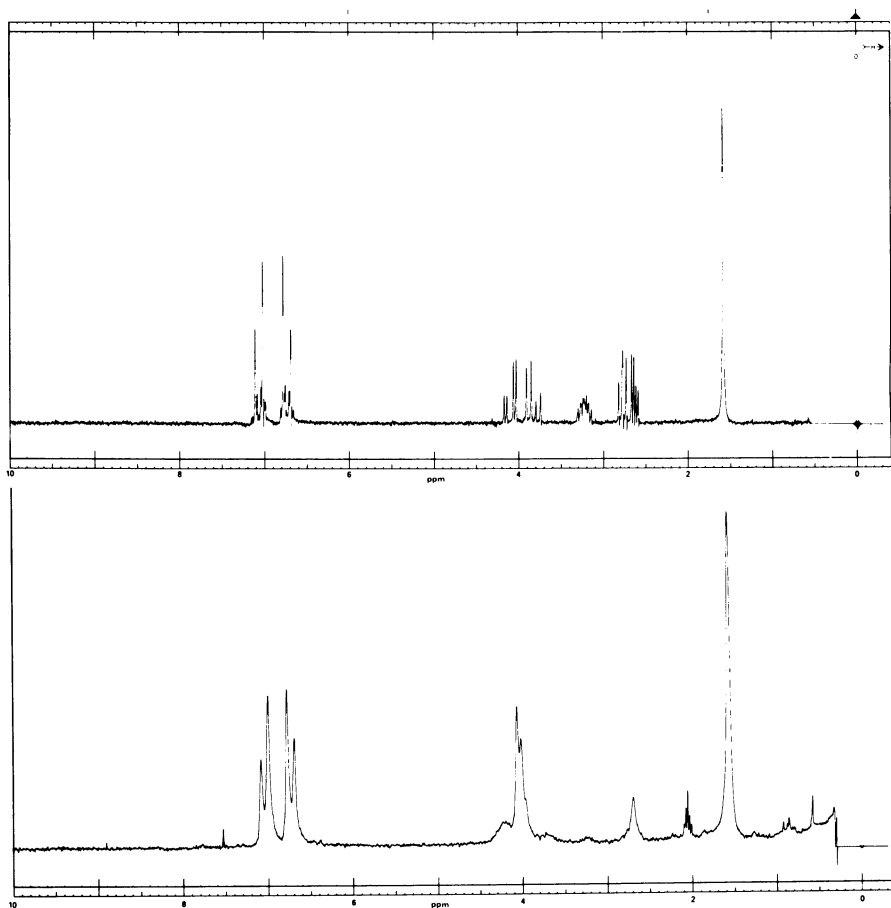
Figure 1.   Proton NMR spectra (100 MHz) of DER 332LC (upper) and Epon 1004 (lower).
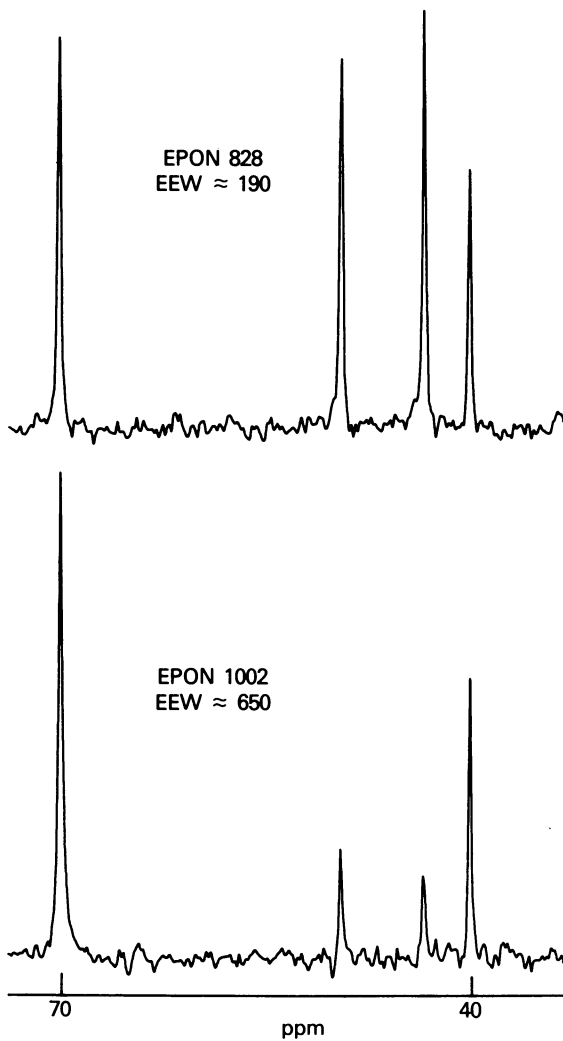
Figure 2. The 40–70 ppm region of the carbon-13 NMR spectra (15 MHz) of
two epoxy resins

This analysis assumes that a particular epoxy resin consists
of only one n-oligomer, which of course is not the true picture.
In order to illustrate that the n derived by the above equation
yields the average n that would be found by chemical analysis, we
generated a set of hypothetical oligomer mixtures and calculated
their EEW's based on carbon-13 nmr and chemical analysis. As
shown in Table I, the two methods give equivalent results.

Table I. Epoxide Equivalent Weights Calculated
for Four Hypothetical Epoxy Formulations

n-oligomer	mole percent of n-oligomer in formulation			
	a	b	c	d
0	5	3	63	3
3	8	5	10	2
5	6	2	8	75
8	10	8	5	9
10	15	72	8	5
15	56	10	6	6
EEW { chemical	1766	1532	568	1012
{ carbon-13	1760	1533	568	1008

Quantitative aspects

Carbon-13 nmr became an important experimental technique
only with the development of Fourier transform (FT) nmr. But
the FT nmr experiment requires attention to a number of factors
in order for the measurements to be quantitatively meaningful
(7,8,9). These may be divided into two catagories: instrumental,
which affect FT nmr of any nucleus; and those related to spin
dynamics, which for some nuclei, including carbon-13, demand
greater attention.

Among the instrumental factors is the power envelope
of the rf interrogating pulse. It must cover the spectral re-
gion of interest uniformly so that all nuclei being studied are
affected to the same degree. The filter used in the detection
system must also have uniform response across the spectrum.
Other instrumental considerations are computer related and in-
clude factors such as memory size, word length and ADC resolu-
tion (9). Most modern FT nmr spectrometer systems are designed
to satisfy the above requirements, but one must always verify
proper operating parameters for the analysis being run.

With regard to spin dynamics, two areas of concern in car-
bon-13 nmr are the spin-lattice relaxation time, T_1, and the

nuclear Overhauser effect,NOE. The relaxation time, T_1, is a measure of the recovery of nuclear magnetization to equilibrium after the rf pulse. In a given molecule, T_1's of the various carbons may vary widely. Since the accumulation of adequate signal to noise ratio in carbon-13 FT nmr is obtained by repetitively pulsing the nuclear system, one must assure that all nuclei have returned to equilibrium between pulses. The NOE is a result of the proton decoupling used to eliminate proton-carbon spin coupling. The carbon nmr signals are enhanced via the proton system, but the enhancement may not be the same for all carbons in a molecule.

Both relaxation effects and NOE can be dealt with in several ways for quantitative carbon-13 measurements (7,8). The approach we used involved gated decoupling to surpress NOE, and a sufficiently long delay time between pulses to assure complete recovery of carbon magnetization.

The delay time was determined by measuring the T_1's of the carbons of interest in several of the epoxy resin systems. The results, given in Table II, show that a delay time between pulses of 16sec (5 times the longest T_1 (8)) would be adequate for these materials. In our EEW determinations, we used a pulse delay of 35sec.

Table II. T_1 Values for Carbons of Interest

Resin		T_1 (sec)	
	44ppm	50ppm	70ppm
EPON 828	1.2	3.2	1.3
EPON 1001	1.2	2.9	0.4
EPON 1002	1.0	2.7	0.3

Results

Table III gives the EEW's we obtained using this carbon-13 approach for a series of commercial epoxy resins. It also gives the values obtained by chemical analysis and the values from the literature (10). The carbon-13 results fall into two groups. For the liquid resins carbon-13 nmr gives results generally lower than the ranges given in the literature. For the solid resins of medium EEW, the carbon-13 results are generally within the literature ranges. Except for two cases, the chemical results are 5-10% higher than the carbon-13 results, and are consistently higher than the literature ranges.

This carbon-13 nmr method for determining EEW has a number of features which make it worth consideration as an alternative

to other methods. The amount of sample required is 0.4g or less.
Neither precision weighings nor standardized solutions are need-
ed. The analyst is free for other tasks while the FT nmr spec-
trometer automatically accumulates the data. In an analytical
laboratory or quality control environment where EEW measurements
are made on a routine basis, calibration curves and standard
data acquisition procedures should result in measurement times
of 20 minutes or less.

Table III. EEW's Found by Carbon-13 nmr and Chemical Analysis

Resin	Carbon-13	Chemical	Literature[a]
DER 332LC	178	178	170-175
EPON 826	172	190	180-188
EPON 828[b]	176	194	185-192
EPON 828[c]	181	196	185-192
EPIKOTE 828	171	193	185-192[d]
ARALDITE 7071	522	529	450-530
EPON 1001	568	600	450-530
EPON 1002	686	762	600-700
EPON 1004	971	1086	875-1025

[a] Reference 10
[b] Manufactured in the United States
[c] Manufactured in Canada
[d] Assumed to be the same as the value for EPON 828

Experimental

The samples for the carbon-13 nmr measurements were $CDCl_3$
solutions (0.2g/ml solvent) of commercial samples of the epoxy
resins in 10mm o.d. sample tubes. The measurements were made at
15MHz with a JEOL FX60Q spectrometer system. A 90°(10μsec) pulse
was used with gated decoupling to surpress the NOE (7). The data
collection block was 2048 points for a spectral width of 2200Hz.
The observation filter was set at 2000Hz, substantially in excess
of the 1100Hz used for best signal to noise in the quadrature
detection mode. This assured negligible attenuation of the
signals of interest due to the Butterworth filter characteris-
tics. The data block was expanded by zero filling to 16,384
points before Fourier transformation. Exponential multiplica-
tion equivalent to a line broadening of 1.6Hz was applied. The
number of accumulations was 512. The pulse repetition rate was
35sec, longer than 10 times the longest T_1 of the carbons of
interest. Relaxation times, T_1, were measured by the inversion/
recovery method (11) on the solutions used for the quantitative
measurements. Chemical analysis (HCl titration, single determi-
nation) of epoxide equivalent weights were performed by Schwarz-
kopf Microanalytical Laboratory, Woodside N. Y.

Literature cited

1. Poranski, Jr., C.F., and Moniz, W.B., J. Coat. Tech., 1977,
   49, (632), 57.
2. Poranski, Jr., C.F., Moniz, W.B., Birkle, D.L., Kopfle, J.T.,
   and Sojka, S.A., "Carbon-13 and Proton NMR Spectra for Char-
   acterizing Thermosetting Polymer Systems: I. Epoxy Resins
   and Curing Agents", Naval Research Laboratory Report 8092,
   Washington, D.C., 1977.
3. Garroway, A.N., Moniz, W.B., and Resing, H.A., "Carbon-13
   NMR in Solving Macromolecular Problems", ACS Symposium
   Series, in press.
4. Zucconi, T.D., "Proceedings of the Fifth Conference on Com-
   posite Materials: Testing and Design", ASTM Special Publica-
   tion, Philadelphia, Pa., 1979, in press.
5. Dorsey, J.G., Dorsey, G.F., Rutenberg, A.C., and Green, L.A.,
   Anal. Chem., 1977, 49, 1144.
6. Hammerich, A.D., and Willeboordse, F.G., Anal. Chem., 1973,
   45, 1696.
7. Werhli, F.W., and Wirthlin, T., "Interpretation of Carbon-13
   NMR Spectra", Heyden and Son, Ltd., New York, 1976, p 264.
8. Shoolery, J.N., Prog. NMR Spectrosc., 1977, 11, 79.
9. Randall, J.C., "Polymer Sequence Determination; Carbon-13
   NMR Method", Academic Press, New York, 1977, Chap. 5.
10. Tanaka, Y., Okada, A., and Tomizuka, I., "Epoxy Resins",
    C. A. May and Y. Tanaka, Eds., Marcel Dekker, Inc., New
    York, 1973, Chap. 2.
11. Mullen, K., and Pregosin, P.S., "Fourier Transform NMR
    Techniques: A Practical Approach", Academic Press, New York,
    1976, p 65.

An Instrumental Method for Measuring the Sterilization Resistance (Blushing) of Can Coatings

W. RAUDENBUSCH, H. C. J. VENSELAAR, and D. M. PAUL

Koninklijke/Shell-Laboratorium, Amsterdam (Shell Research B.V.),
Badhuisweg 3, 1031 CM Amsterdam-Noord, The Netherlands

Of the various coating materials used for food- or beverage-containing cans epoxy resins are some of the most important. World-wide they account for about one third of the total coating materials employed in this market. While epoxies are important to the can-coating market, the reverse is also true: In 1976, epoxy resin consumption for can and container coatings was around 10 000 metric tons both in the US (1) and in Western Europe, making this the largest single outlet for epoxies in the entire coating field. Therefore, as a major producer of epoxy resins, we are devoting a considerable effort to this application.

One result of this development work is an instrument for accurately measuring a key property of can coatings, the sterilisation resistance. First, however, a brief description of can coatings and some of their properties is in order. The discussion will be limited to coatings to be applied to the interior of food- or beverage-containing cans since this application requires the highest chemical resistance. Most of the work described has been carried out with can lacquers of the solid epoxy resin/phenolic-formaldehyde (E/PF) type as these are the predominant type used in Western Europe.

Can Coatings and Some of Their Properties

E/PF can lacquers usually are unpigmented and applied at dry film thicknesses around 5 μm (0.2 mil). On stoving at or above 200 °C glossy, clear coatings with a yellow-golden colour ("gold lacquers") are formed. One of the most important requirements which can linings must meet is a high sterilisation resistance. This implies that the linings should not be damaged by the food contents during a steam sterilisation (or pasteurisation) process applied after filling and closing of the cans. Unsatisfactory sterilisation resistance usually shows up as a haziness or cloudiness in the coating, a phenomenon which is called "blushing". More pronounced blushing is usually accompanied by some loss of surface gloss while in even more extreme cases the coatings become rough and milky-white. Only slight blushing, however, is sufficient to cause the rejection of the corresponding lacquer by the can-coating industry.

Nature and Assessment of Blushing

Some years ago we investigated the nature of the blushing
phenomenon. To this end, E/PF can linings on tinplate panels
were exposed to water and steam at 121 °C for 90 minutes. The
panels were then examined by optical and scanning electron micro-
scopy. From that work the following conclusions could be drawn:

1. The blushing effect is caused by a large number of voids present
   throughout the coatings.
2. The intensity of blushing is proportional to the number of voids.
3. Most of the voids are spherical, with a diameter of around 1 μm
   (0.04 mil), and their size distribution is rather narrow.
4. Voids near the surface tend to result in bubble and/or crater
   formation. Coalescence of several craters may lead to larger
   cavities. This explains the loss of gloss and the surface rough-
   ness observed on heavily blushed specimens.
5. Blushing only becomes visible during cooling of the test panels
   to ambient temperature.

Our theory regarding the formation of these voids is that they are
caused by excess water absorbed homogeneously (i.e. in unit below
the limit of visibility, <25 nm) during the sterilisation test. On
cooling, this water agglomerates in spherical clusters of about 1 μm
diameter. This is analogous with the well-known situation where
excessive water absorbed in other glassy polymers (e.g. polystyrene)
can cause microcavities and visible defects (2,3). The reasons why
some can coatings are more susceptible to excessive water absorp-
tion – and thus blushing – than others still are not completely
clear. One well-known and easily proven fact is that insufficient
cure can lead to blushing. In addition, there are other known
causes, such as the presence of traces of water-soluble materials
(e.g. inorganic salts) in the coatings.

Blushing is usually detected by visual examination of samples
of coatings before and after sterilisation. For more quantitative
assessments sterilised panels are usually compared with a set of
reference panels showing different degrees of blushing, according
to an arbitrary scale such as

     5: no blushing
     4: very weak blushing
     3: weak blushing
     2: blushing
     1: heavy blushing
     0: very heavy blushing.

These methods, however, suffer from various drawbacks:

– Because they rely on visual observation they are subjective.
– Considerable time and practice are required to acquire the obser-
  vational skill necessary for quantitative assessments.
– The colour of the coating, if not exactly the same as that of the
  reference panel, can interfere with the assessment.

- The substrate type and quality as well as the illumination play a critical role in assessments in the weak to very weak blushing range (ratings 3-5). In our experience coatings showing only very weak blushing (4) are generally judged acceptable by the can industry, perhaps because the blushing is then noticeable only under ideal substrate and light conditions.
- Cases of more pronounced blushing (0-2), where the phenomenon as such is readily recognised, are nevertheless difficult to classify. This makes it often problematic to detect trends which might be valuable for further lacquer development work.

For all these reasons the development of an instrumental method which would allow rapid, accurate and reproducible blush measurements was thought very desirable.

The Blushmeter

Several optical techniques were first screened to ascertain their suitability for blush measurement. Of these, the back-scattering of laser light appeared most promising, and this technique was thus pursued further. It is already known from experience that the visual assessment of (weak) blushing is strongly dependent on the angle of observation. According to the scattering theory of Mie (4) it is predicted that the intensity of scattered light should be influenced by the intensity and wavelength of the incident light, the size, number and refractive index of the scattering centres, and the scattering angle. Further, theory predicts that there should be an angle at which the back-scattering intensity reaches a maximum. In our case, however, the theory can only be used to indicate the critical parameters owing to the complexity of the medium to be measured: In addition to the scattering from the inside of the coatings there is reflection and scattering at both the coating/air and the coating/substrate interfaces. Thus the transmitted, reflected and scattered light will also depend strongly on the angle of incidence of the light beam. Further complications arise from imperfections or non-uniformities both in the coatings and on the substrate.

In view of the complexity of the physical situation an adjustable laboratory set-up was constructed first to investigate the theoretical predictions and to define the conditions for an optimised apparatus. The principal components of this arrangement are shown in Fig. 1, and its scattering geometry in Fig. 2. The light source was a 15 mW He-Ne laser whose light was deflected by a mirror onto the test panel. At a distance of about 30 cm from the panel the scattered light was collected by a 1:1.3/50 mm lens and detected by a silicon photodiode whose output was amplified and read out on a digital voltmeter. In order to diminish the effect of accidental coating irregularities (scratches etc.) the collection of the back-scattered light was integrated over a larger surface by expansion of the laser beam. This was accomplished by fitting a beam expander (Oriel, type 1590) in front of the laser. For most of the work a five-fold beam expansion was used; the incident laser beam then had a diameter of 0.5 cm.
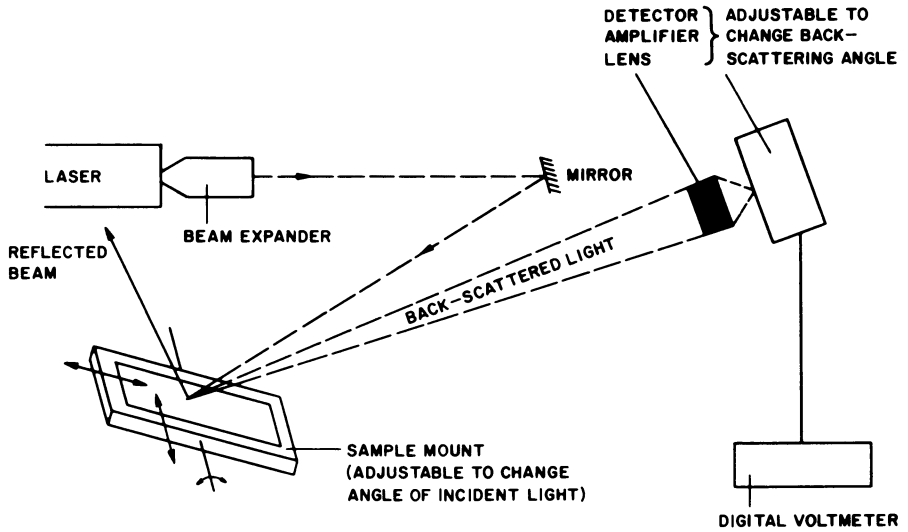
Figure 1.   System components of experimental apparatus
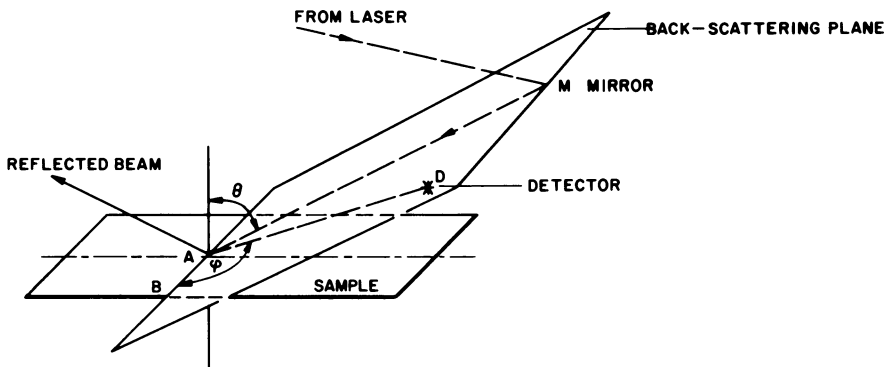
Figure 2.   Scattering geometry

This laboratory set-up permitted accurate variations of both the angle of incidence (θ) and the scattering angle (ϕ). The test panels were mounted magnetically and could be shifted two-dimensionally to allow scanning of their entire surface.

With this apparatus a set of 15 x 6 cm test panels (A-F, 5 µm E/PF coatings on tin plate, stoved at 200 $^\circ$C for 10 min, and sterilised in water at 121 $^\circ$C for 90 min) showing various degrees of blushing was evaluated. At fixed angles of incidence (θ) the scattered light was measured over a range of angles ϕ from 10° to 80° in one quadrant of the backward scattering plane (defined by M, A and B in Fig. 2). A typical plot is shown in Fig. 3, from which it is clear that, in accordance with the theory, there is a back-scattering maximum lying between 70 and 85°. For technical reasons we adopted a standard back-scattering angle ϕ of 70° in our subsequent work. In a similar manner we varied the angle of incident light θ and found a maximum of scattering at about 60° (Fig. 3).

With a fixed optical geometry ($\theta = 60^\circ$, $\phi = 70^\circ$) the set of test panels A-F was then measured systematically. On each panel about 50 individual measurements were made at different spots, covering the whole surface. The mean instrument readings (in mV) correspond very well with the blush levels determined visually by two expert observers (see the table below). In particular, the back-scattering method appeared sufficiently sensitive to distinguish between the various degrees of weak blushing, the range where alternative optical detection methods all had failed.

Test panel	No. of points measured	Mean reading, mV	Standard deviation, mV	Visual blush assessment	Visual rating
A	47	21	4	trace	4-5
B	48	33	5	very weak	4
C	52	49	16	weak-very weak	3-4
D	48	70	24	weak	3
E	52	148	42	blushing	2
F	64	614	113	heavy	1

In further work the 15 mW laser was replaced by a smaller and less expensive one having an output of only 2 mW. Similar good correlation with visual assessment of blushing was found although the actual mV readings of course were lower.

Based on the experience gained with the laboratory set-up, a prototype instrument was then built, the Shell "Blushmeter" (Fig. 4). A 2 mW He-Ne laser is used and the optical arrangement is essentially the same as described above, with ϕ and θ fixed at 70° and 60°, respectively. Flat test panels are clamped magnetically onto a horizontal sample table which can be displaced (at 0.2 cm/s) in the X and Y directions by means of two electric stepping motors. Digital read-out of the actual position permits accurate and reproducible scanning of the entire panel surface.
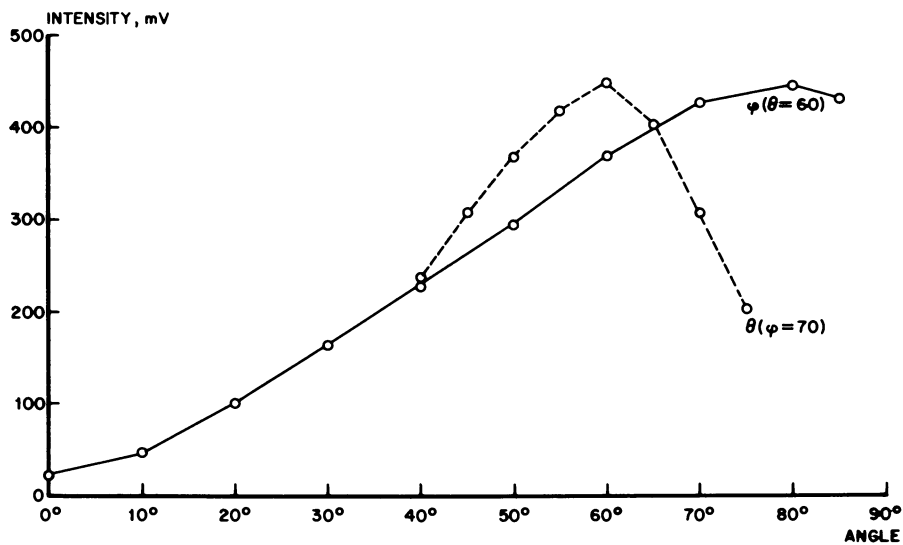
Figure 3.   Dependence of scattered light intensity on back-scattering angle φ and incident beam angle θ
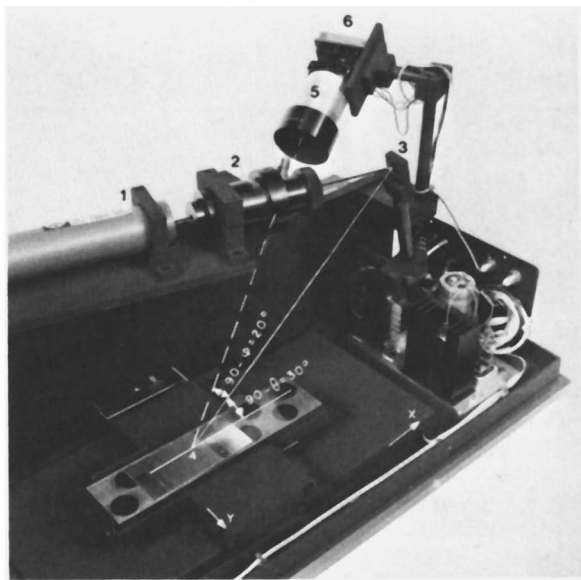
Figure 4.   Prototype blushmeter: (1) laser; (2) beam expander; (3) mirror; (4) panel on sample table; (5) lens; (6) photoamplifier

For the time being, scanning is carried out by manual control of the stepping motors; between 10 and 50 individual readings are taken over the whole panel surface, depending on the uniformity of the blushing effect, in order to obtain a statistically sound value. Since this is somewhat time-consuming, the instrument is currently being modified to allow automatic scanning and data processing.

Typical readings obtained with this instrument for various degrees of blushing were the following:

	Visual rating	Blushmeter reading, mV
No blushing	5	1– 5
Very weak blushing	4	6– 14
Weak blushing	3	28– 35
Blushing	2	64– 69
Heavy blushing	1	120–134
Very heavy blushing	0	226–278

In our experience the prototype "Blushmeter" allows accurate numerical assessment of both weak and heavy blushing. The only requirement for a comparison of the performance of different coatings is that they be applied (at uniform thickness) to flat substrates of the same type and quality. The operation of the Blushmeter is simple and does not require special skills. An interesting observation is that the readings are insensitive to colour changes occurring during the sterilisation test.

In our Amsterdam laboratory the prototype Blushmeter has already helped us to define certain parameters leading to blushing in can lacquers. As a consequence we have been able to adapt certain grades of solid epoxy resin to better meet the needs of the can-coating industry.

Abstract

Internal coatings for food and beverage cans are an important application for epoxy resins. Such coatings must resist the heat sterilisation (or pasteurisation) process to which the filled cans are eventually subjected. Unsatisfactory sterilisation resistance appears as haziness in the otherwise clear coatings, an effect called "blushing". In typical cases the blushing effect was found to be caused by many small (~1 µm) voids inside the coatings. Blushing is customarily assessed by visual methods that require considerable experience and are difficult to quantify. Based on the back-scattering of laser light, an instrument has been developed with which accurate measurements of various degrees of blushing can be made. A 2 mW laser beam is directed onto a flat test panel at an angle of 60°. Back-scattered light is detected by a silicon photodiode, amplified and read out on a digital voltmeter. The

instrument allows reproducible scanning of the whole panel surface.
Instrument readings on coatings showing widely differing degrees
of blushing agreed well with visual ratings. The instrument permits
objective, accurate and reproducible assessments to be made by
inexperienced persons. Moreover, instrument readings were found to
be insensitive to colour changes frequently occurring during
sterilisation.

Acknowledgement

Literature Cited

1. Chemical Economics Handbook, Stanford Research Institute,
   March 1978.
2. Crank, J.; Park, G.S. "Diffusion in Polymers": Academic Press,
   London, 1968.
3. Pogany, G.A. Polymer, 1976, 17, 690.
4. Born, M.; Wolf, E. "Principles of Optics: Electromagnetic
   Theory of Propagation, Interference and Diffraction of Light":
   Pergamon Press, Oxford, 1975.

Phenalkamines—A New Class of Epoxy Curing Agents

ROBERT A. GARDINER and ANTHONY P. MANZARA

3M Company, Saint Paul, MN 55101

Because of proliferating constraints on solvent-based coatings, new materials are being developed for high solids or waterborne coatings. A class of curing agents for epoxy coatings based on proprietary chemistry has been developed by the 3M Company. These materials are called phenalkamines, a term coined to indicate their alkyl-aromatic structure and thereby differentiate them from the currently more familiar curing agents such as polyamides and polyamines.

As a new family of curing agents, the phenalkamines offer a unique combination of properties making them particularly well suited for ambient temperature cured high solids epoxy coatings. Studies on the reactivity of these curing agents and on the properties of certain cured formulations are presented.

Experimental

Materials used were the standard commercially available grades. "CARDOLITE" Brand NC-513 is 3M's monofunctional epoxy reactive diluent; CR-100, 3M's flow control agent; DC-200, Dow-Corning antifoam; Cab-O-Sil[R], Cabot fumed silica; Epon 1001-X-75, Shell solid epoxy resin as 75% solution in xylene; Tint-Ayd[R] EP-30-01, Daniels predispersed titanium dioxide; liquid epoxy resin, standard bis-phenol-A diglycidyl ether of epoxide equivalent weight 190 grams/equivalent.

Amine values are reported as milligrams of KOH equivalent to the base content of one gram of sample, and are obtained by titration with perchloric acid in acetic acid solvent using methyl violet indicator.

The weight per active amine hydrogen is estimated from the assumed chemical structure.

Viscosities were measured using a Brookfield Model LVF Viscometer. Gel times were determined by mixing a quantity of material (50 g unless otherwise stated) manually with a wooden spatula blade and recording the time elapsed before the blade was immobilized by the cured material.

Color was determined by visual comparison of the sample with a set of liquid color standards.

Pigmented coatings were prepared by combining the fillers and additives with the epoxy resin using a high speed high shear mixer, then passing the suspension through a paint mill to disperse the pigment more completely. Curing agent was then added and stirred in manually for the small samples used in the study. Coatings were applied with a knife coater (unless otherwise specified) to a nominal thickness of 10 mils. (0.010 inch.)

Spot tests were done after the one week ambient temperature cure by keeping the test area wet with 15% acetic acid (in water) for 48 hours.

Chemical resistance immersion tests were done on cured discs (20.15 ± 0.15 g) 2.75 inches in diameter and approximately 0.2 inches thick. These were prepared by manually mixing the appropriate ratio of resin and curing agent, removing the air bubbles by centrifugation, and pouring the mixture into tared aluminum dishes. After seven days at room temperature the discs were weighed, their surface hardness measured using a Shore "D" durometer, and then immersed in the test solutions. After the test time period had elapsed, the samples were removed, dried with a paper towel, allowed to stand for one hour at room temperature, and the weight and hardness remeasured.

In near infrared spectroscopic (NIR) cure rate studies, a small amount (10-15 g) of sample was manually combined using the indicated ratio of materials. After the bubbles had been removed via centrifugation, the mixture (about 1 g) was poured onto a microscope slide prepared with a 1 mm spacer window cut from foam tape with adhesive on both sides. Another slide was placed on top, and a zero-time measurement was made on the Cary 14 spectrophotometer. The absorption at 2.205 μ was used as a measure of the amount of unreacted epoxy resin. The sample was kept at the appropriate temperature and spectra were measured at the indicated times.

Results and Discussion.

Curing Agent Properties. Table I gives some specific properties on the three commercial phenalkamines, namely "CARDOLITE" Brand NC-540, NC-541 and NC-542. The three products have gel times ranging from 40 minutes up to 2 hours with a variation in mixing ratio from 40-100 parts per hundred parts resin. Viscosities cover the range from 2500 cps to 40,000 cps.

Young and Howell[1] have suggested that 100% solids epoxy coatings will be most suitable for use as heavy duty maintenance, including marine coatings, in-place decorative coatings, and heat-converted systems for product finishing. Desirable properties for curing agents for "heavy duty maintenance" are low viscosity, superior chemical resistance, and some degree of flexibility. For in-place decorative coatings, the curing agent

requirements are good appearance and epoxy-like properties.

Some features not mentioned by Young and Howell are also important, i.e., handling characteristics, cure rate, safety and cost efficiency. In Table II these desirable properties are listed, and commercial types of curing agents are rated on each property. In the rating scheme used, "*" indicates good, "+" indicates marginally acceptable, and "-" indicates unsuitable.

When rating "appearance", the color of the curing agent itself plus its tendency to blush, ability to self level and sensitivity to moisture in formulated coatings were all taken into consideration. Experience has shown that for a long "pot life" in an ambient cured formulation one must forego a "fast cure". Similarly to obtain a "fast" and/or "low temperature" cure, one must forego a long "pot life". Plural component application equipment resolves this dilemma for those curing agents with immediate compatibility with the epoxy resin. With some state-of-the-art curing agents an induction period is recommended, during which the first stage of reaction produces adducts which are miscible with the resin. 3M's phenalkamines are immediately compatible with epoxy resin, require no induction period, and are ideally suited for use with plural component equipment.

An examination of Table II illustrates the previously mentioned unique combination of properties of the phenalkamines.

Phenalkamine properties are positioned roughly between those of the polyamines and polyamides. They combine the best properties of each of these familiar types of curing agents. The phenalkamines have an intermediate viscosity, the chemical and hydrolytic resistance of the polyamines, and the low toxicity of the polyamides. They have the fast cure and ability to cure at reduced temperatures of the polyamines while exhibiting better compatibility than either the polyamines or the polyamides. The phenalkamines also provide flexibility comparable to the polyamides with similar easy-to-use, relatively non-critical mix ratios.

Table II also rates the properties of amidoamines and cycloaliphatic amines. None of these curing agents appear to satisfy all of the desired properties. There are clearly some unfulfilled needs here; however, the particular combination of properties of the presently commercial phenalkamines comes closest to satisfying the requirements. They are quite suitable for high solids systems.

The presently commercial phenalkamines have exhibited shortcomings for certain applications where lighter color or lower viscosity were required. To offset these limitations, 3M has introduced two new phenalkamines on an experimental basis. These products have properties as shown in Table I. "CARDOLITE" Brand NC-543 is lighter in color but otherwise similar to "CARDOLITE" Brand NC-540, while "CARDOLITE" Brand NC-545 is lighter in color and lower in viscosity than any of the earlier phenalkamines.

The color of the new phenalkamines makes it easier to have

Table I

Phenalkamine Curing Agent Properties

	Commercial			Experimental	
	NC-540	NC-541	NC-542	NC-543	NC-545
Amine value	520	340	470	520	480
N-H Eq. Wt.	70	135	75	75	80
Viscosity, cp, 25°	2500	40,000	3500	2500	350
Color, Gardner	16	17	16	10-12	10-12
Odor	---------Slight Amine------------				
Gel time, min.	40	110	90	45	50
Mixing ratio, phr (Liquid Epoxy)	40-60	50-100	40-60	40-60	40-60

Table II

Comparison of Properties of Classes of Curing Agents[a]

Property	Type of Curing Agent					Cyclo-Ali-phatics
	Phenalkamines Expt'l.	Comm.	Poly-amides	Poly-amines	Amido-amines	
Low viscosity	*	+	-	*	*	*
Chemical resistance	*	*	+	*	-	*
Appearance	*	+	+	+	+	*
Low toxicity	(b)	*	*	-	+	+
Long pot life	-	-	*	-	*	-
Fast cure	*	*	-	*	-	*
Low temperature cure	*	*	-	*	-	+
Epoxy compatibility	*	*	-	+	-	+
Cost effective	*	*	*	*	*	-

(a) *, good; +, marginally acceptable; -, unsuitable
(b) * for NC-543, + to - for NC-545

coatings of any color including white, pastels, and vivid dark colors. The reduced blushing tendency of NC-545 allows the easy preparation of high gloss colored or clear coatings. The lower viscosity of the new material allows formulation of coating systems with less solvent content.

Cure Rate Studies. The literature on curing of epoxies indicated two ways to quantitatively assess the difference in cure rate of various curing agents. Fava has reported on cure mechanism studies using differential scanning calorimetry[2] and Dannenberg of Shell has reported on epoxy-cure mechanism studies by near infrared spectroscopy[3] (NIR).

The use of NIR, in the study of epoxy curing, is also discussed in Lee and Neville's Handbook of Epoxy Resins[4]. The NIR method was selected for this study due to its speed and ease of use.

In the NIR studies, 1 mm thick samples were used, prepared by using a 1 mm spacer between two microscope cover slides. Because of the small size (1 g) and thickness (1 mm) of the samples the results obtained in this study relate very well to the cure which would take place in an actual coating. The absorption at 2.205μ was used as indicative of unreacted epoxy groups. The reaction rate (cure rate) is conveniently plotted as percent unreacted or residual epoxy vs. cure time to get curves such as are shown in Figure I. In these curves degree of cure increases as residual epoxy decreases, i.e., the curve drops.

In the case of a simple mixture of epoxy resin with curing agent, although NC-540 (top curve, Figure I) cures the epoxy rapidly through 24 hours the reaction essentially stops with 25% of the initial epoxy concentration left untouched. This is in spite of use of a stoichiometric amount of curing agent. This behavior is typical for most, or all, curing agents at room temperature because as curing takes place, a three-dimensional structure is formed - which interferes with the free translational movement of the reacting molecules. As rigidity increases, further interference with the vibrational movement of the reacting groups occurs to where they simply can no longer get close enough to each other to react. The reaction becomes arrested or "frozen" in place.

A. M. Partansky[5] has described this effect. He indicates that "completeness" of the reaction can be improved by increasing the mobility of the reacting molecules or groups which can be accomplished in a number of ways, including:

1. Increasing the amplitude of the vibrational movement of the reacting components by increasing their energy - e.g., raising the temperature of the system.

2. Providing for a greater freedom of molecular movement by increasing the fluidity of the system. The use of diluents, either reactive epoxy types or inert solvent types, is one way of increasing the fluidity (and decreasing the crosslink
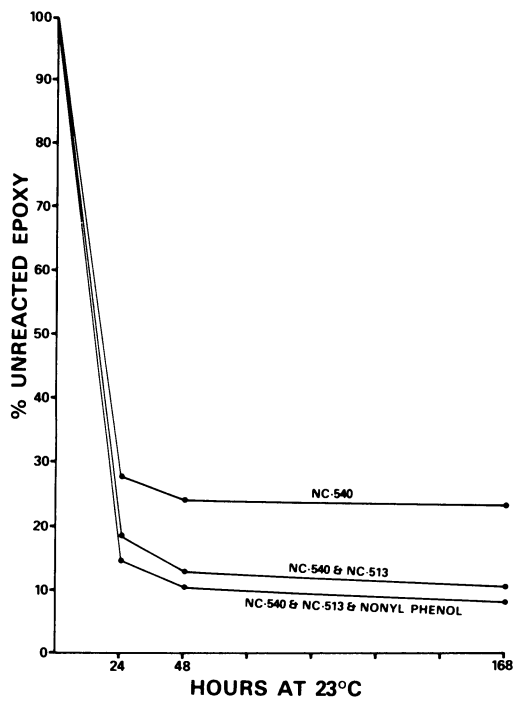
Figure 1.

density) of a given system. Since solid epoxy resins con-
tain fewer epoxy groups for a given weight, their use also
provides lower crosslink density and allows the cure reac-
tion to proceed further to completion.

The effect of adding a mono-epoxy diluent to reduce the
cross-linking density is shown in Figure I, middle curve. The
reactive diluent NC-513 has been added to the NC-540-cured system
and this allows the cure to proceed to where only 11% unreacted
epoxy is present after 7 days of reaction. Surprisingly, the NC-
540/NC-513 system has an extended pot life even though the maxi-
mum cure is achieved faster.

An explanation is apparent by examining the cure curve. Be-
cause the diluent reduces the crosslinking density, it allows the
epoxy to react more completely. The greater extent of reaction
tends to compensate for the otherwise possibly deleterious effect
of the diluent on the properties of the cured system. The use of
diluent also provides the practical advantage of lowered viscosi-
ty in a formulated system. Since excessive use of diluents can
lead to poor chemical resistance and reduced mechanical strength,
recommended amounts should not be exceeded.

An accelerator-diluent such as nonyl phenol can be employed
to increase both the rate of cure and the completeness of cure,
as shown in the bottom curve in Figure I.

In actual coatings applications the first few hours are im-
portant. The cure rate of the NC-540/NC-513 system during this
period is shown in Figure II. It can be seen that better than
75% of the cure is achieved in only seven hours.

Raising the temperature of the system allows one to obtain
proper cure in minutes rather than hours (Figure III). At 65°C
(149°F) complete cure is achieved in 45 minutes. At 100°C
(212°F) it takes only 18 minutes and 150°C (302°F) a mere 6 min-
utes. Actually the cure time at 150°C is probably closer to 2
minutes since equilibration to oven temperature takes 3-4 min-
utes.

Significance of Faster Cure. This rapid and complete cure
of two-part epoxies at a relatively low temperature has not been
exploited in industrial finishing operations to the extent it
might be. Such systems formulated to high solids content would
be quite suitable for many priming applications and could allow
significant time and energy savings by allowing reduced cure-bake
temperatures and/or cure times. Oven through-put could be in-
creased dramatically.

In maintenance applications and other in-place coating work
it is often desirable to have a formulation which cures at tem-
peratures below the normal room temperature. For this reason it
was of interest to investigate the cure rates of various epoxy
resin-curing agent-diluent-accelerator mixtures at lower tempera-
tures.

The effect of reducing the temperature on the NC-540 cured
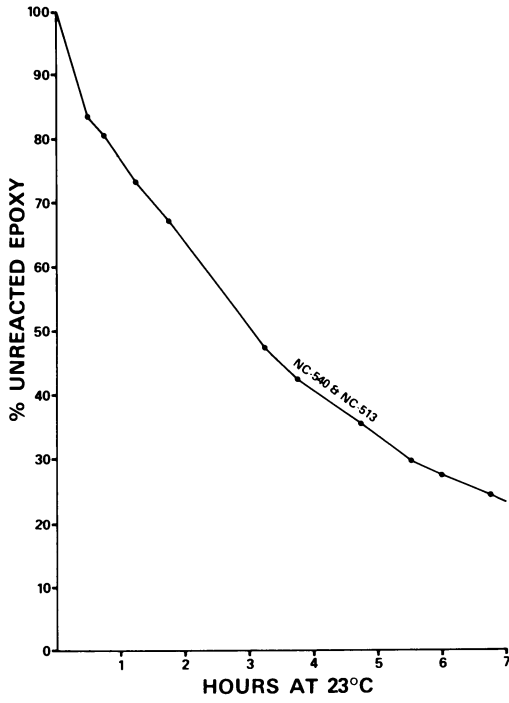
Figure 2.
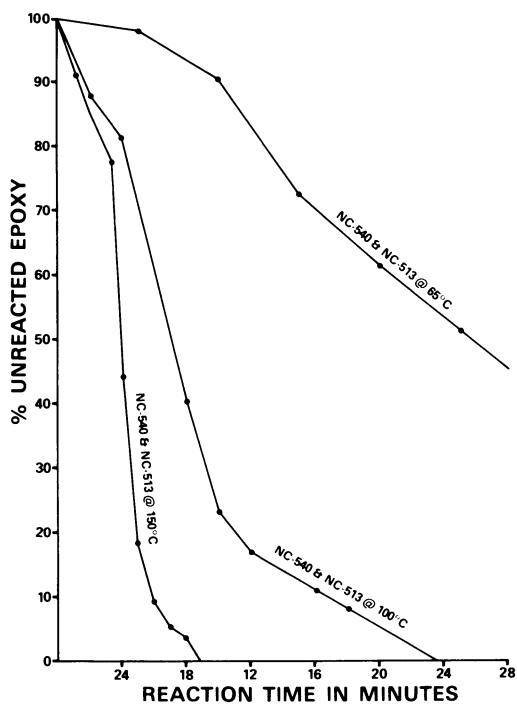
Figure 3.

system is shown in Figure IV. At 4°C (40°F) the cure is slowed
down because of the loss of mobility (viscosity increases) at the
low temperature. Again, the addition of NC-513 and nonyl phenol
helps. In this case, the combination of NC-513 with DMP-30 gives
the most completely cured system. After seven days the cure state
of the DMP-30 accelerated mixture is actually at about the same
position it was at in 7 days at room temperature without the acce-
lerator. However, at room temperature this degree of cure is
attained in 24 to 48 hours.

A number of materials have been examined in the NIR cure rate
studies. Figures V and VI show some comparisons of several curing
agents at 23°C (73°F) and at 4°C (40°F) respectively. In these
cases all of the curing agents were used at stoichiometric ratios
with the liquid Bisphenol A epoxy. In general, the phenalkamines
attain their maximum cure very rapidly at room temperature and
achieve satisfactory cure even at reduced temperatures. This is
in contrast with most of the other types of curing agents. This
property reduces the probability of damage to a phenalkamine-cured
coating should unexpectedly low temperatures prevail between ap-
plication and use.

Formulation and Testing of Coatings. Table III shows two
solvent-free liquid epoxy coating formulations (Formulation I and
2). Although these systems are somewhat limited by their pot life
which is only 30-50 minutes, they are suitable for roller and
brush applications where small amounts are mixed. They are also
suitable for flooring applications where the mixed material is
quickly spread over the prepared surface, which precludes the oc-
currence of an exotherm and allows 2-3 hours working time. For
spray applications, a dual-component airless spray system with an
in-line mixer has been used successfully with these formulations.
In-line mixing requires immediate compatibility of the curing
agent with the resin, a characteristic of phenalkamines.

Modifying the formulations by adding enough solvent converts
them to 85% solids as shown in Table III (Formulations 3 and 4).
Now the viscosities are only 300-500 cps, and they are easily
sprayable using conventional low pressure sprayers. In addition,
the pot life for the NC-542 cured system has been extended to 2
hours and 20 minutes.

Substituting a solid epoxy for the liquid epoxy as shown in
Table III (Formulations 5 and 6), extends the pot life out to 6
hours at 60% volume solids. Both the solid and liquid epoxy based
systems give excellent coatings with good corrosion resistance.

Young and Howell[1] predicted a potential for high to 100% sol-
ids epoxy coatings in heat-converted systems for product finish-
ing. They list potential uses in can coatings, drum linings, coil
coatings, appliance primers, automotive primers, and automotive
guidecoats. Low viscosity applications are possible through em-
ployment of a heated Part A and Part B mixed at the point of ap-
plication. Heating NC-540 and NC-545 to 100°F reduces the
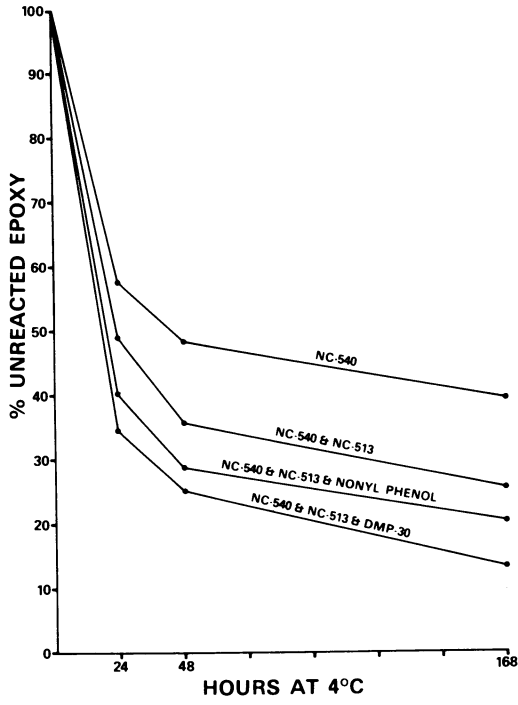
Figure 4.
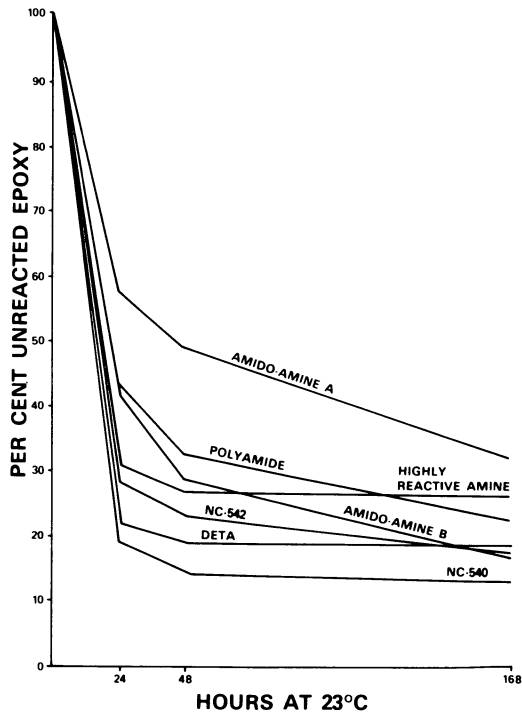
Figure 5.
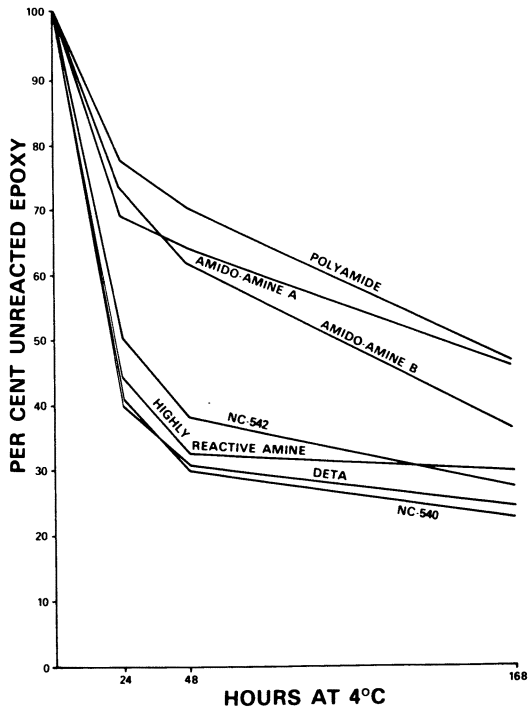
Figure 6.

Table III

Coating Formulations with Phenalkamines

Formulation #	1	2	3	4	5	6
Part A	(Parts	by weight)				
Liquid Epoxy Resin	100	100	100	100	–	–
Solid Epoxy Resin	–	–	–	–	133	133
CARDOLITE NC-513	20	20	20	20	20	20
TiO$_2$	7	7	7	7	7	7
Cab-O-Sil	0.5	0.5	0.5	0.5	0.5	0.5
CR-100	0.2	0.2	0.2	0.2	0.2	0.2
Glycerine	0.15	0.15	0.15	0.15	0.15	0.15
DC-200	0.1	0.1	0.1	0.1	0.1	0.1
Part B						
CARDOLITE NC-542	45	–	45	–	17	–
CARDOLITE NC-545	–	45	–	45	–	16
MIBK/Xylene 50/50	–	–	22	22	42	42
Mix Properties						
Volume % Solvent	–	–	15	15	40	40
Gel time (1 qt., minutes	50	30	140	60	>360	>360
Mix Viscosity	3150	1375	390	240	255	245

Table IV

IMMERSION TEST RESULTS[a]

Curing Agent Phr[b]	NC-540 40	NC-541 50	NC-542 40	NC-543 40	NC-545 40
Initial hardness	85	80	83	83	84
Final properties[c]					
10% aqueous acetic acid					
Weight gain (%)	4.0	1.5	3.5	2.7	11.1
Hardness (Shore D)	83	80	75	80	73
10% aqueous NaOH					
Weight gain (%)	0.45	0.25	0.20	0.3C	0.33
Hardness (Shore D)	83	82	82	83	83
30% aqueous H_2SO_4					
Weight gain (%)	0.5	0.3	0.4	0.4	2.0
Hardness (Shore D)	85	80	82	83	82
H_2O					
Weight gain (%)	0.4	0.4	0.3	0.25	0.29
Hardness (Shore D)	84	80	83	83	83

(a) For procedure see experimental section
(b) Parts per hundred of standard liquid epoxy resin, eew 190
(c) After seven days immersion in specified solvent at 23°C.

viscosity to 100 cps or less. Phenalkamines are excellent for
factory-applied industrial finishes.
    High solids phenalkamine epoxies are used in primers, indus-
trial maintenance coatings, and marine coatings for their improved
chemical and moisture resistance. In acetic acid spot tests on a
liquid epoxy resin coating cured with the designated curing a-·
gents, "CARDOLITE" Brand NC-540 and DETA performed well while the
polyamide-cured coating disintegrated. Immersion tests show excel-
lent retention of hardness and only minor weight gain in aqueous
acids and bases. (See Table IV.)

Conclusions.
    In comparing phenalkamines and other currently available ep-
oxy curing agents against a list of properties desirable for a
curing agent for high-100% solids epoxy coatings, the phenalka-
mines are shown to have the best combination of properties for
such applications. The practical utility of the phenalkamines has
also been demonstrated by their incorporation into high solids and
100% solids epoxy formulations.
    By spot-tests on coatings and immersion-tests on castings the
excellent chemical-resistance of phenalkamine-cured epoxy systems
has been demonstrated. In addition, near-infrared cure studies
have documented the rapid complete cure of epoxies at room temper-
ature and also satisfactory cure at reduced temperatures when
phenalkamines are used as the curing agents.
    This unique combination of properties of the phenalkamines
suggests they should be the curing agents of choice not only for
high solids field applied industrial coatings, but also for heat-
cured factory applied industrial finishes

References.
    1. R.G. Young and W.R. Howell, Jr., "Epoxies Offer Fulfill-
    ment of High Performance Needs", Modern Paint and Coatings,
    43-47 (March 1975)
    2. R.A. Fava, "Differential Scanning Calorimetry of Epoxy
    Resins", Polymer 9, 137-151 (1968)
    3. H. Dannenberg, "Determination of Functional Groups in
    Epoxy Resins by Near-Infrared Spectroscopy", SPE Transactions
    78-88 (January 1963).
    4. H. Lee and K. Neville, "Handbook of Epoxy Resins" Chapter
    4, page 19, McGraw Hill Book Company (1967).
    5. A.M. Partansky, "A Study of Accelerators for Epoxy-Amine
    Condensation Reactions", Advances in Chemistry Series, Epoxy
    Resins, page 92, Chapter 4 (1970).

The Effect of Alkyl Substituents on the Properties of Cured Hydantoin Epoxy Resins

E. H. CATSIFF, R. E. COULEHAN, J. F. DiPRIMA,
D. A. GORDON, and R. SELTZER

Research Department, Plastics and Additives Division, CIBA-GEIGY Corporation, Ardsley, NY 10502

Epoxy resins based on glycidylation of bisphenols, cresol and phenol novolacs, polycarboxylic acids, polyols, amines, and aminophenols have been long known. Epoxidized linear and cyclic olefins have also been used as specialty epoxy resins. More recently, glycidylated heterocycles have been introduced, initially as specialty resins promising improved resistance to weathering. One heterocycle in particular, the hydantoin ring, has become of particular interest as an epoxy substrate (1).

A comprehensive review was given by Habermeier (2) of many types of glycidylated resins based on the hydantoin ring. Much of the emphasis in his account was on the variations possible in the position of the glycidyl groups: direct substitution on either or both of the N atoms of the hydantoin ring, glycidoxy-alkyl substitution in the same positions, and glycidyl esters and ethers based on substituents in those positions. Also shown were bis(hydantoins) in which the hydantoin rings were linked by methylene or other alkylene groups, diester chains, or the β-glycidoxytrimethylene group derived from epichlorohydrin.

Habermeier also pointed out the ready synthesis of hydantoins from aldehydes or ketones; the substituents in the 5-position of the ring were thus determined by the carbonyl compound used as starting material. Most of the examples cited had methyl, ethyl, or cyclopentamethylene substitution in the 5-position. Data were presented on the properties of cured resins with these substituents and with a broad variety of the other structural features mentioned.

In this paper we report on a series of hydantoin resins derived from a somewhat broader choice of aldehydes and ketones, and show how the 5-position substituents interact with several variants of common epoxy curing systems to produce the properties of the final cured systems.

Hydantoin-Based Epoxy Resins

The simplest class of hydantoin epoxy resins are the
1,3-diglycidylhydantoins of Formula II. They were readily
prepared from the 5,5-dialkyl or 5-monoalkylhydantoins and
epichlorohydrin. The hydantoins (Formula I) were prepared
from ketones or aldehydes via the Bücherer reaction.

$$R_1-\overset{O}{\overset{\|}{C}}-R_2 \;+\; HCN \;+\; NH_3 \;+\; CO_2 \;\dashrightarrow\;$$

I
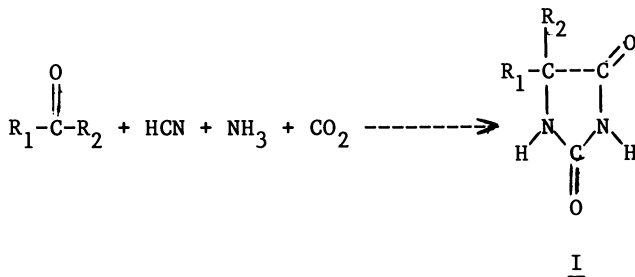
Conversion of the hydantoins to epoxy resins was straight-
forward.

$$\underline{I} \;+\; \underset{CH_2-CH-CH_2Cl}{\overset{O}{\diagup\diagdown}} \;\;\underset{aq.\ NaOH}{\overset{50\%}{\dashrightarrow}}\;$$

II
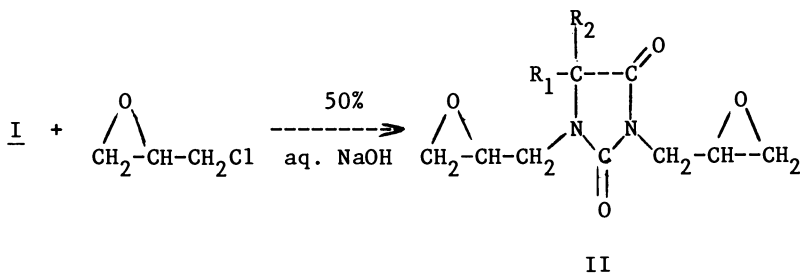
Table I lists typical properties of a baker's dozen of
these resins, produced by typical direct preparations, without
extensive purification. Overall, the viscosities of these
resins were quite low, particularly by comparison to the well
known general purpose epoxy resins based on the diglycidyl
ether of bisphenol A (DGEBA). The more shielded higher alkyl-
substituted hydantoin rings favored lower viscosities. Some
anomalies in these viscosities presumably reflected either a
tendency of certain resins to crystallize, or the presence of
some species of higher molecular weight, formed by reaction of
the glycidyl group with a second hydantoin ring.

In some instances a much purer diglycidylhydantoin species
has been isolated. Pure Resin IIa, 1,3-diglycidyl-5,5-dimethyl-
hydantoin, was a readily crystallizable solid, m. 72-73°C (2),
epoxy content 8.25 eq/kg. The less pure sample described in
Table I tended to supercool for a limited time, and could then
be handled as a liquid. A distilled grade of Resin IIb,

TABLE I

1,3-DIGLYCIDYLHYDANTOINS

Hydantoin, Resin	R_1	R_2	Yield of I	Resin Viscosity mPa·s	Epoxy/Kg.	Theo.
Ia,IIa	CH_3	CH_3	>90%	Solid	7.6	8.32
Ib,IIb	C_2H_5	CH_3	80%	1400	7.3	7.87
Ic,IIc	$i\text{-}C_3H_7$	H	40%	Solid	7.6	7.87
Id,IId	$n\text{-}C_3H_7$	H	40%	3300	7.0	7.87
Ie,IIe	$-(CH_2)_5-$ (a)		90%	Solid	6.8	7.13
If,IIf	$i\text{-}C_4H_9$	CH_3	80%	1300	6.8	7.08
Ig,IIg	$n\text{-}C_4H_9$	CH_3	82%	1300	6.9	7.08
Ih,IIh	$n\text{-}C_5H_{11}$	H	52%	2500	5.9	7.08
Ii,IIi	$i\text{-}C_5H_{11}$	CH_3	90%	2000	6.6	6.75
Ij,IIj	$n\text{-}C_5H_{11}$	CH_3	94%	600	6.7	6.75
Ik,IIk	2-MeBu	C_2H_5	93%	1000	6.2	6.44
Il,IIl	$n\text{-}C_6H_{13}$	CH_3	96%	600	6.3	6.44
Im,IIm	$i\text{-}C_4H_9$	$i\text{-}C_4H_9$	40%	900	6.0	6.16
(DGEBA)	--	--	--	14000	5.3	5.88

(a) cyclopentamethylene group forming a spiro- structure.

1,3-diglycidyl-5-methyl-5-ethylhydantoin, had viscosity 700 mPa.s
and epoxy content 7.52 eq./kg., rather than the values given in
Table I. A distilled grade of Resin IIe, 1,3-diglycidyl-5,5-
cyclopentamethylenehydantoin, was also crystalline, m. 104-106°C
(2), epoxy content 7.07 eq/kg.

Properties of Cured Hydantoin Epoxy Resins - Glass Temperatures

The effect of alkyl substituents in shielding the polar
hydantoin ring was shown by the glass transition temperature Tg
achieved after extensive crosslinking. As a measure of Tg we
used the "initial deformation temperature" (IDT) defined in the
experimental section. The IDT also depended on the stoichio-
metric ratio of curative (hardener) to resin, being highest at
or near exact equivalence. Also, since the reaction rate fell
drastically when enough crosslinking had occurred to bring the
glass transition temperature up to the reaction temperature,
IDT was effectively limited by the latter.

In Table II, the IDT's obtained by curing various diglycidyl-
hydantoins with hexahydrophthalic anhydride (HHPA) are shown.
H/R is the ratio of moles HHPA to actual equivalents of epoxide;
while it was not kept constant throughout the series, experience
has shown that, over the range used (H/R = 0.9 to 1.1), the vari-
ation in IDT was usually less than 10°. In a few cases, the final
cure temperature (150°C) may have limited the IDT, but with the
higher alkyl substituents, clearly it did not.

Note that the highest IDT was obtained with the cyclopenta-
methylenehydantoin resin derived from cyclohexanone. It is
tempting to speculate that this inflexible alkylene moiety was
ineffective in shielding the hydantoin ring, but subsequent com-
parison of the hydrophobic-hydrophilic balance of amine-cured
resins appeared to rule out this explanation; probably the stiff
spiro structure contributed to the high Tg, just as it contri-
buted to the high melting point of the resin itself (IIe).

Aside from this effect, clearly the longer alkyl substit-
uents did reduce interchain interactions so as to lower Tg.
Another steric effect notable in Table II is that Tg was higher
for close-in branching of the alkyl substituents.

As shown in Table III, all of the anhydride-cured resins
were essentially hydrophobic. The amount of water uptake
showed little or no trend with size or branching of the alkyl
substituents. Water uptake was reversible, also.

Hydrophobic-Hydrophilic Balance

A somewhat different aspect of the hydrophobic shielding
effect of alkyl substituents was reflected in the relative
hydrophilicity of aliphatic amine-cured resins. A standard
room temperature-curing polyamine, triethylenetetramine (TETA),
was used to cure a series of resins at room temperature. The

TABLE II

CYCLOALIPHATIC ANHYDRIDE CURING OF 1,3-DIGLYCIDYLHYDANTOINS

Resin	R_1	R_2	H/R		IDT, °C
IIa	CH_3	CH_3	0.9		140
IIb	C_2H_5	CH_3	1.0		148
IIc	$i-C_3H_7$	H	1.1		148
IId	$n-C_3H_7$	H	1.1		139
IIe	$-(CH_2)_5-$ (c)		0.9		153
IIf	$i-C_4H_9$	CH_3	0.9		129
IIg	$n-C_4H_9$	CH_3	0.9		118
IIi	$i-C_5H_{11}$	CH_3	0.9		115
IIj	$n-C_5H_{11}$	CH_3	0.9		112
IIk	2-MeBu	C_2H_5	1.1		123
IIl	$n-C_6H_{13}$	CH_3	1.0		115
IIm	$i-C_4H_9$	$i-C_4H_9$	0.9	(a)	111
(DGEBA)	--	--	1.0	(b)	126

All were cured with HHPA and 2 phr BDMA. Except where noted, all were gelled at 80°C and given a final cure of 2 hr./150°C

(a) gelled at 100°C   (b) final cure 3 hr./150°C

(c) cyclopentamethylene group forming a spiro-structure

TABLE III

CYCLOALIPHATIC ANHYDRIDE CURING OF 1,3-DIGLYCIDYLHYDANTOINS

Resin	R_1	R_2	H/R	Water Uptake, % (b)
IIa	CH_3	CH_3	0.9	1.62
IIb	C_2H_5	CH_3	0.94	1.49
IIc	$i-C_3H_7$	H	1.1	1.58
IId	$n-C_3H_7$	H	1.1	1.80
IIe	$- (CH_2)_5 -$ (c)		0.9	1.09
IIf	$i-C_4H_9$	CH_3	0.9	1.45
IIg	$n-C_4H_9$	CH_3	0.9	1.17
IIi	$i-C_5H_{11}$	CH_3	0.9	1.28
IIj	$n-C_5H_{11}$	CH_3	0.9	1.21
IIk	2-MeBu	C_2H_5	1.1	1.47
III	$n-C_6H_{13}$	CH_3	1.0	1.50
IIm	$i-C_4H_9$	$i-C_4H_9$	0.9 (a)	0.84

All were cured with HHPA and 2 phr BDMA. Except where noted, all were gelled at 80°C and given a final cure of 2 hr/150°C

(a) Gelled at 100°C   (b) 4 weeks, room temperature

(c) cyclopentamethylene group forming a spiro- structure

stoichiometry chosen was one amine hydrogen/actual epoxide equivalent. In most cases, some specimens were given a mild postcure to see the effect of increased crosslinking. The hydrophilicity of the cured systems was judged by weight gain of small specimens after immersion at room temperature in deionized water for periods of one day to four weeks. (In some cases, parallel specimens were exposed at 35°C in a 95% R.H. chamber. These data were generally close to the room temperature immersion results, and with one exception are not reported here.) The flexural modulus of the specimen was also measured at the time of weighing, since the absorbed water acted to plasticize the cured resin.

Both weight gain and plasticization proved to be very sensitive to the alkyl groups present, as shown in Table IV. Note that the mild postcure somewhat improved the more hydrophobic cured resins (those with C_5 and higher substituents), notably permitting TETA-cured Resin IIk to retain 95% of its flexural modulus after four weeks. Mild postcure significantly reduced the rate of water uptake of the hydrophilic cured resins. But note also that even with postcure the hydrophilic cured resins usually absorbed so much water in four weeks that the swelling stresses became greater than the cohesive strength and the specimens broke apart. Even these high water uptakes proved to be reversible; i.e., the water acted only as a swelling agent.

In general, the hydrophobic TETA-cured resins were those which, in Table II, had low IDT. Both properties are attributable to shielding of the hydantoin ring by the 5-position substituents. The principal exception to this correlation was 1,3-diglycidyl-5,5-cyclopentamethylenehydantoin (IIe) which had a high IDT in Table II, but which proved to be quite hydrophobic after room temperature cure with amines (3). Thus it appears that the spiro-joined cycloaliphatic ring was effective in shielding the hydantoin ring, but its relative stiffness raised Tg considerably.

Since the hydrophobic-hydrophilic balance of amine-cured resins was so sensitive to alkyl substituents on the hydantoin ring, it is not surprising that it was also sensitive to the hydrocarbon moieties of the amine curatives. The range of behavior depended on the resin substituents. For example, the already hydrophobic ethyl amyl substituted Resin IIk showed moderate but significant increases in hydrophobicity when cured with cycloaliphatic, highly branched aliphatic, or formulated aromatic amines. See Table V.

At the other extreme, as shown in Table VI, a resin mixture containing only dimethylhydantoin (DMH) rings was quite hydrophilic with all room temperature amine curatives except the formulated aromatic amine mixture based on methylene-dianiline. (See Table VII for identification of the amines in Table V and subsequent tables.) This resin mixture was obtained by hydroxypropylating a portion of the DMH, Ia.

TABLE IV

ROOM TEMPERATURE CURED HYDANTOIN EPOXY RESINS

Resin	R_1	R_2		Water Uptake, %		% Retention of Flex Modulus
				1 Day	4 Wk	4 Wk.
IIa	CH_3	CH_3		27.7	(a)	(c,d)
			(b)	11.7	(a)	15 (d)
IIb	C_2H_5	CH_3		13.4	(a)	10 (d)
			(b)	5.9	29.5	10
IId	$n-C_3H_7$	H		14.5	(a)	10 (d)
IIh	$n-C_5H_{11}$	H		2.6	12.5	50
			(b)	1.8	10.6	65
IIi	$i-C_5H_{11}$	CH_3		2.4	11.5	70
IIl	$n-C_6H_{13}$	CH_3		1.4	6.8	80
			(b)	1.5	3.8	80 (g)
IIk	2-MeBu	C_2H_5		1.2	5.9	70
			(b)	0.8	4.8	95

All were cured with TETA at H/R = 1.0 amine hydrogen/epoxide.
All were cured at room temperature; 14-21 days without postcure
and at least 7 days before postcure. Except where noted, expo-
sure was by immersion in deionized water at room temperature.

(a) Fragmented   (d) At 1 day
(b) Postcured 6 hr./100°C   (g) Exposed to 95% R.H./35°C
(c) Too soft to measure

TABLE V

ROOM TEMPERATURE AMINE CURING OF HYDANTOIN EPOXY RESINS

Resin: IIk [1,3-diglycidyl-5-ethyl-5-(2-methylbutyl)hydantoin]

| Curative | Water Uptake, % | | % Retention of Flex Modulus |
	1 Day	4 Wk	4 Wk
Formulated amine (a)	0.4	1.7	95
TMDA (a)	0.6	2.7	90
MMCHA (a)	0.6	2.6	(b)
TETA (a)	1.2	5.9	70

All were cured at H/R = 1.0 amine hydrogen/epoxide.
All were cured at room temperature 14-21 days.

Except where noted, exposure was by immersion in deionized
water at room temperature.

(a) See Table VII for identification.
(b) Too brittle to cut.
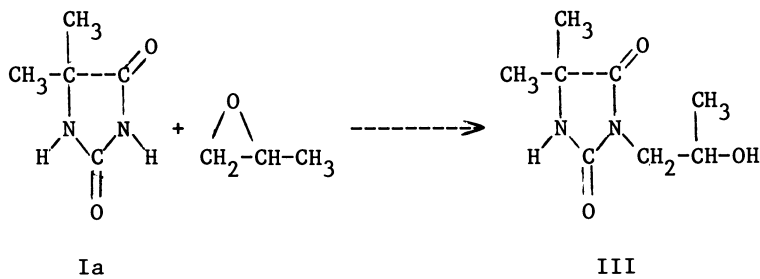
As has been pointed out by Habermeier (2), the non-equiva-
lence of the 1- and 3- positions of the hydantoin ring readily
permitted monosubstitution. Subsequent glycidylation provided
the diepoxide IV.

TABLE VI

ROOM TEMPERATURE AMINE CURING OF HYDANTOIN EPOXY RESINS

Resin: { 70% IIa   (1,3-diglycidyl-5,5-dimethylhydantoin)
       { 30% IV   [1-glycidyl-3-(2-glycidoxypropyl)-
                                 5,5-dimethylhydantoin]

| Curative | Water Uptake, % | | % Retention of Flex Modulus |
	1 Day	4 Wk	4 Wk
Formulated amine (a)	0.8	3.5	70
TMDA (a)	4.7	16.2	5
{ 30%eq TMDA (a) } { 70%eq MCHA (a) }	3.9	11.0	(b)
{ 15%eq TMDA } { 85%eq MCHA }	3.7	10.3	(b)
1,4-BAC (a)	5.2	16.9	35
1,3-BAC (a)	5.2	17.1	20
MXDA (a)	7.4	23.1	(b)
IPDA (a)	6.1	14.3	(b)
PMDA (a)	(c)	--	(b)
TETA (a)	23.4	(c)	(d,e)

All were cured at H/R = 1.0 amine hydrogen/epoxide.
All were cured at room temperature 14-21 days.

Except where noted, exposure was by immersion in deionized
water at room temperature.

%eq = percent of amine equivalents

(a)   See Table VII for identification.
(b)   Too brittle to cut.
(c)   Fragmented
(d)   At 1 day
(e)   Too soft to measure

TABLE VII

IDENTIFICATION OF MATERIALS

Aniline-formaldehyde curative = Jeffamine® AP-22

BAC = bis(aminomethyl)cyclohexane

BDMA = benzyldimethylamine

DGEBA = diglycidyl ether of Bisphenol A

Formulated amine = Liquid amine mixture containing MDA,
                   described by Habermeier (2).

HHPA = hexahydrophthalic anhydride

IPDA = isophoronediamine
     = 3,3 -dimethyl-5-aminomethylcyclohexylamine

MCHA = 4,4'-methylenebis(cyclohexylamine)

MDA = 4,4'-methylenedianiline

MMCHA = 4,4'-methylenebis(2-methylcyclohexylamine)

MXDA = m-xylylenediamine = 1,3-bis(aminomethyl)benzene

PMDA = p-menthanediamine
     = 1-methyl-4-(1-amino-1-methylethyl)cyclohexylamine

TETA = triethylenetetramine = 1,4,7,10-tetraazadecane

TMDA = 2,2,4-trimethylhexane-1,6-diamine

This resin mixture, which had a low viscosity, typically about 2500 mPa.s, was found to avoid the crystallization tendency of pure diglycidyl DMH, IIa. Particular utility has been found for the reversible high degree of swelling of a room temperature cured version of a DMH-based resin, as a water-permeable topcoat for marine antifouling paints (4). The methylethylhydantoin-based Resin IIb, as shown in Table VIII, gave the greatest range of hydrophilicity when the amine curative was varied. This is in keeping with its intermediate degree of alkyl substitution.

A few resins were given elevated temperature cures with aromatic amines; here the effect of alkyl substituents on water uptake could be seen, but the overall behavior was intermediate between the elevated-temperature anhydride cures and the room temperature amine cures.

Solvent/Chemical Resistance

The hydrophobic shielding of the hydantoin ring by alkyl substituents affected all the solvent-solute interactions of cured resins. Two of the resins and the DMH-based resin mixture were cured with a commercially available aromatic amine mixture derived from aniline-formaldehyde condensation, identified in Table VII. Weight gain and solvent plasticization were followed in a number of solvents and aqueous media. Some of the exposure was at 60°C as well as at room temperature.

For the hydrophobic Resin IIk, the results for exposure to various solvents are shown in Table IX. The solvents are listed in increasing order of solubility parameter δ(5). It is evident that (within the limitations of solubility parameter theory) this cured resin was lyophilic in the range of $\delta = 9 - 9.6$; there was also a specific interaction with methanol. Table X shows the generally hydrophobic response of this cured resin in aqueous media (listed in increasing order of pH). Only strong acid had a deleterious effect.

Again at the other extreme, the DMH-based hydrophilic resin mixture was studied, with results shown in Tables XI and XII. This cured resin was hydrophilic (Table XII), though less so than the room temperature amine-cured systems of Table VI, but note its general lyophobicity, as shown in Table XI. Of the non-aqueous media, only methanol and hot trichlorethylene showed much swelling or plasticization in 16 weeks. Presumably the poorly shielded DMH rings permitted strong interchain interactions; this virtual crosslinking provided general solvent resistance.

Resin IIb, which proved somewhat less hydrophilic than the DMH-based resin mixture (see Table VIII), was studied with certain solvents only, as shown in Table XIII. Its lyophobicity was somewhat less than the DMH-based mixture, and in the two aqueous media it was somewhat less affected. Thus, again, its behavior reflected the intermediate degree of alkyl substitution.

TABLE VIII

ROOM TEMPERATURE AMINE CURING OF HYDANTOIN EPOXY RESINS

Resin: IIb (1,3-diglycidyl-5-methyl-5-ethylhydantoin)

		Water Uptake, %		% Retention of Flex Modulus
Curative		1 Day	4 Wk	4 Wk
Formulated amine (a)		0.5	2.4	80
TMDA (a)		1.4	5.3	80
{30%eq TMDA (a) / 70%eq MCHA (a)}		1.5	6.0	(b)
{15%eq TMDA / 85%eq MCHA}		1.5	6.0	(b)
MMCHA (a)		1.1	4.3	(b)
1,4-BAC (a)		2.4	11.4	(b)
1,3-BAC (a)		1.9	10.4	(b)
MXDA (a)		2.4	9.6	(b)
IPDA (a)		(c)	--	(b)
TETA (a)		13.4	(c)	10 (d)

All were cured at H/R = 1.0 amine hydrogen/epoxide.
All were cured at room temperature 14-21 days.

Except where noted, exposure was by immersion in deionized
water at room temperature.

%eq = percent of amine equivalents

(a) See Table VII for identification.
(b) Too brittle to cut.
(c) Fragmented
(d) At 1 day

TABLE IX

SOLVENT RESISTANCE OF AROMATIC AMINE-CURED HYDANTOIN EPOXY RESIN

Resin: IIk [1,3-diglycidyl-5-ethyl-5-(2-methylbutyl)hydantoin]
IDT = 128°C

Solvent	Solubility Parameter(5)	Temp. °C	Solvent Uptake, %		% Retention of Flex Modulus 16 Wk.
			1 Wk.	16 Wk.	
Heptane	7.50	25	0.03	0.54	100
Kerosene		25	0.02	0.10	110
		60	0.3	0.9	95
Xylene	8.9	25	0.08	0.8	100
		60	0.5	5.3	85
Ethyl Acetate	8.91	25	1.9	29.8 (b)	15
Benzene	9.16	25	0.1	1.2	100
Trichlorethylene	9.16	25	3.5	55.1	30 (g)
		60	(a)	--	--
Chloroform	9.16	25	(a)	--	--
Acetone	9.62	25	(a)	--	--
Isopropyl Alcohol	11.44	25	-0.08	0.43	100
Methanol	14.50	25	11.1	20.7	25

All were cured with aniline-formaldehyde curative. See Table VII.
H/R = 1 amine hydrogen/epoxide equivalent
Gelled 16 hr./65°C. Postcured 2 hr./150°C

(a) Fragmented   (b) Cracked   (g) At 8 weeks

TABLE X

CHEMICAL RESISTANCE OF AROMATIC

AMINE-CURED HYDANTOIN EPOXY RESIN

Resin: IIk [1,3-diglycidyl-5-ethyl-5-(2-methylbutyl)hydantoin]
IDT = 128°C

Aqueous Medium	Temp. °C	Liquid Uptake, %		% Retention of Flex Modulus
		1 Wk.	16 Wk.	16 Wk.
25% HCl	25	8.5	38	40
5% Acetic Acid	25	1.3	3.6	105
	60	2.9	4.8	95
Water	25	1.2	3.5	--
	60	2.9	4.4	95
10% NaCl	25	1.1	3.1	--
	60	2.4	3.5	95
10% NH_3	25	1.2	4.3	95
50% NaOH	25	-0.04	0.01	105
	60	0.05	0.14	90

All were cured with aniline-formaldehyde curative. See
Table VII.
H/R = 1 amine hydrogen/epoxide equivalent
Gelled 16 hr./65°C. Postcured 2 hr./150°C

TABLE XI

SOLVENT RESISTANCE OF AROMATIC AMINE-CURED HYDANTOIN EPOXY RESIN

Resin: $\begin{cases} 70\% \text{ IIa} & \text{[1,3-diglycidyl-5,5-dimethylhydantoin]} \\ 30\% \text{ IV} & \text{[1-glycidyl-3-(2-glycidoxypropyl)-} \\ & \quad\quad\quad\quad\quad\quad\quad\quad \text{5,5-dimethylhydantoin]} \end{cases}$

IDT = 125°C

Solvent	Solubility Parameter(5)	Temp. °C.	Solvent Uptake, %		% Retention of Flex Modulus 16 Wk.
			1 Wk.	16 Wk.	
Heptane	7.50	25	0.12	0.84	100
Kerosene		25	0.09	0.29	100
		60	0.5	1.7	105
Xylene	8.9	25	0.04	1.1	--
		60	0.2	2.2	95
Ethyl Acetate	8.91	25	0.06	0.6	100
Benzene	9.16	25	0.07	1.0	100
Trichlorethylene		25	0.15	1.1	95
	9.16	60	0.4	6.8	80
Chloroform	9.16	25	0.1	1.25	100
Acetone	9.62	25	0.11	0.96	95
Isopropyl Alcohol	11.44	25	0.00	0.13	105
Methanol	14.50	25	6.9	21.0	15

All were cured with aniline-formaldehyde curative. See Table VII.
H/R = 1 amine hydrogen/epoxide equivalent
Gelled 16 hr./65°C.   Postcured 2 hr./150°C

TABLE XII

CHEMICAL RESISTANCE OF AROMATIC

AMINE-CURED HYDANTOIN EPOXY RESIN

Resin: 70% IIa [1,3-diglycidyl-5,5-dimethylhydantoin]
30% IV [1-glycidyl-3-(2-glycidoxypropyl)-
5,5-dimethylhydantoin]
IDT = 125°C

Aqueous Medium	Temp. °C.	Liquid Uptake, %		% Retention of Flex Modulus 16 Wk.
		1 Wk.	16 Wk.	
25% HCl	25	(a)	--	--
5% Acetic Acid	25	1.8	10.1	75
	60	8.0	15.9	50
Water	25	1.9	10.6	--
	60	7.7	12.7	60
10% NaCl	25	1.3	6.5	--
	60	4.8	9.5	70
10% NH$_3$	25	1.8	13.7	55
50% NaOH	25	0.005	0.25	110
	60	0.2	-0.15	85

All were cured with aniline-formaldehyde curative.
See Table VII.
H/R = 1 amine hydrogen/epoxide equivalent
Gelled 16 hr./65°C. Postcured 2 hr./150°C

(a) Fragmented

TABLE XIII

SOLVENT/CHEMICAL RESISTANCE OF

AROMATIC AMINE-CURED HYDANTOIN EPOXY RESIN

Resin: IIb [1,3-diglycidyl-5-methyl-5-ethylhydantoin]

IDT = 149°C

Solvent	Solubility Parameter(5)	Temp. °C.	Solvent Uptake, %		% Retention of Flex Modulus 16 Wk.
			1 Wk.	16 Wk.	
Ethyl Acetate	8.91	25	0.01	1.0	105
Trichlorethylene		25	0.3	1.4	105
	9.16	60	2.7	6.5	90
Chloroform	9.16	25	0.3	2.2	100
Acetone	9.62	25	0.12	3.3	85
25% HCl		25	18.7	(a)	--
10% NH$_3$		25	1.3	8.5	90

All were cured with aniline-formaldehyde curative. See Table VII.
H/R = 1 amine hydrogen/epoxide equivalent
Gelled 16 hr./65°C. Postcured 2 hr./150°C

(a) Fragmented

Conclusions

By varying the substituents at the 5-position on the
hydantoin ring, it is possible to control the intermolecular
forces of hydantoin-based epoxy resins. This control is mani-
fested to some extent in the monomeric resins, but is far more
evident in the glass transition temperature of highly crosslinked
resin-curative systems, and particularly in the hydrophilic-
hydrophobic balance of amine-cured systems. Within limits
prescribed by the substituents on the hydantoin ring, the hydro-
philic-hydrophobic balance is also greatly affected by the organic
moieties introduced by the amine curative. Analogous principles
may be invoked in considering the lyophilic-lyophobic balance of
aromatic amine-cured hydantoin epoxy resins.

Experimental Procedures

Mold Construction. Casting molds were prepared from pre-
cleaned mold-release-coated glass plates and square-angled
U-shaped silicone rubber gaskets. The gasket sheets were about
1.6 mm thick and two or more were plied to the casting thick-
ness desired, and spring-clamped between plates. The molds
were set vertically with the top edge open for pouring, and
usually were preheated in an oven to keep the viscous casting
mixture as fluid as possible. The most common plate size used
was about 20 cm square.

Specimen Preparation. The demolded castings were cut
using a circular saw with a diamond cutting wheel to provide
specimens for the various tests.

Casting. Castings of liquid epoxy resins cured with hexa-
hydrophthalic anhydride (HHPA) were prepared by heating the liquid
resin in a stirred 3-necked flask to which the calculated amount
of premelted HHPA was added. A vacuum was drawn to partially
degas the mixture; then 2 phr benzyldimethylamine (BDMA) was added
as accelerator. After further degassing, the mixture was poured
into casting molds prepared as described above. The filled molds
were put into an oven at the desired gelling temperature; subse-
quently, either the oven was reset to the final cure temperature
or the molds were transferred to a second oven, as convenient.
Castings of solid epoxy resins cured with HHPA were pre-
pared similarly, except that the resin also had to be premelted.
Except where noted in Table II, HHPA-cured castings were gelled
at 80°C (at least 3 hours and usually overnight) and then cured
2 hr./150°C.
Castings cured with the commercial aromatic amine derived
from aniline-formaldehyde were prepared like the HHPA-cured
castings, but without accelerator. The aromatic amine mixture
was about 90% methylenedianiline (MDA) and tended to partially

solidify on standing, so it had to be prewarmed and well mixed
before use. In the work reported here, the degassed castings
were gelled 16 hr./65°C and given a final cure of 2 hr./150°C.

For room temperature curing, preheating was used only when
absolutely necessary to reduce viscosity and facilitate mixing.
For this reason, Resin IIe was not considered suitable for room
temperature curing, and Resin IIa was so cured on only a few
occasions, after premelting. Such resins could be used in liq-
uid mixtures, as noted in Tables VI, XI, and XII. In a similar
way, solid amines, such as MDA and methylenebis(cyclohexylamine),
MCHA, could only be used in liquid mixtures.

With all the amine curatives, the stoichiometry used was
one amine hydrogen/epoxide; e.g., TETA, having two primary and
two secondary amines/molecule, would have six equivalents/mole.

The mixture of liquid resin and liquid amine was stirred and
degassed in a 3-necked flask, just as for the thermal castings,
but an ice bath was used to control any exotherm in the flask, so
that rapid viscosity increase due to reaction would not occur to
interfere with degassing. After pouring into the mold, the
casting was kept at room temperature for at least 14 days before
demolding. When a mild postcure was desired, at least 7 days/room
temperature curing preceded it; the postcure was 6 hr./100°C.

Weight Gain and Flexural Modulus. Weight gain and plasti-
cization by absorbed liquid were measured on small flex bar
specimens (7.62 cm x 2.54 cm x 0.32 cm). Most exposure was by
immersion at room temperature, but some specimens were immersed
at 60°C, and some specimens were exposed to 95% R.H. at 35°C in
a controlled-humidity chamber in parallel to their immersion in
water. Deionized water, ten organic solvents, and five aqueous
solutions were used as immersion media, as noted in the appro-
priate tables. Exposure times ranged from 24 hours to 4 weeks
for the water- or humidity chamber-exposed samples, and from 1
to 16 weeks for the solvent- or aqueous media-exposed samples.
At the desired intervals, each specimen was removed from its
environment, rinsed if necessary for safe handling, wiped dry,
and weighed. Then the flexural modulus was measured, to a max-
imum outer-layer strain of 0.5%. Thus, the flex measurement
was essentially non-destructive and the specimen could be
returned to its exposure.

Initial Deformation Temperature (IDT). IDT was determined
as the temperature at which a standard test bar (1.27 cm wide x
0.635 cm deep), centrally loaded on a 100 mm span, deflected an
additional 0.25 mm under a load that gave a maximum (outer-
layer) stress of 1.82 MPa, while being heated at a rate of
2°C/min. The operating procedure followed ASTM Method D648-72
for "Deflection Temperature of Plastics Under Flexural Load"
(6), but the maximum strain reached at the IDT was half that at
the "deflection temperature under load" (DTUL), so IDT was

several degrees lower than DTUL.

Abstract

Hydantoin epoxy resins having glycidyl groups in the 1- and 3-positions and one or two alkyl groups in the 5-position were prepared by the Bücherer reaction, followed by treatment with epichlorohydrin. These resins were crosslinked with hexahydrophthalic anhydride to examine the effect of alkyl substituents on the glass transition temperatures of the cured systems. Higher alkyl substituents shielded the hydantoin rings and gave lower glass temperatures. The same shielding effect was observed in the reduced hydrophilicity of higher alkyl-substituted hydantoin epoxy resins cured with triethylenetetramine.

Steric factors — branching at or close to the hydantoin ring — raised the glass transition temperature while maintaining the shielding effect. Amines of different structures were used as room temperature curatives with a few representative resins, to observe the effect on hydrophilic-hydrophobic balance. Solvent effects were examined on aromatic amine-cured resins; the most hydrophilic cured system proved to have the broadest range of lyophobicity.

Acknowledgement

Literature Cited

1. Catsiff, E. H.; Dee, H. B.; Seltzer, R. Modern Plastics, 1978, 55 (7), 54.

2. Habermeier, J. Angew. Makromol. Chem., 1977, 63 (921), 63.

3. Eldin, S., private communication.

4. Weiss, J. Organic Coatings and Plastic Chemistry, 1978, 39, 567.

5. Hoy, K. L. J. Paint Technol., 1970, 42 (541), 76.

6. Lukens, R.P., Ed. "Annual Book of ASTM Standards;" Am. Soc. for Testing and Materials: Philadelphia, PA, 1976, Part 35, p. 219.

Effect of Cross-Link Density Distribution on the Engineering Behavior of Epoxies

S. C. MISRA, J. A. MANSON, and L. H. SPERLING

Materials Research Center, Lehigh University, Bethlehem, PA 18015

Fundamental knowledge of relationships between characteristics, synthesis or processing, structure, and mechanical and other properties is required of crosslinked networks used for critical and demanding applications. Thus, epoxy resins, which are widely used for engineering purposes, have received great attention in the past decade. Indeed, many papers have covered many aspects of epoxies such as: stoichiometry (1-5), prepolymer structure (6-8), diluents (4,9,12), fillers (13-22), heat treatment (3,22), and effects of cure conditions (23-25). However, relatively little attention has been given to properties such as creep and to the effects of the distribution of crosslink density. Certainly typical commercial epoxy resins usually exhibit a distribution of molecular weights which should result in a distribution of crosslink density in the final network. The broadening of the transition region has been qualitatively attributed to this distribution effect (26). Unfortunately, existing studies were of insufficient scope to permit correlation of the engineering behavior of epoxy networks and the distribution of crosslink density or M_c (the average molecular weight between crosslinks). Because of its relevance to engineering application, such a study was thought to be of considerable interest.

With this in mind, a program was begun to examine the effects of crosslinking and crosslink distribution on several aspects of behavior of high-T_g epoxies (27-31). It was decided that a thorough characterization of viscoelastic behavior in blends of two epoxy resins, each having a quite different molecular weight, should enable correlations of distributions of M_c and other network variables with the engineering behavior. Accordingly, the crosslink density (M_c) was varied by curing a homologous series of bisphenol-A-based epoxy prepolymers with methylene dianiline (MDA). Networks were also prepared at constant crosslink densities by blending low and high-molecular-weight members of the homologous series. This paper summarizes the following properties of the networks: the state of cure, M_c, dynamic mechanical spectroscopy

(DMS), creep, and stress-strain and impact behavior. More
detailed results for each topic will be presented and discussed
separately.

Experimental

    Materials. The following Epon prepolymers (Shell Chemical
Company) were used: Epons 825, 828, 834 (all liquid to semi-
solid); and 1001, 1002, and 1004 (all solids). Approximate com-
positions (degree of polymerization) were determined by gel per-
meation chromatography. Bimodal blends were made by mixing Epon
825 with Epon 1004, as shown in Table 1. Sample preparation and
the method of curing have been described in the preceding paper
(29).

Table I.   Compositions of Homopolymers and Bimodal Blends

Sample	M_c	Epoxy Resin (wt. % in blend)
E-1	308	825 (100)
E-2	326	828 (100)
F-1	326	825 (91) + 1004 (9)
F-2	413	825 (62) + 1004 (38)
F-3	419	825 (60) + 1004 (40)
E-3	430	834 (100)
F-4	430	825 (57) + 1004 (43)
E-5	740	1001 (100)
F-5	740	825 (20) + 1004 (80)
E-7	1004	1400 (100)
E-4	493	834 (100) (with slight excess of curing agent)

    Materials Characterization. Measurements of complex Young's
moduli, including the storage modulus E', loss modulus E", and
loss tangent tan δ, were made using a Rheovibron viscoelastometer,
model DDV-II (Toyo Measuring Instrument Co.). Measurements were
made at 110 Hz over a temperature range from -80°C to about 40°C
above T_g, at a heating rate of 1°C/min. Icing of the specimens at
low temperatures was avoided by sweeping dry nitrogen through the
chamber. Tensile measurements were made using an Instron tester
at room temperature, according to ASTM test D-638-68, type IV
with a crosshead speed of 1mm/min (0.05"/min). Young's modulus,
E, ultimate tensile strength, σ_u, yield strength, σ_y, and ultimate
elongation, ε_u, were determined. In all cases, three to four
specimens per sample were obtained that did not fail prematurely.
Impact tests were conducted according to the ASTM test D-256-70,
method B (Charpy type, notched). On the average, 4 to 5 specimens
were tested.
    Studies of creep as a function of time and temperature were
carried out using a Gehman Torsional Stiffness Tester (32). Creep

experiments covered the entire range of viscoelastic behavior from
the glassy to the rubbery region. Modulus readings were taken at
various intervals of time between 10 sec and 1000 sec. The
inverse time-dependent compliance, $1/J(t)$, was calculated from the
angle of twist of the specimen induced by the torsion wire as
indicated by the apparatus, and the time-dependent Young's modu-
lus, $E(t)$, was assumed to approximately equal $3/J(t)$. Master
curves were obtained by shifting data obtained at various temper-
atures with respect to a reference temperature (129°C in this
case). Each curve of reduced modulus was shifted with respect to
the curve at the reference temperature until all fit together to
form a smooth curve. Master curves for various materials could
then be easily compared. Temperatures corresponding to a value of
0.2 GPa for $E(10 \text{ sec})$ were taken as T_g's.

Average swelling and soluble content measurements were
conducted at room temperature using acetone as the solvent.
Equilibrium swelling was achieved within 15 days, and the swelling
ratio, q, was calculated by the formula:

$$q = \frac{\text{swollen volume of the network}}{\text{extracted, dry volume of the network}} \qquad (1)$$

Density measurements were made at room temperature, $\sim 20°C$, using
the density gradient method. Duplicate runs were made in all
cases.

A differential scanning calorimeter (DSC 1-B, Perkin-Elmer
Corporation) was used to determine the extent of cure; 10-mg to
20-mg specimens were tested at a scanning rate of 10°C/min. An
exothermic peak on the thermograph indicates the heat of reaction
whereas an endothermic peak in the amorphous polymer indicates the
presence of residual stresses or the occurrence of a transition
such as the glass transition. The presence of an exothermic peak
in the DSC-scan of a pre-cured sample is an indication of incom-
plete curing.

The unreacted epoxy and amine groups present in the samples
(degree of cure) were determined by chemical titration, using the
procedure outlined by Bell (33) with a slight modification. Cured
epoxy samples were filed and about 1 g of the resulting powder was
placed in a round-bottomed flask with 50 ml of 0.2N pyridinium
chloride, 50 ml of reagent isopropanol, and 25 ml of distilled
water. The mixture was refluxed for 30 min and stirred continu-
ously with a magnetic stirrer. After cooling to room temperature,
the solution was poured into a 250-ml beaker. Using a potentio-
meter and a buret, standardised 0.505N NaOH was added in 5-ml
increments until the pH increased to 7.0. From this point on,
0.2-ml increments were added until a sharp increase in pH was
noted (pH ~ 10.5). Since the response in the amine titration
region was very slow and the pH did not stablize until 8 to 10 min
after each addition of NaOH, the readings were made at 10-min
intervals.

Results and Discussion

    <u>Distribution of molecular weights in the commercial resins.</u>
Gel permeation chromatography (GPC) indicated that the liquid and
semi-solid prepolymers (Epon 825, 828, and 834) were composed of
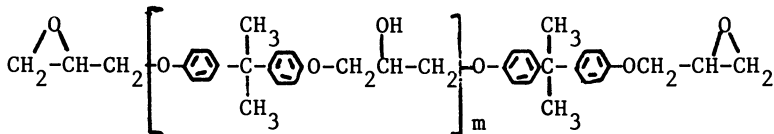
$m = 0$ (M = 340) and $m = 1$ (M = 620) components. The percentage of
$m = 0$ and $m = 1$ species was dependent on the average molecular
weight of the prepolymer, as given in Table II.

Table II. Composition of the Commercial Epoxy Resins

Sample	Epoxy Resin	M	Components present in the prepolymer
E-1	825	352	m=0 (96%) and m=1 (4%)
E-2	828	380	m=0 (86%) and m=1 (14%)
E-3	834	592	m=0 (29%) and m=1 (71%)
E-5	1001	1000	m=1, m=3, and m=7 (major component)
E-6	1002	1360	m=1, m=3, and m=12 (major component)
E-7	1004	1996	m=1, m=3, and m=12 (major component)

The solid prepolymers were composed as follows: Epon 1001, m=7
(M=2328), m=3 (M=1192), and m=1; and Epon 1002 and 1004, m=12
(M=3748), m=3, and m=1 (the major component being m=12). The
exact composition of each component in the solid prepolymers could
not be completely resolved from the peaks of m=7 (Epm 1001) or
m=12 (Epm 1002 and 1004) components.
    Thus, the bimodal blends (Series F) of Epon 825 and Epon 1004
had the following components: m=0, m=1, m=3, and m=12. The
amount of m=0 component was at a maximum in sample F-1 but at a
minumum in sample F-5. On the other hand, samples F-2, F-3, and
F-4 contained both m=0 and m=12 species in appreciable quantities.

    <u>Degree of cure</u>. The titration results given in Table III
reveal that from 98% to 100% of the functional groups had reacted.
Similarly no evidence for incomplete cure was observed by DSC or
by dynamic mechanical spectroscopy (DMS). However, it may be
pointed out that 2% unreacted functional groups could result in
detectable incoherence (see reference <u>29</u>) in the networks prepared
from high-MW epoxy prepolymers.

Table III. Unreacted Epoxy and Amine
Concentration in the Cured Sample

Sample	Epoxy content, meq/g sample	Amine content, meq/g sample
E-1	0.00	0.00
E-2	0.06	-0.02
E-3	0.00	0.00
E-4	0.09	-0.04
E-5	0.04	0.00
E-6	0.03	0.00
F-1	0.00	0.00
F-2	0.00	-0.09
F-3	0.03	0.03
F-4	0.04	0.04
F-5	0.09	0.06

Dynamic mechanical properties. The parameters character-
izing the dynamic mechanical behavior of Series E and Series F are
summarized in Table IV. Several of the viscoelastic parameters
will now be discussed in detail.

Table IV. Dynamic Mechanical Properties of
Series E and Series F Epoxy Networks

Specimen	M_c[a] (theor.)	T_β[b]	Tan δ_{max} (at T_α)		T_g, °C	E', GPa[d] x 10		$-n$[e]
			Value	T, °C		E'_r	E'_g[c]	x10^2
E-1	308	-35	0.62	221	207	0.45	22	5.2
E-2	326	-40	0.75	211	197	0.42	21	5.6
E-3	430	-46	0.90	175	165	0.17	20	6.7
E-4	493	-46	0.95	175	165	0.21	20	6.7
E-5	740	-55	1.25	157	145	0.10	19	9.1
E-7	1400	-60	1.52	138	125	0.065	18	10.0
F-1	326	-40	0.75	211	197	0.42	21	5.6
F-2	413	-45	0.75	185	174	0.21	21	5.6
F-3	419	-45	0.80	175	166	0.17	21	5.9
F-4	430	-46	0.75	168	150	0.17	20	5.6
F-5	740	-55	1.25	157	145	0.10	19	9.1

[a] Based on M_c's of the components
[b] From maximum in tan δ
[c] E' refers to the glassy state
[d] $1 GPa = 10^{10}$ dynes/cm^2
[e] $n = d(\log E')/dT$, at $T_g (\pm 4 °C)$

Glass transition temperature. The effect of the distribution
of M_c on T_g is shown in Figure 1. At M_c = 430, the T_g of the
blend sample F-4 was 13°C lower than that of its commercial
counterpart sample E-3. This indicates that the longer chains,
though present in the same amount as the shorter chains (see
Table I), dominate the final network and thus control the T_g of
the blend sample F-4. Due to the higher reactivity, the longer
molecules react first (29) to give microgels swollen with the
unreacted smaller molecules which react later to form an inter-
penetrating network. Thus the secondary microgels result in a
shell and core type structure (29). On the other hand, at M_c =
326 and M_c = 740, the blend samples F-1 and F-5 did not have a
T_g different from their commercial counterparts, E-2 and E-5,
respectively. At these M_c's, large differences in distribution
between blends and commercial resins could not be obtained because
the number of possible permutations of distribution at these M_c's
was very restricted; at low M_c (326), Epon 825 was the major com-
ponent (90%), whereas at high M_c (740) Epon 1004 was the major
component (80%).

Young's modulus. As expected for the glassy state (in which
long-range segmental motions are frozen), Young's modulus at room
temperature, E_g', was found to be nearly independent of M_c or the
distribution of M_c (Table IV). All values fall within the range
of 2 $\pm$ 0.2 GPa compared to an average of 1.3 GPa obtained from
tensile stress-strain curves (to be discussed later).

Rubbery modulus. Figure 2 shows that the rubbery modulus of
the present networks is unaffected by the distribution of M_c.
Graessley (34) calculated the free energy of deformation and the
equilibrium dimensions of network chains for networks of Gaussian
random coils and showed that the elastic properties of such net-
works depend upon the total number of elastically active chains
(average M_c) and elastically active junctions, but are independent
of the chain length distribution (M_c distribution), junction func-
tionality distribution, and the detailed pattern of connectivity.
Thus, the present experimental results are in agreement with the
theoretical predictions of Graessley.

β-transition temperature. The β-transition temperature
increased with M_c but was unaffected by the changes in the distri-
bution of M_c (Figure 2). This is so because T_β is a result of the
motion of small segments of the main chain, rather than the larger
segments involved in the glass transition. Therefore, T_β should
depend on the average M_c and not on the distribution of M_c.

Height of the tan δ peak. The value of the tan δ_{max}
increased asymptotically with M_c. As expected, the bimodal blend
samples F-2, F-3, and F-4, which showed broader transition regions
than their counterparts the commercial resin samples of Series
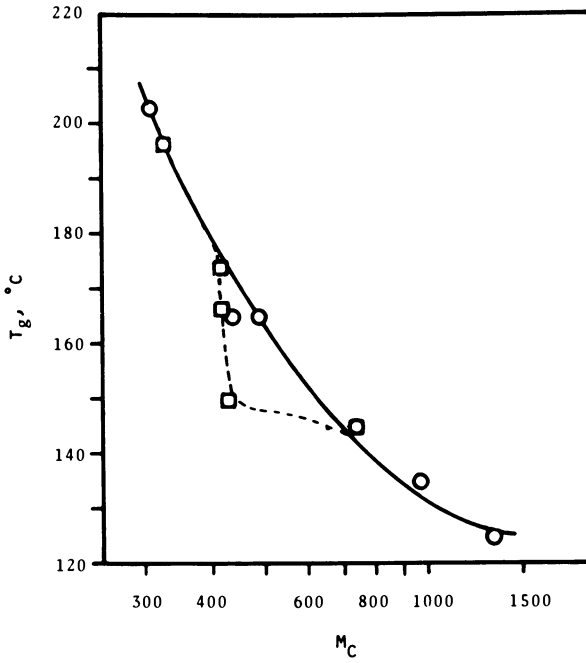
Figure 1.   Glass transition temperature as a function of M_c for Series E and Series F networks: (○) commercial resins; (□) bimodal blends
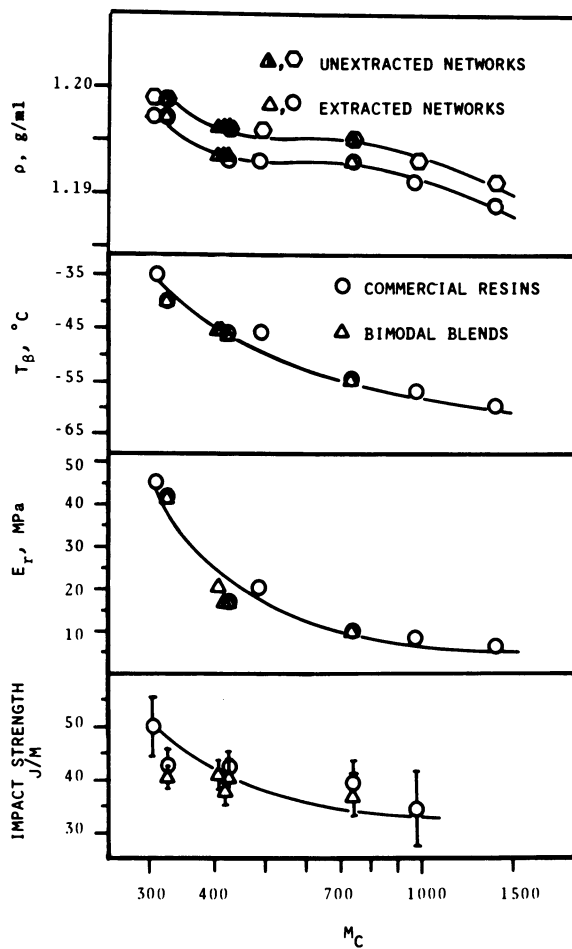
Figure 2. *Impact strength, E_r, T_β, and density as a function of M_c for Series E and Series F networks*

E, also showed broader and flatter tan δ peaks (Figure 3). This broadening is attributed to the broadening of the distribution of M_c.

Slope of the transition region. The slope of the E' vs. temperature curve in the glass transition region also varied with M_c. In accordance to the creep results (discussed later) values of the slope (n), obtained from the dynamic mechanical data (see Figure 3), of the blend samples F-1, F-2, F-3, and F-4 were close to that of the commercial-resin sample E-1. In contrast, the slope of the blend sample F-5 was steeper than that of its commercial counterpart, sample E-5. The broadening of the transition region of the blend samples F-1 to F-4 is attributed to the presence of broad distributions of M_c in them.

Tensile behavior. Tensile properties fell in the following ranges, as shown in Figure 4: (Control Series E), E_g = 1.2 ($+$ 0.3) GPa, σ_u = 71 ($+$ 7) MPa, ε = 11 ($+$ 2) %; (Bimodal Series F), E_g = 1.0 ($+$ 0.3) GPa, σ_u = 69 ($+$ 10) MPa, ε = 9 ($+$ 2) %. No trends as a function of M_c were observed, in contrast to the case of M_c changed by changing stoichiometry (27,28). Thus the tensile properties at room temperature are essentially independent of M_c and its distribution. This general relative insensitivity to changes in M_c and its distribution is not surprising, because the glassy state properties should be more closely related to the cohesive energy density than to network structure (35). Furthermore, the shift factors (log a_T) obtained from creep experiments (see below) indicate that the motion of the main chains of these networks is very restricted. Therefore, as observed experimentally, it can be expected that the room-temperature tensile properties of these epoxy networks having bulky bisphenol-A groups would be independent of average M_c or distribution of M_c.

Impact strengths varied inversely with M_c, values ranging from 50 J/m for E-1 to 34 J/m for E-6. However, as shown in Figure 2, impact strength was not affected by changes in the distribution of M_c.

Creep behavior. Figure 5 shows the composite curve of the shift factors and also indicates that the shift factors in the glass transition region do not follow the WLF equation:

$$\log a_T = -(17.44[T-T_g])/(51.6 + [T-T_g]) \qquad (2)$$

Instead, they follow an equation of the Arrhenius type given below (also see Figure 6):

$$\log a_T = -H_a/2.303\ RT \qquad (3)$$

where R is the gas constant, T is the absolute temperature, and H_a is the apparent activation energy. Thus, shift factors for all the samples of the present study, including samples E-5, E-6, and E-7 which have relatively long chains and would be expected to be
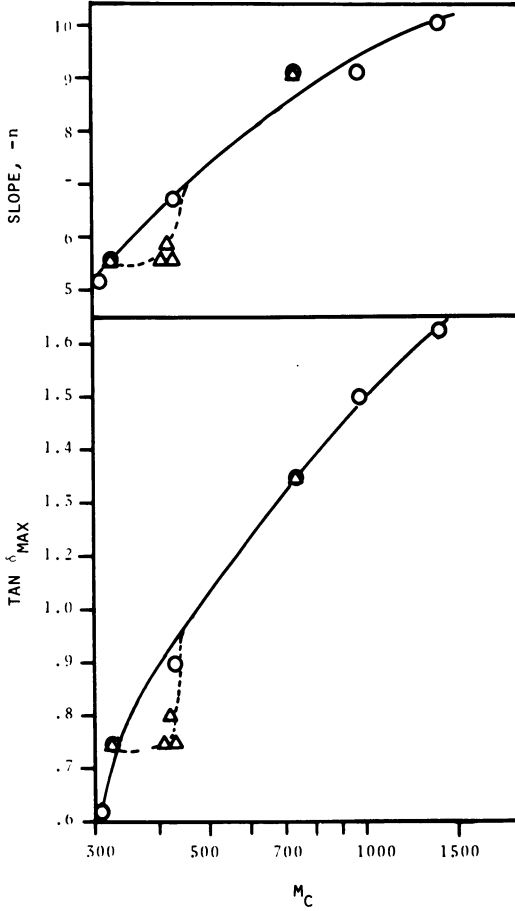
Figure 3.   Tan δ_{max} and slope of the transition region as a function of M_c: ($\bigcirc$) commercial resins; ($\triangle$) bimodal blends
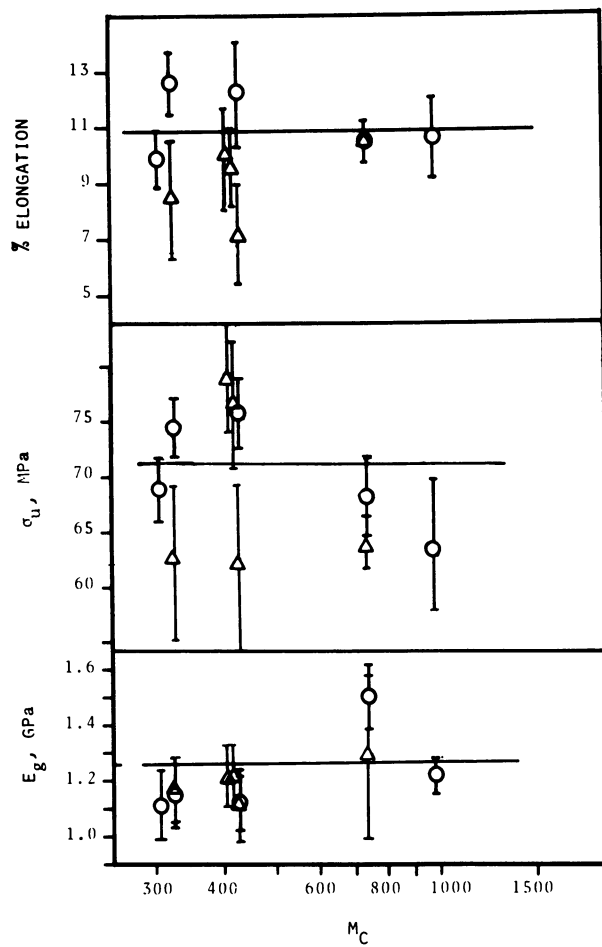
Figure 4.   *Tensile properties of Series E and Series F networks as a function of* M_c: (○) *commercial resins;* (△) *bimodal blends*
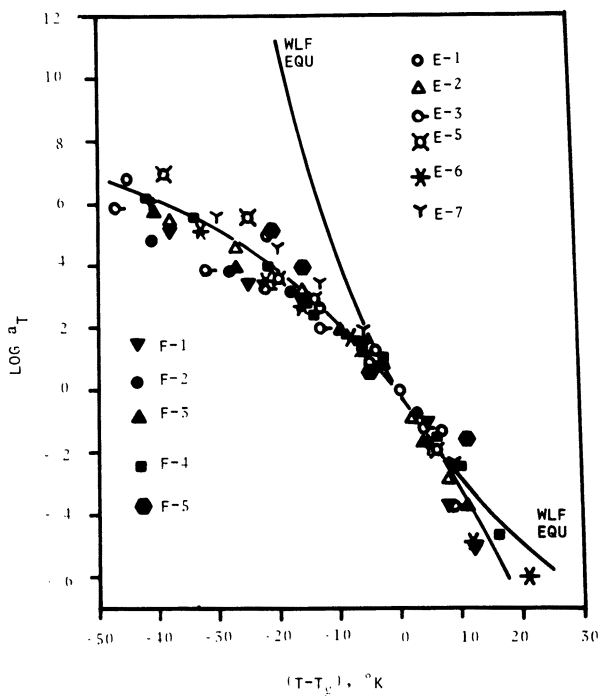
Figure 5. Shift factors as a function of (T − T$_g$) for Series E and Series F networks
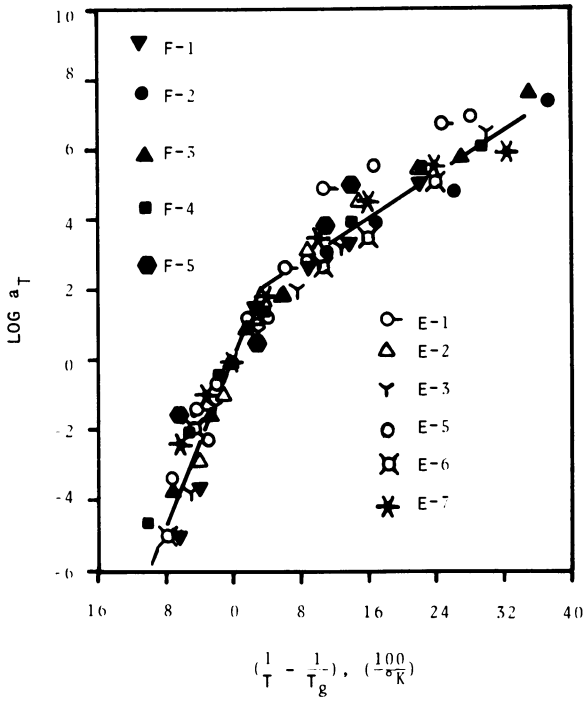
Figure 6. Shift factors as a function of $(1/T - 1/T_g)$ for Series E and Series F networks

flexible, surprisingly gave a better fit to an Arrhenius
relationship as is generally the case for polymers in the glassy
state. Thus it appears that the motion of the main chains of the
present epoxy networks is relatively restricted even beyond the
glassy state. It appears that the bulky bisphenol-A groups are
responsible for the restricted motion of the main chains observed
even beyond the glassy state. It was also noted that the activa-
tion energy was independent of M_c and distribution of M_c in those
networks; values of 230 kcal/mole and 75 kcal/mole above and below
T_g, respectively, fit all samples. The values are in good agree-
ment with values determined here for bisphenol-A-based epoxies
cured with MDA (31) and elsewhere for similar epoxies cured with
amines (37).

To determine the effect of the distribution of M_c on creep,
master curves for all the samples were drawn at 129°C instead of
selecting T_g as the reference temperature. The temperature
corrections were not used to draw the master curves shown in
Figure 7 because these corrections, as mentioned earlier, were
small and the experimental data did not extend to long ranges of
temperature in the rubbery region. The characteristic creep time
(τ_c) was taken as the time required to relax to a value of log
$E(t) = (\log E_g + \log E_r)/2$, where E_g and E_r are the glassy and
rubbery moduli, respectively. The slopes (n) of the master curves
were determined at the time τ_c. The characteristic creep time
(τ_c) was found to be inversely related to M_c by the following
relationship:

$$\log (\tau_c/\tau_{co}) = K_1/M_c \qquad (4)$$

where $\log \tau_{co} = -10.1 = (\tau_c$ at $M_c = \infty$, obtained by extrapolation),
and $K_1 = 5.4 \times 10^3$ (a constant). The statistical correlation
coefficient was 0.99, showing excellent fit.

Figure 8 shows that the blend samples F-1 and F-5 appear to
have higher τ_c's than their counterparts E-2 and E-5, respectively,
which were prepared from commercial resins. On the other hand,
sample F-4 has a lower τ_c than its commercial counterpart E-3.
These results indicate that the differences in distribution of M_c
affect τ_c. Samples E-2 and E-3 have network chains composed of
epoxy molecules having molecular weights of 340 and 620, respec-
tively, whereas the major portions of samples E-5, E-6, and E-7
are composed of epoxy molecules having a M.W. of 2328 or 3748.
Furthermore, the blend samples F-1 and F-5 have a larger propor-
tion of epoxy molecules having a molecular weight of 340 than
their respective counterparts E-2 and E-5 (commercial resins);
this results in a higher τ_c. On the other hand, the blend sample
F-4 has two epoxy species having M.W.'s of 340 and 3748, respec-
tively, in equal amounts and its commercial counterpart sample
E-3 has epoxy species having M.W.'s of 340 and 620. The appreci-
able amount of large molecules in F-4 results in lower τ_c. Thus,
it is concluded that τ_c, besides being sensitive to M_c, is also
very sensitive to the distribution of M_c; τ_c would be larger or
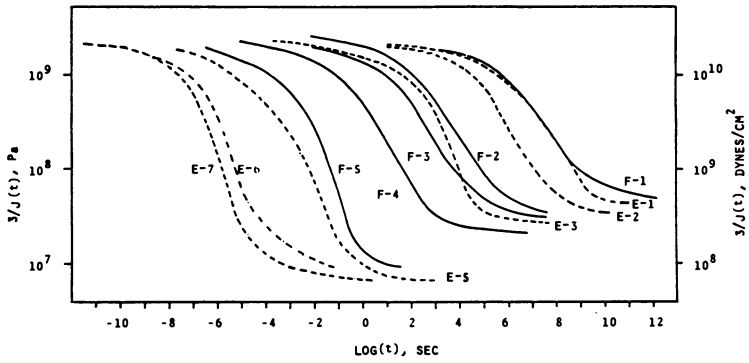
Figure 7.   Master curves for Series E and Series F networks $(T_o = 129°C)$
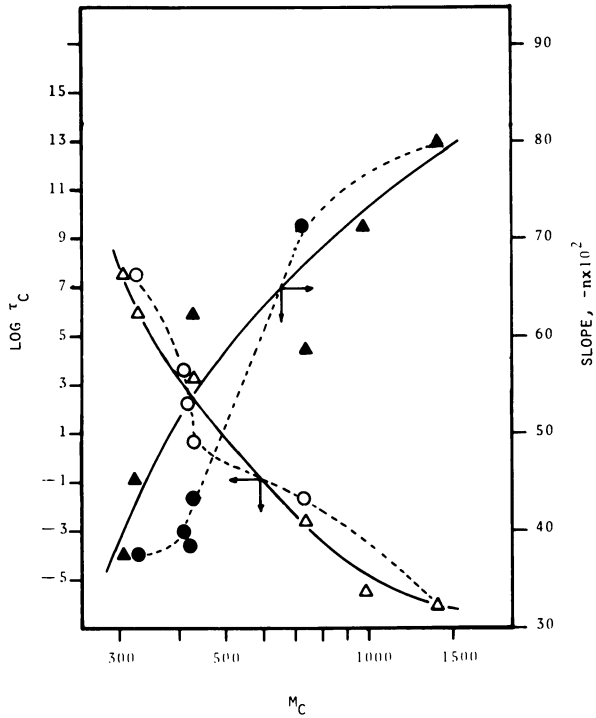
Figure 8.   Characteristic creep time and slope of the transition region as a function of M_c for Series E and Series F networks: $(\triangle, \blacktriangle)$ commercial resins; $(\bigcirc, \bullet)$ bimodal blends

smaller depending upon whether the network has greater amounts of smaller or larger chains, respectively.

The slope of the transition region was found to broaden with a decrease in M_c (Figure 8). These results indicate that an increase in crosslink density results in the broadening of the slope, as is often observed. For example, from dynamic mechanical studies of polyesters, Shibayama and Suzuki (36) had also shown that the dispersion broadens with an increase in crosslink density.

Furthermore, the bimodal blend samples F-1 to F-4 have slopes close to that of sample E-1, prepared from the commercial resin whereas sample F-5 (bimodal blend) has a slope close to that of sample E-7 (commercial resin). The lower values of slope observed in the blend samples F-1 to F-4 are a result of a broader distribution of relaxation times which is not present in the respective counterparts of Series E. Similarly, sample F-5 showed a higher slope than its counterpart E-5 (even though the slope measured for E-5 is lower than it should be), because the former had a narrower distribution of molecular weights which resulted in a narrower distribution of relaxation times (see Table I).

It is concluded that the broadening of the transition region could take place either by an increase in the average crosslink density or by the broadening of the distribution of crosslink density.

Swelling and extraction. Swelling and extraction data are shown in Figure 9. The T_g of the blend sample F-4, which had 57% Epon 825 and 43% Epon 1004, had indicated that Epon 1004 forms the more continuous network. The swell ratio of this sample is the same as that of its commercial counterpart, sample E-3. Similarly the blend samples F-1 and F-5 also have swell ratios that are the same as their respective commercial counterparts E-2 and E-5. This indicates that the swell ratio is not very sensitive to the distribution of M_c. On the other hand, samples F-2 and F-3 have swell ratios that are lower than expected (see Figure 9). These samples have higher proportions of low-molecular-weight prepolymer (i.e. 62 and 60% by weight, respectively). It is highly probable that the composition of these samples is in a critical range in which a phase inversion exists; in other words, some part of the network probably has Epon 1004 as the more continuous phase while another part of the network has Epon 825 as the more continuous phase. Such a mixed network might well result in anomalous swelling behavior, with slightly lower values of the swell ratio than expected if the low-M epoxy network dominates swelling.

The bulk density of the samples at room temperature decreased with M_c and, as expected, was not affected by the distribution of M_c at a constant M_c, as shown in Figure 2.
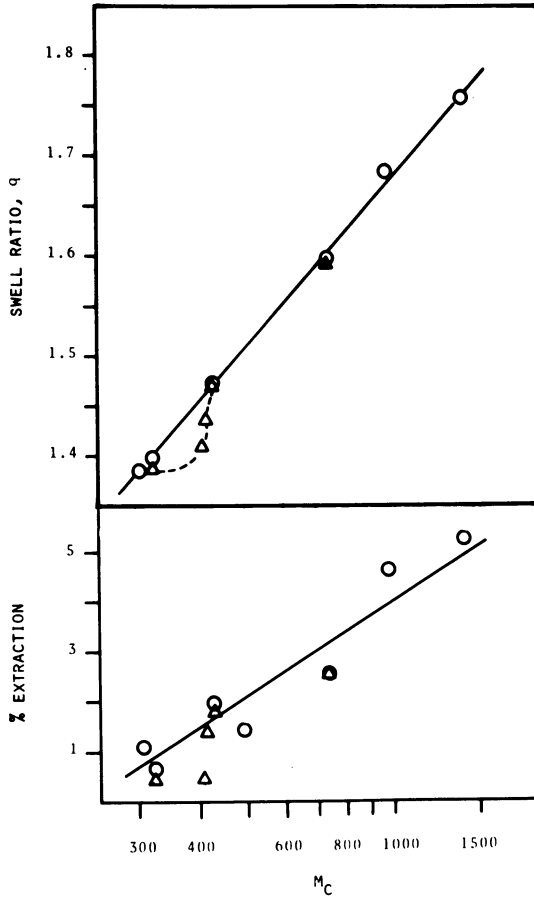
Figure 9.   Swell ratio and % extraction as a function of M_c for Series E and Series F networks: ($\bigcirc$) commercial resins; ($\triangle$) bimodal blends

Conclusions

The effects of M_c and of its distribution may be summarized
in the following conclusions.

Properties affected by the distribution of M_c.
    1. The glass transition temperature, as is well known,
increases with a decrease in M_c. Slight changes in the distribu-
tion of M_c do not affect T_g. However, when significant changes in
the distribution of M_c exist, T_g is governed by the dominant com-
ponent in the final network.
    2. The slope of the transition region at T_g increases
with M_c but decreases (i.e. broadens) with an increase in the
breadth of the distribution of M_c.
    3. The height of the tan δ peak increases with M_c.
Furthermore, as expected, an increase in the breadth of the dis-
tribution of M_c results in a broadening of the tan δ peak along
with a decrease in the height of the peak.
    4. The characteristic creep time (τ_c) is the most sen-
sitive variable to the distribution of M_c. Its value is higher
or lower depending on whether the network is composed of higher
fractions of short or long chains, respectively.

Properties not affected by the distribution of M_c.
    1. The rubbery modulus (E_r) decreases with an increase
in M_c but as predicted theoretically (34) is not affected by the
distribution of M_c.
    2. The room-temperature tensile properties for the pre-
sent epoxy networks are independent of M_c or the distribution of
M_c. This independence is ascribed to the restricted motion of the
main chains, even above T_g, as deduced from the creep experiments.
    3. The soluble content increases steadily with M_c but
is not affected by changes in the distribution of M_c.
    4. The density increases with a decrease in M_c but is
not affected by changes in the distribution of M_c.
    5. The swell ratio increases with M_c but is unaffected
by the distribution of M_c, except in some unusual networks having
a phase inversion.
    6. The room-temperature impact strength increases with
a decrease in M_c but is unaffected by the distribution of M_c.
    7. The β-transition temperature increases with a
decrease in M_c but is not affected by the distribution of M_c.
    8. The experimental shift factors, for DGEBA-epoxy
networks, are independent of M_c or the distribution of M_c.
Instead of following the WLF equation, values of the shift factor
follow an Arrhenius-type relationship with temperature, indicating
that the chain segment mobility is restricted even in the rubbery
state.

Acknowledgements

Literature Cited

1. Murayama, T. and Bell, J. P. J. Polym. Sci. (1970), A-2(8),
    437.
2. Hirai, T. and Kline, D. E. J. Appl. Polym. Sci. (1972), 16,
    3145.
3. Hirai, T. and Kline, D. E. J. Appl. Polym. Sci. (1973), 17,
    31.
4. Whiting, D. A. and Kline, D. E. J. Appl. Polym. Sci. (1974),
    18, 1043.
5. Selby, K. and Miller, L. E. J. Mat. Sci. (1975), 10, 12.
6. Hata, N. and Kumanotani, J., J. Appl. Polym. Sci. (1971), 15,
    2371.
7. Johnson, R. E. and Fricke, A. L. Proc. Conf. Reinf. Plast./
    Compos. Div., Soc. Plast. Ind. (1972), 27, 19F, 1.
8. Kitoh, M. and Suzuki, K. Kobunshi Ronbunshu (1976), 33, 1,
    19.
9. Kenyon, A. S. and Nielsen, L. E. J. Macromol. Sci., Chem.
    (1969), A3(2), 275.
10. Hata, N. and Yamuchi, R. J. Appl. Polym. Sci. (1973), 17,
    473.
11. Hata, N. and Kumanotani, J., J. Appl. Polym. Sci. (1977), 21,
    1257.
12. Moehlenpah, A. E.; Ishai, O.; and Dibenedetto, A. T.
    J. Appl. Polym. Sci. (1969), 13, 1231.
13. Manson, J. A. and Chiu, E. H. ACS Polymer Preprints (1973),
    14(1), 469.
14. Manson, J. A. and Chiu, E. H. J. Polym. Sci.-Symp. No. 41
    (1973), 95.
15. Meeks, A. C. Polymer (1974), 15, 675.
16. DeRosset, W. S. J. Composite Mat. (1975), 9, 114.
17. Bascom, W. D.; Cottington, R. L.; Jones, R. L. and Peyser, P.
    J. Appl. Polym. Sci. (1975), 19, 2545.
18. Galparin, I. J. Polym. Sci. (1967), 11, 1475.
19. Lewis, T. B. and Nielsen, L. E. J. Appl. Polym. Sci. (1970),
    14, 1449.
20. Michael, P.; Ebdon, P.; and Delatycki, O. J. Polym. Sci.,
    Polym. Phy. Ed. (1976), 12, 1555.
21. Peyser, P. and Bascom, W. D. Polym. Preprints (1976), 17(2),
    157.
22. Merrall, G. T. and Meeks, A. C. J. Appl. Polym. Sci. (1972),
    16, 3389.

23. Morgan, R. J. and O'Neil, J. E. in "Chemistry and Properties of Crosslinked Polymers." Ed. by S. S. Labana, Academic Press, N. Y. (1977), p. 289.
24. Suzuki, K., et al., Kobunshi Ronbunshu (1976), 33(5), 271.
25. Brett, C. L. J. Appl. Polym. Sci. (1976), 20, 1431.
26. Nielsen, L. E. J. Macromol. Sci. (1969), C3, 69.
27. Manson, J. A.; Sperling, L. H. and Kim, S. L. Final Report, AFML Contract No. F33615-75-C-5167, 1977 (AFML-TR-77-109.
28. Kim, S. L.; Skibo, M.; Manson, J. A.; Hertzberg, R. W. and Janiszewski, J. ACS Org. Coatings and Plastics Chemistry (1977), 37, 544; in press, Polym. Eng. Sci.
29. Misra, S. C.; Manson, J. A. and Sperling, L. H. This publication, 1978.
30. Misra, S. C. Ph.D. Dissertation, Department of Chemical Engineering, Lehigh University, 1978.
31. Kim, S. L.; Manson, J. A. and Misra, S. C. This publication, 1978.
32. ASTM D-1043, American Society of Testing Materials, Philadelphia, Pa. (1974).
33. Bell, J. P. J. Polym. Sci. (1970), A2(8), 417.
34. Graessley, W. W. Macromolecules (1975), 8(6), 865.
35. Kaelble, D. A. In "Epoxy Resin Chemistry and Technology." Ed. by C. A. May and Y. Tanaka, M. Dekker, 1973, Chap. 5.
36. Shibayama, K. and Suzuki, Y. J. Polym. Sci. (1965), A-3, 2637.
37. Kito, M. and Suzuki, K. Kobunshi Ronbunshu (1976), 33, 19.

Network Morphology and the Mechanical Behavior of Epoxies

S. C. MISRA, J. A. MANSON, and L. H. SPERLING

Materials Research Center, Coxe Laboratory #32, Lehigh University, Bethlehem, PA 18015

Since the properties of thermosetting polymers depend on their network structures, the morphology of such polymers has long been a subject of considerable theoretical and practical interest. Thus, it is well known that the tensile strength of thermoset resins is less than predicted theoretically on the basis of the breakage of primary van der Waal's bonds (1,2), and it was proposed long ago (3) that this discrepancy was due to the rupture of weak regions created during network formation. Indeed, it has been shown (4) that high internal stresses can be developed during curing, especially when the curing rate is low. This view of the role of structural defects is also given credence by modern theories of fracture mechanics (5), which emphasize the concept of the concentration of stress at a flaw.

Two-Phase Networks

Other investigators (4,6-33) have emphasized a view of the network essentially as a composite, with a high-crosslink-density (essentially spherical) phase (often considered as a microgel) embedded in a less-crosslinked matrix. In fact, it is probably generally accepted that, regardless of specific details, the curing of thermosets results in an inhomogeneous, two-phase network. Inhomogeneity has been attributed to incompatibility or to non-optimum curing conditions (8) but has also been proposed to be inherently characteristic of all gelling systems (14). It has also been postulated (7) that these microgels are colloidal in nature, at least for some epoxy systems.

The existence of inhomogeneities has been inferred from results of diverse investigations using techniques such as electron and optical microscopy (13-26,29,30,31,32), thermomechanical measurements (34), differential swelling (12,35), and differential scanning calorimetry (36). In contrast, the use of microtomed thin sections and small-angle x-ray scattering fail to indicate two-phase structures (37). Dispersed phases have been referred to by such terms as "micelles," "globules," "floccules," "nodules," and "microgels." In this study, the term "microgel" will be used.

It has been suggested by Bobalek et al. (27), Solomon (33), and Labana et al. (14) that the two-phase system is produced by microgelation prior to the formation of the macrogel. Some investigators (4,14,16) have postulated that these microgels are loosely connected to the surrounding matrix, and have also suggested (12) that these loose connections are developed during the latter stages of the curing process.

In general, two levels of sizes have been reported in the literature--one (type A) ranging from 6 nm to 40 nm, and the other (type B) ranging from 20 μm to 200 μm. It has also been shown (4) that slow curing rates result in larger microgels (type B), which result in a network having a higher T_g, density, and resistance to etching. The surface properties of the network depend on the surface energy of the mold material and on the atmospheric environment (7,30). The size and density of microgels have also been related to the presence of plasticizer (23), radiation damage (26), prolonged exposure to heat (17) and aging of the resin (24).

Studies of interfaces (30,31) have also shown that certain substrates such as Teflon and silicone-coated sheets give featureless surfaces; however, subsequent etching of the surface reveals a two-phase structure. It was further shown that the microgel size decreases with increasing amounts of catalyst.

Both low tensile strengths and nodular morphology in thermosets have been related to differences in crosslink density (7,10, 14,27,28,32). At the same time, the fact that the yield strength of some epoxies is fairly independent of stoichiometry has been attributed to the role of microgels as primary flow particles (29). Thus, morphology must play an important role in determining network properties. However, surface morphology should not affect the mechanical behavior of the network as much as bulk morphology. Diffusion phenomena, on the other hand, should depend on the morphology of both the outer surface and of the bulk.

Though there have been several postulates of morphological changes during the crosslinking process and of the morphology of the final network, experimental evidence has been scarce. As part of a comprehensive study (38) of the effects of crosslink density on the behavior of epoxies and other polymers, the present morphological investigation was conducted on epoxies with emphasis on the roles of stoichiometry, molecular weight of the epoxy prepolymer, and the distribution of molecular weight between crosslinks (M_c). Bisphenol-A-based prepolymers were used throughout; most were cured with methylene dianiline (MDA), a few were cured with a polyamide.

Experimental

Sample Design. The various formulations are described in Table 1. To examine the effect of stoichiometry, Series A was

prepared using different proportions of Epon 828 with MDA (Shell Chemical Co.). To provide a baseline for examining the effects of M_c <u>at constant stoichiometry</u>, Series E, based on the following prepolymers, was prepared using stoichiometric amounts of MDA as curing agent: Epon 825, 828, 834, 1001, 1002, and 1004 (Shell Chemical Co.) To vary the <u>distribution</u> of M_c, Series F was prepared to yield resins which had the same <u>average</u> M_c values as Epon 828, Epon 834, and Epon 1001. This was done by blending Epon 825 (narrow distribution of molecular weight) with various proportions of Epon 1004. The distributions of M_c thus obtained are essentially bimodal, with little overlap. Finally, to compare behavior with that of a polyamide-cured epoxy, Sample G-1 was prepared by curing Epon 828 with an equivalent proportion of Versamid 140 (General Mills Chemical Co.).

Table I. Compositions of the Samples Prepared in
Epoxy Resin Series A, E, and F.

Series A			Series E and Series F		
Sample No.	Amine/epoxy Ratio	M_c [a,b]	Sample No.	epoxy (wt. %)	M_c [a]
A-7	0.7:1	1523	E-1	825(100)	308
A-8	0.8:1	526	E-2	828(100)	326
A-10	1.0:1	326	F-1	825(91)+1004(9)	326
A-11	1.1:1	370	F-2	825(62)+1004(38)	413
A-14	1.4:1	592	F-3	825(60)+1004(40)	419
A-16	1.6:1	924	E-3	834(100)	430
A-18	1.8:1	1922	F-4	825(57)+1004(43)	430
A-20	2.0:1	∞ (linear)	E-5	1001(100)	740
			F-5	825(20)+1004(80)	740
			E-6	1002(100)	980
			E-7	1004(100)	1400

[a] Calculated using Bell's equation (<u>39</u>).

[b] For reasons discussed by Bell (<u>39</u>), actual M_c values for specimens A-16 to A-20 may be somewhat in error. In any case, the error will not affect the trends observed as a function of stoichiometry.

<u>Resin Preparation</u>. For systems using liquid epoxy prepolymers (e.g., Epon 825 and 828) with MDA as the curing agent, the curing cycle was similar to that used by Bell (<u>39</u>). After heating to 80°C, the resin and curing agent were mixed together, evacuated for 5 to 15 min. to remove air bubbles, and cast and cured as follows: 45 min. in a circulating air oven at 60°C, 30 min. at 80°C, 2.5 hr. at 150°C, and finally slow cooling to room

temperature. The mold assemblies comprised clamped 13-cm by 13-
cm Mylar sheets, separated by 0.5-mm, 1.5-mm, or 6-mm Teflon or
ethylene-propylene-copolymer spacers backed by glass plates.
This cure cycle was reported by Bell to give essentially complete
curing, and was also shown (through chemical titration of the
epoxy and amine groups) to be similarly effective in this labora-
tory (38,41,42).

Solid epoxies were first melted and then evacuated to remove
the entrapped air bubbles. In order to avoid air entrapment, the
curing agent was mixed in, using a magnetic stirrer, under vacuum.
Samples were prepared using the following curing cycle: 1.5 hr.
at 100°C, 2.5 hr. at 150°C, followed by slow cooling to room
temperature. The Versamid-140-cured sample (G-1) was one of the
samples prepared by Manson and Chiu (40), using the following
cure cycle: overnight curing at room temperature, 2 hr. at 60°C,
2 hr. at 100°C, and 4 hr. at 140°C.

Using these techniques, it was possible to prepare reproduc-
ible samples suitable for testing, albeit with considerable
difficulty in the case of solid epoxies.

Electron Microscopy. Various etching techniques were tried
to study the micro- and macro-structures of MDA-cured epoxy net-
works ("macro" implying a morphological feature on the scale of 1
μm or larger). Etching may be presumed to preferentially attack
regions of relatively lower local crosslink density. After the
examination of etched samples under the ETEC Autoscan scanning
electron microscope (SEM), it was concluded that etching for 7 hr.
with 1 M aqueous Cr_2O_3 at 80°C was more effective than the follow-
ing techniques: etching for 30 min with HF; etching for 15 days
with acetone; etching for 10 hr. with argon at high voltage under
vacuum. The study of etching time indicated that at least one hr.
was needed to produce adequate etching with Cr_2O_3. Finally,
etching times of 4 hr. and 7 hr. were found to be convenient for
samples having M_c's above and below 500, respectively. The gross
morphology was examined under the SEM while the fine structure
was examined using a Phillips 300 transmission electron micro-
scope (TEM), using two-stage carbon-platinum replicas of the etch-
ed surfaces. It should be noted that one must be very careful in
interpreting statements about features seen in replicas. Thus a
nodule on a two-stage replica arises from a dimple (not a nodule)
on the polymer surface.

Isolation of Microgels. The following experiments were made
to isolate microgels during the process of curing and from the
etchant solution:

1. The formation of microgels during the curing process was
verified experimentally on samples E-2 and E-5 by dissolving them
in acetone, before gelation. Sample E-2, which has a longer gel-
ation time than E-5, was dissolved after curing at 60°C for 30
min and at 80°C for another 15 min whereas sample E-5 was

dissolved after curing for only 10 min at 100°C. The solution
was diluted to a concentration of 100 ppm, and electron micro-
scope grids were made and examined under the TEM.

2. Etched samples were removed, the etching solution was
diluted with deionized water to a very low concentration, and
electron microscope grids were prepared by platinum shadowing.
Similarly, a less dilute solution (from the etching of sample E-
5) was placed on a clean microscope slide, allowed to dry, and
examined under the SEM.

Results

Figure 1 shows typical macrostructures, with feature sizes
from ca. 10 μm to 40 μm, revealed by progressive etching by the
aqueous Cr_2O_3. The effects of different variables on morphology
are discussed below.

Effect of Stoichiometry. Examination of the etched surfaces
under the SEM (Figures 2 and 3) revealed a two-phase structure.
Dimples were observed on the surface, the dimple size increased
with deviation from equivalent stoichiometry. Samples having an
excess of epoxy appeared to have fewer dimples than samples
having a similar M_c but excess amine. The sizes of the dimples
varied from ca. 10 μm to 70 μm, depending on the percent excess
of reactants, in general agreement with sizes reported by Cuth-
rell (7) and Selby and Miller (37). It was also observed that
above an amine/epoxy ratio of 1.6/1 the morphological differ-
ences were negligible.

The two-stage replicas examined with the TEM also revealed
the existence of two phases on a much finer scale (Figure 4). The
replicas showed nodules on the surfaces, corresponding to dimples
on the polymer surfaces. The dimple sizes in these samples were
in the range of 25 nm to 50 nm except for the case of 100% excess
amine (A-20) where a large distribution of sizes, ranging from
20 nm to 200 nm, was observed. The distribution of phase size
tends to broaden with increasing proportions of excess amine;
the average size also tended to increase with the proportion of
excess amine. On the other hand, an increase in the amount of
excess epoxy did not show significant changes from the morphology
observed at equal stoichiometry. These observations differ from
those of Racich and Koutsky (31), who found that the domain size
decreased with increasing amounts of catalyst and with the pre-
sence of saturated vapor of the curing agent. They argued that
the crosslink density increases with increasing amounts of cata-
lyst, resulting in smaller domain sizes. The present results
indicate that, as reported by Racich and Koutsky, the domain size
tends to increase with a decrease in crosslink density, but only
in the excess-amine case; the domain is not significantly affect-
ed by changes in crosslink density for the excess-epoxy case.
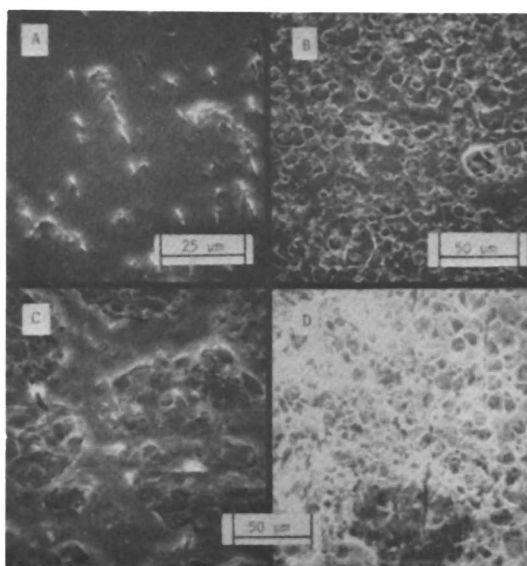
Figure 1.   Micrographs of Cr_2O_3-etched surfaces of Epon 1004-MDA (Specimen E-7). Etching times: (A) 2 hr; (B) 4 hr; (C) 7 hr; (D) 11 hr
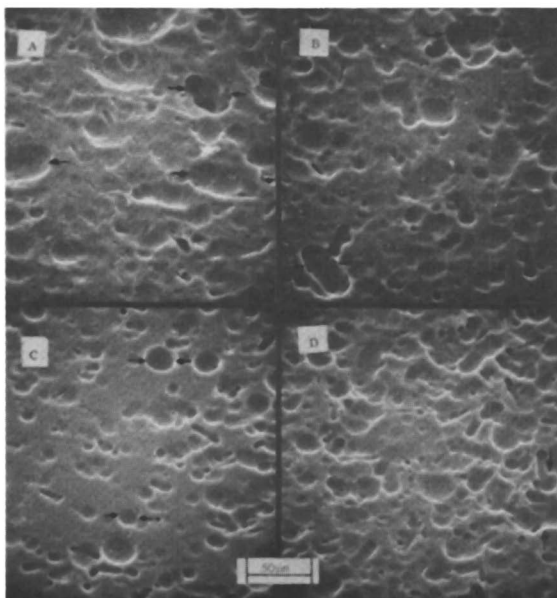
Figure 2. Scanning electron micrographs of 7-hr-etched samples having different stoichiometric ratio of MDA to Epon 828: (A) 0.7/1; (B) 0.8/1; (C) 1/1; (D) 1.1/1
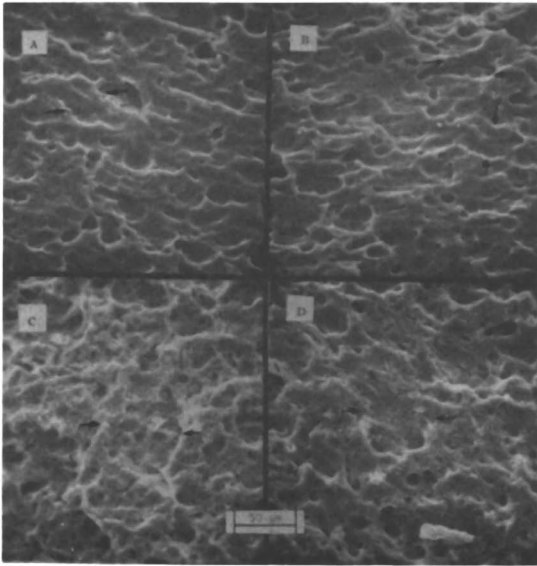
Figure 3. Scanning electron micrographs of 7-hr-etched samples having different stoichiometric ratio of MDA to Epon 828: (A) 1.4/1; (B) 1.6/1; (C) 1.8/1; (D) 2.0/1
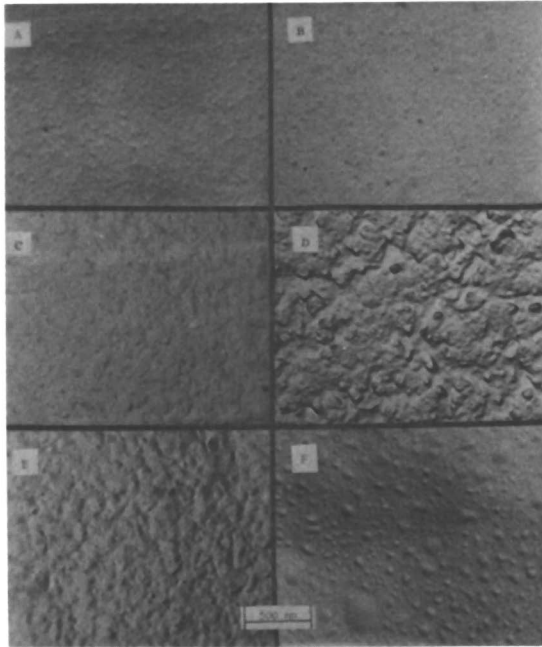
Figure 4. Transmission electron micrographs of replicas of 4-hr-etched samples having different stoichiometric ratio of MDA to Epon 828: (A) 0.7/1; (B) 0.8/1; (C) 1.1/1; (D) 1.4/1; (E) 1.6/1; (F) 2.0/1

Effect of Molecular Weight of the Prepolymer. When the
crosslink density was changed by changing the molecular weight of
the epoxy prepolymers, a two-phase structure, similar to that
found for the case of variable stoichiometry, was observed even
at the macro level (Figures 5 and 6). A marked difference in
morphology was observed in networks prepared from liquid resins
as compared to those from solid or semi-solid resins. The
liquid-resin (Epon 825, 828) samples had dimples which had a dis-
tribution of size ranging from 5 μm to 25 μm. In addition to
dimples, small ridges were also seen in both agglomerated and
isolated forms. In samples from semi-solid and solid resins
(Epon 834, 1001, 1002 and 1004), etch-resistance (and, hence,
presumably highly crosslinked) shells were observed throughout
the cross-section (Figure 7), encapsulating the less crosslinked
material. These shell-and-core-type structures were present in
these samples in a range of sizes from 2.5 μm to 25 μm. It was
found that the range narrowed but that the average size increased
with an increase in the molecular weight of the prepolymer. This
typical morphology was also observed in samples that were solvent
cast from acetone solutions and cured after most of the acetone
evaporated. Since it has been shown that curing does not take
place in the presence of acetone in the Epon-MDA system (39), it
can be assumed that the acetone-cast samples were similar to the
bulk-cured samples. Indeed no differences in mechanical proper-
ties in bulk and acetone-cast samples were observed (41, Ch. 6).
Etched under similar conditions, solvent-cast samples showed the
same shell-and-core-type morphology (Figure 7d), indicating that
this typical morphology was not due to inadequate mixing.

All the samples made from solid or semi-solid prepolymers
had the same fine structure, with the size of the discontinuous
phase in the range from 15 nm to 25 nm, whereas the samples made
from liquid prepolymers had slightly larger discontinuous phases
in the range from 25 nm to 50 nm.

Effect of the Distribution of Molecular Weight in the Pre-
polymer. The gross morphologies (both at macro and micro levels)
in the bimodal blend samples (Series F) appeared to be approxi-
mately similar to those of the counterparts prepared from the
Series E commercial resins (see Figure 8 for a typical compari-
son).

Effect of High-Molecular-Weight Curing Agent. Sample G-1
(cured with Versamid 140) also showed the shell-and-core-type
morphology (Figure 9). The sizes of the shell-and-core structure
(range from 2.5 μm to 25 μm) and the discontinuous phase were
larger than those cured with MDA, probably because this sample
had a higher M_c. Figure 9 shows a shell (encircled in black)
which was not etched open by the chromic acid at the time the
sample was removed. A semi-open shell can also be seen which
looks similar to a dimpled nodule (though of a much larger size)
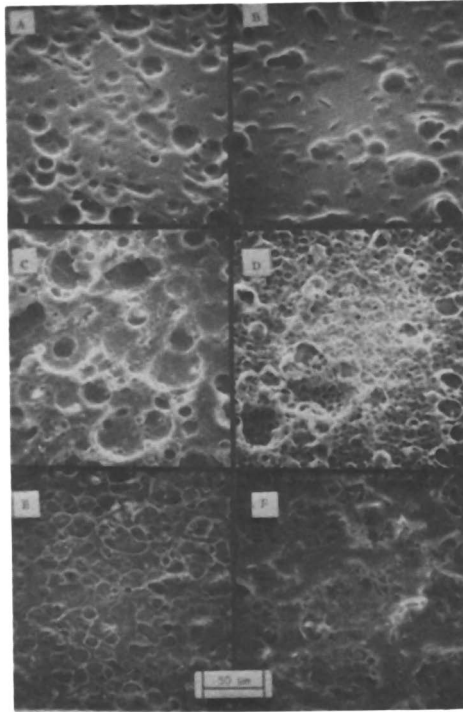
Figure 5. Scanning electron micrographs of 7-hr-etched networks prepared from equivalent stoichiometric amounts of Epon-MDA resins: (A) Epon 825; (B) Epon 828; (C) Epon 834; (D) Epon 1001; (E) Epon 1002; (F) Epon 1004
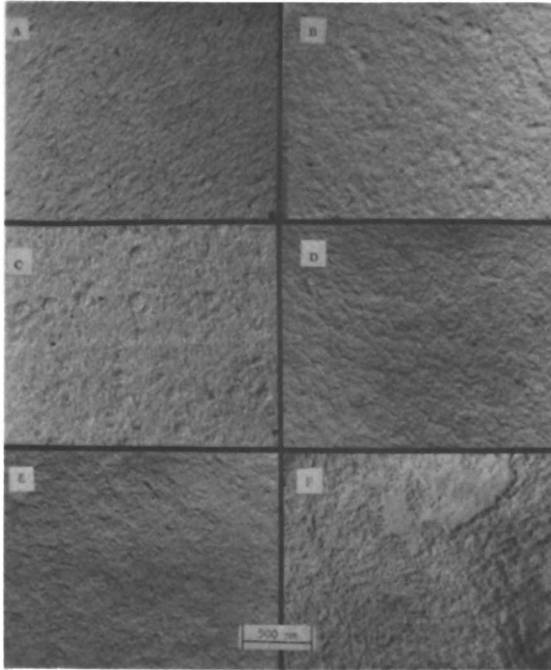
Figure 6. Transmission electron micrographs of replicas of networks prepared from equivalent stoichiometric ratios of Epon-MDA resins etched for 4 hr: (A) Epon 825; (B) Epon 828; (C) Epon 834; (D) Epon 1001; (E) Epon 1002; (F) Epon 1004
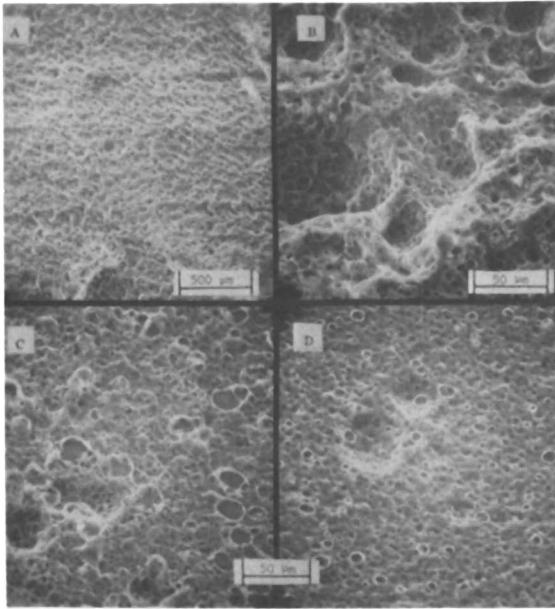
Figure 7. Scanning electron micrographs of Epon 1001-MDA sample (E-5) etched for 7 hr: (A) and (B) sample cross section; (C) sample surface; and (D) surface of solvent-cast sample
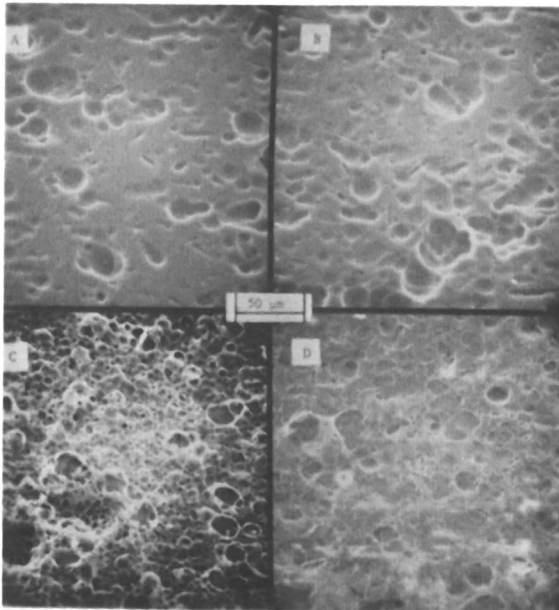
Figure 8.   Scanning electron micrographs of Series F networks along with their Series E counterparts etched for 7 hr: (A) Epon 828; (B) blend (Epons 825 and 1004) equivalent to Epon 828; (C) Epon 1001; (D) blend (Epons 828 and 1004) equivalent to Epon 1001
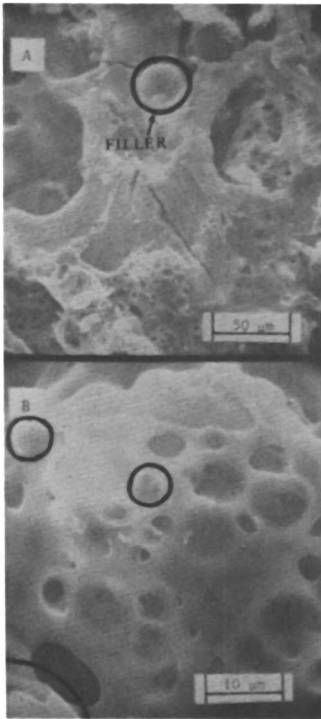
Figure 9. Scanning electron micrographs of Epon 828 resin cured with Versamid 140 (network comprising 25% glass beads by volume; etched for 7 hr)

shown by Racich and Koutsky (31).

To check if the shell-and-core-type structure observed in semi-solid and solid prepolymers was due to fast curing, Epon 828 (liquid prepolymer) and MDA (in stoichiometrically equivalent amounts) were cured at 150°C for 4 hr. This sample, after being etched as described earlier, did not show any difference in morphology from the sample cured through the regular curing cycle. It therefore appears that this peculiar morphology depends on the molecular weight of the prepolymer and not on the rate of curing or inhomogeneous mixing.

Isolated Microgels. The electron micrographs (Figures 10, 11a and 11b) clearly show the individual microgels (ranging in size from 20 nm to 200 nm) and clusters of microgels that were etched out from the network surface. The appearance of these microgels is in good agreement with the observations made on replicas and indicates that sample E-2 (prepared from liquid prepolymers) had larger microgels (sizes from 50 nm to 150 nm) as compared to sample E-5 (prepared from solid prepolymer, sizes from 25 nm to 60 nm). These micrographs prove that the dimples, observed through replicas, on the surfaces of the epoxy networks were due to the etching of the weak connections of the microgels or clusters of microgels and not to the etching of material having a low average crosslink density. The platinum shadows in Figures 11a and 11b indicate that the microgels are solid and nearly spherical in shape (a configuration having minimum surface energy) and can pack in a hexagonal array.

Similarly the electron micrographs (Figures 11c and 11d) show the existence of microgels even before gelation (darker phase) in the size range from 30 nm to 100 nm.

Thus, in both cases discrete microgel particles were observed, indicating that microgel formation takes place before gelation and that the microgels are dispersed and loosely connected to each other and in some cases (non-stoichiometric compositions) to a weaker continuous phase. These results also show that the discontinuous phase (though etched out first as clumps) is composed of microgels that are stronger than the continuous phase. It is the connections between the aggregates that are weak. The size and number of these gels probably continues to increase until the viscosity becomes high enough for physical gelation to take place.

Discussion

General Proposed Model for Network Formation. As mentioned earlier, electron microscopic evidence shows that microgel particles form prior to gelation (Figures 10 and 11), both with low and high molecular weight epoxies and with epoxy and amine-rich systems. This observation is in accord with the suggestions of other investigators (14,27,28). Some investigators have observed
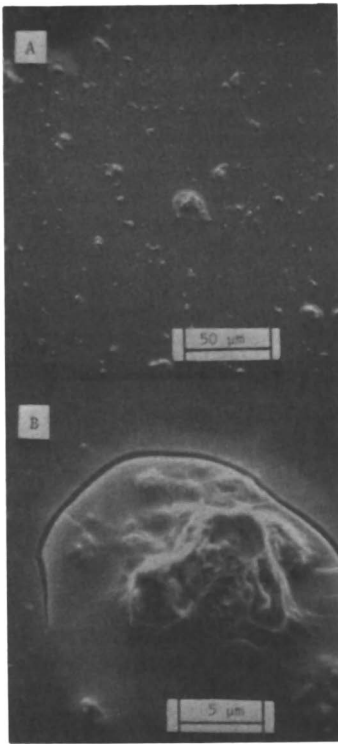
Figure 10. Scanning electron micrographs of isolated secondary microgels from Epon 828-MDA sample (E-2)
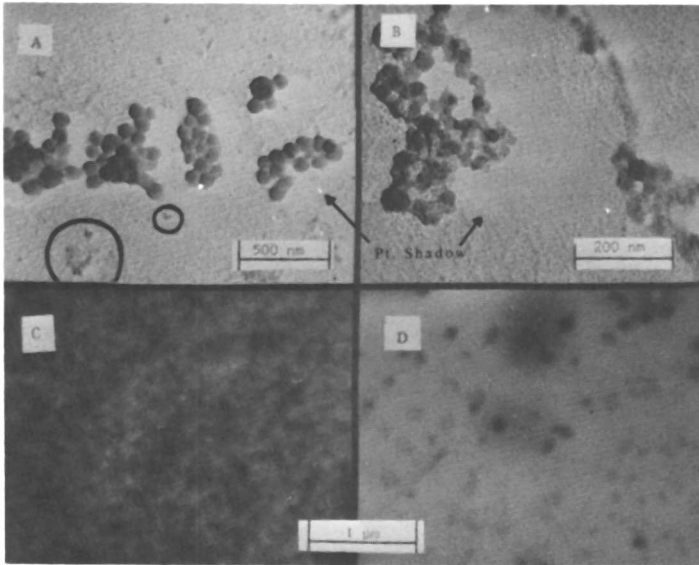
Figure 11.   Transmission electron micrographs of isolated primary microgels: (A) and (B) gel particles etched out by Cr₂O₃ solutions at 70°C after 4 hr; (C) and (D) microgels formed before gelation of the epoxy resins. [A and C—E-2; B and D—E-5]

these microgels in sizes smaller than 0.5 μm while others have reported larger than 5 μm. The present results indicate the presence of microgels at both levels; a lower level (10 nm to 50 nm) and a higher level (2 μm to 50 μm). It is, therefore, probable that the systems studied by other investigators also had microgels at both levels. In order to differentiate between the two size levels, the term <u>primary microgels</u> is used to refer to microgels in the size range from 10 nm to 50 nm, whereas <u>secondary microgels</u> refers to sizes larger than 1 μm.

In view of the morphological and property data at hand, a model for network formation is proposed. The principal points to consider include the following questions: the basic morphological units, the phase continuity, and the crosslink density and other properties of the various entities. The proposed mechanism which essentially comprises a synthesis of the mechanisms proposed by Bobalek et al. (<u>27</u>), Solomon (<u>33</u>) and Labana et al. (<u>14</u>), considers that the formation of the macrogel takes place in three sequential steps (Figure 12): formation of the primary microgels, formation of the secondary microgels, and formation of the macrogel. Following Labana et al. (<u>14</u>), it is also proposed that the secondary microgels and the macrogel are not completely coherent (that is, they have some unconnected dangling chains).

Formation of the Primary Microgels. The reactivities of the primary and secondary amine groups in MDA are approximately in the ratio of 1.4/1 (<u>39</u>). The primary amine groups should, therefore, react first to give a linear structure. Due to a combination of an exothermic heat of reaction with poor heat transfer, the temperature should rise in the vicinity of these molecules, resulting in the reaction of the secondary amine groups. Indeed, it has been shown that the primary and secondary amine groups react almost simultaneously even when their reactivities differ by a factor of two (<u>43</u>), The growth of the nuclei continues until the reactive polymer molecules can diffuse to the reactive sites of the nuclei. During this process several new nuclei are also developed. Therefore, a distribution of size of the primary microgels would be expected at all times during the curing process. This phenomenon has been predicted statistically by Labana et al. (<u>14</u>), who termed it a nucleation process resembling the one that occurs in crystallization.

Formation of the Secondary Microgels. After a certain concentration has been reached, the primary microgels and the growing nuclei begin to interact with each other and give rise to new nuclei for the secondary microgels. These nuclei grow in part due to capillary forces which will encourage physical sintering and in part due to the reaction of unreacted functional groups in the primary microgels. Thus, the secondary microgels are not as coherent as the primary microgels. The size of a particular secondary microgel would depend on the concentration of the
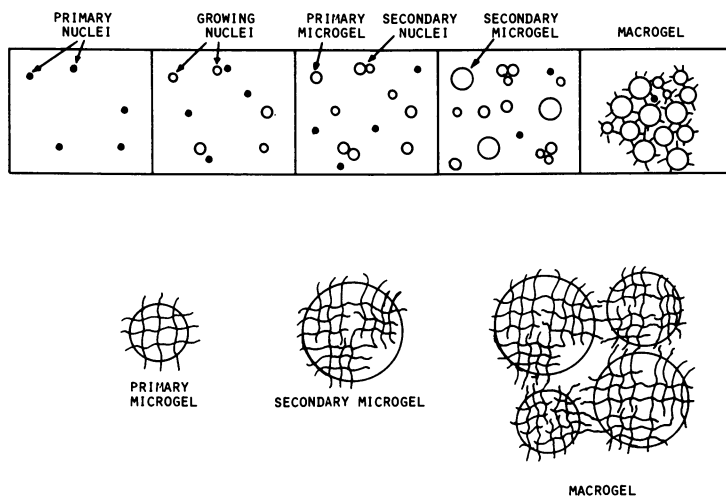
Figure 12.   Proposed model for network formation

primary microgels near the secondary nucleus. A size distribu-
tion in the secondary microgels should also be expected.

Formation of the Macrogel (Final Network). At a critical
solids concentration (~74% for monodispersed spheres arranged in
a hexagonal packing), the secondary microgels pack together and
the experimental gel point is observed. At this stage, phase
inversion takes place during which the secondary microgels become
the matrix and the unreacted or partially reacted prepolymers
become the dispersed phase. By the time of complete reaction,
the secondary microgels become loosely connected to each other
with the help of the interstitial prepolymer or due to self-
diffusion of reactive dangling groups. Thus, the interconnec-
tions between the secondary microgels would be weaker than those
between the primary microgels. The properties of the final net-
work should be affected by the coherence of the network. In net-
works prepared by non-stoichiometric compositions, the secondary
microgels would be embedded in a matrix of lower crosslink den-
sity but still connected to each other through chemical bonds.
Based on the above model, the morphological differences and
mechanical behavior observed in the samples of different series
are interpreted below.

Morphological Differences. In epoxy prepolymers, the
reactivity increases with the number of hydroxyl groups present
in the prepolymer chain (44). Thus, an increase in the molecular
weight of the epoxy prepolymer would not only reduce its diffu-
sivity but would also increase its reactivity, resulting in a
reduced time of microgel formation. This combined effect would
result in a smaller size of the primary microgels, as observed
experimentally.
In the case of non-stoichiometric compositions, the size of
the primary microgels should be expected to be governed both
by the value of M_c and by the structure, because the diffusiv-
ity and the reactivities of the prepolymers should be almost the
same at all stoichiometries. In the Epon 828/MDA system (Series
A), an excess in amine concentration should initially yield many
linear molecules whose length would depend on the amount of
excess amine. The premature reaction of the secondary amines of
these long molecules would result in larger microgels. Thus, in
the case of amine excess, the size of primary microgels, as
observed experimentally, should increase with increasing amounts
of excess amine. In the case of excess epoxy, a branched struc-
ture having four epoxy molecules attached to one amine molecule
is formed (39). Thus, the size of the microgels formed at 100%
epoxy-excess would be much smaller than those formed at 100%
amine excess. The experimental results showed a similar trend.
For systems having a slower rate of reaction (such as
samples of Series A, sample E-1, sample E-2, and sample F-2,
which were made from liquid prepolymers) the higher diffusivity

and lower reactivity result in slightly larger <u>primary</u>
microgels. However, the loose connections of the adjacent
secondary microgels can be readily attacked, resulting in the
etching of the secondary microgels and thus formation of dimples
on the surface (as was observed experimentally). The semi-solid
and solid resins are composed of high-M and low-M prepolymer
components; the amount of low-M component decreases with the
average M of the prepolymer (<u>41</u>, Ch. 3). The more reactive high-
M components form the microgels that get dispersed in the low-M
component, which reacts later to give a high crosslink density
shell. A decrease in the proportion of the low-M component
should increase the size but decrease the number of the shell-
and-core-type of structure as was found experimentally.

   <u>Dynamic Mechanical Spectroscopy</u>. As pointed out above, the
heterogeneous morphology, observed in the present study, implies
network flaws (weak connections between the primary and secondary
microgels). However, the low cyclic strains applied in dynamic
mechanical tests detect only the effect of the basic network
structure and not the network flaws. Therefore, as observed
experimentally (<u>38,41</u>), dynamic mechanical spectroscopy should
not indicate heterogeneity in the samples.

   <u>Soluble Content</u>. The morphological studies indicated an
increase in the dimple size of M_c. A dimple actually represents
a bit of material extracted from the network. This observation
is in good agreement with the extraction results (<u>41,42</u>) that
showed an increase in soluble content with M_c.

   <u>Mechanical Behavior</u>. At present, it is not possible to
reconcile all the diverse dependences on stoichiometry. However,
clearly there is no <u>a priori</u> reason for trends in all properties
to be related. By a modification of the Griffith equation (<u>45</u>)

$$\sigma_u \quad = \quad (\ 2 \ ES \ / \ \underline{a} \ )^{1/2} \qquad\qquad (1)$$

where σ_u = ultimate tensile strength, E = Young's modulus, S =
fracture energy, and $\underline{a}$ = characteristic flaw size. Thus σ_u at
constant E depends on how S varies with $\underline{a}$; S may change while
σ_u does not, if changes in $\underline{a}$ compensate for changes in S. For
the Epon 828/MDA system, both Bell (<u>46</u>) and Kim et al. (<u>45</u>) have
shown that σ_u is almost independent of stoichiometry. Further-
more, it has also been shown that impact toughness is at a maxi-
mum not at 100% stoichiometry but at a 1/1.4 epoxy/amine ratio
(<u>37,45,46</u>). The impact strength for the case of excess epoxy was
also reported to be higher than that at equal stoichiometry.
Under these circumstances, it has been shown that the apparent
critical flaw size $\underline{a}$ is a linear function of the amine/epoxy
ratio, changing from 32 μm to 141 μm (45).

Whether the critical flaw size corresponds to the aggregates first formed prior to phase inversion or whether it corresponds to the inclusions is, of course, not known. Indeed, the reality of a flaw corresponding to the calculated value of a is not proven. Nevertheless, the close agreement between microscopic evidence of the present study and the computed flaw size (45) is strongly suggestive of a correlation.

Though the modulus, E, does not decrease (in fact increases slightly (45,46) with an increase in amine content, the overall plastic deformation should increase due to the plasticizing character of the amine. Hence, S increases (E itself may increase due to enhanced continuity of the network). At the same time, the flaw size increases a little but not as fast as S so that tensile strength actually increases a little. But with an epoxy excess, the decreased flaw size (corresponding to smaller aggregates) more than balances out the lower value of S so that the strength again increases. However, the toughness otherwise seen at high amine contents is vastly reduced by the high loading rate in impact; while with epoxy excess, the smaller flaw size is able to delay fracture.

In the case in which the M_c is varied by varying the molecular weight of the epoxy resin at equal stoichiometry (Series E), the ultimate tensile strength is independent of M_c but the impact strength decreases with M_c (38,41). When the molecular weight of the epoxy is increased, a different behavior occurs. The inherent S of the epoxy components is low compared to that of amine and, hence, the tensile strength does not increase and impact strength decreases.

The Glass Transition Temperature. Samples having a bimodal distribution of molecular weight (Series F) showed the same T_g as their counterparts having a broad distribution in the high (> 700) and the low (< 400) ranges of M_c. At intermediate M_c's, the T_g was found to be lower in samples having a bimodal distribution (42). Though the morphology of the bimodal and broad distribution was the same, the properties of the former will be determined by the dominant component in the final network. If this is a high-molecular-weight resin (which is more reactive), this network may be expected to dominate and T_g will be low, perhaps because the initial fast reaction results in greater incoherence. At intermediate compositions, a judicious balancing may occur and result in a more coherent network. Thus properties may be governed by the low-molecular-weight component.

The fact that small-angle X-ray scattering and stained or unstained microtomed thin sections fail to indicate a two-phase structure (37,41) also supports the present model, which explains that heterogeneity in networks is primarily due to incoherence on a local scale and not to major variations in average crosslink density.

Although this discussion is clearly speculative, it does explain some of the behavior noted and suggests ideas capable of testing in the laboratory.

Conclusions

From the present study and the studies of other investigators (discussed earlier), it is clear that crosslinked networks in many epoxy resins and in some alkyd resins are heterogeneous in nature.

According to the proposed model, small primary microgels ranging in size from 10 nm to 100 nm are formed much before the inset of physical gelation. These primary microgels agglomerate together through weak connections to produce secondary microgels ranging from 0.5 μm to 50 μm. The secondary microgels coalesce together and the experimental gel point is observed. The final crosslinked network is produced after complete reaction of the unreacted prepolymers left in the interstices of the coalesced secondary microgels. As compared to primary microgels, these secondary microgels are generally connected to each other through "weaker" or less coherent links. In networks prepared through non-stoichiometric compositions, the secondary microgels are embedded in a matrix of lower crosslink density but still connected to each other through chemical bonds.

The coherence of the final network (macrogel) depends on the density strength of the connections between the secondary microgels which in turn governs its tensile properties.

In the case in which the prepolymers have a bimodal distribution of molecular weight, the properties of the network are governed by the component that is more dominant in the microgels.

Though sufficient experimental evidence is not presently available, the optimization of curing conditions should also play an important role in achieving maximum coherence in the network.

Acknowledgements

Literature Cited

1. deBoer, J. H. Trans. Faraday Soc., 1936, 36, 10.
2. Lohse, F.; Schmid, R.; Batzer, H.; and Fisch, W. Br. Poly. J., 1969, 1, 110.
3. Houwink, R. J. Soc. Chem. Ind., London 1936, 55, 247; Trans. Faraday Soc., 1936, 32, 122.
4. Cuthrell, R. E. J. Appl. Polym. Sci., 1967, 11, 949.
5. Andrews, E. H. "Fracture in Polymers," American Elsevier, 1968.

6. Solomon, D. H. and Hopwood, J. J. J. Appl. Polym. Sci., 1966, 10, 1898.
7. Cuthrell, R. E. J. Appl. Polym. Sci., 1968, 12, 1263.
8. Kaelble, D. H. In "Epoxy Resins, Chemistry and Technology," ed. by C. A. May and Y. Tanaka, Marcel Dekker, NY, 1973, Chapter 5.
9. Blockland, R. and Prins, W. J. Polym. Sci., 1969, A-2(7), 1595.
10. Gallacher, L. and Bettelheim, F. A. J. Polym. Sci., 1962, 58, 697.
11. Balyuzi, H. H. M. and Burge, R. E, Nature, 1970, 227, 489.
12. Kenyon, A. S. and Nielsen, L. E. J. Macromol. Sci.-Chem., 1969, A-3(2), 275.
13. Kardos, J. L. Trans. N. Y. Acad. Sci., 1973, 11, 35(2), 136.
14. Labana, S. S.; Newman, S.; and Chompff, A. J. In "Polymer Networks," ed. by A. J. Chompff and S. Newman, Plenum Press, 1971, p. 453.
15. Erath, E. H. and Spurr, R. A. J. Polym. Sci., 1959, 35, 391.
16. Erath, E. H. and Robinson, M. J. Polym. Sci., 1960, C-3, 65.
17. Spurr, R. A. Ind. Eng. Chem., 1957, 49, 1839.
18. Miyamoto, T. and Shibayama, K. Kobunshi Kagaku (Eng. Ed.) 1973, 2, 203.
19. Loskutov, A. I.; Zagrebennikova, M. P. and Arsen'eva, L. A. Vysokomol. Soedin, 1974, B-16, 334.
20. Wohnsiedler, H. P. J. Polym. Sci., 1963, C-3, 77.
21. Rochow, T. G. Anal. Chem., 1961, 33, 1810.
22. Rochow, T. G. and Rowe, F. G. Anal. Chem., 1949, 21, 461.
23. Kessenikh, R. M.; Korshunova, L. A.; and Petrove, A. V. Poly. Sci. USSR, 1972, 14, 2339.
24. Basin, V. Y.; Korunskii, L. M.; Shokal'skaya, O. Y.; and Aleksandrov, N. V. Poly. Sci. USSR, 1972, 14, 2339.
25. Carswell, T. S. "Phenoplasts, Their Structure, Properties and Chemical Technology," Interscience: New York, 1947, Chapter 5.
26. Neverov, A. N. Vysokomol. Soedin, 1968, A-10, 463.
27. Bobalek, E. G.; Moore, E. R.; Levy, S. S.; and Lee, C. C. J. Appl. Polym. Sci., 1967, 11, 1593.
28. Solomon, D. H.; Loft, B. C.; and Swift, J. D. J. Appl. Polym. Sci., 1967, 11, 1593.
29. Morgan, R. J. and O'Neal, J. E. Polym. Plast. Tech. Eng., 1975, 5, 173.
30. Racich, J. L. and Koutsky, J. A. J. Appl. Polym. Sci., 1976, 20, 2111.
31. Racich, J. L. and Koutsky, J. A. "Chemistry and Properties of Crosslinked Polymers," ed. by S. S. Labana, Academic Press, Inc.: New York, 1977, p. 303.
32. Morgan, R. J. and O'Neal, J. E. "Chemistry and Properties of Crosslinked Polymers," ed. by S. S. Labana, Academic Press, Inc.: New York, 1977, p. 289.

33. Solomon, D. H. J. Macromol. Sci., (Rev.), 1967, C-1(1), 179.
34. Batzer, H.; Lohse, F.; and Schmid, R. Agnew Makromol. Chem., 1973, 29/30, 349.
35. Funke, W. J. Polym. Sci., 1967, C-16, 1497.
36. Kreibick, U. T. and Schmid, R. J. Polym. Sci., 1975, Symp. No. 53, 177.
37. Selby, K. and Miller, L. E. J. Material Sci., 1975, 10, 12.
38. Manson, J. A.; Sperling, L. H.; and Kim, S. L. Final Report, AFMC Contract No. F33615-75C-5167, April 1977, AFML-TR-77-109.
39. Bell, J. P. J. Polym. Sci., 1970, A-2(8), 417.
40. Manson, J. A. and Chiu, E. H. J. Polym. Sci., 1973, Symp. No. 41, 95.
41. Misra, S. C. Ph.D. Dissertation, Lehigh University, 1978.
42. Misra, S. C.; Manson, J. A.; and Sperling, L. H. This volume, 1978.
43. Acitelli, M. A.; Prime, R. B.; and Sacher, E. Polymer, 1971, 12, 335.
44. Bowen, D. O. and Whiteside, R. C. Jr. "Epoxy Resins" in Advances in Chemistry Series, American Chemical Society: Washington, D.C., 1970, 92, 48.
45. Kim, S. L.; Skibo, M.; Manson, J. A.; Hertzberg, R. W.; and Janiszewski, J. Presented at American Chemical Society meeting, Chicago, August 1977; Poly. Eng. and Sci., in press, 1978.
46. Bell, J. P. J. Appl. Polym. Sci., 1970, 14, 1901.

13

Creep Behavior of Amine-Cured Epoxy Networks: Effect of Stoichiometry

S. L. KIM[1], J. A. MANSON, and S. C. MISRA

Materials Research Center, Coxe Laboratory #32, Bethlehem, PA 18015

Creep studies are not only important in the theory of viscoelasticity but also of great practical importance in any engineering application in which the polymer must sustain loads for long times. With a thermoset resin, creep can vary a great deal, depending on the degree of crosslinking, the perfection, and the morphology of the network structure.

While many studies of the effects of crosslinking on behavior have been made, most have been restricted in scope and many have used relatively uncharacterized materials. For this reason, a systematic examination was conducted to elucidate the effects of crosslink density and its distribution on a wide range of properties including basic viscoelastic response, stress-strain and impact· behavior, and fatigue crack propagation. The same base prepolymer type and curing agent were used throughout, and a given crosslink density was obtained by changing the stoichiometry and by changing the molecular weight of the pre-polymer at constant stoichiometry.

Related Studies

In some epoxy systems (1,2), it has been shown that, as expected, creep and stress relaxation depend on the stoichiometry and degree of cure. The time-temperature superposition principle (3) has been applied successfully to creep and relaxation behavior in some epoxies (4-6) as well as to other mechanical properties (5-7). More recently, Kitoh and Suzuki (8) showed that the Williams-Landel-Ferry (WLF) equation (3) was applicable to networks (with equivalence of functional groups) based on nineteen-carbon aliphatic segments between crosslinks but not to tighter networks such as those based on bisphenol-A-type prepolymers cured with m-phenylene diamine. Relaxation in the latter resin followed an Arrhenius-type equation.

[1]Current address: Fiber and Polymer Product Research Division, Goodyear Tire & Rubber Co., Akron, Ohio 44316.

     In this study, the imperfection of the networks was varied
by varying the stoichiometry of an Epon 828–methylene dianiline
system. Related studies of morphology, other properties, and
creep as a function of molecular weight and distribution of the
prepolymer are described elsewhere (9–13).

Experimental

     The materials used were Epon 828 epoxy resin and methylene
dianiline (Tonox), both from the Shell Chemical Co. The resin
and curing agent were melted together, mixed, degassed, and cast
between glass plates. The cure cycle was as follows: 45 min at
60°C, 30 min at 80°C, and 2.5 hr at 150°C; then slow cooling to
room temperature. The amine to epoxy ratio (A/E) was varied from
0.7 to 2.0 (in terms of equivalents). Compositions are given in
Table I.

Table I. Composition of Epoxy Specimens for Creep Study

Sample	Amine/Epoxy Ratio	M_c [a]
A–7	0.7	721
A–8	0.8	457
A–10	1.0	303
A–12	1.2	420
A--20	2.0	1381

[a] M_c is calculated based on the rubbery moduli from dynamic
mechanical measurements (10), and used as a relative and effec-
tive M_c throughout this study.

     Creep was measured using a Gehman torsional tester (14).
[In fact, the shear compliance J(t) was measured explicitly; the
data are presented as moduli by taking $E(t) \simeq 3/J(t)$.] Master
curves were obtained in the usual manner (3).

Results and Discussion

     Typical creep–modulus behavior is shown in Figure 1; visco-
elastic parameters deduced from the master curve are given in
Table II, and discussed below.

     Glass-transition temperature (T_g). The modulus–temperature
curves for all the specimens were composed by plotting the 10-sec
modulus at each temperature, as shown in Figure 2. The glass-
transition temperatures (corresponding to a modulus of 0.2 GPa)
are given in Table I. Calculations show that T_g is inversely
proportional to the average molecular weight between crosslinks
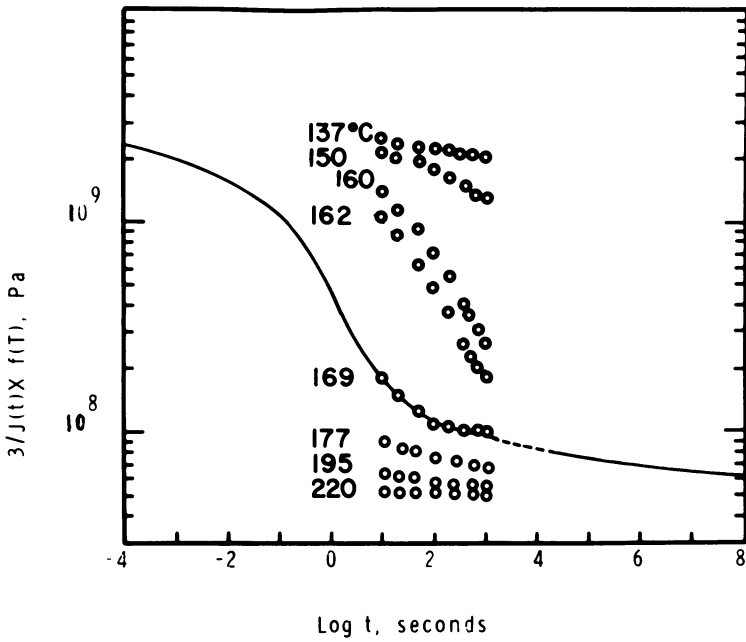
Figure 1. Typical curves of creep modulus vs. log t at different temperatures (epoxy specimen A-10). Master curve at 169°C shown as solid curve.
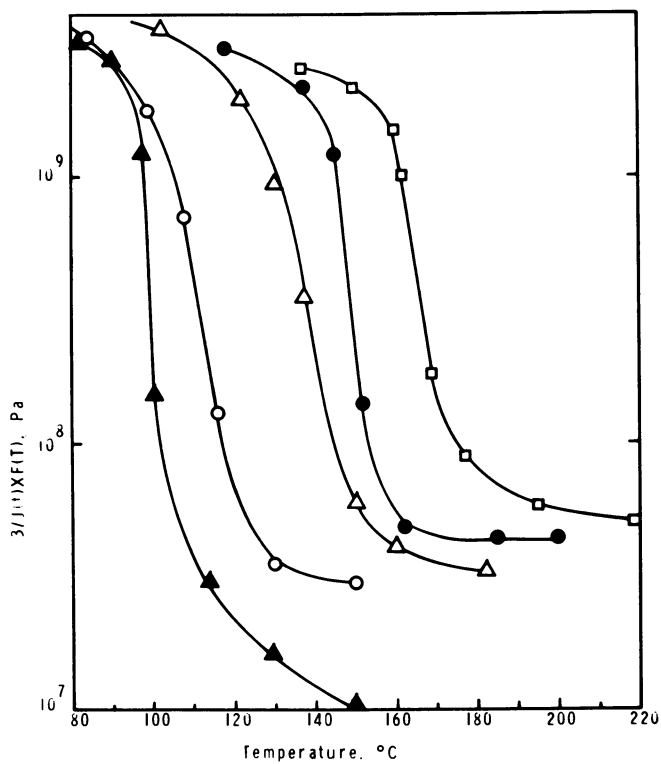
Figure 2. Dependence of creep modulus (10-sec) on temperature for series of epoxy resins: (○) A-7; (△) A-8; (□) A-10; (●) A-12; (▲) A-20

(M_c); as proposed by Nielson (15):

$$T_g - T_{g,o} = \frac{k}{M_c} \qquad (1)$$

where $T_{g,o} = 350°K$, the extrapolated value of T_g for $M_c \rightarrow \infty$, and $k = 2.9 \times 10^4$. Results are in excellent agreement with those from other tests (Table II) such as dynamic mechanical spectroscopy and differential scanning calorimetry (10).

TABLE II. Creep Characteristics of Epoxy Resins

No.	$T_g{}^a$,C°	$T_g{}^b$,°C	$T_g{}^c$,°C	E_r,MPa	log τ_c	n^d
A-7	132	101	114	30	-9.7	-0.36
A-8	162	127	140	33	-2.5	-0.38
A-10	198	164	168	50	4.0	-0.42
A-12	185	146	151	44	0.3	-0.38
A-20	119	93	100	10	-13.0	-0.63

[a] By dynamic mechanical spectroscopy at 110 Hz (9).
[b] By differential scanning calorimetry (9).
[c] From the temperature dependence of creep modulus (Figure 2).
[d] From slope of transition region in creep curves;
$$n = d[\ln 3/J(t)] / d(\ln t)$$

Shift factor (a_T). Experimental shift factors were determined by composing smooth master curves from the data at various temperatures, taking T_g as the reference temperature in each case. Temperature corrections were made only for the data above T_g; the corrections were found to be small ($\sim 10\%$).

A smooth composite curve was obtained by plotting log a_T vs. $(T-T_g)$ for all the specimens, as shown in Figure 3. The composite curve following the prediction of WLF equation (3) only in the limited range between $(T_g - 10°C)$ to $(T_g + 20°C)$. While one does not expect the WLF predictions to hold below T_g, the predictions are usually good to temperatures as high as $(T + 100°C)$. In fact, the data could be represented over the entire temperature range by plotting the shift factors against $1/T$ (i.e., in an Arrhenius-plot fashion), as shown in Figure 4.

When the data were plotted against $(1/T - 1/T_g)$, two straight lines for all the specimens were obtained as shown in Figure 5, consistent with an Arrhenius-type relationship:

$$\log a_T = \frac{-E_a}{2.303 \, RT} \qquad (2)$$

where R is the gas constant, T is the absolute temperature, and E_a is the apparent activation energy. From the slopes of the straight lines, the activation energies were found to be 950 kJ/mole (227 kcal/mole) above T_g and 356 kJ/mole (85 kcal/mole)
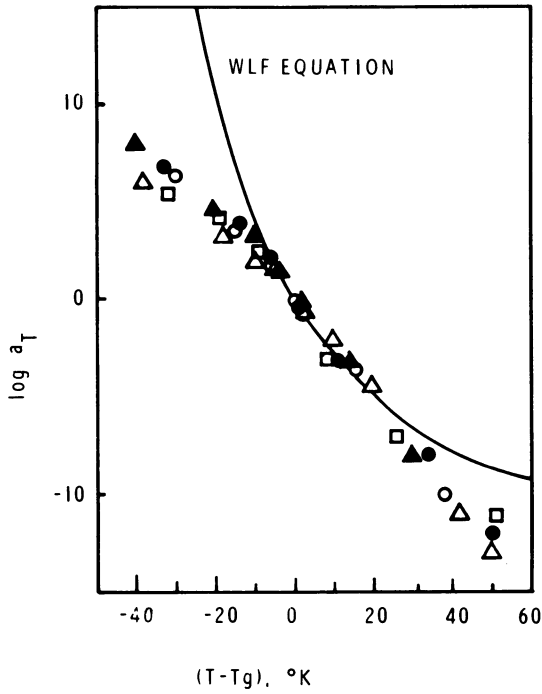
Figure 3. Composite curve of experimental shift factors as a function of $(T - T_g)$ *(symbols are as in Figure 2). The curve predicted by the WLF equation (3) is indicated by the solid line.*
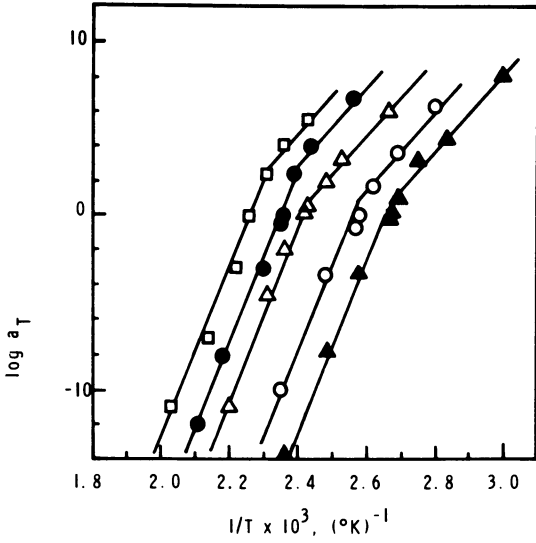
Figure 4. Plots of experimental shift factors for epoxy specimens vs. inverse temperature (symbols are as in Figure 2)
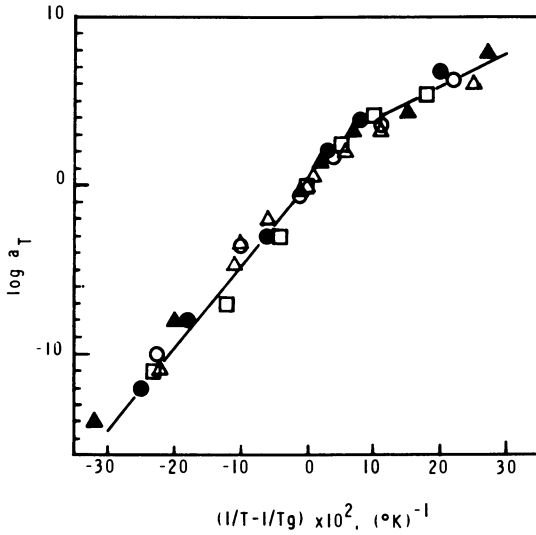
Figure 5. Composite plot of experimental shift factors for all epoxy specimens as a function of $(1/T - 1/T_g)$ (symbols are as in Figure 2)

below T_g. As shown in Table III, these values are in excellent
agreement with the values observed by Kitoh and Suzuki (8) in a
bisphenol-A-type epoxy cured with phenylene diamine: 962 kJ/mole
(230 kcal/mole) above T_g and 381 kJ/mole (91 kcal/mole) below T_g.
Values also agree reasonably well with the apparent activation
energies that were determined in our parallel study in which M_c
was varied by changing prepolymer molecular weight (13). In com-
parison, apparent energies of activation [at T_g, assuming a
viscosity of 10^{12} N.s.m^{-2} (16, p.   )], are calculated to range
between 900 kJ/mole (215 kcal/mole) for T_g = 100°C and 1259 kJ/
mole (301 kcal/mole) for T_g = 168°C. Further, the WLF equation
predicts a continuous decrease in E_a as T increases above T_g.

Table III. Comparison of Apparent Energies of
Activation for Relaxation in Epoxies

Range of T	E_a, kJ/mole (kcal/mole)		
$T > T_g$	950^a (227)	960^b (230)	962^c (230)
$T < T_g$	360^a (86)	356^b (75)	381^c (91)

[a] This study.
[b] Parallel study with M_c changed by changing prepolymer
molecular weight (13).
[c] Kitoh and Suzuki (8), for bisphenol-A-type resin cured
with m-phenylene diamine.

Thus, while our values of E_a (as well as those in references
8 and 13) agree well with WLF predictions at T_g when $T_g \simeq 100$°C,
they do not agree quantitatively or qualitatively for higher-T_g
specimens at T_g or for any specimens at $T \gg T_g$. Interestingly,
other authors (5,14) have reported validity of the WLF treatment
for less-densely-crosslinked epoxy systems. Also, we find that a
plot of data by Murayama et.al. (17) shows that an Arrhenius-type
treatment of dynamic mechanical shift factors is preferred for
oriented poly(ethylene terephthalate).

Characteristic creep time. All master curves were empiri-
cally shifted to the most convenient common temperature, 150°C,
as shown in Figure 6. For convenience, only transition regions
are shown. An increase in crosslink density (nearing to equiva-
lent stoichiometry) shifts the curves to longer times as expected.
The chracteristic creep time, τ_c, was taken as the time to creep
to a modulus value of log E(t) = (log E_g + log E_r)/2, where E_g
and E_r are the glassy and rubbery modulus, respectively. [While
τ_c is analogous to a retardation time, the latter designation is
not used, because our τ_c is determined from plots of 3/J(t), not
J/(t), and is hence not numerically equal to the corresponding
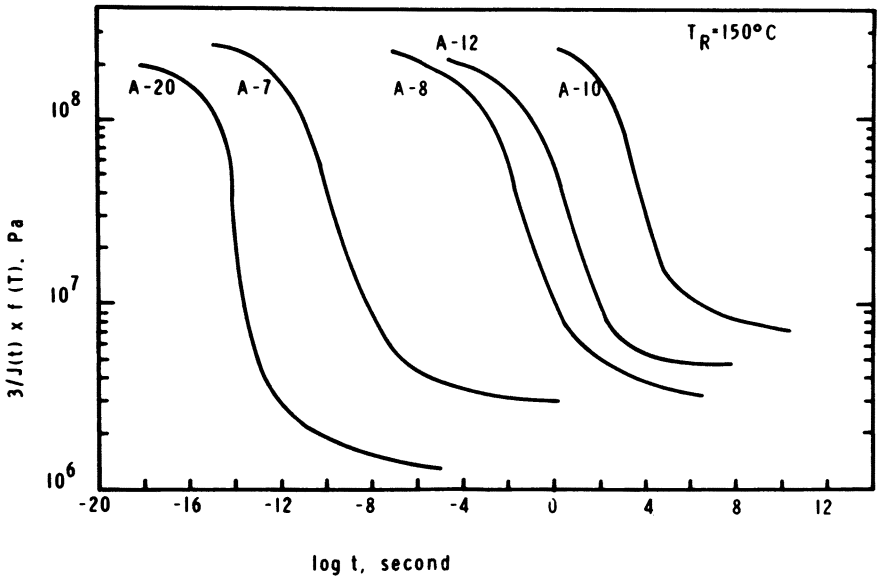
Figure 6.   Creep-modulus master curves for all epoxy specimens as a function of log t at a reference temperature of 150°C

retardation time. τ_c is, strictly speaking, a relaxation time.]
Characteristic creep time is shown as a function of the A/E ratio
and also as a function of $1/M_c$ (Figure 7). The good straight-
line relationship between $\log \tau_c$ and $1/M_c$ again shows consistency
in the behavior of these specimens:

$$\log \frac{\tau_c}{\tau_{c_\infty}} = \frac{7.7 \times 10^3}{M_c} \tag{3}$$

where $\log \tau_{c_\infty}$ is found by extrapolation to equal −18, which is
the characteristic creep time at about 150°C for a network having
an infinite value of M_c.

Since both τ_c and T_g are inversely related to M_c and the
activation energies of the shift factors are independent of M_c, a
common segmental motion must be involved in the creep behavior of
all these specimens varying the crosslink density merely shifts
the curves along the time axis.

Distribution of relaxation times, H(τ). In this
discussion, using plots of 3/J(t), we shall discuss the distribu-
tion of characteristic response times in terms of relaxation
times. The relaxation-time spectrum, H(τ), can be determined as
a first approximation (18) by the following relationship:

$$H(\tau) = - d[E(t)] / d (\log t) \Big|_{t=\tau}$$
$$= -E(t) \left[\frac{d [\log E(t)]}{d (\log t)} \right]_{t=\tau} \tag{4}$$

Plots of H(τ) vs log t for all specimens are given in Figure 8.
When data are replotted at the T_g of each specimen, the distri-
bution of relaxation times for the 5 different specimens nearly
coincide with each other until the rubbery region, where some
scatter is seen (Figure 9). This confirms that the same mechan-
ism for relaxation is involved for all 5 specimens. The slope of
H(τ) (i.e., d[log H(τ)]/d (log t)] at the glass transition region
(the right-hand part of Figure 9) is about −0.42, which compares
fairly well with the value of −0.33 obtained by Kitoh and Suzuki
(8) for a bisphenol-A epoxy resin cured with m-phenylene diamine,
considering the differences in the epoxy system and in the testing
modes. Clearly the data for our parallel study (13) in which M_c
is varied by changing prepolymer molecular weight are indis-
tinguishable from those of this study (note triangles in Figure 9).

Conclusions

In conclusion, the temperature dependence of shift factors
for the networks studied here do not follow the WLF equation, but
rather an Arrhenius-type relationship. The apparent activation
energies are independent of stoichiometric variation [as they are
when M_c is varied by changing prepolymer molecular weight (13)].
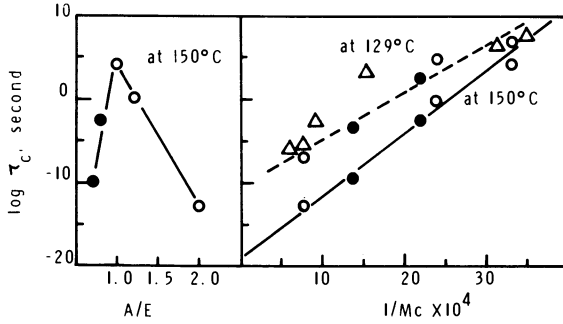
Figure 7. Characteristic creep time for all epoxy specimens as a function of stoichiometry and M_c: (●) epoxy-rich; (○) amine-rich; (△) different series with M_c varied by changing prepolymer molecular weight (13)

log t, second
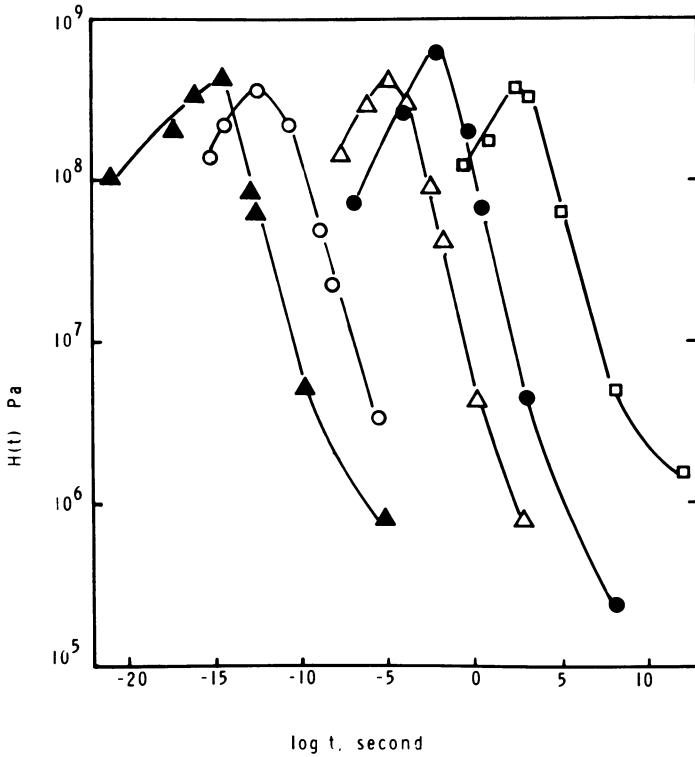
Figure 8. Distribution of relaxation times for all epoxy specimens as a function of log t (symbols as in Figure 7)
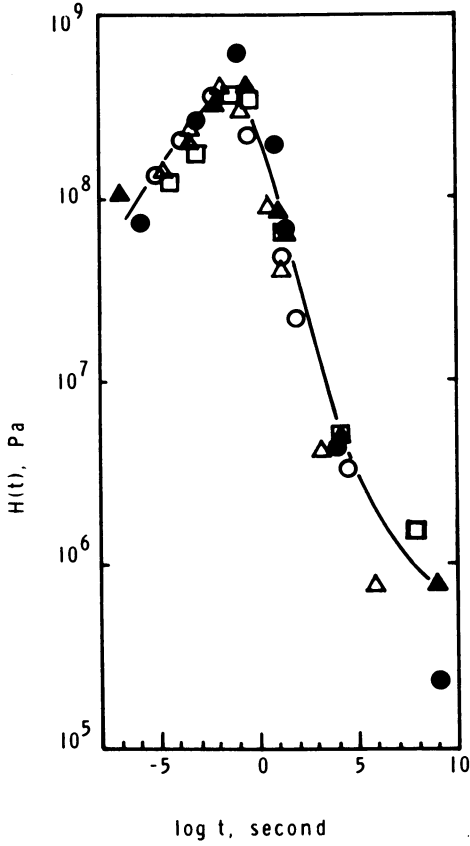
Figure 9.

Nearing to stoichiometry (decrease in M_c) merely shifts the creep curves to a longer time scale. Although the crosslink density was lowered (increase in M_c) more than four-fold by varying the A/E ratio, apparently the aromatic rings in the bisphenol-A and diamine group must be controlling (stiffening) the segmental motions in the networks. Thus, considering the results of this work and those of Kitoh and Suzuki (8) and Murayama et. al. (17), we might expect an Arrhenius-type relationship in the temperature dependence of shift factors for relatively rigid networks.

Acknowledgement

Literature Cited

1. Kosuga, N. and Tsugawa, S. Kobunshi Ronbunshu, 1975, 32, 252.
2. Delmonte, J. Plastics Technol., 1958, 4, 913.
3. Ferry, J. D. "Viscoelastic Properties of Polymers," 2nd Ed., John Wiley & Sons, Inc., New York, NY, 1970, Chap. 11.
4. Theocaris, P. Rheol. Acta, 1962, 2, 92.
5. Kaelble, D. H., J. Appl. Polym. Sci., 1965, 9, 1213.
6. Shito, N. and Sato, M. J. Polym. Sci.-C., 1967, 16, 1069.
7. McCrum, N. G. and Pogany, G. A. J. Macromol. Sci.-Phys., 1970, B4(1), 109.
8. Kitoh, M. and Suzuki, K. Kobunshi Ronbunshu, 1976, 33, 19.
9. Manson, J. A.; Sperling, L. H. and Kim, S. L. "Influence of Crosslinking on the Mechanical Properties of High-T_g Polymers," Technical Report AFML-TR-77-109, July 1977.
10. Kim, S. L. and Manson, J. A. "Dynamic Mechanical Behavior of Amine-Cured Epoxy," 19th Canadian High Polymer Forum, Ottawa, Canada, August 1977, to be published.
11. Kim, S. L.; Skibo, M.; Manson, J. A.; Hertzberg, R. W. and Janiszewski, J. Polym. Eng.-Sci., 1977.
12. Misra, S. C. Ph.D. Thesis, Lehigh University, 1978.
13. Misra, S. C.; Manson, J. A. and Sperling, L. H. This publication, 1979.
14. ASTM D-1043, American Society of Testing Materials, Philadelphia, PA.
15. Nielson, L. E. J. Macromol. Sci.-Rev. Macromol. Chem., 1969, C3(1), 69.
16. Nielsen, L. E. "Mechanical Properties of Polymers," Van Nostrand Reinhold, New York, 1962.
17. Murayama, T.; Dumbleton, J. H. and Williams, M. L. J. Polym. Sci., 1968, part A-2, 6, 787.
18. Tobolsky, A. V. "Properties and Structure of Polymers," John Wiley & Sons, Inc., New York, NY, 1960, Chap. 3.

Self-Cross-Linkable Polyepoxides

YOSHIO TANAKA

Research Institute for Polymers & Textiles, 4 Sawatari, Kanagawa, Yokohama 221, Japan

The literature contains numerous references to the reactive copolymers of 2,3-epoxy-1-propyl esters such as 2,3-epoxy-1-propyl methacrylate, acrylate and vinyl-sulfonate with other vinyl compounds like propionitrile, methyl acrylate, and vinylbenzene (1), and to the addition reaction of amino, carboxy, and hydroxy compounds with the epoxy ring of these copolymers (2). 2,3-Epoxy-1-propyl-2-propenyl ether is found (2) to have a strong tendency to limit the molecular weight of a polymer by chain transfer through the allyl portion of the molecule. Relatively little attention has been paid to the copolymers of 2,3-epoxy-1-propyl ethers such as 1-ethenyl-4-(2,3-epoxy-1-propoxy) benzene, and to the self-addition reaction of the epoxy group with catalytic or reactive functional groups, being capable of opening or adding to the epoxy ring, in the copolymers. This paper, therefore, reports the radical copolymerization of 2,3-epoxy-1-propyl methacrylate or 1-ethenyl-4-(2,3-epoxy-1-propoxy)benzene with 4- and 2-vinylpyridines and with 5-ethyl-2-vinylpyridine, and the self-crosslinking reaction of these copolymers.

Experimental

Reagent-grade 2,3-epoxy-1-propyl methacrylate and vinylpyridines were distilled at reduced pressure, and the middle fractions were collected for use. 1-Ethenyl-4-(2,3-epoxy-1-propoxy)benzene was prepared from 4-ethenylphenol and 1-chloro-2,3-epoxypropane by a two-step process (1). 2,2'-Azoisobutyronitrile was recrystallized from its alcoholic solution.

An epoxide and a vinylpyridine were dissolved in 10 ml of dry tetrahydrofuran followed by the addition of 0.5 mole-% of the initiator. The solution was transfered to a polymerization tube, cooled in a liquid nitrogen bath, degassed, and sealed under vacuum after

flushing with a stream of oxygen-free nitrogen. The
tube was then placed in a constant temperature bath
at 60.0 ± 0.2°C for several hours. At the end of the
reaction time the tube was cooled and opened. The
reaction mixtures was dissolved in a small amount of the
solvent and poured into anhydrous petroleum ether. The
insoluble material was collected and washed with cold
petroleum ether. A fluffy yellow or brown solid was
purified by redissolving twice and reprecipitating in a
large excess of nonsolvent. It was finally dried to
constant weight under vacuum at a room temperature. Co-
polymer compositions calculated from carbon and nitrogen
analyses. The reactivity ratios were calculated by
Mayo-Lewis technique (3).

Viscosities of the polymeric materials were ob-
tained in tetrahydrofuran with an Ubbelohde-type viscom-
eter at 30.00 ± 0.02°C. The infrared absorption spectra
in the region of 400-4000/cm were measured for the sam-
ple by Hitachi Model EPI-G3 infrared spectrophotometer.
The samples were prepared by the KBr pellet technique.
The thermal behavior of the specimens was observed with
a Rigakudenki DSC-TGA apparatus. The X-ray diffraction
pattern of the powdered polymer was taken in the region
of 3-37° by a Rigakudenki Model 3D-F X-ray diffrac-
tometer with the use of Ni-filtered copper K   radiation.

Results and Discussion

Copolymerization of the epoxides with these vinyl-
pyridines in tetrahydrofuran under reduced pressure with
2,2'-Azoisobutyronitrile at 60°C gave stable yellow or
brownish polymeric materials. In Figure 1-3, the con-
centration of M_2 (vinylpyridine) in the monomer mixture
are plotted against the corresponding mole fraction M_2
of vinylpyridine in the copolymer. The lines in the
figures were calculated from the monomer reactivity
ratios and the points represent experimental data. The
reactivity ratios for these epoxy compounds with the
present comonomers have not yet been reported, but can
be compared with those predicted by the Q-e scheme. The
Q-e values for the individual vinylpyridine were calcu-
lated by assuming Q=0.78 and e=-0.02, Q=0.85 and e=0.10,
and Q=0.87 and e=0.40 for 2,3-epoxy-1-propyl methacry-
late; these are given in Table I. Assuming Q=1.30 and
e=-0.50 for 2-vinylpyridine, and Q=1.37 and e=-0.74 for
5-ethyl-2-vinylpyridine, the Q-e values for the epoxide
were also calculated and are shown in Table I, compared
with those obtained from Price's (4) or Tamikado's (5)
Q-e values for the pyridine. The Q-e values for 1-
ethenyl-4-(2,3-epoxy-1-propoxy) benzene were also cal-
culated by assuming Q=0.82, e=-0.20 for 4-vinylpyridine,
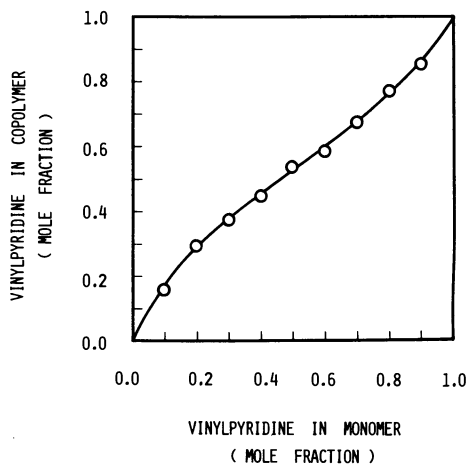
Journal of Polymer Science, Polymer Chemistry Edition

Figure 1. Monomer–copolymer composition curve for 1-ethenyl-4-(2,3-epoxy-1-propoxy) benzene (M_1) with 4-vinylpyridine (M_2): (——) $r_1 = 0.467$ and $r_2 = 0.638$
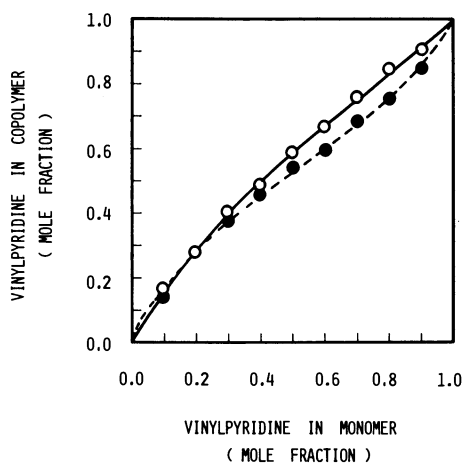
Journal of Polymer Science, Polymer Chemistry Edition

Figure 2. Monomer–copolymer composition curves for 1-ethenyl-4-(2,3-epoxy-1-propoxy) benzene (M_1) or 2,3-epoxy-1-propyl methacrylate (M_1) with 2-vinyl-pyridine (M_2): (——) 1-ethenyl-4-(2,3-epoxy-1-prpoxy) benzene with $r_1 = 0.556$ and $r_2 = 1.25$; (– – –) 2,3-epoxy-1-propyl methacrylate with $r_1 = 0.51$ and $r_2 = 0.62$
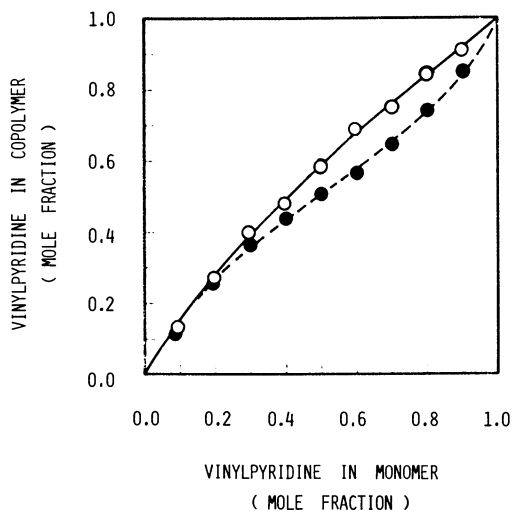
Figure 3.   Monomer–copolymer composition curves for 1-ethenyl-4-(2,3-epoxy-1-propoxy) benzene or 2,3-epoxy-1-propyl methacrylate (M_1) with 5-ethyl-2-vinyl-pyridine (M_2): (———) 1-ethenyl-4-(2,3-epoxy-1-propoxy) benzene with $r_1 = 0.639$ and $r_2 = 1.38$; (– – –) 2,3-epoxy-1-propyl methacrylate with $r_1 = 0.57$ and $r_2 = 0.62$

Table I

Monomer Reactivity Ratios and Q-e Values in Copolymerization of 2,3-Epoxy-1-propyl Methacrylate (M_1) with Vinylpyridines (M_2)[a]

M_2	r_1	r_2	e_1	e_2	Q_1	Q_2
2-Vinylpyridine	0.51	0.62	-0.02[b,c]	-0.85	0.78[b,c]	1.15
			0.10[b,d]	-0.73	0.85[b,d]	1.14
			0.40[b,e]	-0.43	0.87[b,e]	0.91
			0.54	-0.50[b,d]	1.23	1.30[b,d]
			-1.17	-0.1[b,f]	1.55	1.07[b,f]
			-1.67	-0.6[b,g]	0.93	1.09[b,g]
5-Ethyl-2-vinylpyridine	0.57	0.62	-0.02[b,c]	-1.04	0.78[b,c]	1.40
			0.10[b,d]	-0.92	0.85[b,d]	1.35
			0.40[b,e]	-0.62	0.87[b,e]	1.02
			0.28	-0.74[b,d]	1.04	1.37[b,d]

a   Polymerization conditions: 0.02 mole of monomers; polymerization in tetrahydrofuran with 0.5 mole-% of 2,2'-azoisobutyronitrile at 60°C.

b   Reference data used for calculation of Q-e values.

c   Data of Young (J. Polym. Sci., 1961, 54, 411).

d   Data of Young and Kennedy (in Copolymerization, G. E. Ham, Ed., Interscience, New York, 1964, Appendix B.).

e   Data of Iwakura et al. (Makromol. Chem., 1960, 44/46, 570).

f   Data of Price (J. Polym. Sci., 1948, 3, 772).

g   Data of Tamikado (J. Polym. Sci., 1960, 43, 489).

Q=1.30, e=-0.50 for 2-vinylpyridine, and Q=1.37, e=-0.74 for the other pyridine; these are given in Table II. The monomer-copolymer compostion curve calculated from the monomer reactivity ratios, r_1=0.514 and r_2=0.715, gave a poorer fit to the experimental points with 4-vinylpyridine. To describe the data obtained with 2-vinylpyridine, the calculated curve with Q=1.5 and e=-1.2 was poorer fit than that with Q=1.4 and e=-1.1, but better than that with Q=1.2 and e=-1.0 for 1-ethenyl-4-(2,3-epoxy-1-propoxy)benzene. These calculated with Q=1.5, e=-1.2; Q=1.3, e=-1.1; and Q=1.2, e=-1.0 for 1-ethenyl-4-(2,3-epoxy-1-propoxy)benzene gave an excellent fit corresponding closely to the points with 5-ethyl-2-vinylpyridine.

The copolymers with these pyridines have a characteristic band due to an intermolecular hydrogen bond ν(OH) of OH group of polymers about at 3500/cm as shown in Figure 4. The bands at 1660 to 1640/cm assigned to the stretching modes of the C=C bond of olefinic hydrocarbons are not observed. The bands assigned to the in-plane and the out-of-plane bending modes for olefinic CH groups are also not observed distinctly in the 1450-1300/cm and 1000-800/cm regions of the infrared spectra of the copolymers. The symmetrical and the asymmetrical stretching bands of the epoxy ring seem to occur near 1250/cm and 910/cm, respectively. The intensity of the band at 910/cm decreased and disappeared in the spectra of the heated samples which became insoluble and infusible.

The homo- and copolymers of these epoxides with the vinylpyridines were highly amorphous as judged by the X-ray diffractograms Under the experimental conditions, the resulting copolymers were soluble in organic solvents such as tetrahydrofuran, chloroform, and N,N-dimethylformamide, while in a humid atmosphere the copolymers, especially those with 4-vinylpyridine, were apt to be converted to the insoluble materials during reprecipitation or drying at a room temperature. Differential scanning calorimetry and thermogravimetry studies show these copolymers do not melt but react autocatalytically at 90-200°C and degrade extensively above 300°C.

The polymeric materials were crushed, mixed with KBr powder and pressed into the form of a KBr disk. The samples were heated in a forced draft oven, taken out at convenient intervals, cooled in a desiccator, and the intensity of the band at 910/cm was measured. The intensity of IR absorption spectrum of the epoxy group at 910/cm was found to decrease in proportion to the decrease of the epoxy compound in the reaction system (2).

Table II

Monomer Reactivity Ratios and Q-e Values in Copolymerization of 1-Ethenyl-4-(2,3-epoxy-1-propoxy)benzene (M_1) with Vinylpyridines (M_2)[a]

M_2	r_1	r_2	e_1	e_2[b]	Q_1	Q_2[b]
4-Vinylpyridine	0.467[c]	0.638[c]	-1.3	-0.20	1.6	0.82
	0.514[c]	0.715[c]	-1.2[d]		1.4[d]	
2-Vinylpyridine	0.531[c]	1.15[c]	-1.2[d]	-0.50	1.5[d]	1.30
	0.556	1.25	-1.1		1.4	
	0.560[c]	1.39[c]	-1.0[d]		1.2[d]	
5-Ethyl-2-vinylpyridine	0.630[c]	1.28[c]	-1.2[d]	-0.74	1.5[d]	1.37
	0.639	1.38	-1.1		1.3	
	0.675[c]	1.38[c]	-1.0[d]		1.2[d]	

a Polymerization conditions: 0.02 mole of monomers; polymerization in tetrahydrofuran with 0.5 mole-% of 2,2'-azoisobutyronitrile at 60°C.
b Reference data used for calculation of Q-e values.
c Calculated values from the assumed Q-e values.
d Assumed values used for calculation of r_1 and r_2 values.
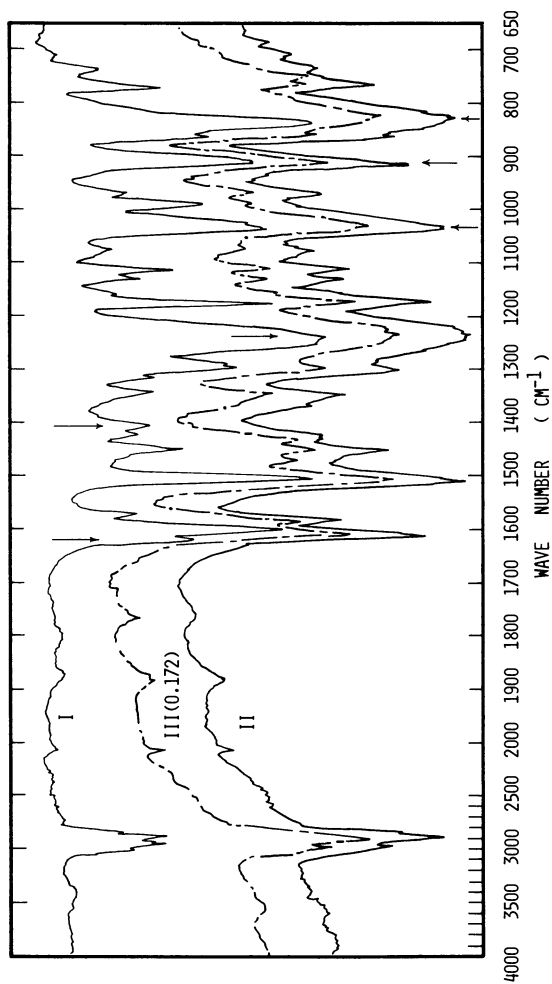
Figure 4. IR spectra of 1-ethenyl-4-(2,3-epoxy-1-propoxy) benzene and its homopolymers and copolymers with 2-vinylpyridine. Number in parentheses shows the mole fraction of pyridine in the copolymer: (I) monomer; (II) homopolymer; (III) copolymer

Journal of Polymer Science, Polymer Chemistry Edition

The characteristic bands of the methyl or methylene, and
the phenyl groups at 1440 and 1505/cm were used as stan-
dards for copolymers of these epoxides, respectively,
because their intensities did not change during the
reactions.   The results of typical experiments with the
copolymers of 1-ethenyl-4-(2,3-epoxy-1-propoxy)benzene
are plotted in Figure 5, in which the relative intensity
changes of 910 to 1505/cm are plotted against the reac-
tion time and follow, in some cases, sigmoidal curves
showing an induction period.   The induction period was
found to be dependent on the reaction temperature and on
the content of the vinylpyridine unit in copolymers.
     The relationship of the rate of consumption of the
epoxy group, $-d(M_{1,t}/M_{1,o})/dt$, with the epoxy groups
remaining $M_{1,t}/M_{1,o}$, in the copolymers of 1-ethenyl-
4-(2,3-epoxy-1-propoxy)benzene is shown in Figure 6.
$M_{1,i}$ is the content of the epoxy group at reaction
time i.   The maximum rate of consumption of the epoxy
group increased as the mole fraction of the pyridine to
the epoxy group increased.   At the maximum rate of
reaction the rate of consumption of the epoxy group
reached the stationary stage, independent of the
content of the epoxy group, the region of which became
longer as the fraction of the pyridine increased.   The
slope of the linear part of the curve obtained for the
relationship decreased with increasing the content of
the pyridine unit except in the initial stage of the
reaction.   Then, the rate of disappearance of the epoxy
group varies with the mole fraction of the epoxy group
and the order of reaction with respect to the concentra-
tion of the epoxy group cannot be determined by this
experiment.   The time-conversion curves, however, are
similar to those observed in the tertiary amine-cata-
lyzed oligomerization of epoxy compounds ($\underline{2}$), in which
the rate is first-order with respect to the epoxy com-
pound except in the initial stage of the reaction.
     If the rate of reaction is given as a function of
the concentrations of the epoxy and the pyridyl groups,
the rate equation is shown by:

$$- dM_1/dt = k\ f(M_1)\ g(M_2)$$

and may be rewritten as:

$$- \int dM_1/f(M_1) = k\ g(M_2)\ t_i$$

where $f(M_1)$ and $g(M_2)$ are functions of the concentra-
tions of the epoxide and the pyridine, k is the rate
constant, and t_i is the reaction time when the conver-
sion of the epoxy group reaches i.   Assuming that $g(M_2)$
is constant under the condition, we can obtain

$$g(M_2)\ t_i = K_i$$

where K_i is a constant shown by $-[\int dM_1/f(M_1)]/k$.
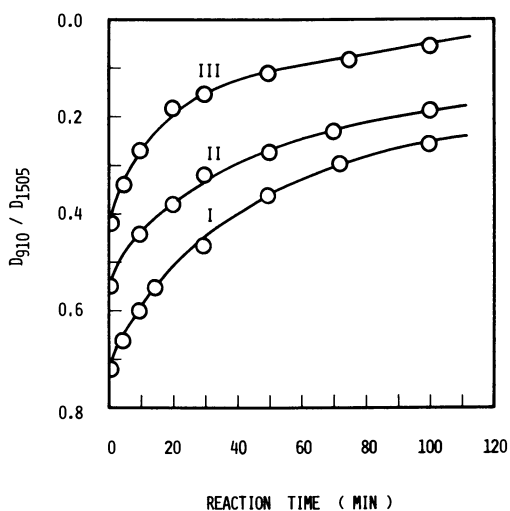
Figure 5. Time–conversion curves for the epoxy group of poly[1-ethenyl-4-(2,3-epoxy-1-propoxy)benzene] in KBr pellet at 105°C for copolymers with various mole fractions of pyridine: (I) 0.274; (II) 0.399; (III) 0.584
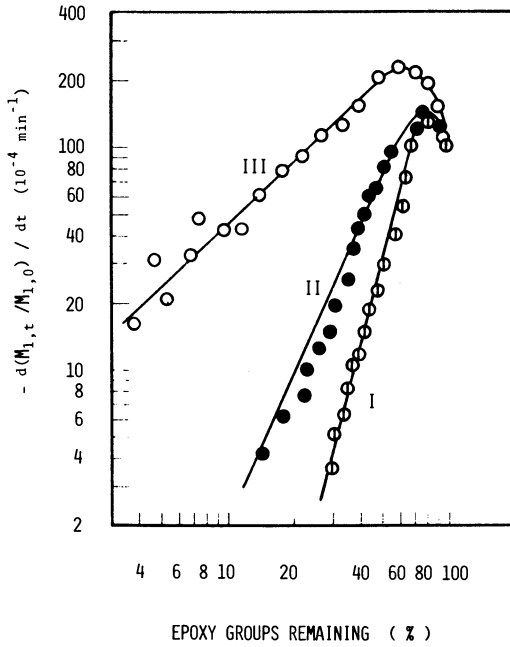
Figure 6.   Dependence of the rate of consumption of the epoxy group at 130°C on the remaining epoxy group in copolymers obtained at reduced pressure with various mole fractions of pyridine: (I) 0.258; (II) 0.502; (III) 0.597

Thus, various reciprocal values of the reaction time t_i, at which the conversion of the epoxy group reaches i, are plotted against the mole fraction of the pyridine, M_2, as shown in Figure 7. The reaction rate increases with increasing the content of the pyridyl group, reaches a maximum value about at 0.5 or 0.6, and then decreases with the fraction of the pyridine. The ring-opening reaction of the epoxy group in these co-polymers may be carried out in the presence of the pyridyl group by the cocatalytic action of the hydroxyl group in the polymer chain. The mechanism of this self-crosslinking reaction of the copolymers seems to be similar to those (2) proposed for the oligomerization of the epoxy compound and the curing of the epoxy resin by a tertiary amine. The reactivity difference in these self-crosslinking reactions between these copolymers seems to be described mainly by the polar effect of any of the possible organic moieties of the copolymer except the epoxy group.

The ring-opening reaction of the epoxy compound can be generally explained by the modified Taft equation (6). As a linear relationship has been observed between the polar substituent constant $\sigma*$ and the basicity of ethers (2), the reactivity towards nucleophilic species will decrease and that towards electrophilic reagents may increase as the basicity of the epoxy compound increases, i.e., as the $\sigma*$ value decreases. The $\sigma*$ values for the substituents $R[R=CH_2CHC_6H_4OCH_2$ and $CH_2C(CH_3)CO_2CH_2]$ of the epoxy compounds, OCH_2CHR, can not be found in the literature, but their relative order may be estimated from those ($\sigma*=0.600$ and 1.9) (6) for C_6H_5 and CH_3CO, $\sigma*$ for 1,2-epoxypropane ($R=CH_3$) being 0. Therefore, the reactivity of the epoxy group in the copolymers of 1-ethenyl-4-(2,3-epoxy-1-propoxy)benzene can be considered to be higher towards electrophilic species and to be lower towards nucleophilic compounds than that in the copolymers of 2,3-epoxy-1-propyl methacrylate. In the self-crosslinking reaction, actually, the former was converted to the insoluble materials faster and at a lower temperature than the latter.

The pKa values of unsubstituted, 2-vinyl and 4-vinylpridines are 5.17, 4.92-4.98, and 5.62 (7). A methyl or an ethyl group in 2- or 6-position of the pyridine nucleus causes an increase in basicity as well as that in 3- or 4-postion. Consequently, a similar increase in rate would be anticipated if the rate was proportional to the basicity of the pyridyl group in co-polymers. Nevertheless, the rate of reaction catalyzed by 2,5-disubstituted pyridyl group are not larger but smaller than 2- or 4-substituted pyridyl group as shown
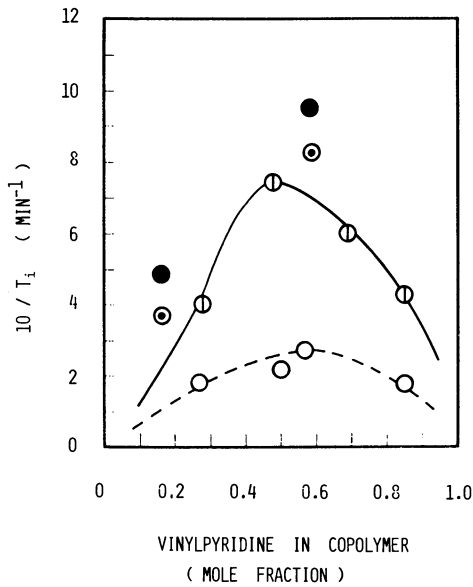
Figure 7.   Effect of the mole fraction of pyridine on the reaction at 130°C of the epoxy group in copolymers of 1-ethenyl-4-(2,3-epoxy-1-propoxy) benzene (⊕, ⊙, ●) or 2,3-epoxy-1-propoxy methacrylate (○) with various vinylpyridines. Where 10/t$_i$ at 30% conversion of the epoxy group is plotted: (⊙) copolymers with 2-vinylpyridine; (●) copolymers with 4-vinylpyridine; (⊕) and ○ copolymers with 5-ethyl-2-vinylpyridine.

in Figure 7. This might be attributed to the steric
effect of any of the possible organic moieties of the
copolymer except the pyridyl group. The similar iden-
tity of these results has been retained in the reaction
of 2,3-epoxy-1-propyl phenyl either with benzoic acid
catalyzed by substituted pyridines and in many other
reactions (2).

Synopsis

        Soluble and self-crosslinkable linear copolymers
with pendant epoxy and pyridyl groups were obtained from
1-ethenyl-4-(2,3 epoxy-1-propoxy) benzene or 2,3-epoxy-1-
propyl methacrylate and vinylpyridines by the action of
2,2'-azoisobutyronitrile. The monomer reactivity ratios
were determined in tetrahydrofuran at 60°C, and the Q
and e values for these epoxides were calculated with the
reported Q-e values for these pyridines. The intrinsic
viscosities of the copolymers were found to be 0.15-0.38
in tetrahydrofuran at 30°C and to be dependent on the
copolymer composition. The copolymers were amorphous,
had no clear melting points, and became insoluble cross-
linked polymers under heating without further addition
of any curing agents. The reactivity difference in
these self-crosslinking reactions among these copolymers
was described by the steric as well as the polar effect
of any of the possible organic moieties of the copoly-
mers.

Literature Cited

1.   Tanka, Y; Okada, A; Tomizuka, I.,in "Epoxy Resins";
      May, C. A., Tanaka, Y., Ed.; Dekker: New York, 1973;
      Chap. 2.
2.   Tanaka, Y.; Mika, T. F., in "Epoxy Resins"; May,
      C. A., Tanaka, Y., Ed.; Dekker: New York, 1973;
      Chap. 3.
3.   Mayo, F. R.; Lewis, F. M., J. Amer. Chem. Soc.,
      1944, 66, 1594.
4.   Price, C. C., J. Polym. Sci., 1948, 3, 772.
5.   Tamikado, T., J. Polym. Sci., 1960, 43, 489.
6.   Taft, R. W. Jr., in "Steric Effects in Organic
      Chemistry"; Newman, M. S., Ed.; Wiley: New York,
      1956; Chap 13.
7.   Perrin, D. D. Ed., "Dissociation Constants of
      Organic Bases in Aqueous Solution"; Butterworths:
      London, 1965.

Some Studies on the Preparation of Glycidyl 2-Ethylhexanoate

D. A. CORNFORTH, B. G. COWBURN, K. M. SMITH,
C. W. STEPHENS, and C. G. TILLEY

Anchor Chemical Company Ltd., Clayton, Manchester M11 4SR, England

The preparation of glycidyl 2-ethylhexanoate has been studied in order to gain an insight into the general mechanism of the reaction of epichlorohydrin with carboxylic acids. The investigation was carried out in two stages. The first stage of the reaction involves the catalysed addition of 2-ethyl-hexanoic acid to epichlorohydrin to yield 2-hydroxy-3-chloropropyl 2-ethylhexanoate. The reaction is then completed by de-hydrochlorination of 2-hydroxy-3-chloropropyl 2-ethyl-hexanoate to yield glycidyl 2-ethylhexanoate (Fig. 1). This compound was selected in order to give intermediates and products of acceptable volatility to allow gas chromatography to be used as the principal analytical tool.

Results and Discussion

Reaction of Epichlorohydrin with 2-Ethylhexanoic Acid

The cetyl trimethylammonium bromide catalysed addition of epichlorohydrin to 2-ethylhexanoic acid has been studied at levels of 1, 5 and 7 molar ratios of epichlorohydrin to 2-ethylhexanoic acid. The reactions were carried out in toluene in order to facilitate removal of water from the final product (glycidyl 2-ethylhexanoate) by azeotropic distillation. A further advantage in using toluene as solvent is that where glycidyl esters of high molecular weight are being considered the solution viscosities may be kept sufficiently low to effect filtration, if required, before final distillation. The reaction products were determined by gas chromatography. The rate of consumption of the starting materials was also determined by gas chromatography and other standard analytical techniques.

R - COOH   +   CH₂ - CH - CH₂ - Cl

R - CO - O - CH₂ - CH - CH₂ - Cl
                         OH

R - COO - CH₂ - CH - CH₂

Figure 1.   Overall reaction scheme

Figure 2.   Reaction of epichlorohydrin with 2-ethylhexanoic acid (1:1 mol ratio)

1:1 Molar Ratio of Epichlorohydrin to 2-Ethylhexanoic Acid

The concentration-time curve for the reactants is shown in Fig. 2, and the concentration-time curve for the products is depicted in Fig. 3. Examination of Fig. 3 shows that as well as the desired reaction product (the chlorohydrin ester), there are two other major product components. These were identified as 1,3-dichloropropan-2-ol (α-dichlorohydrin) and glycerol – 1,3-di(2-ethylhexanoate) (hydroxy diester). The structure of the hydroxy diester was confirmed by its independent synthesis from glycidyl 2-ethyl hexanoate and 2-ethyl hexanoic acid. The yield of chlorohydrin ester was only 50.4%, the remainder of the 2-ethylhexanoic acid being converted to the undesirable hydroxy diester. Fig. 4 shows the structure of the products obtained in the 1:1 reaction. Fig. 5 depicts the formation of the hydroxy diester from glycidyl 2-ethylhexanoate and 2-ethyl-hexanoic acid.

A mechanism which is consistent with the experimental observations for the production of the chlorohydrin ester is given in Fig. 6. The first stage of the reaction involves ionisation of 2-ethylhexanoic acid by the catalyst cetyltri-methylammonium bromide. Subsequent attack of the carboxyanion on epichlorohydrin leads ultimately to the desired reaction product of the first stage of the reaction. Examination of Fig. 3 shows that the rate of formation of α-dichlorohydrin and the hydroxy diester closely follow each other indicating that their formation is interdependent. The by-product formation seems best accommodated by the mechanism shown in Fig. 7 which involves breakdown of the intermediate chloro-oxy anion by internal nucleophilic displacement, to yield glycidyl 2-ethyl-hexanoate. The glycidyl 2-ethylhexanoate subsequently reacts with the carboxyanion to yield ultimately the hydroxy diester. The α-dichlorohydrin may be formed by chloride ion attack on epichlorohydrin with subsequent protonation of the dichloro-oxy anion.[1] Further evidence for this mechanism is also provided by the direct synthesis of the hydroxy diester from glycidyl 2-ethylhexanoate and 2-ethylhexanoic acid (Fig. 5). It is also possible that the chlorohydrin may break down thermally to give the undesirable by-products (Fig. 8).

Summary of 1:1 Reaction

The reaction of epichlorohydrin with 2-ethylhexanoic acid in a 1:1 molar ratio gives rise to only 50% of the desired product, the chlorohydrin ester. The mechanism depicted above indicates that the undesirable hydroxy diester is formed by reaction of 2-ethylhexanoic acid with glycidyl 2-ethylhexanoate. It appears therefore that formation of the hydroxy diester competes directly with the chlorohydrin ester formation (Fig. 9).
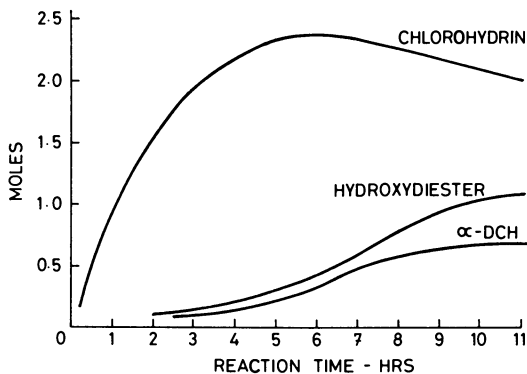
Figure 3.   Reaction of epichlorohydrin with 2-ethylhexanoic acid (1:1 mol ratio; product composition)

① R - CO - O - CH₂ - CH - CH₂
                         | |
                        OH   Cℓ

2 - HYDROXY - 3 CHLOROPROPYL - ⌈2 - ETHYLHEXANOATE⌉
⌈CHLOROHYDRIN⌉

② Cℓ - CH₂ - CH - CH₂ - Cℓ
                |
               OH

1,3 - DICHLOROPROPAN - 2 - OL
⌈α - DICHLOROHYDRIN⌉ α-DCH

③ R - CO - O - CH₂ - CH - CH₂ - O - CO - R
                         |
                        OH

GLYCEROL - 1,3 - DI - ⌈2 - ETHYLHEXANOATE⌉
⌈HYDROXYDIESTER HDE⌉
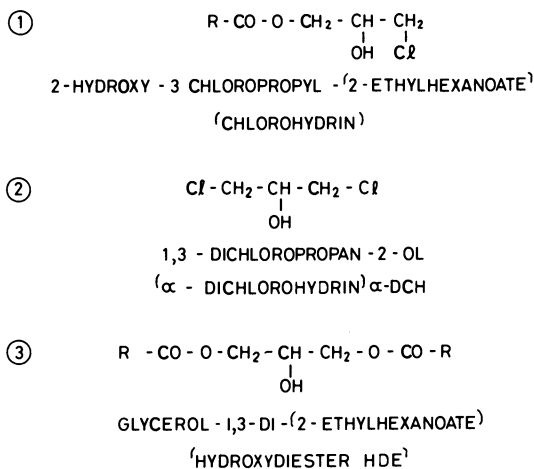
Figure 4.   Product structures

$$RCO_2H + RCO_2\,CH_2\,CH-CH_2 \longrightarrow RCO_2\,CH_2\,CHCH_2\,CO_2\,R$$

$$\left[\; R = C_4\,Hg \bullet CH - \;\atop\qquad\qquad\;\; C_2H_5 \right]$$
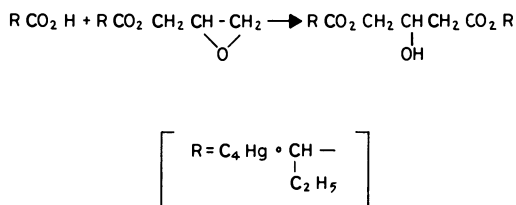
Figure 5. Glycerol-1,3-di-2-ethylhexanoate synthesis
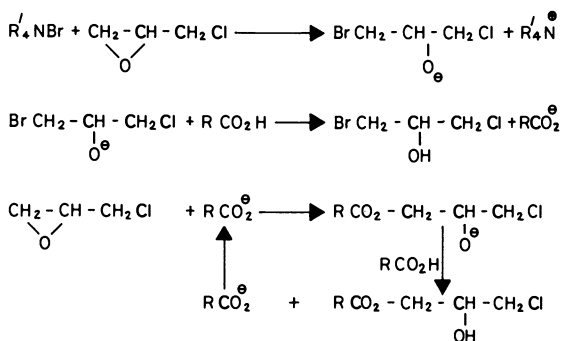
Figure 6. Proposed reaction mechanism Part A
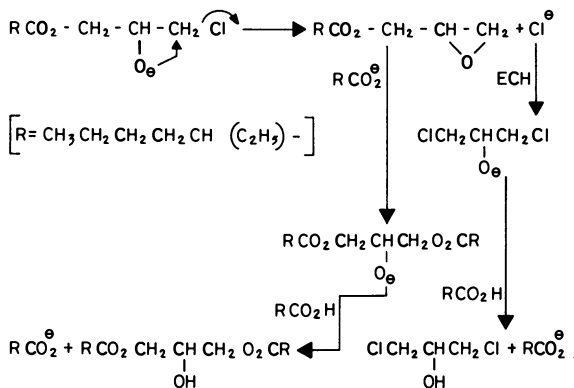
Figure 7. Proposed reaction mechanism Part B

$R\,CO_2\,CH_2\,CH\,CH_2\,Cl \longrightarrow R\,CO_2\,CH_2\,CH\,CH_2\,+\,HCl$
                         | \O/
                        OH

                                                          ECH

$R\,CO_2\,H$

$R\,CO_2\,CH_2\,CH\,CH_2\,O_2\,CR \longleftarrow \quad Cl\,CH_2\,CH\,CH_2\,Cl$
                     | |
                    OH   OH

Figure 8.   By-product formation

$CH_2-CH\,CH_2\,Cl$
      \O/

                        $R\,CO_2\,CH_2\,CH\,CH_2\,Cl$
                                        |
                                       OH

$R\,CO_2\,H$

                        $R\,CO_2\,CH_2\,CH\,CH_2\,CO_2\,R$
                                        |
                                       OH

$R\,CO_2\,CH_2\,CH-CH_2$
                \O/

Figure 9.   Competition reaction

Figure 10.   Reaction of epichlorohydrin with 2-ethylhexanoic acid (5:1 mol ratio; product composition)

It is apparent therefore that an increase in the epichlorohydrin concentration should promote the formation of the chlorohydrin ester, at the expense of the hydroxy diester.

5:1 and 7:1 Molar Ratio of Epichlorohydrin to 2-ethylhexanoic acid

The concentration-time curve for the products of the 5:1 reaction are shown in Fig. 10 and that for the 7:1 reaction depicted in Fig. 11. As expected the chlorohydrin ester is produced almost exclusively at the expense of the hydroxy diester, the yield of the latter compound being reduced to 2.9% in the 5:1 reaction and 1.4% in the 7:1 reaction (ca 50% in the 1:1 reaction).

Examination of Figs. 10 and 11 show that the chlorohydrin ester formation reaches a maximum after 3 to 4 hours, this maximum coinciding with the consumption of all the 2-ethylhexanoic acid. Interestingly if the reaction is allowed to continue for an excess period the concentration of the chlorohydrin ester begins to decrease in the reaction mixture. The decrease in chlorohydrin ester concentration is concomitant with the formation of glycidyl 2-ethylhexanoate and is accompanied by the formation of α-dichlorohydrin. This shows that the chlorohydrin is breaking down (thermally or catalytically) as depicted in Fig. 12. At this point in the reaction all the acid has been consumed and it is therefore not available to underto further reaction with the epoxy compound to give the hydroxy diester as in the 1:1 reaction.

At first sight it may not seem undesirable to allow the reaction to continue, in order to allow conversion of the chlorohydrin ester to the epoxy compound (Fig. 12) as the ultimate aim is, in fact, to form glycidyl 2-ethylhexanoate by ring closure of the chlorohydrin ester intermediate. However it was noted that formation of the epoxy compound is accompanied by formation of α-dichlorohydrin, and it was shown in a separate experiment that further reaction of these two compounds could be effected under the reaction conditions, probably giving rise to further undesirable by-products (Fig. 13).

Conclusion

The products formed during the reaction of epichlorohydrin with 2-ethylhexanoic acid are governed by the relative concentrations of the two reactants. Epichlorohydrin must be present in excess in order to achieve a high yield of chlorohydrin ester. In order to optimise the yield of chlorohydrin ester the reaction must be terminated when all the acid has been consumed otherwise the reaction is complicated by decomposition and further reactions of this material.

Figure 11.   Reaction of epichlorohydrin with 2-ethylhexanoic acid (7:1 mol ratio; product composition)

Figure 12.   Chlorohydrin ester decomposition

Figure 13.   Further by-product formation

Stage II Ring Closure Reaction

In order to study the ring closure reaction in detail a
masterbatch of the chlorohydrin ester was prepared in 50%
toluene solution using a 5:1 molar excess of epichlorohydrin to
2-ethylhexanoic acid.

The first ring closure process investigated used a
technique whereby 50% aqueous sodium hydroxide was added at a
constant rate under conditions where the water was removed by
azeotropic distillation with the excess epichlorohydrin and
toluene solvent, giving a dehydrochlorination under essentially
anhydrous conditions.   Fig. 14 shows the conversion of
chlorohydrin ester to glycidyl 2-ethylhexanoate using two
different rates of addition of sodium hydroxide solution (0.25
mol. hr.$^{-1}$ and 0.125 mol. hr.$^{-1}$).   Excellent conversion to
glycidyl 2-ethylhexanoate was obtained which may be seen to be
relatively independent of the rate of sodium hydroxide addition.
However in order to attain high yields (>99%) it may be seen
that 40-50% excess (based on chlorohydrin ester) sodium
hydroxide was required.

The epichlorohydrin concentration was also followed during
the reaction and it can be seen (Fig. 14) that this component
was also consumed during the ring closure reaction (12-14%
conversion).   It can be seen therefore that epichlorohydrin
competes with the chlorohydrin ester for sodium hydroxide during
the dehydrochlorination reaction.   Two competing reactions are
essentially taking place and indeed it was found that the
excess sodium hydroxide required was directly attributable to
hydrolysis of epichlorohydrin.   Epichlorohydrin hydrolysis is
highly undesirable in the ring closure reaction as it leads to
polymer formation in the final product[2,3].

The polymeric material was isolated from the reaction
mixture as a colorless water insoluble material.   The polymer
was tentatively assigned the cross-linked structure depicted in
Fig. 15 based on mass spectrometric evidence.   Interestingly
the mass spectrum did not show any chlorine containing
structures in the polymer showing that sodium hydroxide was in
fact hydrolysing the chlorine atom of epichlorohydrin either
before or after polymerisation.

In an attempt to overcome epichlorohydrin hydrolysis in
the ring closure reaction an alternative approach using sodium
hydroxide/sodium carbonate solution was sought.   A patent[4]
is held by the Dow Chemical Company which describes the use of
a solution of an alkali metal hydroxide and an alkali metal
carbonate to effect dehydrochlorination.   The patent claims
that using this technique epichlorohydrin hydrolysis is greatly
reduced.   Accordingly this technique was investigated whereby
a mixture containing sodium carbonate (9.8%), sodium hydroxide
(15.7%) and water (74.5%) was stirred with the chlorohydrin
ester masterbatch prepared above.   The reaction was studied in
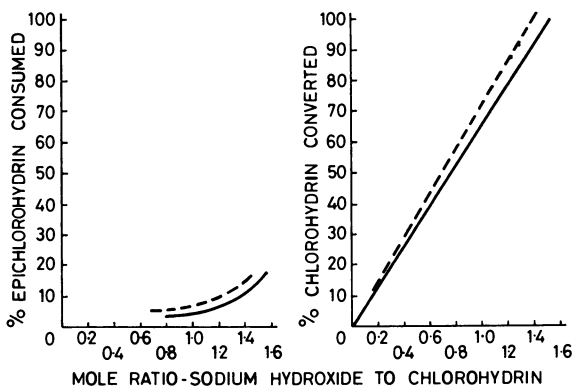
Figure 14. Conversion of chlorohydrin and epichlorohydrin in the presence of sodium hydroxide under azeotropic conditions: (———) NaOH added 0.25 mol/hr; (— — —) NaOH added 0.125 mol/hr
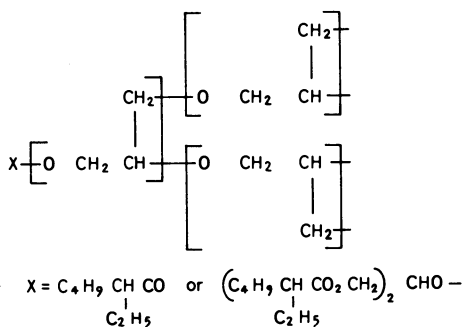
Figure 15.   Polymer isolated from product

detail at 40ºC and 75ºC using a molar ratio of sodium hydroxide to chlorohydrin ester of 2:1. The reactions were monitored by gas chromatography. Fig. 16 shows the rate of conversion of chlorohydrin ester to glycidyl 2-ethylhexanoate and the rate of epichlorohydrin hydrolysis at both temperatures.

It may be seen that at 75ºC epichlorohydrin hydrolysis is in fact the major reaction (51.7% conversion) and that only 30% conversion to glycidyl 2-ethylhexanoate is obtained. The graph clearly shows that at 75ºC the low yield is not due to consumption of the chlorohydrin ester in an undesirable manner, but is simply due to removal of sodium hydroxide by rapid hydrolysis of epichlorohydrin. The reaction at 40ºC was more encouraging. After 6.5 hours, at which time all the sodium hydroxide had been consumed, a 75% conversion of chlorohydrin ester to glycidyl 2-ethylhexanoate was obtained. However, it can be seen that even at 40ºC epichlorohydrin hydrolysis is occurring (15.6% conversion) and a large amount of sodium hydroxide is consumed in this reaction.

The organic phase from the above reaction was removed and retreated with a further portion of the sodium hydroxide/ sodium carbonate mixture and the reaction continued at 40ºC. A high conversion to glycidyl 2-ethylhexanoate was ultimately achieved by this technique (>99%) although by this time the epichlorohydrin hydrolysis (24.3%) was considered to be too high for this method to be used commercially.

In an attempt to reduce the overall epichlorohydrin hydrolysis the effect of removal of this component from the reaction system was investigated. A sample of the above reaction mixture was removed after the initial treatment with sodium hydroxide/sodium carbonate solution and the excess epichlorohydrin and toluene removed by vacuum distillation. The resulting mixture of chlorohydrin ester and glycidyl 2-ethylhexanoate was resolvated with toluene and retreated with a further portion of sodium carbonate solution at 40ºC. However it was found that no further conversion of the chlorohydrin ester to epoxy compound was obtained indicating that epichlorohydrin is required in the reaction system to effect ring closure.

Indeed, in a patent held by the Dow Chemical Company[1] it is observed that epichlorohydrin (or other suitable 1,2-epoxide) is required in order to obtain high yields of glycidyl esters from 2-hydroxy-3-chlorophenyl esters. A mechanism involving transepoxidation was proposed (Fig. 17). No polymer formation was observed in the above reaction; however, some water soluble organic components were detected by gas chromatography which were presumably derived from hydrolysis of epichlorohydrin. Analysis of the aqueous residues showed that the sodium carbonate was essentially unchanged during the reaction, which lead to examination of
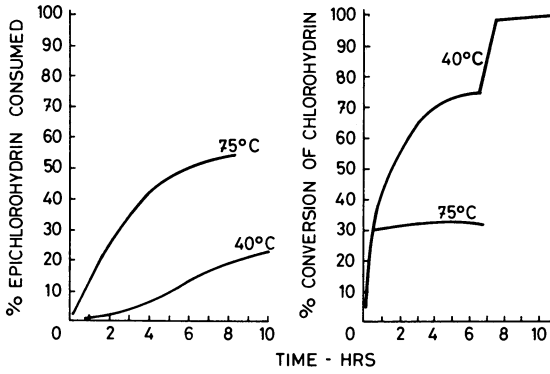
Figure 16.   The % conversion of chlorohydrin and % epichlorohydrin consumed at 40°C and 75°C in sodium hydroxide/sodium carbonate aqueous solution
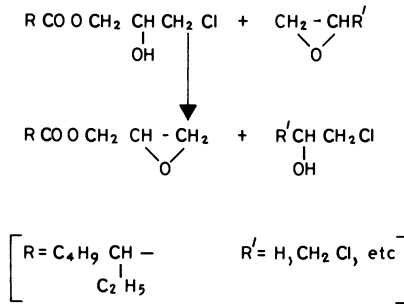
Figure 17.   Transepoxidation reaction
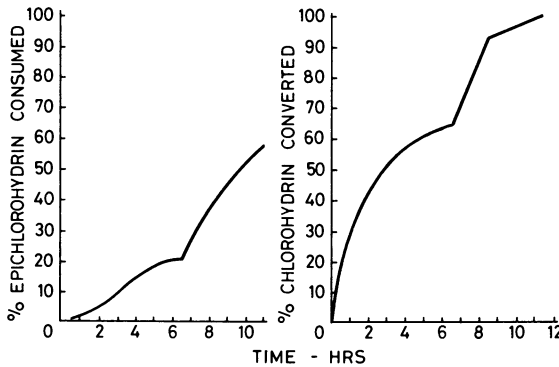
Figure 18.   Product composition in aqueous sodium hydroxide at 40°C

the use of aqueous sodium hydroxide alone to effect ring
closure.

   Accordingly, sodium hydroxide (17% aqueous solution) was
stirred with the chlorohydrin ester masterbatch prepared above.
The reaction was followed at 40°C using a molar ratio of sodium
hydroxide to chlorohydrin ester of 2:1.   The reaction was
followed by gas chromatography.   Fig. 18 shows the rates of
conversion of epichlorohydrin and chlorohydrin ester during the
reaction.   Again, it was shown that after 6.5 hours all the
sodium hydroxide had been consumed (cf. sodium hydroxide/sodium
carbonate reaction at 40°C) at which time only 64% conversion
to the epoxy compound was observed.   Correspondingly the
epichlorohydrin hydrolysis (25%) had increased in comparison to
the sodium hydroxide/sodium carbonate method (15.6% at 40°C).
In order to continue the comparison of the aqueous sodium
hydroxide dehydrochlorination with the aqueous sodium hydroxide/
sodium carbonate method the organic phase from the above
reaction was removed and retreated with aqueous sodium
hydroxide (a further 2 molar excess).   Ultimately a 98%
conversion to glycidyl 2-ethylhexanoate was achieved but by
this time very extensive epichlorohydrin hydrolysis had
occurred (56%).   It was also found difficult to separate the
organic phase from this reaction due to emulsification with the
aqueous phase in order to carry out the final purification
stage by distillation.

Conclusion

   Three techniques were evaluated for the ring closure
reaction:

   1.   Aqueous sodium hydroxide/sodium carbonate

   2.   Aqueous sodium hydroxide

   3.   Azeotropic system

In aqueous systems it was shown that a temperature of 40°C was
most practical.   At higher temperatures epichlorohydrin
hydrolysis was too rapid to give rise to a viable process.
Although at 40°C good conversion to the glycidyl ester could be
obtained, a high proportion of sodium hydroxide (based on
chlorohydrin) had to be used (up to 4 molar excess).   However
even at 40°C the hydrolysis of epichlorohydrin was a serious
competitive reaction to the ring closure.   The epichlorohydrin
hydrolysis using a mixture of sodium carbonate/sodium hydroxide
was considerably reduced in comparison to that obtained by
using sodium hydroxide (24.3% in the former reaction: 56% with
NAOH).   This is in agreement with the Dow patent.

The best technique for ring closure evaluated to date involves continuous addition of 50% aqueous sodium hydroxide to the reaction mixture at such a rate that water may be obtained by azeotropic distillation. Although polymeric material is formed during the reaction this can be removed, along with the salt formed during dehydrochlorination, prior to isolation of the glycidyl ester by distillation.

Future Process Optimisation

Modifications to the above techniques may be envisaged for process improvement. In the above reactions epichlorohydrin is present in excess after the initial formation of the chlorohydrin ester (4 molar excess) as a consequence of the requirements of the stage I reaction. However it has been shown that epichlorohydrin hydrolysis competes with the required reaction in stage II of the process. It would therefore be desirable to reduce the concentration of epichlorohydrin prior to ring closure. It has however been shown that epichlorohydrin is required to effect ring closure (transepoxidation) and work is in hand to optimise the concentration of this component during the dehydrochlorination reaction.

LITERATURE CITED

1.   D. R. Smith, U.S. Patent 3,335,156 (1967)

2.   I. Ondus, Chem Prum., 21 (4), 168 (1971)

3.   L. N. Finyakin, V. V. Kafarov, M. F. Sorokin, L. G. Shode and G. V. Onosov, Tr. Mosk.Khim. - Teknol. Inst., No. 70, 80 (1972).

4.   D. R. Smith, U.S. Patent 3,372,142 (1968).

RECEIVED May 21, 1979.

Reactions in a Typical Epoxy–Aliphatic Diamine System

JOHN J. KING and JAMES P. BELL

University of Connecticut U-139, Storrs, CT 06268

A large amount of work has been reported in the literature concerning the nature of the reaction of epoxides with aliphatic amines (1-12). Schecter, Wynstra and Kurkjy (1) suggested that only reactions (1), (2) and (3) need be considered in the absence of strong tertiary amines:

$$RNH_2 + \overset{O}{\overset{\frown}{C-CR'}} \xrightarrow{k1} RNHC-\overset{OH}{\underset{}{CR'}} \qquad (1)$$

$$RNHC-\overset{OH}{\underset{}{CR'}} + \overset{O}{\overset{\frown}{C-C-R'}} \xrightarrow{k2} RN\overset{OH}{\underset{\substack{C \\ C-OH \\ R'}}{C-CR'}} \qquad (2)$$

$$RN\overset{OH}{\underset{R''}{C-CR'}} + \overset{O}{\overset{\frown}{C-C-R''}} \rightarrow RN\overset{}{\underset{R'\,R'}{C-C}}-O-C-\overset{}{\underset{OH}{C}}-R'' \qquad (3)$$
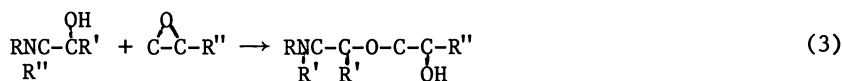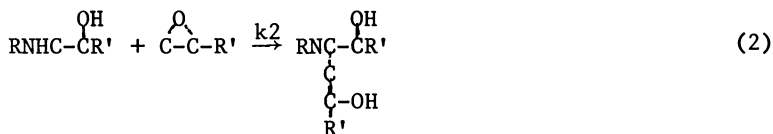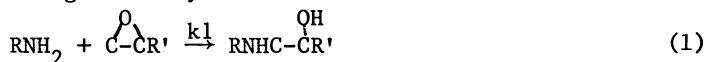
Of these, they determined (3) was negligible for most near-stoichiometric amine concentrations, leaving (1) and (2) with rate constants k_1 and k_2 respectively.

Ingbermand and Walton (2) found that the secondary aliphatic amino hydrogen reacted as readily as the primary. This is in contrast to Oshior et al, (3,4) Harrod, (5) Kakurai et al,(6) and Isaacs and Parker (7) who found an unequal activity of primary and secondary amino groups to epoxy.

The difference in activity among various amines may be attributed to steric hinderances of and substituent groups on the reactants. Kakurai et al (6) found a decrease in reactivity of amines as the bulkiness of the side chains increased. Data collected by Iwakura et al, (8) Allen et al (9) and Ingberman et al (2) suggest that hydroxyl substituted amines react more readily by forming a reactive transition state, reaction (4).

$$A-OH + \overset{O}{\overset{\frown}{C-C-R}} \rightarrow \overset{HO-A}{\overset{O}{\overset{\frown}{C-C-R}}} \qquad (4)$$
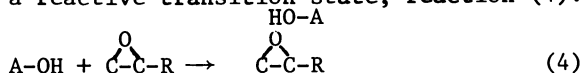
An increase in consumption of reactants has been noted in
the presence of certain Lewis acids. This catalytic effect has
been related to the pK_a values of the various groups, with acti-
vities arranged as: acids > phenols > water > alcohols
nitriles > aromatic > hydrocarbons > dioxane > diisopropylether
(6,10). The alcohols are included in this list due to their
weakly acidic nature. The accelerating effect of alcohols is de-
pendent on structure: methanol > ethanol > n-propanol > tert-
butanol > n-butanol > isobutanol > cyclohexanol (6,10).

It was suggested by Harrod (5) that the ratio k_2/k_1 is
virtually independent of temperature and composition but depen-
dent on the amine and epoxide used. Dusek et al (11) state that
k_1 and k_2 depend on the autocatalytic effect of the hydroxyls and
retardation caused by hydroxyl complexing with amine hydrogens
but present no evidence to support this statement. They also
mention data to support the constancy of k_2/k_1.

The presence of hydroxyl groups during the reaction should
be included within the rate expressions. Schecter et al (1) first
proposed a termolecular mechanism to describe the effect of
hydroxyl groups on the reaction, reactions (5) and (6).

$$R_2NH + C\text{-}CR' + HO\cdot X \rightarrow R_2NH\text{---}C\text{-}C\text{-}R' \qquad (5)$$
$$\overset{O}{\underset{HO\cdot X}{\overset{\diagdown}{\diagup}}}$$

$$R_2NH\text{---}C\text{-}CR' \rightarrow R_2NC\text{-}CR' + HO\cdot X \qquad (6)$$
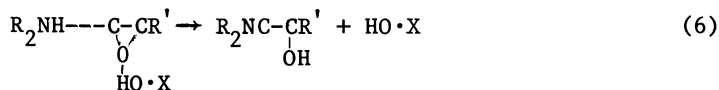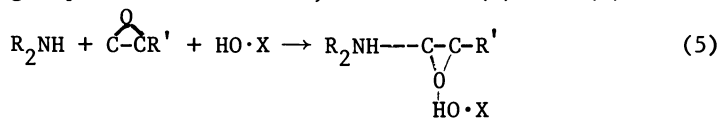
In this system, hydroxyl groups in the solvent accelerate the
epoxy ring opening by hydrogen bonding to the epoxy group during
transition.

Smith (10) proposed a variation of this mechanism. He
suggests that a hydrogen bond forms between the acid and the oxy-
gen on the epoxide ring followed by a three molecule transition
state which is rate determining, reactions (1a), (1b) and (1c),
Figure 1.

$$C\text{-}CR' + HX \rightleftharpoons R'C\text{-}C \qquad (1a)$$

$$R_2NH + R'C\text{-}C \rightleftharpoons \left[\begin{array}{c}R_2NH\\C\text{-}CR'\\HX\end{array}\right] \qquad (1b)$$

$$\left[\begin{array}{c} R_2NH \\ C-CR' \\ \diagdown O \diagup \\ HX \end{array}\right] \xrightarrow{\text{slow}} \begin{array}{c} R_2NH \\ C-CR' \\ O-HX \end{array} \xrightarrow{\text{fast}} \begin{array}{c} R_2N \\ C-CR' \\ OH \end{array} + HX \qquad (1c)$$
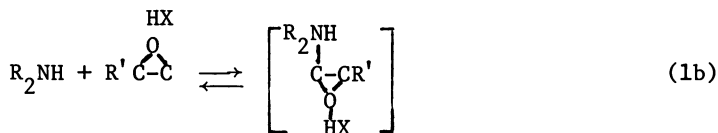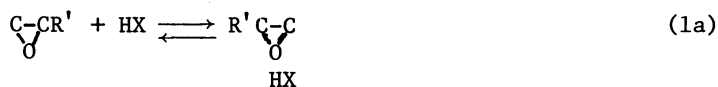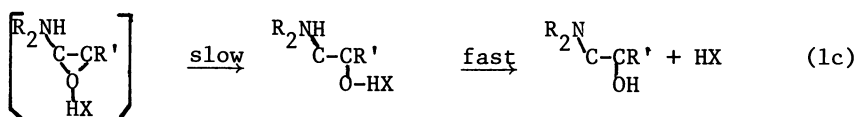
Figure 1.

More recently Mika and Tanaka (12) suggested a mechanism based on the hydrogen bonding of amine to a hydrogen donor, reactions (2a), (2b) and (2c).

$$R_2NH + HX \rightleftharpoons [R_2NH \cdots HX] \qquad (2a)$$

$$[R_2NH \cdots HX] + \underset{O}{C-CR'} \rightleftharpoons \left[\begin{array}{c} R_2NH \cdots C-CR' \\ XH \cdots O \end{array}\right] \qquad (2b)$$

$$\left[\begin{array}{c} R_2NH \cdots C-CR' \\ XH \cdots O \end{array}\right] \longrightarrow R_2N-C-CR' + HX \qquad (2c)$$
$$ OH$$
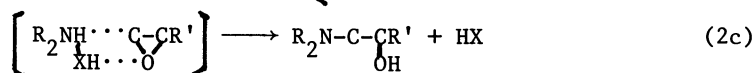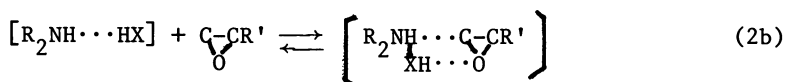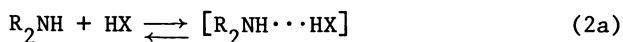
Figure 2.

This system is supported by the work of Iwakura et al (8) who studied the reaction of amines and epoxide in acrylonitrile-glycidyl methacrylate copolymers. An accelerating effect by formed hydroxyl groups was noted but the cyano group, which should retard activity, by the hypothesis of Smith, acted as an accelerator by its interaction with amine. Harrod (13) observed hydrogen bonding in epoxy-amine systems with both nitrogen and oxygen. Equilibrium hydrogen bonding would be more favorable between hydroxyl and amine groups than epoxy and hydroxyls due to the difference in basicity. It was also found that epoxy reacted more readily when the added water was equal to amine.

Mika and Tanaka also suggested that if reaction (10) occurs, then the retardation effect caused by maleic and phthalic acids, ketones and esters may be attributed to formation of imides, ketimines and amides. The inhibition caused by dioxane, tetrahydrofuran and diisopropyl ethers may be attributed to the fact that the ($R_2NH \cdots HX$) reacts with ethers to yield a complex, thereby preventing the epoxides from reacting. This would be expected because the four, five and six member rings are better hydrogen donors than three component epoxy rings.

This report compares the three mechanisms in light of data collected for an Epon 828/diaminobutane epoxy system. It also studies the effect of low molecular weight hydroxyl groups on the mechanisms and rate of reaction.

Experimental

Materials. The diglycidyl ether of bisphenol A, DGEBA, (Epon 828) (Registered trademark of Shell Chemical Co.), having the structure shown in Structure 1 (n $\doteq$ 0.2) was used in all tests.

$$CH_2\text{-}CH\text{-}CH_2\text{-}\left[O\text{-}\phi\text{-}\overset{\overset{CH_3}{|}}{\underset{\underset{CH_3}{|}}{C}}\text{-}\phi\text{-}O\text{-}CH_2\text{-}\overset{\overset{OH}{|}}{CH}\text{-}CH_2\right]_n \quad \text{-}O\text{-}\phi\text{-}\overset{\overset{OH_3}{|}}{\underset{\underset{CH_3}{|}}{C}}\text{-}\phi\text{-}O\text{-}CH_2\text{-}CH\text{-}CH_2$$
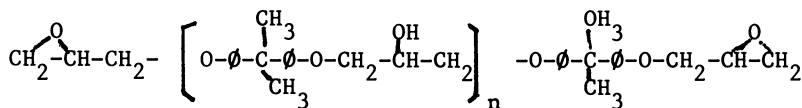
Structure 1

The resin was placed in a vacuum of 30 in Hg for two hours, then sealed in a nitrogen atmosphere. Resin with a higher hydroxyl content was prepared in a similar manner except before sealing the bottle, isopropyl alcohol (Reagent, Lehigh Valley Chemical) was added. Characterization of these materials by a modified procedure of Knoll et al (14) gave the epoxide content, Table I. Hydroxyl content was calculated from the structural formula. These epoxy values were used to determine the stoichiometric ratios of curing agent.

1-4, Diaminobutane, DAB (Aldrich), Di-n-Butylamine, DBA (Aldrich), and Tri-n-Butylamine, TBA (Eastman Organic Chemicals), were used as curing agents. Each was distilled under Helium at one atmosphere and sealed. The amine analysis of Critchfield and Johnson (15)was conducted to determine purity, Table I. The purity and the theoretical equivalence were used to determine the weight of amine needed for a given weight of resin.

Curing Process. Two to five grams of resin were weighed into a 10 milliliter beaker. The appropriate amount of amine was added and mixed thoroughly by stirring with a spatula for 30 seconds. This mixture was placed in several 1 cc syringes which served as batch reactors during the cure.

Every half hour, 0.5 to 1.0 milliliter of sample was added to a reagent solution for analysis. All reagent solutions used stopped the cure almost immediately. The syringe was weighed before and after the addition to obtain the exact sample weight.

For these studies it was desirable to maintain a constant temperature of about 22° C (room temperature). Since the amine-epoxy polymerization is an exothermic process, the syringes must have sufficient surface area to dissipate the evolved heat rapidly. Tests with Leeds and Northrup Potentiometer and a small alumel-chromel thermocouple, inserted into the center of the syringe, showed a maximum temperature rise of less than 2° C during the entire reaction time. This was sufficiently small to assume that isothermal conditions were maintained.

Analytical Methods. The analytical methods utilized for this paper were a combined epoxy-amine analysis as described by Bell (16) and a spectrophotometric determination for primary and secondary amines based on work by Toome and Manhart (17).

Pyridinium Chloride Analysis. The pyridinium method of analysis was developed by Bell (16) based on methods described

Table I - Starting Materials

Resin	Epoxy meq/g - sample	Hydroxyl meq/g - sample
Epon 822 Resin	5.16	0.52
Prepared Resin I	4.65	2.12
Prepared Resin II	4.10	3.82
Prepared Resin III	2.92	6.72

Curing Agent	Purity
1,4-Diamino butane (DAB) $H_2N-(CH_2)4-NH_2$	97%
Di-n-butylamine (DBA) $(CH_3CH_2CH_2CH_2)_2NH$	99%
Tri-n-butylamine (TBA) $(CH_3CH_2CH_2CH_2)_3N$	98.6%

by Knoll et al (14) and Critchfield and Johnson (15). Epoxy
first reacts with excess pyridinium chloride in the reagent solu-
tion, the remaining pyridinium chloride is titrated with 0.5N
NaOH to a pH endpoint of about 11.0. The difference between a
blank run and this first endpoint is the epoxy equivalent present.
Carbon disulfide is added; this reacts with primary and secondary
amine hydrogens to form their corresponding thiocarbamic acids.
The acid is then titrated with 0.5N NaOH to a pH endpoint of
around 10.0. The difference between the first and second end-
point is the amount of primary and secondary amine.

Spectrophotometric Analysis. Florescamine (Fluram*, Roche
Diagnostics) is a nonfluorescent compound that reacts with pri-
mary and secondary amines to form fluorescent compounds. It has
been used chiefly in the spectrophotometric investigation and
assays of biological compounds. This investigation utilized the
compound to determine concentrations of primary and secondary
amines.

Excess Fluram reacts with primary and secondary amine
forming structures that have absorptions of 375 – 410 and 310 –
320 nm, respectively. The remaining Fluram is hydrolyzed by
water. The procedure developed was based on work done by Toome
and Manhart (17).

The change in primary and secondary amine concentrations
versus time is shown in Figure 3. The system used is Epon 828
and DAB. Both curves are accurate when compared with primary
and secondary amine points obtained by another method (16).

The secondary amine peak was found to disappear at 2.0 hours.
This is explainable by the large size of the Fluram molecule. At
90 minutes tertiary amine production is initiated; this is where
branching of the molecule most likely starts. When 2 hours is
reached, a highly branched molecule is present. At this point
the secondary amines are probably too sterically hindered to
allow the large planar Fluram molecule to react. The primary
amine is still available because it is a dangling end, exposed
to the reagent solution.

Results

A set of material balances were developed to determine the
concentrations of various reactive groups based on data collec-
ted by the method of Bell (16). These material balances assume
that any side reactions are negligible.

A_0 – initial primary amine concentration
A   –primary amine concentration
B_0 – initial epoxy concentration
B   – epoxy concentration
R_0 – initial secondary amine concentration
R   – secondary amine concentration
S_0 – initial tertiary amine concentration
S   – tertiary amine concentration
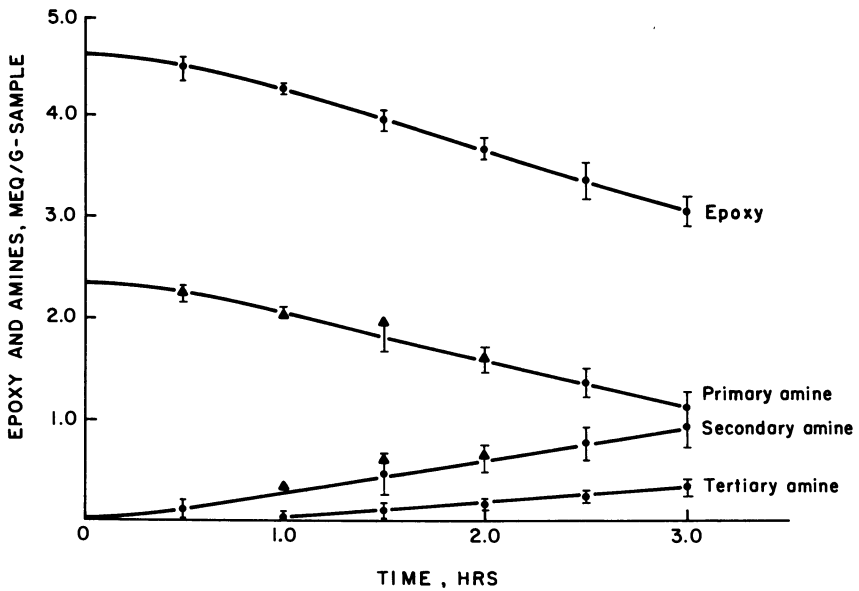
Figure 3.   Change in epoxy and primary, secondary, and tertiary amines vs. time: (⦚) method of Bell (16), calculated with 95% confidence limits, compared to (▲) spectrophotometric method (1.0:1.0 epoxy to amine stoichiometry)

Given: A_O, B_O and $R_O = S_O = 0.0$
Data collected: B, (A + R)
It follows that:

$$S = A_O - (A + R) \tag{7}$$

$$0.0 = (B - B_O) + (R - R_O) + 2.0(S - S_O) \tag{8}$$

$$A = R - (A + R) \tag{9}$$

This data alone is sufficient to determine all reactive groups present, that is, epoxy, hydroxyl and primary, secondary and tertiary amines, provided no significant reactions take place other than between the amino hydrogens and epoxy resin, reactions (1) and (2).

To date, investigations have supported this absence of side reactions (1,6,18,19) with some special exceptions; low amine concentrations (20,21) less than a 1.0:1.0 amine:epoxy stoichiometry, yield etherification, reaction (3). High curing temperature has had the same effect (6).

Since the stoichiometry of epoxy to amine is not less than 1.0:1.0 and the cure proceeds at a low temperature, one would predict that only reactions (1) and (2) would take place. To test this assumption for the DAB-DGEBA system, several identical runs were analyzed by the method of Bell (16). Utilizing the material balances found above (which assume no side reactions), the various reactive groups were determined and averaged with 95% confidence limits. A similar run using the spectro-photometric method gave the amounts of primary and secondary amines separately. This yields a calculated and actual concentration of primary and secondary amines. Provided there are no side reactions, the two values should be identical. The results were plotted in Figure 3 and found to fall on the same curve, within experimental error. This verifies the assumption that only reactions (1) and (2) need be considered.

DBA and TBA, a secondary and tertiary amine respectively, when used as curing agents at 1.0:1.0 stoichiometries, showed no noticeable reaction with Epon 828 over a period of five hours. After two days, however, the DBA-resin mixture turned into a clear glassy solid. Hydroxyl groups were calculated from the structure of epoxy given in Structure 1 with n = 0.2. For each epoxy consumed one hydroxyl was produced.

OH - hydroxyl concentration

OH_a - added hydroxyl concentration (isopropyl alcohol)

$$OH = 0.1 (B) + OH_a + (B_O - B) \tag{10}$$

Original data and calculated values used in the development of this paper appear in Tables II through VII.

Table II – Data for 1.0:1.0 epoxy amine stoichiometry. Initial hydroxyl concentration = 0.46 meq/g-sample

	Experimental Data		Calculated Data			
Time	Epoxy (meq/g)	Primary and Secondary amine (meq/g)	Hydroxyl (meq/g)	Primary amine (meq/g)	Secondary amine (meq/g)	Tertiary amine (meq/g)
0	4.62	2.30	0.46	2.30	0.0	0.0
30	4.41	2.30	0.67	2.09	0.21	0.0
60	4.15	2.31	0.93	1.83	0.47	0.0
90	3.96	2.29	1.12	1.67	0.64	0.01
120	3.70	2.21	1.38	1.47	0.74	0.09
150	3.41	2.09	1.67	1.30	0.79	0.21
180	3.24	2.01	1.84	1.21	0.80	0.29

Table III – Data for 1.0:2.0 epoxy-amine stoichiometry. Initial hydroxyl concentration = 0.42 meq/g sample

	Experimental Data		Calculated Data			
Time	Epoxy (meq/g)	Primary and Secondary amine (meq/g)	Hydroxyl (meq/g)	Primary amine (meq/g)	Secondary amine (meq/g)	Tertiary amine (meq/g)
0	4.17	4.21	0.42	4.21	0.0	0.0
30	3.81	4.22	0.78	3.84	0.38	0.0
60	3.33	4.21	1.26	3.37	0.84	0.0
90	2.95	4.19	1.64	3.01	1.18	0.02
120	2.52	4.09	2.07	2.68	1.41	0.12
150	2.02	3.88	2.57	2.39	1.49	0.33
180	1.73	3.73	2.86	2.25	1.48	0.48

Table IV – Data for 1.0:3.0 epoxy–amine stoichiometry. Initial hydroxyl concentration = 0.38 meq/g sample

	Experimental Data		Calculated Data			
Time	Epoxy (meq/g)	Primary and Secondary amine (meq/g)	Hydroxyl (meq/g)	Primary amine (meq/g)	Secondary amine (meq/g)	Tertiary amine (meq/g)
0	3.82	5.71	0.38	5.71	0.0	0.0
30	3.35	5.71	0.85	5.24	0.47	0.0
60	2.67	5.71	1.53	4.56	1.15	0.0
90	2.12	5.71	2.08	4.01	1.70	0.0
120	1.59	5.61	2.61	3.56	2.05	0.10
150	0.90	-	3.30	-	-	-
180	0.54	5.04	3.66	3.10	1.94	0.67

Table V - Data for 1.0:1.0 epoxy-amine stoichiometry. Initial hydroxyl concentration = 1.91 meq/g sample

	Experimental Data		Calculated Data			
Time	Epoxy (meq/g)	Primary and Secondary amine (meq/g)	Hydroxyl (meq/g)	Primary amine (meq/g)	Secondary amine (meq/g)	Tertiary amine (meq/g)
0	4.20	2.12	1.91	2.12	0.0	0.0
30	3.62	2.00	2.49	1.66	0.34	0.12
60	3.24	1.97	2.87	1.31	0.66	0.15
90	2.84	1.83	3.27	1.05	0.78	0.29
120	2.61	1.83	3.50	0.82	1.01	0.29
150	2.36	1.75	3.75	0.65	1.10	0.37

Table VI – Data for 1.0:1.0 epoxy–amine stoichiometry. Initial hydroxyl concentration = 3.50 meq/g sample

Time	Experimental Data		Calculated Data			
	Epoxy (meq/g)	Primary and Secondary amine (meq/g)	Hydroxyl (meq/g)	Primary amine (meq/g)	Secondary amine (meq/g)	Tertiary amine (meq/g)
0	3.76	1.85	3.50	1.85	0.0	0.0
30	3.11	1.80	4.53	1.25	0.55	0.05
60	2.81	1.66	4.83	1.09	0.57	0.19
90	2.43	1.59	5.21	0.78	0.81	0.26
120	2.16	1.56	5.48	0.54	1.02	0.29
150	–	–	–	–	–	–
180	1.71	1.32	5.93	0.33	0.99	0.53

Table VII – Data for 1.0:1.0 epoxy-amine stoichiometry. Initial hydroxyl concentration = 7.08 meq/g sample

| Time | Experimental Data | | Calculated Data | | | |
---	Epoxy (meq/g)	Primary and Secondary amine (meq/g)	Hydroxyl (meq/g)	Primary amine (meq/g)	Secondary amine (meq/g)	Tertiary amine (meq/g)
0	2.74	1.33	7.08	1.33	0.0	0.0
30	-	-	-	-	-	-
60	1.80	1.21	8.29	0.51	0.70	0.12
90	1.49	1.07	8.60	0.34	0.73	0.26
120	1.33	0.86	8.76	0.39	0.47	0.47
150	1.17	0.73	8.92	0.36	0.37	0.60
180	-	-	-	-	-	-

Figures 4, 5, and 6 show the concentration of various re-
actants as a function of time for varying stoichiometries. In
all three cases, the epoxy drop seems relatively linear through-
out the test period and shows an increasing rate of consumption
as the stoichiometric amount of amine increases. Tertiary amine
formation is not apparent until 1.5 hours of reaction for all
amine concentrations.

Figures 7, 8, and 9 demonstrate the effect of increased
hydroxyl concentration (by adding isopropyl alcohol) on the rate
of production or consumption of the various reactive groups. The
rate of epoxy drop is no longer constant in contrast with the
earlier situation when no alcohol was added, but varies with time.
The production of tertiary amine is immediate in all cases where
hydroxyl groups were added; this is also in contrast to the
earlier case.

Discussion

The Effect of Hydroxyl Concentration on Epoxy-Amine Reactions.
Prior work completed with polyamine-epoxy systems has indicated
a second order rate law, supporting the S_n2 mechanism for nucleo-
philic attack on the epoxy ring. (8,10,22,23) Figure 10 is the
result of an initial rate analysis, described by Levinspiel, (24)
of the present epoxy resins containing low molecular weight hy-
droxyls, Resins I, II, III, Table I. The graph demonstrates a
possible second order reaction. This is in contrast, however, to
the apparent zero order dependence of the epoxy reaction shown in
Figures 4, 5 and 6. To be valid, any model must be able to re-
solve this difference in order.

The mechanisms of Smith (10) and Mika and Tanaka (12),
although differing, both contain an intermediate complex, Struc-
tures 2 and 3:

$$\left[\begin{array}{c} R_2NH \\ C-CR' \\ O \\ HX \end{array} \right] \qquad \left[R_2NH\cdots C-CR' \\ XH\cdots O \right]$$
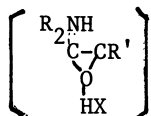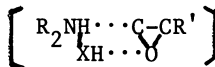
Structure 2   Structure 3
    Smith   Mika and Tanaka

It can be seen by examination of the two mechanisms, Figures 1
and 2, that if the hydroxyl groups, when complexing to form their
intermediates, Structures 4 and 5, in equations (1a) and (2a),
are sterically hindered (thereby being less reactive) causing a
slow rate of epoxy consumption, a small amount of intermediate
is formed.
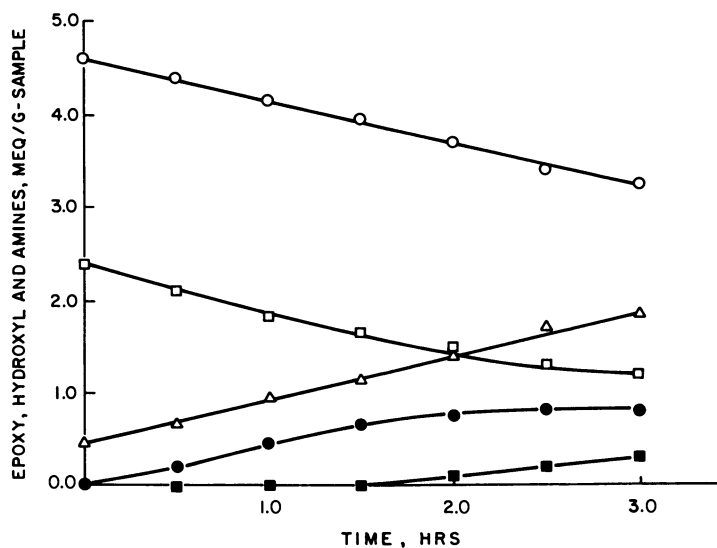
Figure 4.   Change in primary, secondary, and tertiary amines, epoxy, and hydroxyl groups vs. time for 1.0:1.0 stoichiometry (initial hydroxyl concentration = 0.46 meq/g-sample) (○) epoxy; (□) primary amine; (△) hydroxyl groups; (●) secondary amine; (■) tertiary amine
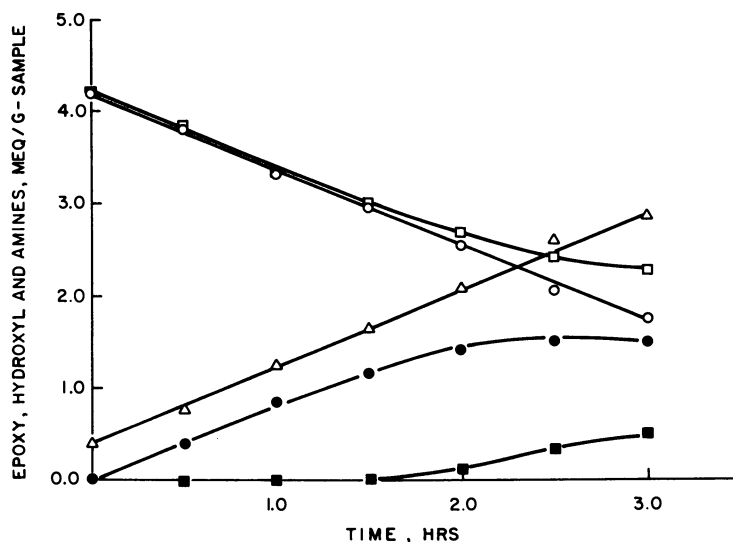
Figure 5.   Change in primary, secondary, and tertiary amines, epoxy, and hydroxyl groups vs. time for 1:2 stoichiometry (initial hydroxyl concentration = 0.42 meq/g-sample) (○) epoxy; (□) primary amine; (△) hydroxyl groups; (●) secondary amine; (■) tertiary amine
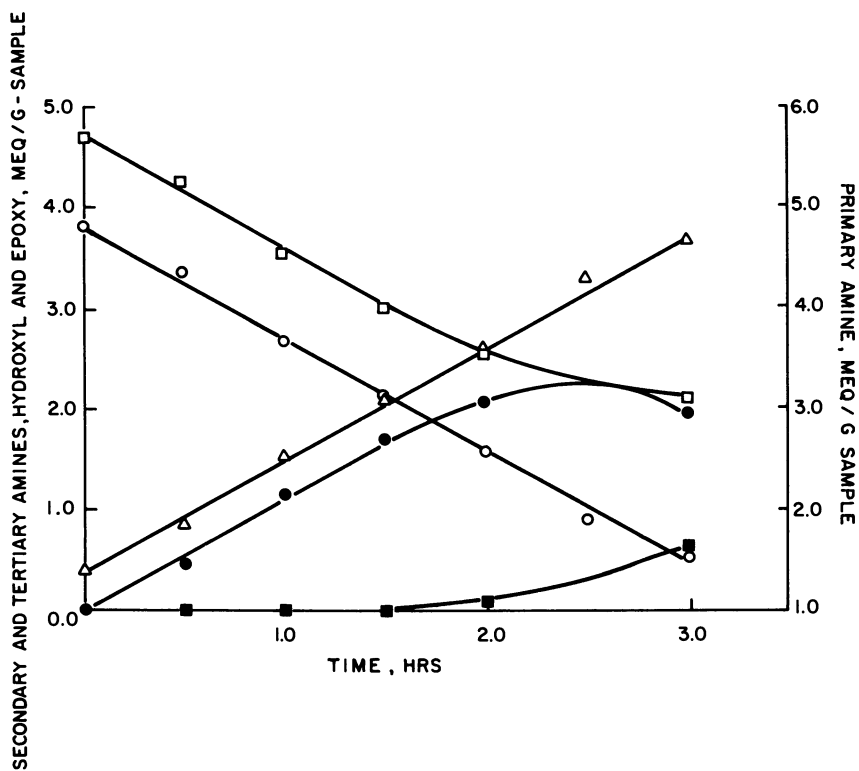
Figure 6. Change in primary, secondary, and tertiary amines, epoxy, and hydroxyl groups vs. time for 1.0:3.0 stoichiometry (initial hydroxyl concentration = 0.38 meq/g-sample) (○) epoxy; (□) primary amine; (△) hydroxyl groups; (●) secondary amine; (■) tertiary amine
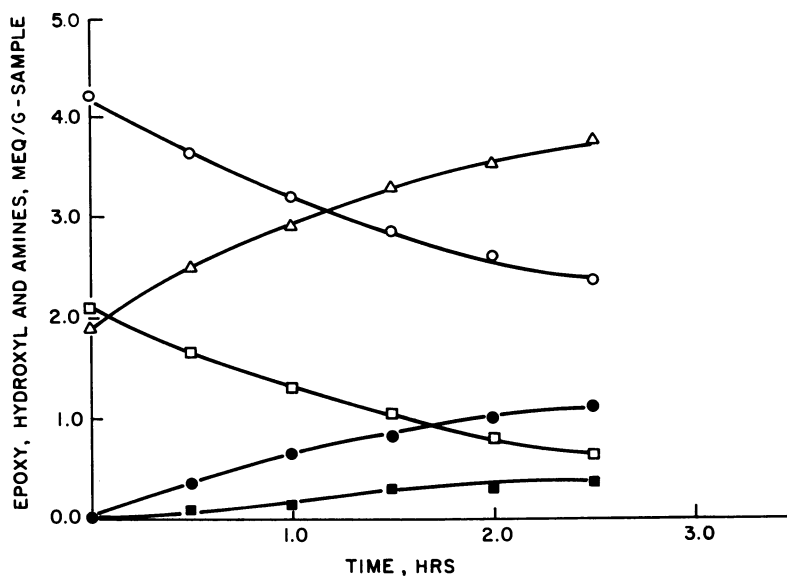
Figure 7.   Change in primary, secondary, and tertiary amines, epoxy, and hydroxyl groups vs. times for 1.0:1.0 stoichiometry (initial hydroxyl concentration = 1.91 meq/g-sample) (■) tertiary amine; (○) epoxy; (□) primary amine; (△) hydroxyl groups; (●) secondary amine
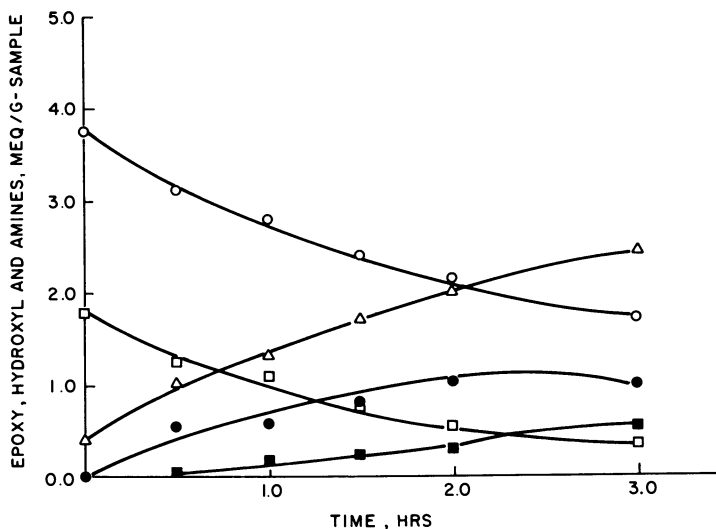
Figure 8. Change in primary, secondary, and tertiary amines, epoxy, and hydroxyl groups vs. time for 1.0:1.0 stoichiometry (initial hydroxyl concentration = 3.50 meq/g-sample) (○) epoxy; (□) primary amine; (△) hydroxyl groups; (●) secondary amine; (■) tertiary amine
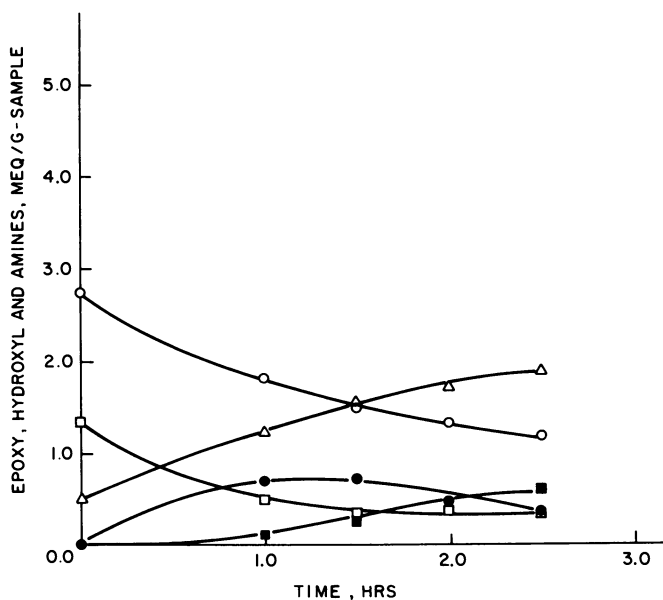
Figure 9. Change in primary, secondary, and tertiary amines, epoxy, and hydroxyl groups vs. time for 1.0:1.0 stoichiometry (initial hydroxyl concentration = 7.08 meq/g-sample) (○) epoxy; (□) primary amine; (△) hydroxyl groups; (●) secondary amine; (■) tertiary amine
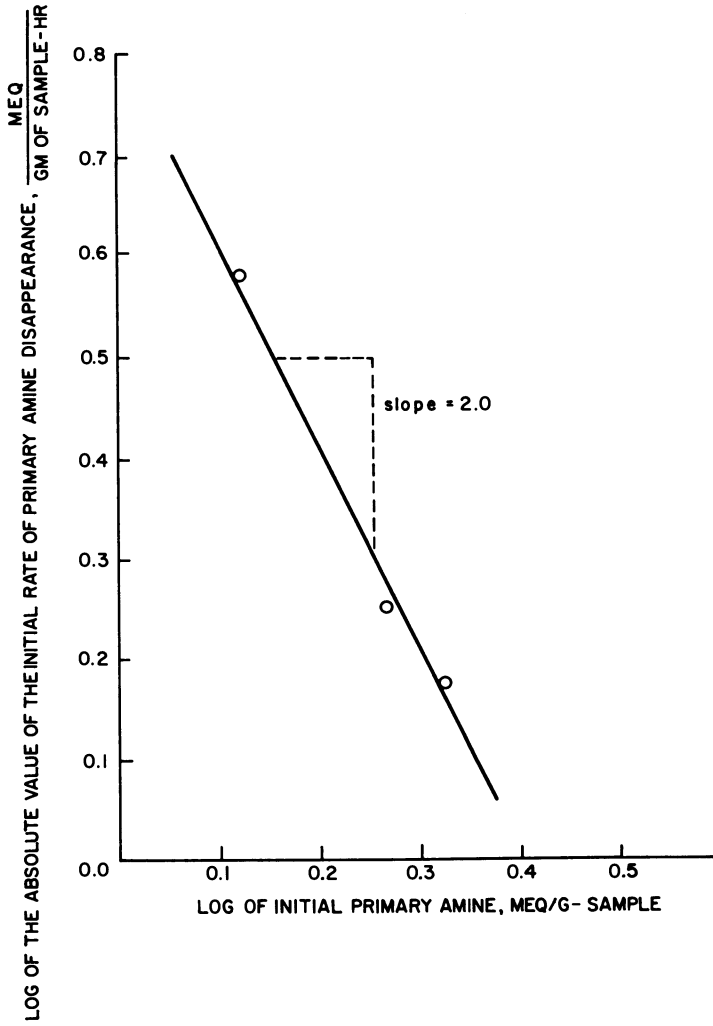
Figure 10. Log of the initial rate of consumption of primary amine vs. the log of the initial primary amine concentration to determine the reaction order

$$\left[\begin{array}{c} R'\overset{}{\underset{O}{C}}-\overset{}{\underset{HX}{C}} \end{array} \right]$$

Structure 4
Smith

$$\left[\begin{array}{c} R_2NH\cdots HX \end{array} \right]$$
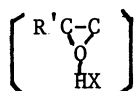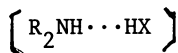
Structure 5
Mika and Tanaka

An equilibrium is set up in equations (1b) and (2b) and the zero order behavior observed for the epoxy consumption may be attributed to the slow breakdown and low concentration of the ternary intermediate, Structures 2 and 3. On the other hand, if the hydroxyls are more reactive, equilibrium formation of the intermediates, Structures 4 and 5 will be far to the right and equations (1a) and (2a) may be neglected. It may also be assumed that when the hydroxyls are much more tightly bound to the amine or epoxy, shifting equations (1b) and (2b) to the left, then the association of hydroxyl complexes with epoxy or amine, equations (1b) and (2b), tend to control the rate of reaction and not the breakdown of ternary complex, equations (1c) and (2c). This would cause an apparent second order reaction.

Figure 11 represents the fractional epoxy drop for the data shown in Figures 4, 5 and 6. It may be noted that as the stoichiometric amounts of amine increase by factors of two and three, the slopes of the corresponding lines increase by the same factor. Figures 12 and 13 are plots of the fractional drops of primary amine and production of tertiary amine, respectively. A single curve may be drawn through the data for the different stoichiometries.

Taking the value of epoxy present as one, it can be observed in the model of Mika and Tanaka, (12) that as the amine concentration is increased by factors of two and three, the intermediate present, Structure 5, increases by that factor thereby increasing the consumption of epoxy by the same factor. When the amine is taken as one, then the epoxy is reduced by factors of a half and a third. Assuming that the concentration of Structure 5 is low, due to the low reactivity of the hydroxyls, then the consumption of amine would remain constant due to the large excess of epoxy ready to react. The same line of reasoning may be used to explain the mechanism of Smith (10). When the epoxy is one, then the equilibrium established in equation (1a) is constant and as the amine is increased by factors of two and three, the disappearance of epoxy is accelerated by the same factor. If the amine is unity and the equilibrium in equation (1a) produces a sufficient amount of intermediate, Structure 4, to react with the amine then the rates of amine consumption in equation (1b) could be the same for lower epoxy concentrations. This line of reasoning also supports the model of Smith (10). Figures 14 and 15 summarize the possible effects of hydroxyl groups on the two mechanisms.
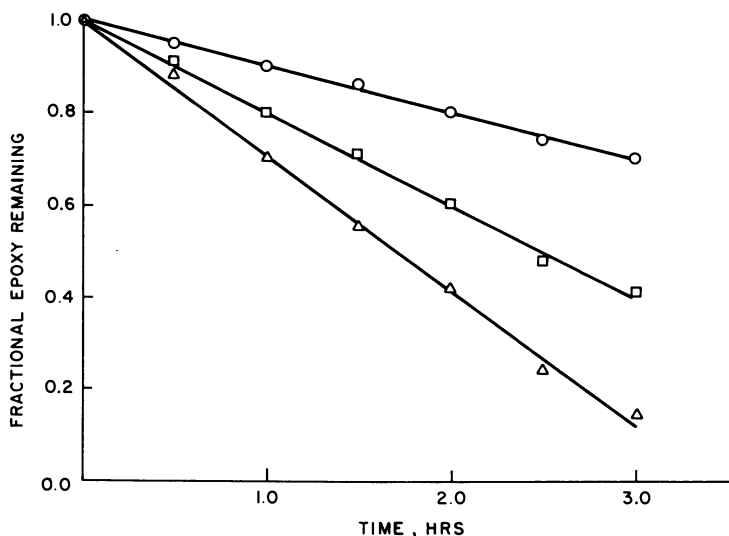
Figure 11. Effect of initial epoxy: amine stoichiometries on the fractional consumption of epoxy (○) 1.0:1.0, epoxy:amine; (□) 1.0:2.0, epoxy:amine; (△) 1.0:3.0, epoxy:amine
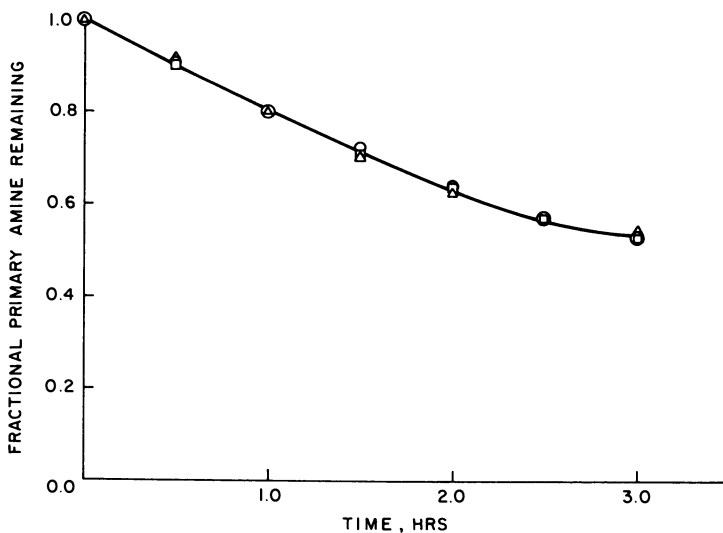
Figure 12. Effect of initial epoxy:amine stoichiometries on the fractional consumption of primary amines (○) 1.0:1.0, epoxy:amine; (□) 1.0:2,0, epoxy:amine; (△) 1.0:3.0, epoxy:amine
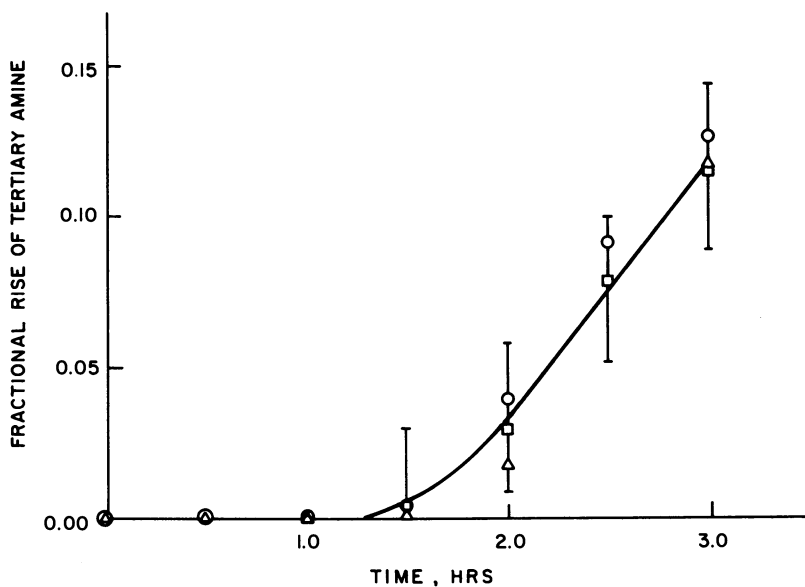
Figure 13. *Effect of initial epoxy:amine stoichiometries on the fractional rise of tertiary amine. Total conversion to tertiary amine is 1.0. (○) 1.0:1.0, epoxy:amine; (□) 1.0:2.0, epoxy:amine; (△) 1.0:3.0, epoxy:amine*

Slightly reactive hydroxyl groups:

$$R_2NH + HX \rightleftharpoons [R_2NH\cdots HX]$$

$$[R_2NH\cdots HX] + C-CR_1 \xrightarrow{\text{fast}} \left[\begin{matrix}R_2NH\cdots C-CR_1 \\ XH\cdots O\end{matrix}\right]$$

$$\left[\begin{matrix}R_2NH\cdots C-CR_1 \\ XH\cdots O\end{matrix}\right] \xrightarrow{\text{slow}} R_2N-C-CR_1 + HX \\ OH$$

Highly reactive hydroxyl groups:

$$R_2NH\cdots HX + C-CR_1 \xrightarrow{\text{slow}} \left[\begin{matrix}R_2NH\cdots C-CR_1 \\ XH\cdots O\end{matrix}\right]$$

$$\left[\begin{matrix}R_2NH\cdots C-CR_1 \\ XH\cdots O\end{matrix}\right] \xrightarrow{\text{fast}} R_2N-C-CR_1 + HX \\ OH$$
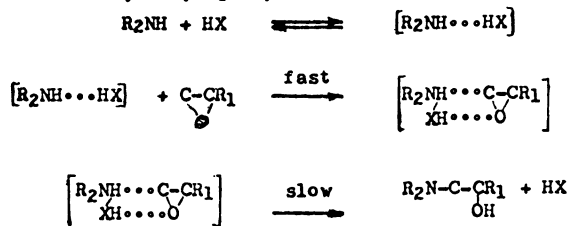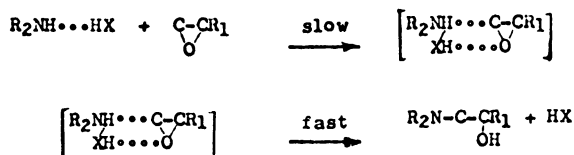
Figure 14. Possible effect of hydroxyl groups on the mechanism of Mika and Tanaka

Slightly reactive hydroxyl groups:

$$C-CR_1 + HX \rightleftharpoons R_1 C-C \\ O \\ HX$$

$$R_2NH + R_1 C-C \xrightarrow{\text{fast}} \left[\begin{matrix}R_2NH \\ C-CR_1 \\ O \\ HX\end{matrix}\right]$$

$$\left[\begin{matrix}R_2NH \\ C-CR_1 \\ HX\end{matrix}\right] \xrightarrow{\text{slow}} R_2NH \\ C-CR_1 \\ OHX \xrightarrow{} R_2N \\ C-CR_1 + HX \\ OH$$

Highly reactive hydroxyl groups:

$$R_2NH + RC-C \xrightarrow{\text{slow}} \left[\begin{matrix}R_2NH \\ C-CR \\ O \\ HX\end{matrix}\right]$$

$$\left[\begin{matrix}R_2NH \\ C-CR \\ O \\ HX\end{matrix}\right] \xrightarrow{\text{fast}} R_2N \\ C-CR + HX \\ OH$$
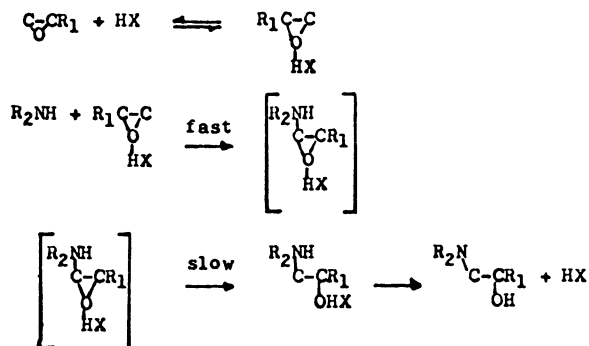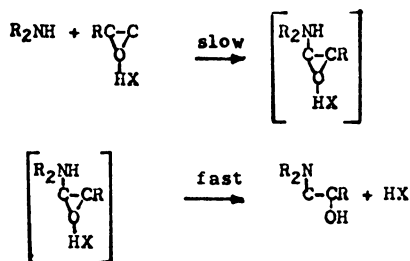
Figure 15. Possible effect of hydroxyl groups on the mechanism of Smith

The Effect of pK$_a$ Values on the Reaction of Amines with Epoxy.
According to Mika and Tanaka (12), an acid-amine equilibrium is
first established, equation (2a). This would require two equi-
libria to be present for the reaction of primary amine, one for
the primary and the other with the formed secondary, reactions
(11) and (12).

$$R-NH_2 + HX \rightleftharpoons (RNH_2 \cdots HX) \tag{11}$$

$$R_2NH + HX \rightleftharpoons (R_2NH \cdots HX) \tag{12}$$
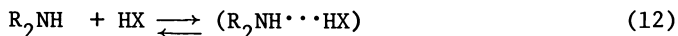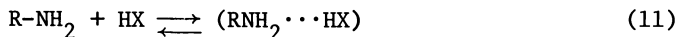
Such an association would depend on many factors, including the
relative ease of removal of the amine hydrogen, i.e., basicity.
This ability may be related to the pK$_a$ values of the amine. DAB
consists of two primary amine groups separated by four carbons.
It has been found that these two amines have differing pK$_a$
values (25) of 11.15 and 9.71. Such values would be interpreted
to mean that the first primary amine could react more quickly
than the remaining one. Damusis (26) found that the reaction of
two to six carbon, aliphatic diamines is rapid for the first
amino group, but the reaction of the second primary group is not
detectable, being achieved only by catalytic action. It is also
indicated (25) that aliphatic secondary amines have a pK$_a$ value
of around 10.7, falling between the values of the two primary
groups.

    If the hydroxyl groups present are not very reactive, as in
the high molecular weight resins, then it would be assumed that
the first group on the diamine would react first, followed by
the secondary amine and the second primary amine group.

    Figure 12 shows a leveling out of the primary amine concen-
tration at 50%, suggesting that later in the reaction the pri-
mary does not react as quickly as the secondary. Figure 16 is
a plot of the percent of tertiary amine produced versus primary
amine consumed. As can be seen, only primary amine reacts until
about 30% consumption then tertiary amine is produced. At about
50% primary amine remaining, the rate of secondary amine reacting
is twice that of primary. This would tend to indicate a three-
step reaction which could be described by a two-step primary and
a secondary reaction.

    The secondary-alcohol amine has been found to be more re-
active due to the hydroxyl group (8). Laird and Parker (27)
have suggested and presented evidence that the hydroxyl group
has an intermolecular "self-solvating" effect; a similar state-
ment was made by Allen and Hunter (28). A hypothetical inter-
mediate being formed between the secondary-alcohol amine and
epoxy is presented in Structure 6.
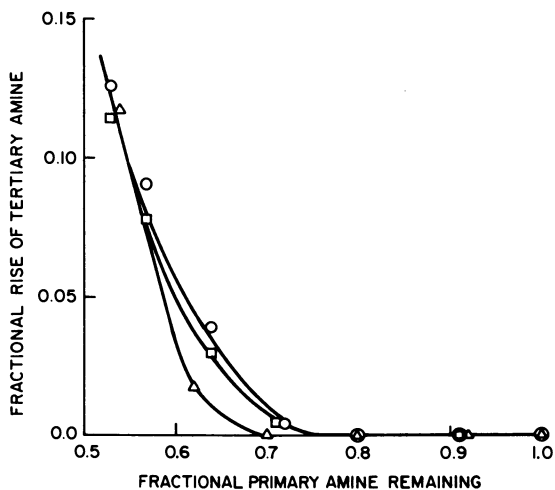
Figure 16.   Primary vs. tertiary amine, fractional changes for varying stoichiometries (○) 1.0:1.0, epoxy:amine; (□) 1.0:2.0, epoxy:amine; (△) 1.0:3.0, epoxy:amine
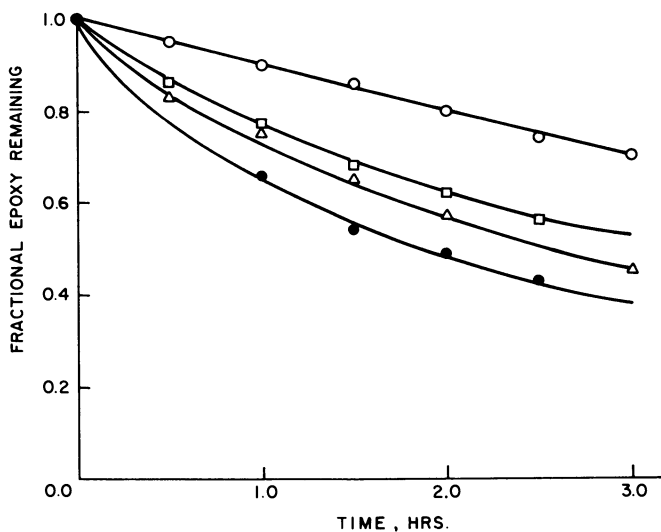
Figure 17.   Effect of initial hydroxyl concentration on the fractional drop of epoxy for a 1.0:1.0 stoichiometry (○) intial hydroxyl = 0.46 meq/g-sample; (□) initial hydroxyl = 1.91 meq/g-sample; (△) initial hydroxyl = 3.50 meq/g-sample; (●) initial hydroxyl = 7.08 meq/g-sample

$$\begin{array}{c} CH_2 \longrightarrow CHR \\ \diagdown O \diagup \\ RNH \diagup \diagdown H \\ CH_2 \quad O \\ \diagdown CH \\ R \end{array}$$
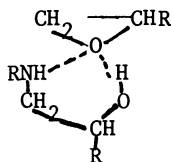
Structure 6

Further evidence of the probability of the Mika and Tanaka model (of hydroxyls complexing with amine) is an observation during experimentation. In Resin III, the isopropyl alcohol was not totally soluble; when the mix was homogenized it formed an emulsion. As amine was added, the mixture became miscible as evidenced by the almost immediate disappearance of turbidity.

Added low molecular weight hydroxyl groups accelerate the reaction between amines and epoxy as noted in Figure 17. This representation shows the fractional loss of epoxy for Epon 828 and Resin systems I, II and III, each of which has increasing hydroxyl concentrations, Table I. There is an obvious disappearance of linearity when one compares Epon 828 to systems I, II and III; this change is probably due to the more active added hydroxyls as opposed to the formed hydroxyls.

Figure 18 demonstrates the increased reactivity of the amine groups when in the presence of hydroxyls. It plots the change of primary to tertiary amines. Resins with high hydroxyl group concentrations are more reactive and show an immediate production of tertiary amine.

A relation was developed in Figure 19 for effect of the hydroxyl to epoxy ratio on the initial rate of reaction. As the hydroxyl concentration rises, the initial rate of reaction increases; this would probably hold true until dilution effects dominate. Similar relations have been developed by Bowen and Whiteside (29). It should be further noted that this curve represents isopropyl alcohol as the hydroxyl source. The slope would shift for other alcohols depending on their reactivity.

Kinetic Modeling Approaches. This section contains some possible approaches to modeling of the data and mechanisms proposed in this paper. It also includes recommendations for future work to analyze the validity of the suggested models. The cases presented take into account the zero order behavior at low hydroxyl concentrations (Case I) and the second order reaction observed at high hydroxyl concentrations in conjunction with the three step mechanism proposed previously (Case II).

Case I:

Case I examines the runs made with low initial concentrations of high molecular weight hydroxyls. This data is represented in Figures 4, 5 and 6.
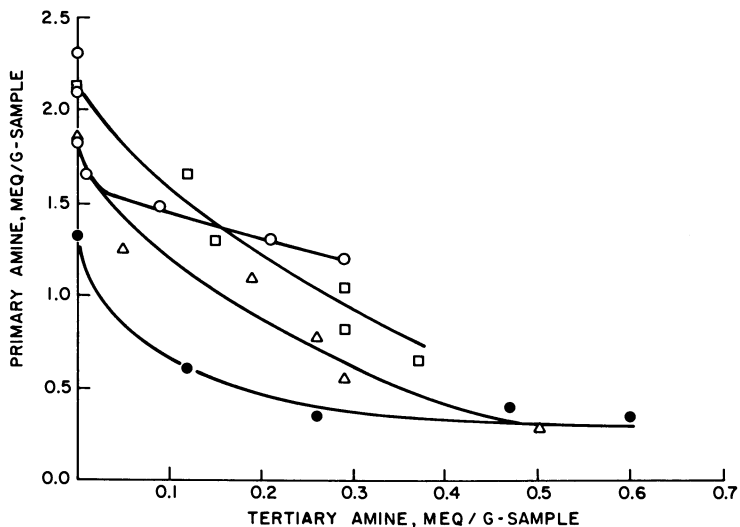
Figure 18. Effect of initial hydroxyl concentration on primary vs. tertiary amine for a 1.0:1.0 stoichiometry (○) hydroxyl = 0.46 meq/g-sample; (□) hydroxyl = 1.91 meq/g-sample; (△) hydroxyl = 3.50 meq/g-sample; (●) hydroxyl = 7.08 meq/g-sample
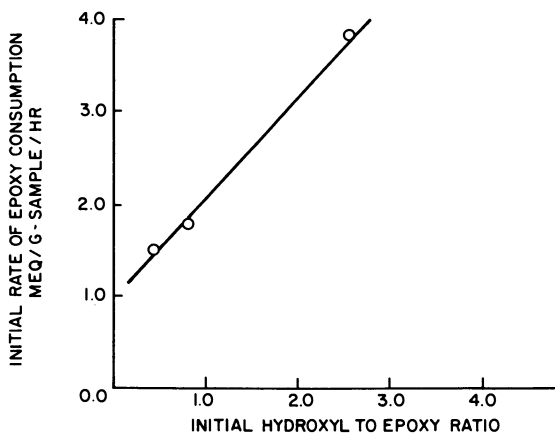
Figure 19. Initial hydroxyl to epoxy ratio vs. initial rate of epoxy consumption for a 1.0:1.0 stoichiometry

Figure 11 shows that the consumption of epoxy is apparently zero order. It also shows that as the amount of amine increases, the rate of epoxy consumption increases proportionally. This is in contrast to the normal zero order equation that states:

$$r_B = \frac{dB}{dt} = k \tag{13}$$

This equation has no provision for changes in stoichiometry. To explain this, one must take into account the complexing of hydroxyls with amine as shown in Figure 15. Assume:

1) hydroxyls only complex with amines
2) all amine–hydroxyl complexes are equally reactive with epoxies.

Initially only primary amines are present. An increase in the amount of amine will cause a proportional increase in the amount of hydroxyl intermediate formed:

$$A + H \underset{k_2}{\overset{k_1}{\rightleftharpoons}} A \cdot H \tag{14}$$

$$K = \frac{k_1}{k_2} = \frac{(A \cdot H)}{(A)\,(H)} \tag{15}$$

Increasing the amine, then, does not change the value of the equilibrium constant but does allow for a proportional increase in the amount of hydroxyl intermediate present, which in turn, is available to react with the epoxy. This would account for the paradoxial effect of the varying rates in Figure 11. Assume:

3) rate of reaction is dependent only on the breakdown of the ternary intermediate (zero order); all ternary complexes breakdown at the same rate
4) consumption of various reactive groups is dependent only upon their relative composition in the hydroxyl complex state.

Given: A = 1st primary amine
        B = 2nd primary amine
        C = secondary amine
        H = hydroxyl
        E = ternary complex
        D = epoxy
        F = tertiary amine

The first reaction is the hydroxyl complexing with amine:

$$A + H \underset{k_2}{\overset{k_1}{\rightleftharpoons}} A \cdot H \tag{16}$$

$$B + H \underset{k_2'}{\overset{k_1'}{\rightleftharpoons}} B \cdot H \tag{17}$$

$$C + H \underset{k_2''}{\overset{k_1''}{\rightleftharpoons}} C \cdot H \tag{18}$$

Assume:
  5) the complexing of epoxy with the hydroxyl complex is
      rapid.

$$A \cdot H + D \longrightarrow E_A \qquad\qquad (19)$$

$$B \cdot H + D \longrightarrow E_B \qquad\qquad (20)$$

$$C \cdot H + D \longrightarrow E_C \qquad\qquad (21)$$

$$E_x \longrightarrow products + 2H \qquad\qquad (22)$$
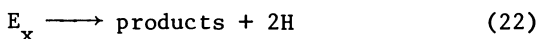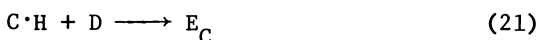
From the above assumptions the following model is proposed:
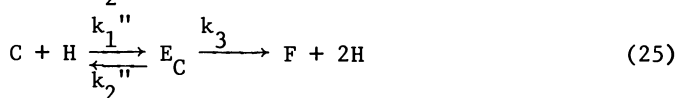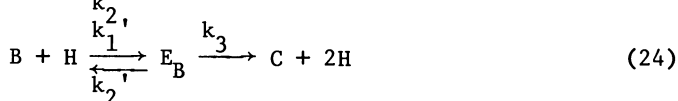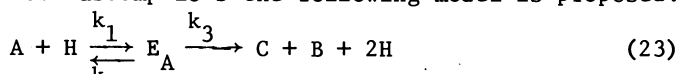
$$A + H \underset{k_2}{\overset{k_1}{\rightleftarrows}} E_A \overset{k_3}{\longrightarrow} C + B + 2H \qquad\qquad (23)$$

$$B + H \underset{k_2'}{\overset{k_1'}{\rightleftarrows}} E_B \overset{k_3}{\longrightarrow} C + 2H \qquad\qquad (24)$$

$$C + H \underset{k_2''}{\overset{k_1''}{\rightleftarrows}} E_C \overset{k_3}{\longrightarrow} F + 2H \qquad\qquad (25)$$

The disappearance of the various reactants may be described by
the following differential equations:

$$\frac{dA}{dt} = r_A = - k_1 (A)(H) + k_2 (E_A) \qquad\qquad (26)$$

$$\frac{dB}{dt} = r_B = - k_1' (B)(H) + k_2' (E_B) + k_3 (E_A) \qquad\qquad (27)$$

$$\frac{dC}{dt} = r_C = - k_1'' (C)(H) + k_2'' (E_C) + k_3 (E_A + E_B) \qquad (28)$$

The consumption of epoxy would equal the breakdown of E_x and be
described by the zero order reaction observed in Figure 11

$$\frac{dD}{dt} = -k_3 \qquad\qquad (29)$$

Therefore the slope of the 1.0:1.0 stoichiometric case would yield
the value of k_3. It is recommended that the k_1 and k_2 rate con-
stants be determined by equilibrium experiments done separately
with the use of IR to determine the extent of hydrogen bonding.
The use of IR for determination of E_A, E_B and E_C would be im-
possible in the reaction mixture since the absorption bands for
these three components would fall within the same area; an over-
all amount of hydrogen bonding may be calculated by IR. It

should be noted that hydroxyls need not only associate with
amines but may also bond with epoxies simultaneously.

Case II.

Case II examines the runs made with added low molecular
weight hydroxyls. The data is shown in Figures 7, 8 and 9.

Figure 15 shows the proposed sequence of reactions in the
presence of these low molecular weight hydroxyl groups. Based
on this and the following assumptions, a model may be proposed.
Assume:

    1) the formation of hydroxyl intermediate is rapid and

$$A = A \cdot H \tag{30}$$
$$B = B \cdot H \tag{31}$$
$$C = C \cdot H \tag{32}$$

    2) the breakdown of the ternary intermediate is rapid when
        compared to the formation.

From these assumptions the following mechanism may be proposed:
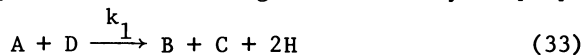
$$A + D \xrightarrow{k_1} B + C + 2H \tag{33}$$

$$B + D \xrightarrow{k_2} C + 2H \tag{34}$$

$$C + D \xrightarrow{k_3} F + 2H \tag{35}$$

The disappearance of the various reactants may be described by
the following differential equations:

$$\frac{dA}{dt} = r_A = -k_1 \, (A) \, (D) \tag{36}$$

$$\frac{dB}{dt} = r_B = k_1 \, (A) \, (D) - k_2 \, (B) \, (D) \tag{37}$$

$$\frac{dC}{dt} = r_C = k_1 \, (A) \, (D) + k_2 \, (B) \, (D) - k_3 \, (C) \, (D) \tag{38}$$

dividing the first two equations we obtain:

$$\frac{dB}{dA} = \frac{k_2}{k_1} \frac{(B)}{(A)} - 1 \tag{39}$$

When this is solved, using the initial and final concentrations
of A and B as limits, the following equation is obtained:

$$B = -\frac{A}{1-k'} + \left(B_o A_o^{-k'} + \frac{A_o^{1-k'}}{1-k'} \right) A^{k'} \tag{40}$$

This would then yield values for $k' = k_2/k_1$. When equation 3 is divided by equation 1, the following differential equation is obtained:

$$\frac{dC}{dA} = -1 - k' \frac{(B)}{(A)} + k'' \frac{(C)}{(A)} \qquad (41)$$

where $k'' = \frac{k_3}{k_1}$. Substituting equation (40) into (41)

$$\frac{dC}{dA} = -1 + \frac{k'}{1-k'} - k' (B_o A_o^{-k'} + \frac{A_o^{1-k'}}{1-k'}) A^{k'-1} + k'' \frac{C}{A} \qquad (42)$$

This equation may then be integrated using the initial and final concentrations of A and C as limits. k_1/k_3 then may be calculated.

The above descriptions provide an initial approach to modeling the data. A final model should be able to take into account the effect of hydroxyls on all epoxy systems in general. Such a model would be a combination of Cases I and II and would probably be much more difficult than the two cases individually.

Conclusion

Hydroxyl groups are an important constituent in the reaction between amines and epoxy. The hydroxyls have an accelerating effect accompanied by an increase in the order of reaction from zero to two. They most likely interact with amines to form complexes as described by Mika and Tanaka (12). In the case of DAB there are three distinct reactions involved, the first primary amine, the second primary amine and the formed secondary alcohol amine reaction. The rates of these reactions are probably determined by the relative bascities of the amines present, thereby controlling their ability to complex with hydroxyls. If amines, such as diethelenetriamine (DETA), containing secondary amines were used, a fourth reaction would most likely come into play.

The reaction appears to be more complicated than assumed initially and an attempt to describe parameters in terms of a generalized simple model would be difficult.

The authors appreciate the help of Mr. W. Ku in formulation of the model.

References
1.   L. Schecter, J. Wynstra and R. E. Kurkjy, Ind. Eng. Chem., 48, 94 (1956).
2.   A. K. Ingberman and R. K. Walton, J. Polymer Sci., 28, 468 (1958).
3.   Y. Oshiro, M. Ochiai, S. Komori, Kogyo Kagaky Zasshi, 64, 1588 (1961).

4. Y. Oshiro, T. Tsunoda, S. Komori, <u>Kogyo Kagaky Zasshi</u>, <u>64</u>, 2132 (1961).
5. J. F. Harrod, <u>J. Appl. Polymer Sci.</u>, <u>6</u>, 863 (1962).
6. T, Kakurai and T. Noguchi, <u>J. Soc. Org. Chem. Japan</u>, <u>18</u>, 485 (1960).
7. N. S. Isaacs and R. E. Parker, <u>J. Chem. Soc.</u>, <u>1960</u>, 3497.
8. Y. Iwakura, T. Kurosaki, Y. Imai, <u>Makromol. Chem.</u>, <u>86</u> (1957).
9. F. J. Allen and W. M. Hunter, <u>J. Appl. Chem.</u>, <u>7</u>, 86 (1957).
10. I. T. Smith, <u>Polymer</u>, <u>2</u>, 95 (1961).
11. K. Dusek, M. Ilavsky, S. Lunak, <u>J. Polymer Sci.</u>, Symposium <u>53</u>, 29 (1975).
12. Y. Tanaka and T. F. Mika in <u>Epoxy Resins Chemistry and Technology</u> (C. A. May and Y. Tanaka, eds.) Marcel Dekker, New York, 1973, p. 135.
13. J. F. Harrod, <u>J. Polymer Sci.</u>, <u>1A</u>, 385 (1963).
14. Knoll et al in <u>Handbook of Epoxy Resins</u> (H. Lee and K. Neville, Eds.) McGraw-Hill, New York, 1967, Chap. 4, p. 17.
15. F. E. Critchfield and J. B. Johnson, <u>Anal. Chem.</u>, <u>29</u>, 957 (1957).
16. J. P. Bell, <u>J. Poly. Sci.</u>, A-2, <u>6</u>, 417 (1972).
17. V. Toome and K. Manhart, <u>Anal. Let.</u>, <u>8</u> (7), 441 (1975).
18. L. A. O'Neill and C. P. Cole, <u>J. Appl. Chem.</u>, <u>6</u>, 356 (1956).
19. H. Dannenberg, <u>SPE Trans.</u>, <u>3</u>, 78 (1963).
20. T. K. Kwei, <u>J. Polymer Sci.</u>, <u>IA</u>, 2985 (1963).
21. H. C. Anderson, <u>SPE Journal</u>, <u>16</u>, 1241 (1960).
22. C. Potter and W. C. MacDonald, <u>Cand. J. Reas.</u>, <u>25 B</u>, 415 (1947).
23. N. B. Chapman, N. S. Isaacs, R. E. Parker, <u>J. Chem. Soc.</u>, <u>1959</u>, 1925.
24. O. Levinspiel, <u>Chemical Reaction Engineering</u>, John Wiley and Sons Inc., New York, 1972, p. 70.
25. <u>Handbook of Chemistry and Physics</u>, (R. C. Weast, Ed.) Chemical Rubber Co., Cleveland, 1972, p. D-117.
26. Damusis, ACS Symposium, Atlantic City, September, 1956.
27. R. M. Laird and R. E. Parker, <u>J. Chem. Soc.</u>, <u>1965</u>, 4784.
28. F. J. Allen and W. M. Hunter, <u>J. Appl. Chem.</u>, <u>7</u>, 154 (1964).
29. D. O. Bowen and R. C. Whiteside in <u>Epoxy Resins</u>, (R. F. Gould, ed.) ACS Publications, Washington, D.C., 1970, p. 48.

Epoxy Resins Containing a Specific Vulnerability

JAMES R. GRIFFITH

Chemistry Division, Naval Research Laboratory, Washington, DC 20375

The concept of a coating with a built in vulnerability to destruction by specific reagents has been used successfully in some applications. For example, floor finishes which can be removed readily when renewal is required by the application of dilute ammonia, or another mild reagent, are available and convenient. The extension of this concept to rugged, durable coatings, such as epoxies, entails the requirement that a means be found to degrade an "infinite network" molecular structure which is inherently resistant to attack. A need exists for such materials, however, because the factors of toughness and durability which are desirable when epoxy coatings are applied become expensive, troublesome obstacles to removal when the time arrives for renewal. The present work concerns some efforts to synthesize epoxy resins which contain a cleavable weak link that allows the cured network to be chemically degraded into smaller fragments. The consequence of such degradation should be that such coatings would peel from surfaces or become soluble in common solvents after treatment with a "triggering" reagent. For convenience, such a selectively destructible polymer is called a command-destruct resin.

Properties of An Ideal Command-Destruct Resin

An ideal command-destruct resin should retain the desirable properties of conventional epoxies; including, reasonable cost, cure by available curing agents, ability to be compounded with solvents, pigments, etc. to form high-quality paints, and provide long service life. In addition, the cured coatings should retain the ability to be destroyed quickly and effectively by selected reagents not likely to be encountered in the service environment. A high degree of destruct agent specificity insures against accidental loss of the coating. Also, the destruct

agents should be mild chemicals without harmful environmental effects.

All of the ideal properties may never be found in real systems because of a multiplicity of problems concerning economics, synthesis possibilities, destruct effectiveness limitations and environmental stability. However, some of the necessary attributes of effective materials are being incorporated into the following resin types.

Cleavage of Olefinic Bonds

One approach to an effective command-destruct epoxy is that of incorporating one or more olefinic bonds into each molecule such that the final network can be degraded by the well-known reaction of olefins with powerful oxidizing agents, such as acidic permanganate:

$$[O]$$

$$R-CH=CH-R' \longrightarrow RCOOH + HOOCR'$$
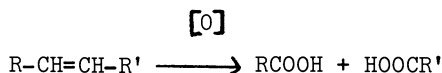
One of the simpler compounds of this type is the diglycidyl ether of 4,4-dihydroxystilbene, although the expense and high-melting point ($284°C$) of this diphenol make the substance impractical:

$$CH_2CHCH_2O \langle O \rangle CH=CH \langle O \rangle OCH_2CH CH_2$$
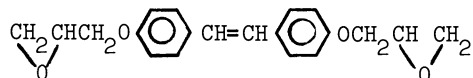
The product obtained in a standard diglycidyl ether reaction with epichlorohydrin and alkali was an off-white crystalline powder melting at $191°-193°C$.

A lower melting diphenol which contains several oxidizable sites is curcumin. This is an intensely colored pH indicator which undergoes various vivid color changes during the synthesis of the diglycidyl ether. The following formula shows the simplest form, although the actual products obtained to date have apparently been polymeric:

$$CH_2CHCH_2O \overset{H_3CO}{\langle O \rangle} CH=CHCCH_2CCH=CH \overset{OCH_3}{\langle O \rangle} OCH_2CH CH_2$$
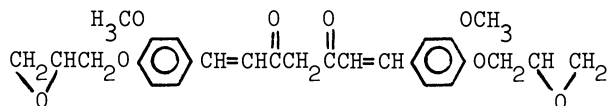
A third compound of the olefinic type, and the most promising obtained to date, is the diglycidyl ether of 2,6-divanillylidene cyclohexanone, which is produced by the conventional reaction of the diphenol with epichlorohydrin:
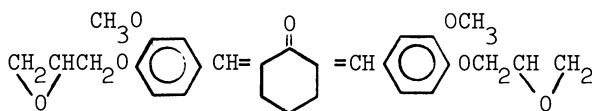
This bright yellow, crystalline compound has a melting range of 143°-148°C, and it is virtually insoluble in common epoxy solvents. However, it will react with polyamide curing agents, and films of good quality have been produced by use of dimethyl sulfoxide as solvent. The films so produced are readily destroyed by a solution of potassium permanganate in 50% acetic acid – water. Permanganate in water alone is ineffective, and the solvency of the acetic acid is necessary in order to swell and soften the cured films enough for the permanganate to penetrate to the olefinic sites. After degradation, the film residue may be easily brushed away from the surface to which the film was formerly tightly bonded.

Another approach to a diglycidyl ether of this type which results in a product of improved solubility characteristics is the reaction of two moles of a pure diglycidyl ether of Bisphenol-A with one mole of 2,6-divanillylidene cyclohexanone. This results in a resin with glycidyl ether terminals which is partially soluble in ketone solvents, particularly methyl ethyl ketone.

Further work will be necessary to produce practical paints from the 2,6-divanillylidene cyclohexanone system, but as an example of the possibilities of the olefinic approach to cleavable epoxy resins, it has been reasonably successful.

Cleavable Tertiary Carbamate Epoxy Resins

Tertiary carbamates, or urethanes, are not produced as readily as the primary and secondary compounds, but an effective synthesis has been described (1). This molecular unit can be readily cleaved by warm solutions of mineral acids (2), and the ease of cleavage may be controlled by proper selection of the components of the tertiary radical:

$$R'R''R''' \ \underset{\Delta}{\overset{O \ \ \ \ \ H+}{C O C N H R} \longrightarrow} R'R''R''' COH + CO_2 + H_2NR$$
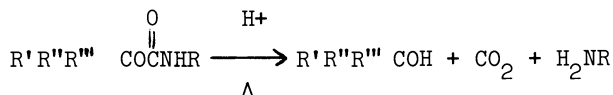
Epoxy resins may be produced which contain tertiary carbamates by the use of glycidol as the chain-terminating alcohol in a diisocyanate – diol reaction. For example, a stepwise reaction has been used in which one equivalent of glycidol has been reacted with 1,6-hexamethylene diisocyanate to produce a mixture represented ideally by the reaction:

$$CH_2CHCH_2OH + O=C=N(CH_2)_6N=C=O \longrightarrow$$

$$CH_2CHCH_2O\overset{\overset{\text{O}}{\|}}{C}NH(CH_2)_6N=C=O$$

The available remaining isocyanate may then react with a
tertiary alcohol when dibutyl tin diacetate is used as
catalyst. An interesting diol containing both primary and
tertiary terminals is hydroxycitronellol, a derivative of
natural products:

$$\underset{\underset{CH_3}{|}}{HOC}\overset{\overset{CH_3}{|}}{(CH_2)_3}\overset{\overset{CH_3}{|}}{C}CH_2CH_2OH$$

The complex epoxy resin obtained from this system is a low-
melting wax which is nominally represented by the formula:

$$CH_2CHCH_2O\overset{\overset{O}{\|}}{C}NH(CH_2)_6NH\overset{\overset{O}{\|}}{C}O\overset{\overset{CH_3}{|}}{\underset{\underset{CH_3}{|}}{(CH_2)_3}}\overset{CH_3}{C}CH_2CH_2O\overset{\overset{O}{\|}}{C}NH(CH_2)_6NH\overset{\overset{O}{\|}}{C}OCH_2CH CH_2$$

This resin may be melted and blended with amine curing agents to
produce tough polymers which are vulnerable to cleavage at the
tertiary linkage.
        As with the olefin - containing epoxies, much is yet to be
done with tertiary carbamate epoxies in order to produce
practical systems, but the synthesis possibility has been
established. A variety of diisocyanates and tertiary alcohols
are available. A general synthesis effort is needed to screen
the most effective compositions with regard to solvency,
compounding, cure, environmental stability, and the effectiveness
of various destruct agents and conditions.

Literature Cited

1. Bailey, W. J. and Griffith, J. R. Polymer Preprints, 1964,
    5 (1), 266-278.

2. Bailey, W. J. and Griffith, J. R. Polymer Preprints, 1964,
    5 (1), 279-290.

RECEIVED May 21, 1979.

INDEX